Topics in Conformal Regge theory

Aaditya Salgarkar
Physics and Astronomy
Faculty of Sciences, University of Porto
2023

Supervisor
Dr Miguel Costa, Faculty of Sciences, University of Porto

PhD

Universidade do Minho

U.PORTO
FACULDADE DE CIÊNCIAS
UNIVERSIDADE DO PORTO

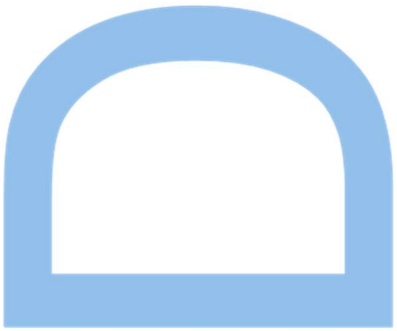

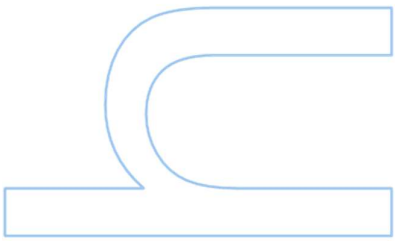

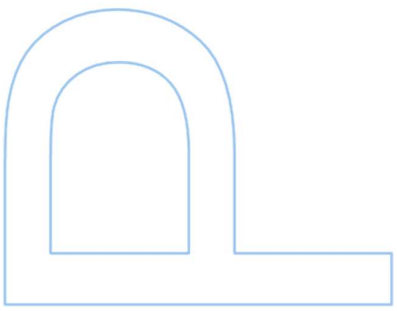

Sworn statement

I, Aaditya Salgarkar, enrolled in the Doctor's Degree of Physics at the Faculty of Sciences of the University of Porto hereby declare, in accordance with the provisions of paragraph a) of Article 14 of the Code of Ethical Conduct of the University of Porto, that the content of this thesis reflects perspectives, research work and my own interpretations at the time of its submission. By submitting this thesis, I also declare that it contains the results of my own research work and contributions that have not been previously submitted to this or any other institution. I further declare that all references to other authors fully comply with the rules of attribution and are referenced in the text by citation and identified in the bibliographic references section. This thesis does not include any content whose reproduction is protected by copyright laws. I am aware that the practice of plagiarism and self-plagiarism constitute a form of academic offense.

Acknowledgements

First, I would like to thank my advisor, Professor Miguel Costa, for giving me the opportunity do work in the group. I would specially like to thank for making part of the Simons Collaboration on nonperturbative bootstrap which helped me understand the important ideas in the field by joining stimulating discussions in the conferences. His high standards for the research were instrumental in my development as a researcher and the work in this thesis. I thoroughly enjoyed working with him and I am grateful for his guidance, support and specially his patience.

I would also like to thank the Simons foundation (grant ID 488637) for providing me the funding throughout my PhD as well as several conferences.

I was fortunate to have several amazing collaborators during my PhD. I am grateful to them for the exchange of ideas and discussions about finished projects, as well as the several ideas for future projects. Therefore, I would like to thank António, Balt VR, Vasco, João P, João VB, Sourav, Miguel.

I would like to thank all the friends I have made during my time in Porto inside and outside the university.

Finally, I would like to thank my parents for all the support they have provided me throughout my life and specially the patience during my PhD, without which this work would not have been possible. This thesis is dedicated to them.

To Aai, Baba

UNIVERSITY OF PORTO

Abstract

Faculty of Sciences
Departament of Physics and Astronomy
Centro de Física do Porto

Doctor of Philosophy

Topics in Conformal Regge theory

by Aaditya SALGARKAR

In this thesis, we discuss two aspects of conformal field theory, more specifically, the conformal Regge theory. Conformal field theories are a special class of quantum field theories with enhanced symmetry under the group of conformal transformations. Regge limit is a special kinematical limit of observables in conformal field theories analogous to the high energy limit of the flat space scattering amplitude. First, we discuss the generalization of Optical theorem from flat space to AdS space, in the Regge limit. We discuss its relation to the flat space optical theorem in the appropriate limit. Second, we discuss the generalization of conformal Regge theory to higher point correlation functions. In particular, we propose the kinematics in the position space for the higher point correlation functions and show that they are equivalent to a natural generalization from the multi Regge limit of the flat space scattering amplitude.

UNIVERSITY OF PORTO

Resumo

Faculty of Sciences
Departament of Physics and Astronomy
Centro de Física do Porto

Doutor de Ciência

Tópicos em teoria de Regge conforme

por Aaditya SALGARKAR

Nesta dissertação, discutimos dois aspetos da teoria de campos conformes, particularmente, a teoria de Regge conforme. As teorias de campos conformes são uma classe especial de teorias de campos quânticos com simetria aprimorada sob o grupo de transformações conformes. O limite de Regge é um limite cinemático especial de observáveis em teorias de campos conformes, análogo ao limite de alta energia da 'Scattering amplitude' de espaço plano. Em primero lugar, discutimos a generalização do teorema ótico de espaço plano para o espaço AdS, no limite de Regge. Adicionalmente, discutimos a sua relação com o teorema ótico de espaço plano no limite apropriado. Em segundo lugar, discutimos a generalização da teoria conforme de Regge para funções de correlação com mais de quatro pontos. Em particular, propomos a cinemática no espaço de posição para funções de correlação de mais de quatro pontos e mostramos que são equivalentes a uma generalização natural do limite multi Regge da 'Scattering amplitude' de espaço plano.

Contents

List of Figures

List of Tables

Publications

During the period of his PhD, the author contributed to the publication of the three works below. This thesis focuses on the first and the last publication of this list

1. A. Antunes, M. S. Costa, T. Hansen, A. Salgarkar, and S. Sarkar, The perturbative CFT optical theorem and high-energy string scattering in AdS at one loop, JHEP 04 (2021) 088, [arXiv:2012.0151],

2. A. Antunes, M. S. Costa, J. a. Penedones, A. Salgarkar, and B. C. van Rees, Towards bootstrapping RG flows: sine-Gordon in AdS, JHEP 12 (2021) 094, [arXiv:2109.1326],

3. M. S. Costa, V. Gonçalves, A. Salgarkar, and J. Vilas Boas, Conformal multi-Regge theory, To appear.

Abbreviations

CFT	Conformal Field Theory
QFT	Quantum Field Theory
AdS	Anti de-Sitter
SYM	super Yang-Mills

Chapter 1

Introduction

Two of the most beautiful theories developed in the 20^{th} century are Quantum mechanics and General theory of relativity. Generically, the theory of quantum mechanics is crucial in the description of phenomenon at the atomic scale, where the deviation from classical mechanics governed by Newton's law is significant. On the other hand, general theory of relativity is important for the description astronomical phenomenon, where, again, the deviation from the Newton's law is significant. One of the most important problem at our hand is to find a consistent framework that unifies both these theories, dubbed the problem of 'quantum gravity'.

An important milestone in the quest for quantum gravity was achieved with the framework of perturbative quantum field theories. This framework successfully combines quantum mechanics and special theory of relativity. The breadth of this framework includes, but not limited to, the scattering of particles at the Large Hadron Collider, the description of the boiling water, exploration of the exotic phases of matter and Hawking radiation coming out of black hole.

Among all quantum field theories, there is a class of theories with enhanced symmetry when compared to the Lorentz invariance of special relativity. This includes all the transformations of the spacetime which preserve angles between two lines, in addition to the transformations that preserve the Lorentzian length. This class of theories is called 'conformal field theories' (henceforth CFTs), the central topic of this thesis.

Conformal field theories appear in a variety of physical phenomenon. An important class of them appear at the end of renormalization group flow. Generically, the coupling constants in quantum field theories depend on the energy scale at which one probes the said theory, called 'running coupling constant'. This flow of the coupling constant can stop due to coincidences, at which point the theory becomes independent of the energy at which it is

probed. Precisely this independence on the energy scale leads to the enhancement of symmetries from Lorentz length invariance to scale invariance. These 'fixed points' of the flow of couplings are described by scale invariant theories. In addition, one hypothesizes that this scale invariance is enhanced to 'conformal invariance'. Thus, these 'end points of the flow' are described by CFTs.

Another context in which this class of theories appear is the criticality of the statistical physical models. Ising models in various dimensions provide a detailed model of magnetization. This model is exactly solved in two dimensions on the lattice. It is also solved in four dimensions since the mean field approximation is exact. However, in three dimensions, both these techniques fail to be tractable. One simplification can be made in this case by considering the case of criticality. In this case, the fluctuations becomes scale independent, and therefore amenable to be analyzed using the tools of CFT.

Yet another context where the study of CFTs is important pertains the 'AdS/CFT correspondence'. While a first principle construction of nonperturbative theory of quantum gravity, mentioned above, is still unclear, the 'AdS/CFT' correspondence provides an indirect formulation of such a framework. In its strongest form, it postulates the duality between two theories. On one hand, there is the nonperturbative completion of certain type of string theory in asymptotically AdS backgrounds, certain highly symmetric solutions of Einstein equation. On the other hand, there is a maximally supersymmetric and conformal invariant cousin of quantum chromodynamics. This conformal invariant theory can be understood in the framework of CFTs, and therefore furnish *a* definition of nonperturbative theory of quantum gravity.

Conformal field theories

CFTs are a class of quantum field theories with enhanced symmetries. Thus, they combine quantum mechanics with conformal invariance. The central aspect of quantum mechanics is 'Unitarity', which encodes the preservation of information. This is an appropriate generalization of the Liouville theorem, which states that the number of possible physical states in a classical system can neither decrease nor increase. In essence, the quantum generalization states that the number of possible physical states remain preserved, and therefore all the probabilities add to 1. In particular, this means that the probability of any physical process must be between 0 and 1. In quantum theories, the physical states are described by rays in the Hilbert space, and the corresponding probability is given by the square of the norm of the corresponding vector, as per 'Born rule'.

Conformal invariance means invariance of the observables in the quantum theory under conformal transformations. In d dimensional Euclidean space, they are encoded in the group

$SO(d+1,1)$, as opposed to the Lorentzian theory, where it is $SO(d,2)$. An important class of observables in CFTs are the correlation functions of local operators, denoting the amount of correlation in the respective local operators. These can be defined in both Euclidean and Lorentzian setup, and are related to each other via the Wightman functions. These correlation functions depends on the types of the local operators and the respective location of these operators. However, their form is highly constrained due to conformal invariance more than one might naively imagine. Naively, a correlation function of n operators can be a function of $4n$ variables, namely, the spacetime coordinates of the n operators,

$$\langle O_1(x_1) O_2(x_2) \dots O_n(x_n) \rangle = f(x_i). \tag{1.1}$$

Two and three points are highly constrained by conformal invariance, up to certain numbers depending on conformal representation theory. Two point function can be written in terms of squared distances $x_{ij}^2 = (x_i - x_j)^2$ to be [1]

$$\langle O_{\Delta,J=0}(x_1) O_{\Delta',J=0}(x_2) \rangle = \frac{\delta_{\Delta,\Delta'}}{x_{12}^{2\Delta}}. \tag{1.2}$$

However, four point correlation functions are not fixed entirely like the two and three point case. This follows from the nontrivial dependence on the 'cross ratios' [1]

$$U = \frac{x_{12}^2 x_{34}^2}{x_{14}^2 x_{32}^2}, \qquad V = \frac{x_{13}^2 x_{24}^2}{x_{14}^2 x_{23}^2}. \tag{1.3}$$

Conformal invariance can be used to write the correlation function in terms of a function of these cross ratios by choosing some appropriate scaling behavior. A key object in the analysis of this correlator is the 'conformal block'. It encodes the contribution of a certain exchanged primary operator and all its descendants in a single function of cross ratios. Any Euclidean correlator can be expanded into these kinematical objects. This allows us to separate the kinematical part of the correlation function from the dynamical part. We will discuss these details in the next chapter.

Conformal Regge theory

The topic of this thesis is a particular aspect of CFTs, namely, Conformal Regge theory. The main idea is to consider certain limit of the correlation function where the dependence on the spacetime point is even more constrained which leads to more direct and analytical study of the observables of the CFTs. This idea is rooted in the analogous simplification that occurs in the S-matrix theory, called the Regge theory.

Consider two to two scattering in a generic quantum field theory. Conservation of momentum and Lorentz invariance forces the scattering amplitude A for such a process to be dependent on only two 'Mandelstam' variables: $s = (p_1 + p_2)^2$, $t = (p_1 + p_3)^2$. Regge limit concerns the study of this amplitude in the limit large s for fixed t . In this limit, the amplitude is expected to have a simple structure,

$$A(s,t) \to s^{\alpha(t)} f(t) . \tag{1.4}$$

This scaling behavior of the scattering amplitude is experimentally verified [2].

In fact, this limit provided the crucial insight to prescribe a model of meson scattering consistent with Unitarity, proposed by Veneziano. Providing a first principle derivation of this scattering amplitude lead to the 'model of dual resonances'. This paved the way to the analysis of perturbative string theory.

Important insight from the analysis of Regge limit can be summarized in the Chew-Frautschi plot. In this plot, one considers spin angular momentum in the x axis and squared mass in the y axis. Then, one plots the exchanged particles in the scattering process as points in this space. These plots from the experiments have an approximate structure of a straight line. Thus, the idea is to consider these particles as a 'Regge trajectory' rather than individual particles. In particular, the spin quantum number is not necessarily quantized, but rather is a general complex number.

While perturbative string theory in the asymptotically flat spacetime is rather well understood, its analogue in the curved spacetime is unclear due to technical difficulties. However, one expects a similar structure as in the flat spacetime. To begin understanding this structure, it is useful to consider anti de-Sitter space in $d+1$ dimensions, since they are maximally symmetric backgrounds.

AdS/CFT correspondence [3] states the equivalence of string theory in these spacetime with an independently defined CFT. Therefore, Regge limit of string theory in AdS should reflect itself as some limit in the dual CFT description. Two to two scattering amplitude admits a dual description in terms of the four point correlation function. The role of the Mandelstam invariants in CFT case is played by the cross ratios. Therefore, one considers analogous limit of the correlation functions. As described in [4], this limit can be pictured in the Lorentzian cylinder as in Figure 1.1.

Outline

This sets the stage for the work in this thesis. First, we describe the implications of the Regge theory on the CFT data extracted from one loop string theory. While independent

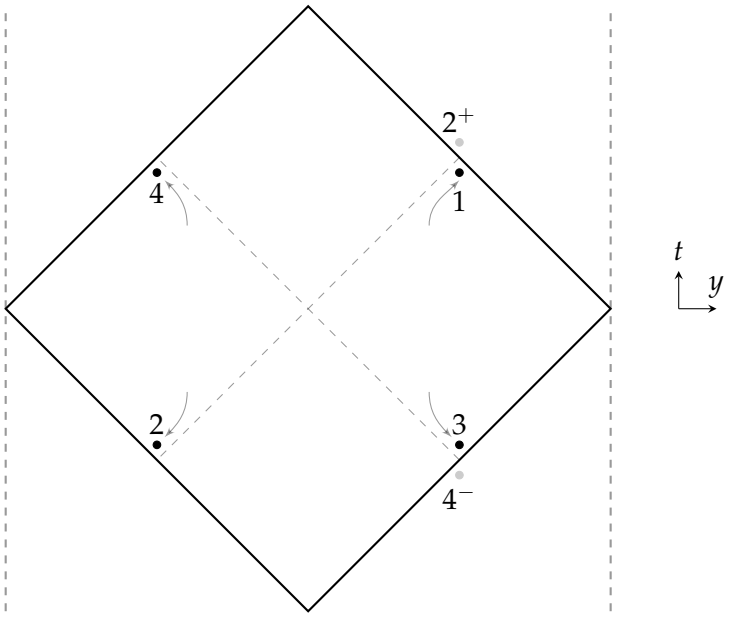

FIGURE 1.1: Regge limit configuration in the Lorentzian cylinder.

computation of the string theory amplitudes are available mainly in flat space and some AdS_3 backgrounds, we can employ bootstrap techniques to arrive at a subset of data in AdS_5. We can also use the flat space string theory analysis to constrain the amplitude in AdS_5, since effectively AdS_5 acts like a one parameter extension of flat space background.

In the latter part, we discuss the generalization of the Conformal Regge theory to many point correlation functions. We first review the case of multi-Regge limit in the many particle scattering amplitude in quantum field theories. Then, we discuss its generalization to the conformal field theories.

1.1 Kinematics of conformal field theory

Now, we turn to a detailed introduction of the theories considered in this thesis.

In this section, we discuss the kinematics of conformal field theory. Conformal field theories in d dimensions are a class of quantum field theories with additional symmetries that are not present in the standard quantum field theories. In the Euclidean space, the conformal field theories are invariant under the Euclidean conformal group, $SO(d+1,1)$, while in the Lorentzian space they are invariant under the Lorentzian conformal group, $SO(d,2)$. The generators of the Euclidean conformal group can be written in terms of the spacetime

derivative ∂_μ as

$$\text{Translations} \qquad P_\mu = \partial_\mu, \tag{1.5}$$

$$\text{Rotations} \qquad M_\mu = i\left(x_\mu \partial_\nu - x_\nu \partial_\mu\right), \tag{1.6}$$

$$\text{Dilatations} \qquad D = i x^\nu \partial_\nu, \tag{1.7}$$

$$\text{Special conformal transformations} \qquad K_\mu = i\left(2x_\mu \left(x^\nu \partial_\nu\right) - x^2 \partial_\mu\right). \tag{1.8}$$

However, some of these generators act nonlinearly on the spacetime points. Therefore, it is useful to consider 'Embedding space':

$$X^A = \left(\frac{1+x^2}{2}, \frac{1-x^2}{2}, x^\mu\right), \tag{1.9}$$

with the signature $(-,+,\ldots,+)$. The Euclidean conformal group acts linearly on X. This simplifies several calculations, for instance, the inner product in the physical space given by $\left(x_\mu - y_\mu\right)\left(x_\nu - y_\nu\right)\delta^{\mu\nu}$ becomes $X \cdot Y = X_A Y_B \eta^{AB}$. Here, X, Y are respective embedding coordinates for x, y. This allows us to identify the dependence on the spacetime variables of the correlations functions.

The physical observables in conformal field theory are the correlation functions of the local operators in the theory. The local operators are characterized by quantum numbers of the generators of the conformal group. We consider a special set of operators, called 'primary' operators. They are precisely the operators which are annihilated by special conformal transformations $K_\mu O = 0$. All the other operators are 'descendants' of one of these operators, namely, they are of the form: $\left(P_\mu\right)^n O$. In particular, the operators are labeled by the quantum numbers for dilatations: Δ and rotations: λ, a Young tableux diagram for the representation. Thus, a representation of the conformal group R is labeled by (Δ, λ). In the simple case of symmetric traceless representation, λ can be replaced by the number of boxes in λ, representing the spin.

Two and three points correlation functions of the primary scalars, the primary operators with spin 0 and scaling dimensions Δ_i can be written in terms of the embedding space as follows [1],

$$\left\langle \phi(X)\, \phi(Y) \right\rangle = \frac{\delta_{\Delta_1 \Delta_2}}{(X \cdot Y)^{\Delta_1}}, \tag{1.10}$$

$$\left\langle \phi(X)\, \phi(Y)\, \phi(Z) \right\rangle = \frac{c}{(X \cdot Y)^{\alpha_{123}} (Y \cdot Z)^{\alpha_{231}} (Z \cdot X)^{\alpha_{132}}}. \tag{1.11}$$

We have chosen the normalization of the operators such that the two point function numerators are 1. The numerator in the three point function, c, is called 'operator product expansion coefficient' (OPE coefficient). We have also used $\alpha_{ijk} = \left(\Delta_i + \Delta_j - \Delta_k\right)/2$.

The set of representations R's of the local primary operators and their respective OPE coefficients c_{R_1,R_2,R_3} consitute a useful characterization of the observables in conformal field theory, called '*CFT data*'.

While it is easy to see that the spactime dependence of the two and three point functions are fixed by the conformal invariance, the situation changes for higher point functions. The four point function is not fixed by the conformal invariance because there exist conformal invariant 'cross ratios'

$$U = \frac{X_{12}X_{34}}{X_{13}X_{24}},\ V = \frac{X_{14}X_{23}}{X_{13}X_{24}}. \tag{1.12}$$

The dependence on these cross ratios can not be fixed by conformal invariance alone. This allows us to write the four point correlation function of identical scalars as

$$\langle \phi(X_1)\,\phi(X_2)\,\phi(X_3)\,\phi(X_4)\rangle = \frac{1}{X_{12}^{\Delta}X_{34}^{\Delta}} A(U,V)\,. \tag{1.13}$$

A denotes an unknown function of cross ratios. However, since the operators ϕ's are identical, their correlation function is permutation invariant. It is easy to see that this leads to a constraint on A, namely [1]

$$A(U,V)\left(\frac{V}{U}\right)^{\Delta} = A(V,U)\,. \tag{1.14}$$

This is called as the '*crossing constraint*'.

The goal of conformal bootstrap is to use the consistency conditions of the conformal field theory to constrain the CFT data. In particular, we use consistency of the four point function to arrive at constraint on the lower point functions.

In conformal field theories, one can use '*operator product expansion*'.

$$\phi(x)\,\phi(y) = \sum_{primary\ O} c_{\phi\phi O}\left(x-y,\partial_{x-y}\right) O(y)\,. \tag{1.15}$$

Unlike a generic quantum field theory, this expansion has a finite radius of convergence. This is an operator level statement and therefore is valid in all correlation functions. In particular, it can be used to write down a four point correlation function in terms of the lower point correlation function.

$$\langle \phi(x)\,\phi(y)\times\phi\ldots\phi\rangle = \sum_{primary\ O} c_{\phi\phi O}\left(x-y,\partial_{x-y}\right)\langle O(y)\,\phi\ldots\phi\rangle. \tag{1.16}$$

Note that the right hand side correlation function has fewer operator insertions than the left hand side correlation function.

In this thesis, we will concern outselves with unitary quantum field theories. Unitarity of conformal field theory, which is also a quantum field theory imposes constraint on the CFT data. This leads to a nontrivial constraint on the four point correlation function when expanded in terms of the lower point correlation functions.

These constraints are used in the program of Euclidean conformal bootstrap. However, in this thesis, we are mainly concerned with the constraints coming from the Lorentzian consistency of the conformal field theory. In the following, we discuss the necessary tools to discuss correlation function in the Lorentzian setup and its relation to the Euclidean correlation function.

1.2 Wightman functions

In this section, we discuss the Wightman functions and their properties. The Wightman functions are useful in going back and forth between the properties of Lorentzian correlators and their Euclidean counterparts. We closely follow the discussion in [5].

For concreteness, we consider the correlation function of four identical scalars ϕ. First, we discuss the Euclidean correlation function in the Euclidean space with time direction denoted by τ and space directions labelled by y_i. As discussed before, such a correlation function is fixed up a function, A, of two cross ratios U, V. We define a rewriting of the cross ratios $U = z\bar{z}$ and $V = (1-z)(1-\bar{z})$. This rewriting is especially useful when we use the conformal symmetry to fix three out of the four points to be at $0, 1, \infty$. The point that is not fixed can be brought to the same plane as the other three points by a conformal transformation. The location of this point is precisely z in the complex plane $i\tau + y$. We choose the second point to be written in terms of z. Thus, the Euclidean correlation function is given by $A(z, \bar{z} = z^*)$. Note that in the Euclidean setup, we have $\bar{z} = z^*$, since τ is real. Now, we would like to discuss the procedure to convert this correlation function to a Lorentzian correlation function. In this case, the Euclidean time becomes purely imaginary. Therefore, $z, \bar{z}$ are no longer complex conjugates of each other, but are in fact complex numbers.

In the Lorentzian setup, commutator of two operators spacelike separated.

$$[O_1(x_1), O_2(x_2)] = 0 \qquad\qquad x_1 \approx x_2. \tag{1.17}$$

In particular, if we move the point x_2 from the region spacelike separated from x_1 to the region timelike separated from x_1, the commutator encounters a jump. This jump is reminiscant of branch cut behaviour. In fact, the correlation function in the Lorentzian setup is given by an appropriate analytic continuation of the Euclidean correlation function. One expects

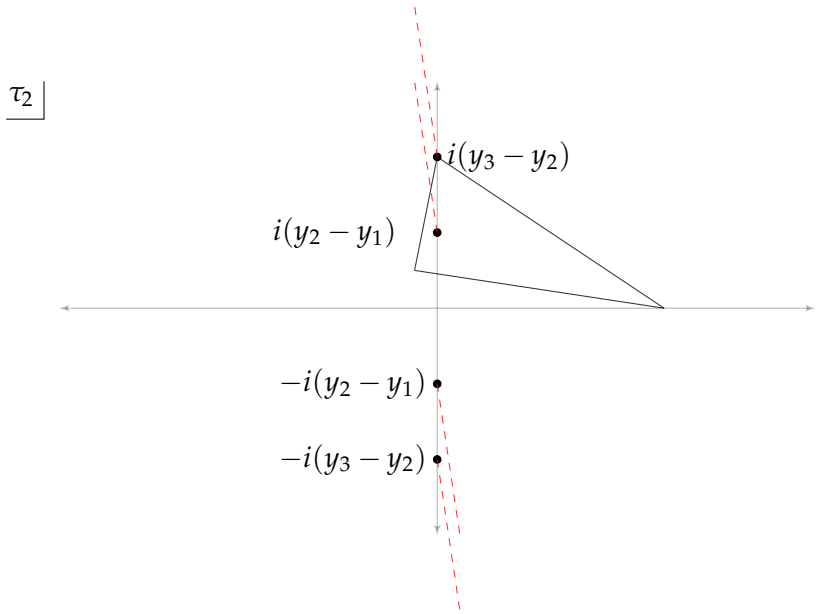

FIGURE 1.2: Location of cuts in the complex τ plane. The grey lines are the possible path, with or without crossing the branch cuts.

that the function A admits a branch cut when two of the points in the correlation function become lightlike separated.

We study the correlation function by first starting in the Euclidean setup with points fixed at

$$\begin{aligned} x_1 &= (0, 0, \ldots, 0)\,, & x_2 &= (\tau_2, y_2, \ldots, 0)\,, \\ x_3 &= (0, 1, \ldots, 0)\,, & x_4 &= (0, \infty, \ldots, 0)\,. \end{aligned} \tag{1.18}$$

Now, the idea is to move the second point away from the Euclidean space positions to Lorentzian space positions. This involves a Wick rotation $\tau \to it$ with appropriate $i\epsilon$ prescription. While doing so, one can encounter a branch cut due to the presence of the light-cones in the Lorentzian spacetime. It is easy to see that the location of the branch cuts in τ_2 is as depicted in figure 1.2. Going from Euclidean to Lorentzian, the value of τ_2 goes from a real number to a purely imaginary number.

One can study the implications of this branch cuts on the correlation function as a function of the cross ratios. This branch cuts implies a branch cut in the correlation function at $z, \bar{z} \in (1, \infty)$.

This exotic branch structure allows us to probe more constraints on the correlation function. In particular, there are constraints coming from the Lorentzian consistency which are hard to see from the Euclidean CFT understanding. Euclidean correlation functions are simplified in the 'OPE limit', when two of the points are colliding. This is a somewhat singular limit, but allows us to study the correlation function analytically. This corresponds to $z \to 0, 1$ or ∞ limit in the correlation function A. The complicated structure of cuts allows us access to a

bigger set of singular structure of the correlation function. We can choose to cross some of these branch cuts *before* taking the limit $z \to 0, 1$ or ∞. Study of such limits of the correlation function is called 'Regge theory'.

An important aspect of this limit is that we access the sheets of the correlator which are not principal. Principal sheet corresponds to the Euclidean configurations. However, we can use many paths to go away from this region. For instance, consider the configuration of the correlation function when $2 > 3$ and $1 < 4$ whereas all the other pairs are spacelike separated. This allows us to reach the following Wightman functions,

$$\begin{aligned}
&\langle \phi(x_4)\, \phi(x_1)\, \phi(x_2)\, \phi(x_3) \rangle, \\
&\langle \phi(x_4)\, \phi(x_1)\, \phi(x_3)\, \phi(x_2) \rangle, \\
&\langle \phi(x_1)\, \phi(x_4)\, \phi(x_2)\, \phi(x_3) \rangle, \\
&\langle \phi(x_1)\, \phi(x_4)\, \phi(x_3)\, \phi(x_2) \rangle.
\end{aligned} \tag{1.19}$$

It is easy to see that in this configuration, $1,2$ OPE converges on the right vacuum in the second Wightman function as 1 can be commuted with 3. Similarly, it converges on the left vacuum in the third Wightman function since 2 and 4 are spacelike separated. However, the first and the fourth Wightman functions do not have a convergent $1,2$ OPE. Therefore, they can not be arrived at by naive analytic continuation of the Euclidean correlation function without encountering monodromy. One can track the path in the cross ratio space $z, \bar{z}$ during this analytic continuation of x_i. It amounts to taking $\bar{z}$ going across the cut $\bar{z} = 1$ in the clockwisek or counterclockwise direction, for the fourth and the first Wightman function, respectively. Thus, these Wightman functions are $A^{\circlearrowleft}, A, A, A^{\circlearrowright}$, respectively.

These four Wightman functions can be combined to write an interesting quantity, dDisc. This quantity serves as a generalization of imaginary part of the scattering amplitude, in a sense that it is manifestly positive. It is also an important quantity since the analogue of the inversion formula feeds on it. Formally, it is defined as

$$\text{dDisc}A(z,\bar{z}) = \cos(\pi(a+b))\, A(z,\bar{z}) - \frac{1}{2}\left[e^{i\pi(a+b)} A^{\circlearrowright}(z,\bar{z}) + e^{i\pi(a+b)} A^{\circlearrowleft}(z,\bar{z})\right]. \tag{1.20}$$

Here, we have used $a = \frac{\Delta_2 - \Delta_1}{2}$, $b = \frac{\Delta_3 - \Delta_4}{2}$. The phase factors come from changing the time ordering of the unequal operators. For equal scalars, the phase factors become 1. Incidently, this quantity also admits an elegent formulation in terms of 'double commutator',

$$\langle [\phi_1, \phi_4]\, [\phi_2, \phi_3] \rangle = x_{12}^{-2\Delta_\phi} x_{34}^{-2\Delta_\phi} \text{dDisc}(A). \tag{1.21}$$

1.3 Regge theory

We discuss some aspects of Regge theory in this section. Regge theory concerns the study of the correlation function in the 'Regge limit'. This is a generalization of the 'Regge limit' in the scattering amplitudes, which concerns the high energy limit.

Consider the case of two to two scattering amplitudes. They are described in terms of the momenta of the external particles, p_1, p_2, p_3, p_4. However, due to conservation of momenta as well as Lorentz invariance of the theory, they depend only on the two invariants, $s = -(p_1 + p_2)^2$ and $t = -(p_1 + p_3)^2$. Regge limit concerns an extreme high energy scattering limit wherein s is large while t is fixed.

Analogously, the correlation functions of four operators in a Lorentzian conformal field theory depend on two cross ratios, U, V, defined in equation 1.12. In terms of these cross ratios, one can consider various limits. One can consider the 'OPE limit' where two of the four operators approach each other. This amounts to $U \to 0, V \to 1$ with $(V-1)/\sqrt{U}$ fixed. The latter, ξ, is the analogue of the scattering angle in the S-matrix case. One can also consider the limit where one of the operators approach the lightcone of the other. This is called the 'lightcone limit'. This amounts to $U \to 0$ for any V.

In the Regge limit, we are concerned with a certain generalization of the OPE limit. As described in the previous section, the correlation function has interesting analytic structure. Therefore, one has a lot more freedom to consider the generalization of the lightcone limit. Several lightcones of the form $x_{ij}^2 = 0$ are related to nontrivial analytic structure such as branch points and branch cuts in terms of the cross ratio space U, V. Regge limit concerns the OPE limit, however, it is taken after crossing the cuts in V cross ratio at $V = 1$.

In the following, we study the effect of this limit on the correlation function of four operators, ϕ. Using conformal symmetry, we first represent the correlation function in terms of the cross ratios, $A(U, V)$. It admits an expansion in terms of certain kinematical functions of cross ratios called 'conformal blocks', denoted by G.

$$A(U, V) = \sum_O \lambda_{\phi\phi O}^2 G_O(U, V) \tag{1.22}$$

These objects are defined for each primary O and come from summing over all the descendants of a given primary O. Each primary is a representation of the Euclidean conformal group, and therefore labeled by scaling dimensions, Δ and the representation of the rotation group, Λ. For the symmetric traceless representation of the rotation group, it is just the spin quantum number. While these are interesting objects themselves, it is useful to rewrite the expansion in terms of 'conformal partial waves', F_O. Similar to the S-matrix partial waves, these partial waves have a well defined orthogonality properties. They can be expressed as

a linear combination of the conformal block as follows

$$F_O = G_O + \frac{\kappa_{\tilde{O}}}{\kappa_O} G_{\tilde{O}}. \tag{1.23}$$

The expressions for κ can be found in [4]. The orthogonality holds for the operators on the 'principle series representations'. These are operators whose scaling dimensions is $\nu = d/2 + i\mathbb{R}$. The orthogonality relation can be written in terms of some weight function μ as [6]

$$\int dU dV \, \mu(U,V) \, F_O(U,V) \, F_{O'}(U,V) = n_O \delta_{O\,O'}. \tag{1.24}$$

Since these partial waves form a complete basis, we can consider the partial wave expansion in spacetime dimensions $d = 2h$ [4, 6],

$$A(U,V) = \sum_J \int_{h+i\mathbb{R}} \frac{d\nu}{2\pi i} b_{\nu,J} F_{\nu,J}(U,V). \tag{1.25}$$

Here, we have introduced the 'OPE function' $b_{\nu,J}$

$$b_{\nu,J} = \frac{\lambda^2_{\phi\phi O}}{\nu^2 - (\Delta - h)^2}. \tag{1.26}$$

It is an analytic function of ν with poles at the location of the physical operators.

We discuss the analytic structure of the correlation function in the Regge limit as a function of V. The lightcones result in two branch point singularities at $V = 1$ and $V = \infty$. To separate them, we write a decomposition of the correlator [4] as follows

$$A = A^+ + A^-, \tag{1.27}$$

such that the first one has no nontrivial monodromy around $V = 1$, whereas the later has no nontrivial monodromy around $V = \infty$. Corresponding to each, we define the 'signatured OPE function', $A^{\theta=\pm}$. They are the coefficient of the partial wave expansion of the signatured correlator

$$A^\theta(U,V) = \sum_J \int_{h+i\mathbb{R}} \frac{d\nu}{2\pi i} b^\theta_{\nu,J} F_{\nu,J}(U,V). \tag{1.28}$$

They get contributions from even and odd spins, respectively. It is now known that these 'signatured OPE functions' are also analytic functions of J [6]. Thus, even and odd spins form 'Regge trajectories'. These are interesting analytic manifolds with analyticity in J.

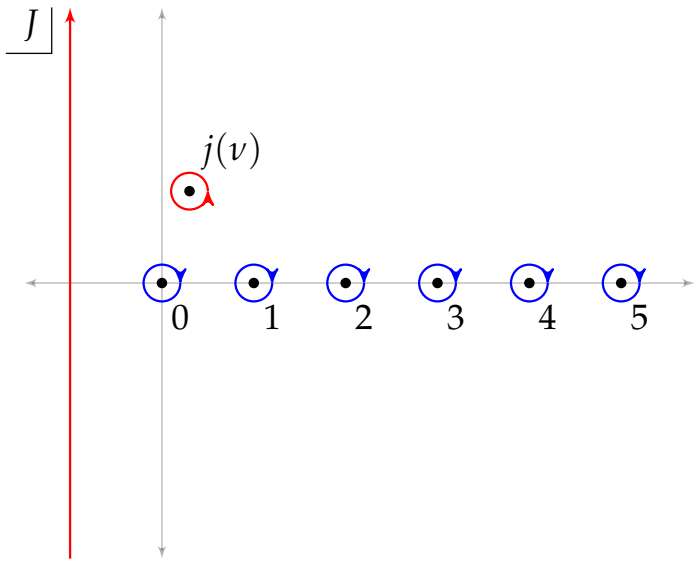

FIGURE 1.3: Location of poles in the complex J plane. In blue, the spins in the Euclidean conformal field theory are shown. $j(\nu)$ denotes the special poles in the complex plane that dominates the Regge limit of the correlator.

First, we discuss the limiting behaviour of the conformal partial wave in the Regge limit. This limit can be written as $\sigma \to 0$ with fixed ξ where we use

$$\sigma^2 = z\bar{z}, \qquad \xi = \frac{1}{2}\left(\sqrt{\frac{z}{\bar{z}}} + \sqrt{\frac{\bar{z}}{z}}\right). \tag{1.29}$$

As we will discuss later in the thesis, the Regge limit of the partial wave in generic dimensions is σ^{1-J}. Thus, the leading contribution to the correlator comes from the operators with higher spins. However, operators with arbitrarily large spin appear in the spectrum. To make sense of this sum over spins, we use the techniques from complex analysis.

We will use the analyticity in spin in the following. We discuss the evaluation of the correlator in the Regge limit described above. First, we replace the sum over spins by a contour integral over the positive real line, shown in blue in Figure 1.3. Then, we consider deforming this contour to the red contour. In the process, we pick any pole that we may encounter [4]. This pole is called 'the pomeron'. Furthermore, the integral over ν can also be performed in the saddle point approximation in certain cases [7]. Thus, the leading behaviour of the correlator in the Regge limit is given by σ^{1-j^*}, where j^* is the location of the circled pole in Figure 1.3 evaluated at the saddle point in the ν integral.

1.4 An inversion formula

In the previous section, we discussed the representation of the conformal correlator in terms of the CFT data via conformal block expansion. The goal of this section is to discuss the

'inverse' of that expansion, called as an 'inversion formula'.

First, we present a toy model from a single variable complex analysis that captures the essence of the main formula. Consider an analytic function A of a complex variable w. We would like to consider its Taylor series expansion around $w = 0$,

$$A(w) = \sum_{J=0}^{\infty} a_J w^J. \tag{1.30}$$

A priori, the expansion coefficients a_J are independent of each others. In other words, one can change, say, a_{134} by a small amount without changing any other a_J.

Now, we take an alternate point of view at the same expansion formula. It uses the orthogonality of the power laws, playing the role of partial waves

$$\oint dw\, w^a w^b = \delta_{a,-1-b}. \tag{1.31}$$

This is essentially the Cauchy formula for the contour circling the origin. The Euclidean inversion formula implied by this is

$$a_J = \oint \frac{dw}{2\pi i}\, w^{-1-J} A(w). \tag{1.32}$$

If we assume that the function A has a nice behavior at ∞, we can deduce more properties of the function a_J. Let us say A is bounded as

$$A(w) \leq 1 \qquad\qquad w \to \infty. \tag{1.33}$$

Naively, this appears impossible to achieve as all the power laws w^J blow up at large w, for $J > 1$. Thus, imposing the boundedness constraint provides highly nontrivial relations among all a_J's.

The best way to make use of this is to consider the contour deformation of the orthogonality relation, as in Figure 1.4. Assume that the function has a cut on the positive real axis starting at 1. Then, the blue contour can be deformed into the red contour. Boundedness at infinity allows us to drop the circle at infinity in the Figure 1.4. The only nontrivial ingredient is the evaluation of the integrand on the two sides of the cut. This is essentially the *discotinuity* of the function A,

$$\text{Disc}\left[A(w)\right] \equiv A(w + i\epsilon) - A(w - i\epsilon). \tag{1.34}$$

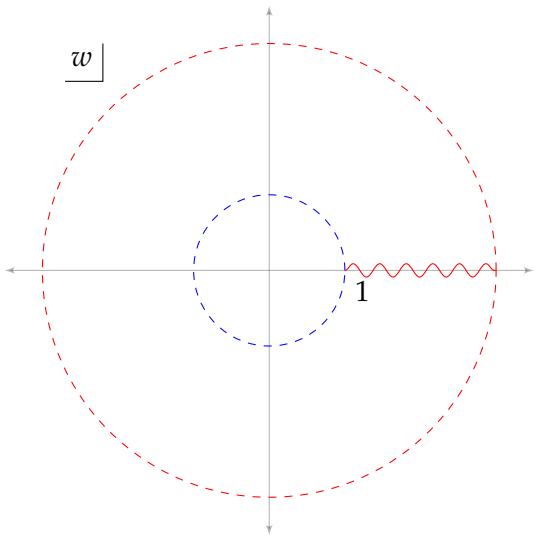

FIGURE 1.4: Contour deformation for the toy model in single variable complex analysis. Analyticity implies that the contour integral over the region between blue and red contours is zero.

In terms of this discotinuity, one can write the formula for a_J,

$$a_J = \frac{1}{2\pi i}\int_1^\infty \frac{dw}{w^{J+1}} \text{Disc}\left[A\left(w\right)\right]. \tag{1.35}$$

Note that, we have dropped the circle at infinity assuming the boundedness behavior. However, the power law w^J for $J = 0$ is already bounded in the large w limit. Thus, the Equation (1.35) does not constrain the coefficient a_0 and the Equation (1.35) is valid only for $\text{Re}\, J > 0$.

Let us consider a concrete example of a function $A = \log\left(1 - w\right)$. It's discotinuity across the cut is simply a constant, $-2\pi i$. This leads to an analytic formula for a_J,

$$a_J = -\frac{1}{J}, \text{Re}\left(J\right) > 0. \tag{1.36}$$

The analyticity in the variable J is best visualized as in the Figure 1.5.

The goal of Lorentzian inversion formula is to produce a formula that displays the analyticity in spin in conformal field theories. As we showed the analyticity in J, the example from the single variable complex analysis serves as a good toy model of the Lorentzian inversion formula.

Casimir equation

Our goal is to introduce the Lorentzian inversion formula in a simple setting of two dimensions. Most of the technical details are analogous in the generic dimensions. We list the

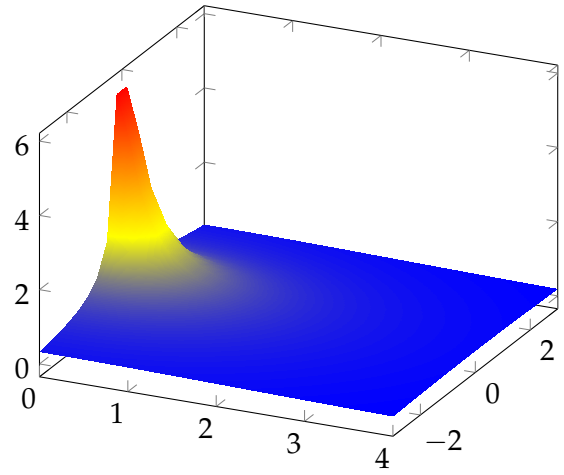

FIGURE 1.5: We plot the absolute value of a_J with respect to real and imaginary part of J. The orthogonality relation would only lead to the points corresponding to the positive integer values of J. However, analyticity in J suggests that a more appropriate way to think about a_J is the whole colored manifold, rather than just the isolated points.

analogies with the toy model discussed above in Table 1.1.

	Toy model	CFT
Orthogonal partial wave	w^J	$F_{h+i\nu,J}(u,v)$
Orthogonality relation	$\oint \frac{dw}{2\pi i} w^J w^{J'} = \delta_{-1-J,J'}$	$\int du\, dv\, \omega\, F_{h+i\nu,J}\, F_{h+i\nu',J} = (n_{\nu,\nu'}\delta_{\nu,\nu'} + \text{shadow})$
Coefficient function	a_J	$c_{\nu,J}$

TABLE 1.1: Analogy between the toy model and the conformal field theories

We summarize some useful properties of conformal blocks here [8]. The operator product expansion of two external operators can be arranged into families of operators such that all the operators are either a primary or its descendant

$$\phi \times \phi = \sum_O \lambda_O O. \tag{1.37}$$

This allows us to write the correlator as a sum over blocks with contribution coming from this primary

$$A(u,v) = \sum_O \lambda_O^2 G_O(u,v). \tag{1.38}$$

However, we can use conformal symmetry to characterize the blocks in a different way. Since they are functions of two variables u, v, or alternatively, of $z, \bar{z}$, they can be written as solutions to the differential equation, called the Casimir equation

$$C_2\, G_{\Delta,J} = c_2\, G_{\Delta,J}. \tag{1.39}$$

Here, we have used the notation that $a = (\Delta_2 - \Delta_1)/2$ and $b = (\Delta_3 - \Delta_4)/2$,

$$\begin{aligned} C_2 &= D_z + D_{\bar{z}} + (d-2)\frac{z\bar{z}}{z-\bar{z}}\left[(1-z)\partial_z - (1-\bar{z})\partial_{\bar{z}}\right], \\ c_2 &= \frac{1}{2}\left[J(J+d-2) + \Delta(\Delta-d)\right] \\ D_z &= z^2\partial_z(1-z)\partial_z - (a+b)z^2\partial_z - abz. \end{aligned} \tag{1.40}$$

For equal external scalars, these simplify due to $a = b = 0$. The solutions to this equation admit several symmetries which they inherit from the Casimir eigenvalue, which correspond to swapping two elements in the following tuples,

$$(J \leftrightarrow 2-d-J), \quad (\Delta \leftrightarrow d-\Delta), \quad (\Delta \leftrightarrow 1-J). \tag{1.41}$$

It can be seen that the differential equation in Equation (1.40) admits a power law solution in $z, \bar{z}$ if we strip out a pure power law as a leading behavior. Thus, we define a 'pure' solution to the differential equation as the solution with the boundary condition

$$\begin{aligned} g_{\text{pure},\Delta,J}(z,\bar{z}) &= z^{\frac{\Delta-J}{2}}\bar{z}^{\frac{\Delta+J}{2}}\,(1 + \text{subleading power laws}) \\ 0 &\ll z \ll \bar{z} \ll 1. \end{aligned} \tag{1.42}$$

Thus, there are 8 solutions to the differential equation of the form $g_{\text{pure},\Delta,J}$. Each of which can be obtained by doing the swaps in Equation (1.41) to the main pure solution $g_{\text{pure},\Delta,J}$. A general solution to the differential equation is a linear combination of these 8 solutions.

Two of the most important solutions are called the conformal block $G_{\Delta,J}$ and the conformal partial wave $F_{\Delta,J}$. Conformal block resums the contribution of the primary and its descendant, whereas partial wave is a linear combination of the conformal block and its 'shadow', $\Delta \to d - \Delta$. In two dimensions, the conformal block can be written in a closed form in terms of the hypergeometric functions

$$G_{\Delta,J} = \frac{1}{1+\delta_{J,0}}\left[k_{\Delta-J}(z)\,k_{\Delta+J}(\bar{z}) + k_{\Delta-J}(z)\,k_{\Delta+J}(\bar{z})\right]. \tag{1.43}$$

The two terms here are equivalent to g_{pure}. Here, we have defined

$$k_\beta^{a,b}(z) = z^{\beta/2}{}_2F_1\left(\begin{matrix}\beta/2+a, \beta/2+b \\ \beta\end{matrix}; z\right). \tag{1.44}$$

The conformal blocks in general dimensions can be written in a similar fashion. We use the shorthand g to denote g_{pure}.

$$G_{\Delta,J} = g_{\Delta,J} + \frac{\Gamma(J+d-2)\,\Gamma\left(-J-\frac{d-2}{2}\right)}{\Gamma\left(J+\frac{d-2}{2}\right)\Gamma(-J)} g_{\Delta,2-d-J}. \tag{1.45}$$

A more useful object for our purpose is the conformal partial wave, $F_{\Delta,J}$, as it admits nice orthogonality properties. It is defined as the unique linear combination of the conformal block, $G_{\Delta,J}$, and its shadow, $G_{d-\Delta,J}$, that is single valued in the Euclidean signature. Here, Euclidean signature means $\bar{z} = z^*$,

$$F_{\Delta,J} = \frac{1}{2}\left[G_{\Delta,J} + \frac{K_{d-\Delta,J}}{K_{\Delta,J}} G_{\Delta,J}\right]. \tag{1.46}$$

We suppress the definition of K and refer to [6], for the definitions of K.

Alternatively, these can be thought of as the solutions of the Sturm-Liouville problem defined by the Casimir equation. In particular, they admit an orthogonality property for the scaling dimensions $\Delta = d/2 + i\nu$ when ν is a real number [6],

$$I_{J,\nu,J',\nu'} = \int d^2z\, \mu(z,\bar{z})\, F_{\frac{d}{2}+i\nu,J} F_{\frac{d}{2}+i\nu',J'}. \tag{1.47}$$

Here, $I_{J,\nu,J',\nu'}$ acts as a delta function along with some normalization factor, n. One needs to use the properties of the Gegenbauer polynomials, the spherical polynomials in d dimensions, in order to show the orthogonality property.

It can be used to write the Euclidean inversion formula, as follows,

$$c_{\Delta,J} = n_{\Delta,J} \int d^2z\, \mu(z,\bar{z})\, F_{\Delta,J}(z,\bar{z})\, A(z,\bar{z}). \tag{1.48}$$

This can be rewritten in a useful way in terms of $\sigma = \sqrt{z\bar{z}}$ and $w = \exp(i \arccos(\xi))$. We remind that the angle

$$\xi = \frac{1}{2}\left(\sqrt{\frac{z}{\bar{z}}} + \sqrt{\frac{\bar{z}}{z}}\right), \tag{1.49}$$

and w is a phase factor associated with it. The integral over the Euclidean region can be recast as an integral over σ in $(0,1)$ and w on a unit circle. This is shown as the blue contour in the Figure 1.6. This is analogous to the orthogonality relation of the power laws in the toy model presented above. Now, we move to the contour deformation of this blue contour.

In order to do this, we need to discuss the behavior of the pure blocks when we analytically continue them away from the Euclidean region. This can be done by studying the analytic

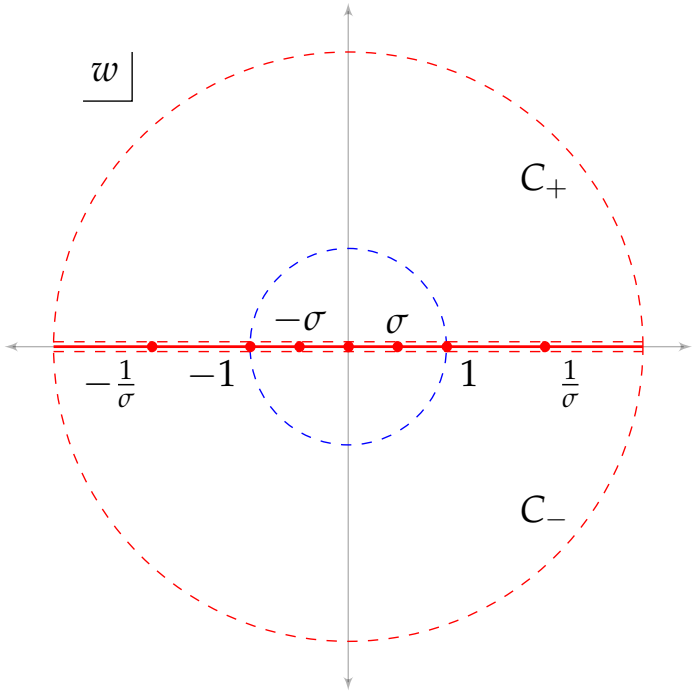

FIGURE 1.6: Contour deformation in the inversion formula. Blue contour corresponds to the Euclidean inversion formula. The cuts lie at the whole real axis for various branch points shown in red. Dashed red contour corresponds to the Lorentzian formula.

structure of the lightcone limit of these blocks, $0 \ll z \ll \bar{z}$ without taking any limit for $\bar{z}$. In this limit,

$$g_{\Delta,J} \to z^{\frac{\Delta-J}{2}} k_{\Delta+J}(\bar{z}). \tag{1.50}$$

Since the analytic continuations happen in $\bar{z}$ around 1, we would like to know the monodromy of this function around around 1. We note a useful identity,

$$\begin{aligned} {}_2F_1(a,b;c;z) = &\frac{\Gamma(c)(1-z)^{-a-b+c}\Gamma(a+b-c)}{\Gamma(a)\Gamma(b)} {}_2F_1(c-a,c-b;-a-b+c+1;1-z) \\ &+ \frac{\Gamma(c)\Gamma(-a-b+c)}{\Gamma(c-a)\Gamma(c-b)} {}_2F_1(a,b;a+b-c+1;1-z). \end{aligned} \tag{1.51}$$

This can be used to map the nontrivial monodromy at $\bar{z}=1$ to monodromy of the power laws at $\bar{z}=0$. As a result, one can show that, for some functions α and β of the operator data Δ, J

$$g^{\circlearrowleft}_{\Delta,J}(z,\bar{z}) = \alpha_{\Delta,J} g_{\Delta,J}(z,\bar{z}) + \beta_{\Delta,J} g_{1-J,1-\Delta}(z,\bar{z}). \tag{1.52}$$

Similar formula can be written for $g^{\circlearrowright}$. As any solution to the Casimir equation can be written as a linear combination of these $g_{\Delta,J}$, we can deduce the analytic continuation of any such solution along any path in the complex $\bar{z}$ plane.

Lorentzian formula

In the toy model, we used Cauchy formula to deform the contour to arrive at a novel representation of the coefficient function that displays the nice analyticity properties. We would like to use the same idea for the Euclidean inversion formula. We outline the key steps involved in the derivation.

We would like to analyze the cut structure of the correlation as well as the weight of the orthogonality relation. The branch points corresponding to those nontrivial analytic behaviors are plotted in Figure 1.6. For the purpose of this section, we will use the cross ratios $\rho, \bar{\rho}$:

$$\rho = \frac{1-\sqrt{1-z}}{1+\sqrt{1-z}}, \qquad \bar{\rho} = \frac{1-\sqrt{1-\bar{z}}}{1+\sqrt{1-\bar{z}}}. \tag{1.53}$$

In the Lorentzian setup, they become lightcone coordinates as shown in Figure 1.7. To make contact with toy model, it is useful to change the variables further to

$$\rho = \sigma w, \qquad \bar{\rho} = \frac{\sigma}{w}. \tag{1.54}$$

These are precisely the variables used in the Equation (3.117). We will use these variables to rewrite the Euclidean inversion formula Equation (3.117) as

$$c_{\Delta,J} = n_{\Delta,J} \int_0^1 \sigma \, d\sigma \oint \frac{dw}{i\,w} \, \mu(\rho,\bar{\rho}) \, A(\rho,\bar{\rho}) \, F_{\Delta,J}(\rho,\bar{\rho}) \,. \tag{1.55}$$

The contour for w is shown in red in the Figure 1.6. The branch points corresponds to the lightcones as well as the branch points of the weight function.

We would deform this contour in two ways. First, we split the integrand according to the part which diverges at $w = 0$ and the part which does not. Then, for the part that converges at $w = 0$, we deform the contour inward, whereas for the other part we deform the contour outward. This will result in two contours as shown in Figure 1.6. Individually, these contour contribute 0, since the function inside them is analytic.

Note that, we have also made an assumption to drop the arcs at ∞ and at 0. This is the assumption of boundedness in the Regge limit.

In practice, we do these contour manipulations using the ideas from representation theory of the conformal group. The most general solution to Casimir equation is represented by 8 functions with various weights $g_{\Delta,J}$. They can be simple understood as the values of Δ, J such that the Casimir eigenvalue $C_2 = \Delta(\Delta - d) + J(J + d - 2)$ remains unchanged. Again, the contour integral over $C_\pm$ is 0 for all of them.

The count of 8 can be achieved from the analytic continuation of the conformal partial waves, as follows. The conformal partial wave $F_{\Delta,J}$ is already a sum of two conformal blocks, $G_{\Delta,J}$

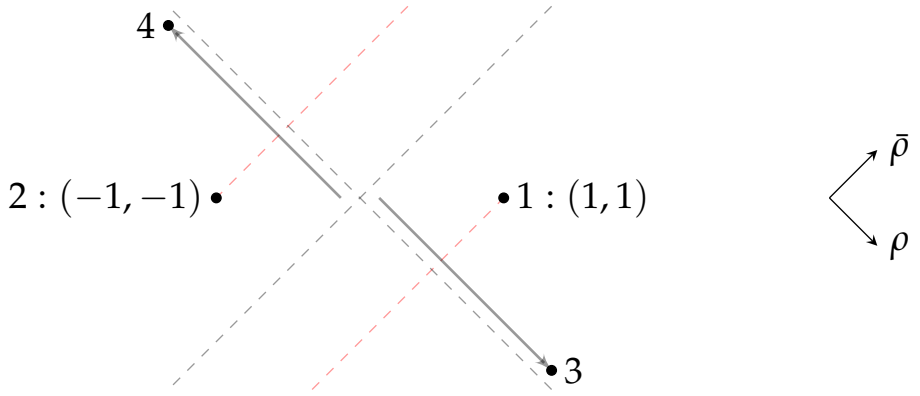

FIGURE 1.7: Regge limit configuration in the Lorentzian cylinder. The red lines correspond to the lightcones crossed by the points 3 and 4.

functions, as shown in Equation (3.113). Each of the blocks is a sum of two $g_{\Delta,J}$ functions. However, after analytic continuation, each of the $g_{\Delta,J}$ functions picks monodromy which contains yet another $g_{\Delta,J}$ function, as shown in Equation (1.52).

The analytic continuation can be done using these formulae. Since we have dropped the arcs at ∞, we arrive at only an integral over the real axis with small positive or negative imaginary part, for $C_{\pm}$. By splitting these integrals into intervals separated by the various branch points on the real axis $\sigma, 1, 1/\sigma, -\sigma, -1, -1/\sigma$, we get several integrals over the ranges such as $w \in (0, 1/\sigma)$. The cuts with $w > 0$ and $w < 0$ are treated separately. The contributions from the four regions with $w > 0$ combie to give a dDisc (A). The regions with negative w give rise to the integral that is the same as the positive w region, but with an extra factor of $(-1)^J$. The final formula for $c_{\Delta,J} = c^t_{\Delta,J} + c^u_{\Delta,J}$ in terms of $z, \bar{z}$ looks as follows [6],

$$c^t_{\Delta,J} = \frac{\kappa_{\Delta+J}}{4} \int_0^1 dz\, d\bar{z}\, \mu(z,\bar{z})\, G_{J+d-1,\Delta+1-d}(z,\bar{z})\, \text{dDisc}\left[A(z,\bar{z})\right]. \tag{1.56}$$

The main implication of the analyticity property is to show the rigidity in the spectrum of the conformal field theories. The claim of analyticity is not just an abstract mathematical statement, but can be seen at weak coupling theories as in Figure 1.8. Analyticity is also useful in justifying the large spin expansion of the CFT data. A priori, such an expansion of the CFT data is only asymptotic. However, analyticity in J shows that for $\text{Re}\, J > 1$, the coefficient function is analytic. Therefore, it can be expanded around $J = \infty$ to yield a convergent series [9]. This can be checked with the analysis from the numerical bootstrap as shown in the Figure 1.9.

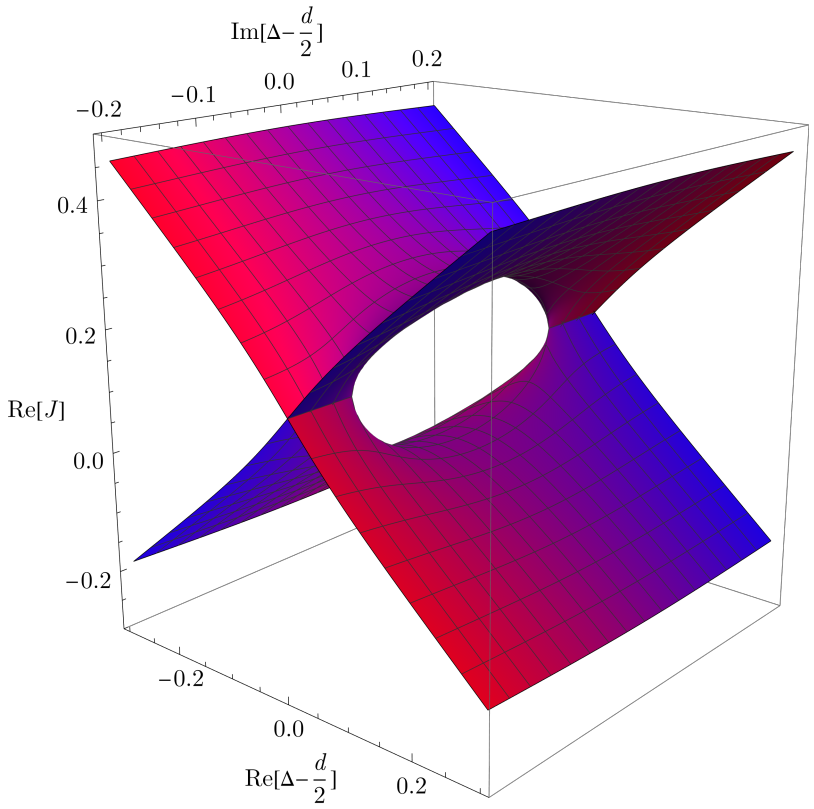

FIGURE 1.8: The figure taken from [10]. An $\mathbb{R}^3$ projection of the $\mathbb{C}^2$ Chew-Frautschi plot of the leading Regge trajectory in Wilson-Fisher theory near the intercept at $O(\epsilon^4)$. The imaginary part of J is shown by color, with negative values in blue and positive values in red. Even though the two branches appear to intersect, they do not – in order to intersect in $\mathbb{C}^2$, they need to intersect in this $\mathbb{R}^3$ projection and also have the same color. The plot is made at $\epsilon = 0.3$.

1.5 Plan of the thesis

The discussion of the analyticity in spin sets the stage for the thesis. The goal of the thesis is to consider two aspects of Regge theory.

Optical theorem in AdS

In recent years it has been shown that powerful analytical results for scattering amplitudes in quantum field theory, namely the Froissart-Gribov formula and dispersion relations, have equally powerful CFT analogues in the Lorentzian inversion formula [6, 11–14] and the two-variable CFT dispersion relation [15, 16]. Dispersion relations reconstruct a scattering amplitude from the discontinuity of the amplitude, while the Froissart-Gribov formula extracts the partial wave coefficients from the discontinuity and makes their analyticity in spin manifest. The utility of these methods as computational tools for scattering amplitudes stems from the fact that the discontinuity of an amplitude (or that of its integrand) in perturbation theory is

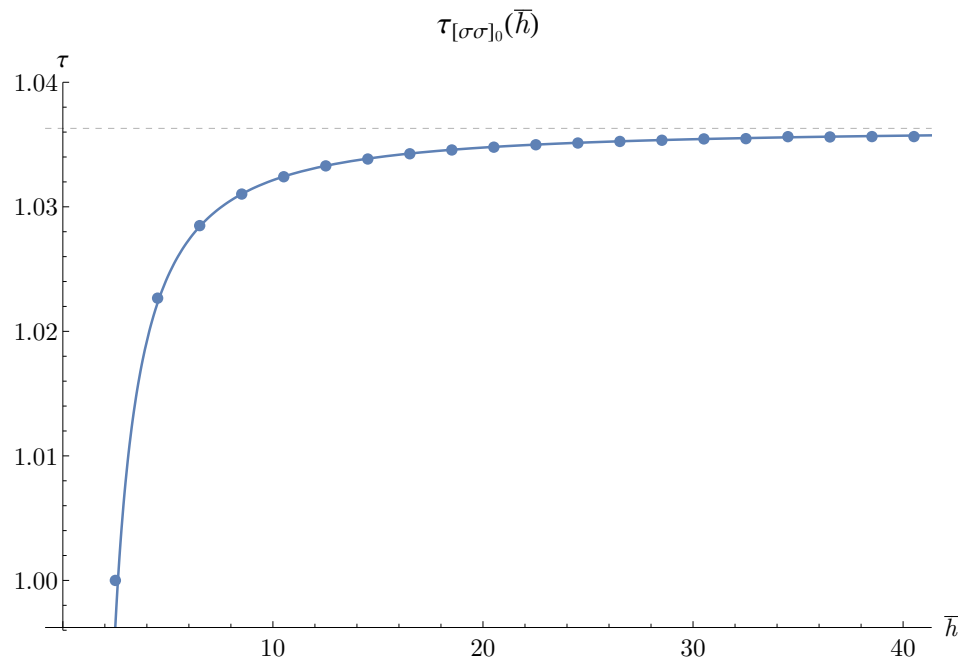

FIGURE 1.9: Results from the numerical analysis [9]. It depicts the spectrum of operators in the operator product expansion of $\sigma \times \sigma$. To facilitate the comparison with analytic result, the vertical axis plots $\tau = \Delta - J$, 'twist' and $\bar{h} = \frac{\Delta+J}{2}$. Notice the present of stress-tensor with $\Delta = 3, \tau = 1$. The continuous line is the extrapolation of the large spin perturbation theory around $J = \infty$. While the spin $J = \bar{h} - h$ is as small as 2, we find a remarkable agreement with the numerics.

determined in terms of lower-loop data by the optical theorem, which in turn is a direct consequence of unitarity. The CFT analogue of the discontinuities of amplitudes, which contain the dispersive data and are of central importance in the aforementioned analytical results, is the double discontinuity (dDisc) of CFT four-point functions. The Lorentzian inversion formula computes OPE data (anomalous dimensions and OPE coefficients) from the dDisc of four-point functions and establishes the analyticity in spin of OPE data. The CFT dispersion relation, much like its QFT inspiration, directly reconstructs the full correlator from the dDisc. There also exist simpler single-variable dispersion relations in terms of a single discontinuity (Disc) of the correlation function that determine only the OPE coefficients while the anomalous dimensions are required as inputs [17].

The unitarity based methods to compute amplitudes inspire the development of similar unitarity methods for CFT, in particular, for the dDisc of four-point functions one gains a loop or leg order for free. It was first noticed in large spin expansions [18–20] and later understood more generally in terms of the Lorentzian inversion formula that OPE data at one-loop can be obtained from tree-level data [21, 22]. Generically, in perturbative CFT calculations the dDisc at a given order only depends on OPE data from lower order or lower-point correlators. More recently, in the context of the AdS/CFT correspondence [3, 23, 24], these unitarity methods for CFT have been related to cutting rules for computing the dDisc of one-loop

Witten diagrams [25] from tree-level diagrams [26–28]. See also the earlier work of [29].

However, so far we have been missing a direct adaptation of the optical theorem to CFT correlation functions. More concretely, we lacked the ability to express the dDisc of a perturbative correlator, at a given order in the perturbative parameter, in terms of lower order correlators, without the detour via the OPE data and without making explicit reference to AdS Witten diagrams. In the first chapter, we provide a direct CFT derivation of such unitarity relations. In particular, we present an optical theorem for 1-loop four-point functions wherein the dDisc is fixed in terms of single discontinuities of lower-loop correlators.

Conformal multi-Regge theory

Constraints from the bootstrap analysis of the four point correlation functions are known to be powerful in obtaining remarkable accurate and precise physical data such as critical exponents of the theories appearing in the nature. The main idea is that any function of two cross ratios can not be a valid correlation function.

This suggests that there might be more constraints in the consistency of higher point correlation functions. Since higher point functions can be decomposed into correlation functions with fewer number of points, these constraints are implicitly present in the four point bootstrap analysis. However, we might need to explore *infinitely* many four point functions to probe them. For instance, a single five point correlation function can be decomposed into infinitely many four point functions. This calls for a careful study of such high point functions.

In the third chapter, our goal is to initiate such a program. The goal is to introduce a useful definition of Regge limit for five point correlation functions in conformal field theories. First, we review the relevant literature from S-matrix theory. In particular, we discuss the multi-Regge limit of five point string theory amplitudes.

Inspired by this analysis, we propose the generalization to the conformal field theory. Since the natural analogue of the Mandelstam invariants is the Mellin space, we discuss this generalization mainly in Mellin space. We also show its relation to position space and the corresponding spacetime structure.

Furthermore, we comment on the relation between the Reggeized correlator and the CFT data such as the OPE coefficients and the scaling dimensions of the operators on the leading Regge trajectory. In passing, we also discuss several interesting kinematical aspects of higher point correlation functions. We expect them to be useful in generalizing the discussion of the inversion formula and the dispersion relation to the higher point functions.

Now, we turn to the analysis of the optical theorem in AdS.

Chapter 2

Optical theorem in AdS

2.1 Introduction

Let us briefly describe the logic that underlies the perturbative CFT optical theorem. Throughout this chapter we will consider the correlator

$$A(y_i) = \langle \mathcal{O}_1(y_1)\mathcal{O}_2(y_2)\mathcal{O}_3(y_3)\mathcal{O}_4(y_4)\rangle \,. \tag{2.1}$$

We begin by expanding the dDisc of this correlator in t-channel conformal blocks. We may do this by expanding in conformal partial waves and then projecting out the contribution of the exchange of the shadow operator $\tilde{\mathcal{O}}$. The advantage of this procedure is that when writing the partial waves as an integrated product of three-points functions, the dDisc operation factorizes as a product of discontinuities,

$$\text{dDisc}_t A(y_i) = -\frac{1}{2}\sum_{\mathcal{O}} \int dy dy' \ \text{Disc}_{23}\langle \mathcal{O}_2\mathcal{O}_3\mathcal{O}(y)\rangle \langle \tilde{\mathcal{O}}(y)\tilde{\mathcal{O}}(y')\rangle \ \text{Disc}_{14}\langle \mathcal{O}_1\mathcal{O}_4\mathcal{O}(y')\rangle\Big|_{\mathcal{O}}\,, \tag{2.2}$$

where we use the shorthand notation $d^d y \equiv dy$. Notice that the sum runs over all operators in the theory. We give the precise definitions of the double and single discontinuities of the correlator in section 2.2.

Next, let us assume that the correlator admits an expansion in a small parameter around mean field theory (MFT). The example we have in mind is the $1/N^2$ expansion,

$$A = A_{\text{MFT}} + \frac{1}{N^2}A_{\text{tree}} + \frac{1}{N^4}A_{\text{1-loop}} + \cdots \,. \tag{2.3}$$

We can then separate the sum over intermediate operators $\mathcal{O}$ into single-, double-, and higher-trace operators, and rewrite the multi-trace contributions as higher-point functions of single-trace operators. The contribution of single-trace operators to the t-channel expansion

of dDisc in (2.2) is left unchanged and is still given in terms of discontinuities of three-point functions

$$\text{dDisc}_t A(y_i)\Big|_{\text{s.t.}} = -\frac{1}{2}\sum_{\mathcal{O}\in s.t.}\int dy dy'\ \text{Disc}_{23}\langle\mathcal{O}_2\mathcal{O}_3\mathcal{O}(y)\rangle\langle\tilde{\mathcal{O}}(y)\tilde{\mathcal{O}}(y')\rangle\,\text{Disc}_{14}\langle\mathcal{O}_1\mathcal{O}_4\mathcal{O}(y')\rangle\Big|_{\mathcal{O}}\,. \tag{2.4}$$

Here no simplifications occur, however this contribution is already simple as loop corrections come from corrections to the three-point functions of single-trace operators.

The essential simplification that we call the perturbative optical theorem arises for the contributions of double-trace operators to (2.2), which are now expressed in terms of discontinuities of four-point functions of single-trace operators

$$\text{dDisc}_t A_{1-\text{loop}}(y_i)\Big|_{\text{d.t.}} = -\frac{1}{2}\sum_{\substack{\mathcal{O}_5,\mathcal{O}_6\\ \in\, s.t.}}\int dy_5 dy_6\ \text{Disc}_{23}\, A^{3652}_{\text{tree}}(y_k)\ \mathbf{S}_5\mathbf{S}_6\,\text{Disc}_{14}\, A^{1564}_{\text{tree}}(y_k)\Big|_{[\mathcal{O}_5\mathcal{O}_6]}\,.. \tag{2.5}$$

Here and henceforth, we shall use the notation $A^{abcd}(y_k) = \langle\mathcal{O}_a\mathcal{O}_b\mathcal{O}_c\mathcal{O}_d\rangle$ to denote the correlator of a set of operators other than $\langle\mathcal{O}_1\mathcal{O}_2\mathcal{O}_3\mathcal{O}_4\rangle$, which we denote simply as $A(y_i)$. $\mathbf{S}_5\mathbf{S}_6 A^{1564}$ is defined as the shadow transform of A^{1564} with respect to the operators $\mathcal{O}_5$ and $\mathcal{O}_6$. The operators $\mathcal{O}_5$ and $\mathcal{O}_6$ are summed over all single-trace operators for which the tree-level correlators exist. These may have spin, in which case the indices are contracted between the two tree-level correlators. Importantly, in this case dDisc is of order $1/N^4$ and can be computed from the product of the discontinuities of tree-level four-point functions, each of order $1/N^2$.

Together equations (2.4) and (2.5) compute the full double discontinuity at one-loop in large N CFTs, since the contributions from higher traces will start at higher loops. Their analogue is of course the optical theorem for amplitudes which computes discontinuities of one-loop amplitudes in terms of two- and one-line cuts. Note that although we use the notation A_{tree} and $A_{\text{1-loop}}$, these refer to conformal correlation functions and in general are not Witten diagrams. The notation with the terms "one-loop" and "tree" for the correlators is used only because we always refer to a perturbative expansion. The result is valid for CFTs with an expansion in a small parameter around MFT. The fact that it naturally handles cuts of spinning particles gives an advantage over previous CFT unitarity methods that work in terms of OPE data.

In the second part of the chapter, we employ the perturbative CFT optical theorem in the context of the AdS/CFT correspondence [3, 23, 24] to study high-energy scattering of strings in AdS, which is governed by the CFT Regge limit [30, 31]. This is illustrated in figure 2.1. High-energy string scattering in flat space has been of interest for a long time, both in the

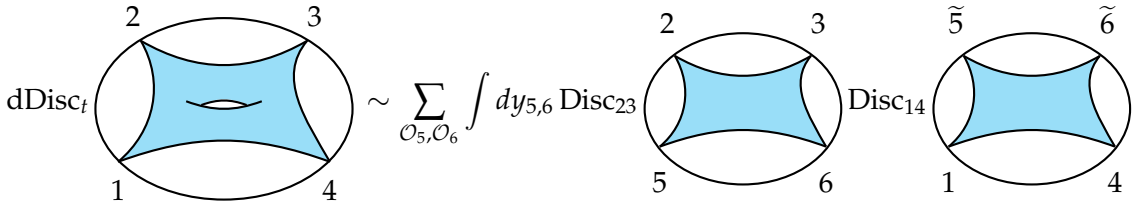

FIGURE 2.1: In the Regge limit the dDisc of the genus one closed string amplitude in AdS is given by the perturbative CFT optical theorem in terms of genus zero amplitudes.

fixed angle case [32, 33] and in the fixed momentum transfer Regge regime [34–36]. This second set of works studied the effects of the finite string size on the exponentiation of the phase shift (eikonalization) in the Regge limit. In particular, it was shown that the amplitudes indeed eikonalize provided we allow the phase shift to become an operator acting on the string Hilbert space, whose matrix elements account for the possibility of the external particles becoming intermediate excited string states, known as tidal excitations. The phase shift $\delta(s,b)$, which depends on the Mandelstam s and on the impact parameter b, is obtained by Fourier transforming the amplitude with respect to momentum transfer in the directions transverse to the scattering plane. This gives a multiplicative optical theorem of the form

$$\mathrm{Im}\delta_{\text{1-loop}}(s,b) = \frac{1}{2}\sum_{\substack{m_5,\rho_5,\epsilon_5\\ m_6,\rho_6,\epsilon_6}} \delta^{3652}_{\text{tree}}(s,-b)^*\,\delta^{1564}_{\text{tree}}(s,b)\,, \tag{2.6}$$

where the sum is over all possible exchanged particles, characterized by their mass m_i and Little group representation ρ_i, and their polarization tensors ϵ_i. In [35] the one-loop amplitude for four-graviton scattering in type IIB string theory was presented in a particularly nice form, where the tidal excitations, which constitute a complicated sum in (2.6), are packaged into a single explicit scalar function, the so-called vertex function.

To study the analogous process in AdS we derive an AdS/CFT analogue of (2.6) by transforming the correlators in the CFT optical theorem (2.5) to AdS impact parameter space [30, 31]. This gives the following multiplicative optical theorem for CFTs

$$-\mathrm{Re}\mathcal{B}_{\text{1-loop}}(p,\bar{p})\Big|_{\text{d.t.}} = \frac{1}{2}\sum_{\mathcal{O}_5,\mathcal{O}_6\in s.t.} \mathcal{B}^{3652}_{\text{tree}}(-\bar{p},-p)^*\,\mathcal{B}^{1564}_{\text{tree}}(p,\bar{p})\Big|_{[\mathcal{O}_5\mathcal{O}_6]}\,. \tag{2.7}$$

Here $\mathcal{B}$ denotes the impact parameter transform of A. These transforms depend on two cross ratios S and L, respectively interpreted as the square of the energy and as the impact parameter of the AdS scattering process, that can be expressed in terms of two d-dimensional vectors p and $\bar{p}$, as will be detailed below. When $\mathcal{O}_5$ or $\mathcal{O}_6$ have spin, $\mathcal{B}$ has tensor structures that depend on p and $\bar{p}$. Equations (2.7) and (2.6) are related through the flat space limit for the impact parameter representation, where the radius of AdS is sent to infinity and where

$\mathcal{B}(p,\bar{p})$ is mapped to $i\delta(s,b)$. In this way, each of the infinite number of tree-level correlators with spinning particles 5 and 6 that appear on the right hand side of (2.7) is partially fixed by the corresponding flat space phase shift. Moreover, we will be able to efficiently describe the summed result in terms of an AdS vertex function, which is in turn constrained by the one-loop flat space vertex function, as constructed for example for type IIB strings in [35].

For neutral scalar operators of dimension four in $d = 4$, the four-point function considered here is dual to the scattering of four dilatons in the bulk of AdS_5. There are two expansion parameters that we need to consider, the loop order parameter $1/N^2$, and the 't Hooft coupling λ. The large λ limit is given by supergravity in AdS. In this limit the tree-level four-point function is dominated by graviton exchange [30, 31] and beyond tree-level one can safely resum the $1/N$ expansion by exponentiating the single graviton exchange [37, 38]. For finite λ, string effects are included at tree-level via Pomeron exchange [39] and can be described using conformal Regge theory [4, 40]. A very non-trivial question we address in this chapter is the inclusion of string effects beyond tree-level.

To account for such effects in the Regge limit, the earlier works [40–42] conjectured the exponentiation of the tree-level Pomeron phase shift, assuming stringy tidal excitations to be negligible [43]. More recently [44], the loop effects of Pomeron exchange were systematically taken into account from the CFT side in the AdS high-energy limit $S \gg \lambda \gg 1$, with the crucial use of CFT unitarity to obtain higher-loop amplitudes from the lower-loop ones. This work also pointed out the suppression of tidal excitations in the supergravity limit $\lambda \gg 1$, in agreement with [40–42]. In the present work, we take finite λ (or α') and include all tidal or stringy corrections. This is made possible because the perturbative CFT optical theorem is able to describe cuts involving spinning operators, so we can take into account intermediate massive string excitations that are exchanged in the t-channel.

This chapter has the following structure. In section 2.2 we first motivate how (2.2) for double-trace operators leads to the perturbative CFT optical theorem (2.5) using the technique of "conglomeration" [29], and then give a detailed derivation of (2.5) using tools from harmonic analysis of the conformal group. Then in section 2.3 we review some important ideas from flat space scattering, including impact parameter space, unitarity cuts and the vertex function, both to guide the AdS version and to serve as a target for the flat space limit. We subsequently move to the holographic case in section 2.4, where we transform the correlator to CFT impact parameter space to write a multiplicative optical theorem for phase shifts. We use conformal Regge theory in the case of arbitrary spinning operators leading to the derivation of the AdS vertex function. In section 2.5 we recover the results for the one-loop correlator in the large λ limit [44] and also derive new t-channel constraints on CFT data at finite λ. We give the details of the flat space limit prescription in section 2.6, and consider the

specific four-dilaton amplitude of type IIB strings in section 2.7, constraining several spinning tree-level correlators of the dual $\mathcal{N} = 4$ SYM theory. We conclude and briefly discuss some generalizations and applications of our work in section 2.8. Many technical details and additional considerations about spinning amplitudes are relegated to the appendices.

2.2 Perturbative CFT optical theorem

In this section we will give a derivation for the perturbative CFT optical theorem in (2.5) using results from harmonic analysis of the conformal group following [11], but first let us motivate (2.5) and (2.4) using the conglomeration of operators [29].

Unitarity in CFT can be formulated as completeness of the set of states corresponding to local operators

$$1 = \sum_{\mathcal{O}} |\mathcal{O}| \,. \tag{2.8}$$

The right hand side is a sum over projectors associated to a primary operator $\mathcal{O}$. Such projectors can be formulated in terms of a conformally invariant pairing known as the shadow integral [45, 46]

$$|\mathcal{O}| = \int dy \, |\mathcal{O}(y)\rangle \langle \mathbf{S}[\mathcal{O}](y)| \Big|_{\mathcal{O}} \,, \tag{2.9}$$

which defines the projector to the conformal family with primary operator $\mathcal{O}$, automatically taking into account the contribution of descendants of $\mathcal{O}$. Here we used the shadow transform, defined by

$$\mathbf{S}[\mathcal{O}](y) = \frac{1}{N_{\mathcal{O}}} \int dx \, \langle \widetilde{\mathcal{O}}(y) \widetilde{\mathcal{O}}^{\dagger}(x) \rangle \mathcal{O}(x) \,, \tag{2.10}$$

with an index contraction implied for spinning operators. We normalize the two-point functions to unity and

$$N_{\mathcal{O}} = \pi^d (\Delta - 1)_{|\rho|} (d - \Delta - 1)_{|\rho|} \frac{\Gamma\left(\Delta - \frac{d}{2}\right) \Gamma\left(\frac{d}{2} - \Delta\right)}{\Gamma(d - \Delta + |\rho|) \Gamma(\Delta + |\rho|)} \,. \tag{2.11}$$

Note that with this normalization of $\mathbf{S}[\mathcal{O}]$, $\mathbf{S}^2$ is $1/N_{\mathcal{O}}$ times the identity map. $|\rho|$ is the number of indices of the operator $\mathcal{O}$. The shadow transform is a map from the operator $\mathcal{O}$ to $\widetilde{\mathcal{O}}$, where $\widetilde{\mathcal{O}}$ is in the representation labeled by $(\widetilde{\Delta} = d - \Delta, \rho)$. $\mathcal{O}^{\dagger}$ is an operator with scaling dimension Δ but transforming in the dual $SO(d)$ representation ρ^*.

Inserting the projector (2.9) into a four-point function, one finds the contribution of the t-channel conformal partial wave $\Psi_{\mathcal{O}}$ to the four-point function

$$\langle \mathcal{O}_2 \mathcal{O}_3 | \mathcal{O} | \mathcal{O}_1 \mathcal{O}_4 \rangle \propto \Psi_{\mathcal{O}}^{3214} \,. \tag{2.12}$$

The conformal partial wave is a linear combination of the conformal blocks for exchange of $\mathcal{O}$ and its shadow $\widetilde{\mathcal{O}}$. This explains the notation $|_{\mathcal{O}}$ adopted in (2.9), since we need to project onto the contribution from $\mathcal{O}$ and discard that of $\widetilde{\mathcal{O}}$.

In the large N expansion of CFTs, there exists a complete basis of states spanned by the multi-trace operators. In a one-loop four-point function of single trace operators, with an expansion as shown in (2.3), only single- and double-trace operators appear

$$A(y_i) = \sum_{\mathcal{O}\in\mathcal{O}_{\text{s.t.}},\,\mathcal{O}_{\text{d.t.}}} \langle \mathcal{O}_2\mathcal{O}_3|\mathcal{O}|\mathcal{O}_1\mathcal{O}_4\rangle\,. \tag{2.13}$$

The right hand side involves three-point functions with single- and double-trace operators. The double-trace operators are composite operators of the schematic form

$$[\mathcal{O}_5\mathcal{O}_6]_{n,\ell} \sim \mathcal{O}_5\partial^{2n}\partial_{\mu_1}\ldots\partial_{\mu_\ell}\mathcal{O}_6\,, \tag{2.14}$$

and have conformal dimensions

$$\Delta_5 + \Delta_6 + 2n + \ell + O\big(1/N^2\big)\,. \tag{2.15}$$

Below we often omit the n and ℓ labels when talking about a family of double-trace operators. To obtain an optical theorem resembling the one in flat space, we would like to project onto states created by products of single-trace operators $|\mathcal{O}_5(y_5)\mathcal{O}_6(y_6)\rangle$, rather than the often infinite sum over n and ℓ of the double-trace operators $|[\mathcal{O}_5\mathcal{O}_6]_{n,\ell}(y)\rangle$. This can be achieved by relating these two states using the technique of conglomeration [29], which amounts to using the formula

$$|[\mathcal{O}_5\mathcal{O}_6]_{n,\ell}(y)\rangle = \int dy_5 dy_6\, |\mathcal{O}_5(y_5)\mathcal{O}_6(y_6)\rangle\langle \mathbf{S}[\mathcal{O}_5](y_5)\mathbf{S}[\mathcal{O}_6](y_6)[\mathcal{O}_5\mathcal{O}_6]_{n,\ell}(y)\rangle\,. \tag{2.16}$$

This shows that we can define a projector onto double-trace operators in terms of a double shadow integral

$$|\mathcal{O}_5\mathcal{O}_6| = \int dy_5 dy_6\, |\mathcal{O}_5(y_5)\mathcal{O}_6(y_6)\rangle\langle \mathbf{S}[\mathcal{O}_5](y_5)\mathbf{S}[\mathcal{O}_6](y_6)|\Big|_{[\mathcal{O}_5\mathcal{O}_6]}\,, \tag{2.17}$$

and thus (2.16) is just the projection

$$|\mathcal{O}_5\mathcal{O}_6|[\mathcal{O}_5\mathcal{O}_6]_{n,\ell}\rangle = |[\mathcal{O}_5\mathcal{O}_6]_{n,\ell}\rangle\,. \tag{2.18}$$

The notation $|_{[\mathcal{O}_5\mathcal{O}_6]}$ means that we project onto the contributions from the double-traces of the physical operators and discard contributions coming from the shadows, which, as we will discuss below, can be generated when using this bi-local projector. Using this projector,

together with (2.9) for the single-traces, we can write the one-loop four-point function in (2.13) as

$$A(y_i) = \sum_{\mathcal{O}\in\mathcal{O}_{\text{s.t.}}} \langle \mathcal{O}_2\mathcal{O}_3|\mathcal{O}|\mathcal{O}_1\mathcal{O}_4\rangle + \sum_{\mathcal{O}_5,\mathcal{O}_6\in\mathcal{O}_{\text{s.t.}}} \langle \mathcal{O}_2\mathcal{O}_3|\mathcal{O}_5\mathcal{O}_6|\mathcal{O}_1\mathcal{O}_4\rangle \,. \tag{2.19}$$

The important step in (2.19) is that we replaced the sum over double-trace operators with a double sum over the corresponding single-trace operators. This is already close to the single- and double-line cuts that appear in the flat-space optical theorem at one-loop.

The main difference of (2.19) with the flat space optical theorem is that in flat space one needs to sum only over cuts of internal lines, while if we express (2.19) in terms of Witten diagrams it would also contain contributions from external line cuts. Another way to see this is that even the disconnected correlator for $\mathcal{O}_1 = \mathcal{O}_2$ and $\mathcal{O}_4 = \mathcal{O}_3$ has contributions of the form

$$\langle \mathcal{O}_2\mathcal{O}_3|\mathcal{O}_2\mathcal{O}_3|\mathcal{O}_2\mathcal{O}_3\rangle \,, \tag{2.20}$$

while internal double line cuts in a diagram can only appear starting at one-loop. This problem is resolved by acting on (2.19) with the double discontinuity. This procedure shifts the contributions of external double-traces to a higher order in $\frac{1}{N}$. In the context of (2.5) that we propose for conformal correlation functions (and not for Witten diagrams specifically), taking the double discontinuity suppresses the contributions of the external double-trace operators $[\mathcal{O}_2\mathcal{O}_3]$ and $[\mathcal{O}_1\mathcal{O}_4]$. We will expand on this further in section 2.2.3.

We will make the definitions of the double discontinuity and the single discontinuities more precise in sec. 2.2.3 but for now, let us mention that the double discontinuity can be written in the following factorized form

$$\text{dDisc}_t A(y_i) = -\frac{1}{2}\,\text{Disc}_{14}\,\text{Disc}_{23}\,A(y_i)\,. \tag{2.21}$$

The discontinuities on the right hand side are defined in terms of analytic continuations of the distances y_{14}^2 and y_{23}^2 to the negative real axis,

$$\text{Disc}_{jk}\,A(y_i) = A(y_i)|_{y_{jk}^2\to y_{jk}^2 e^{\pi i}} - A(y_i)|_{y_{jk}^2\to y_{jk}^2 e^{-\pi i}}\,. \tag{2.22}$$

Note that each term in this discontinuity is defined through a Wick rotation of the two coordinates y_j and y_k while we hold the other points Euclidean (or spacelike separated).

The result (2.4) for the exchange of single-trace operators comes from the first term on the right hand side of (2.19) with the double discontinuity taken on both sides. This are simply the single-trace terms in the conformal block expansion of the correlator. For the more interesting result (2.5), let us use the explicit form of the projector (2.17) in the second term on the

right hand side of (2.19). This gives

$$\sum_{\mathcal{O}_5,\mathcal{O}_6\in\mathcal{O}_{\text{s.t.}}}\int dy_5 dy_6\,\langle\mathcal{O}_3\mathcal{O}_2|\mathcal{O}_5(y_5)\mathcal{O}_6(y_6)\rangle\langle\mathbf{S}[\mathcal{O}_5](y_5)\mathbf{S}[\mathcal{O}_6](y_6)|\mathcal{O}_1\mathcal{O}_4\rangle|\Big|_{[\mathcal{O}_5\mathcal{O}_6]}\,. \tag{2.23}$$

We can now take the double discontinuity on the left hand side using (2.21), while on the right hand side we can take Disc_{23} on the first correlator and Disc_{14} on the second. This gives the result (2.5). In the next subsections we provide a detailed proof of this perturbative CFT optical theorem using results from harmonic analysis of the conformal group [11].

2.2.1 Conformal blocks and partial waves

A conformal correlator can be expanded in s-channel conformal blocks as follows,

$$A(y_i)=T^{1234}(y_i)\mathcal{A}^{1234}(z,\bar{z})\,,\quad \mathcal{A}^{1234}(z,\bar{z})=\sum_{\mathcal{O}}c_{12\mathcal{O}}c_{34\mathcal{O}}\,g^{1234}_{\mathcal{O}}(z,\bar{z})\,, \tag{2.24}$$

with the kinematical prefactor

$$T^{1234}(y_i)=\frac{1}{y_{12}^{\Delta_1+\Delta_2}y_{34}^{\Delta_3+\Delta_4}}\left(\frac{y_{14}^2}{y_{24}^2}\right)^{\frac{\Delta_{21}}{2}}\left(\frac{y_{14}^2}{y_{13}^2}\right)^{\frac{\Delta_{34}}{2}}\,, \tag{2.25}$$

where $\Delta_{ij}=\Delta_i-\Delta_j$ and the cross-ratios are defined as

$$z\bar{z}=\frac{y_{12}^2y_{34}^2}{y_{13}^2y_{24}^2},\qquad (1-z)(1-\bar{z})=\frac{y_{14}^2y_{23}^2}{y_{13}^2y_{24}^2}\,. \tag{2.26}$$

The t-channel OPE is obtained by exchanging the labels 1 and 3, thus

$$A(y_i)=T^{3214}(y_i)\mathcal{A}^{3214}(z,\bar{z})\,,\quad \mathcal{A}^{3214}(z,\bar{z})=\sum_{\mathcal{O}}c_{32\mathcal{O}}c_{14\mathcal{O}}\,g^{3214}_{\mathcal{O}}(1-z,1-\bar{z})\,, \tag{2.27}$$

Note that although $A^{jklm}(y_i)$ is invariant under permutations of the $jklm$ labels, the ordering of the labels is meaningful in $\mathcal{A}^{jklm}(z,\bar{z})$ because of the pre-factor $T^{jklm}(y_i)$. For the conformal blocks we will also use the notation

$$G^{1234}_{\mathcal{O}}(y_k)=T^{1234}(y_k)\,g^{1234}_{\mathcal{O}}(z,\bar{z})\,, \tag{2.28}$$

and similarly for t-channel blocks.

In order to perform harmonic analysis of the conformal group, one expands the four-point function not in conformal blocks but in conformal partial waves of principal series representations $\Delta=\frac{d}{2}+i\nu$, $\nu\in\mathbb{R}^+$ [47]. A conformal correlator can be expanded in terms of

s-channel conformal partial waves as follows

$$A(y_i) = \sum_{\rho} \int_{\frac{d}{2}}^{\frac{d}{2}+i\infty} \frac{d\Delta}{2\pi i}\, I_{ab}^{1234}(\Delta,\rho)\Psi_{\mathcal{O}}^{1234(ab)}(y_i) + \text{discrete}, \tag{2.29}$$

where the operator $\mathcal{O}$ is labeled by the scaling dimension Δ and a finite dimensional irreducible representation ρ of $SO(d)$, which we take to be bosonic. I_{ab} is the spectral function carrying the OPE data, and it can be extracted from the correlator using the Euclidean inversion formula. We will assume that there are no discrete contributions. The conformal partial waves are defined as a pairing of three-point structures

$$\Psi_{\mathcal{O}}^{1234(ab)}(y_i) = \int dy\, \langle \mathcal{O}_1\mathcal{O}_2\mathcal{O}(y)\rangle^{(a)} \langle \mathcal{O}_3\mathcal{O}_4\widetilde{\mathcal{O}}^{\dagger}(y)\rangle^{(b)}\,, \tag{2.30}$$

where a and b label different tensor structures in case the external operators have spin. The conformal partial wave $\Psi_{\mathcal{O}}^{1234(ab)}$ is related to the conformal block $G_{\mathcal{O}}^{1234(ab)}$ and to the block for the exchange of the shadow by

$$\Psi_{\mathcal{O}}^{1234(ab)} = S(\mathcal{O}_3\mathcal{O}_4[\widetilde{\mathcal{O}}^{\dagger}])^b{}_c\, G_{\mathcal{O}}^{1234(ac)} + S(\mathcal{O}_1\mathcal{O}_2[\mathcal{O}])^a{}_c\, G_{\widetilde{\mathcal{O}}}^{1234(cb)}\,. \tag{2.31}$$

The matrices $S(\mathcal{O}_i\mathcal{O}_j[\mathcal{O}_k])^a{}_b$ are part of the action of the shadow transform (2.10) on three-point functions,

$$\langle \mathcal{O}_1\mathcal{O}_2\mathbf{S}[\mathcal{O}_3]\rangle^{(a)} = \frac{S(\mathcal{O}_1\mathcal{O}_2[\mathcal{O}_3])^a{}_b}{N_{\mathcal{O}_3}} \langle \mathcal{O}_1\mathcal{O}_2\widetilde{\mathcal{O}}_3\rangle^{(b)}\,, \tag{2.32}$$

with $N_{\mathcal{O}_3}$ as defined in (2.11). Acting with the shadow transform on an operator within a three-point structure also rotates into a different basis of tensor structures. The shadow coefficients/matrices S act as a map between the two bases. Note that the inverse of $S(\mathcal{O}_1\mathcal{O}_2[\mathcal{O}_3])^a{}_b$ is $(1/N_{\mathcal{O}_3})S(\mathcal{O}_1\mathcal{O}_2[\widetilde{\mathcal{O}}_3])^a{}_b$.

The usual conformal block expansion (2.24) can be obtained from (2.29) by inserting (2.31) and using the identity

$$I_{ab}(\Delta,\rho)\, S(\mathcal{O}_3\mathcal{O}_4[\widetilde{\mathcal{O}}^{\dagger}])^b{}_c = I_{bc}\big(\widetilde{\Delta},\rho\big)\, S(\mathcal{O}_1\mathcal{O}_2[\widetilde{\mathcal{O}}])^b{}_a\,, \tag{2.33}$$

to replace the contribution of the shadow block with an extension of the integration region to $\frac{d}{2} - i\infty$,

$$A(y_i) = \sum_{\rho} \int_{\frac{d}{2}-i\infty}^{\frac{d}{2}+i\infty} \frac{d\Delta}{2\pi i}\, C_{ab}^{1234}(\Delta,\rho)\, G_{\mathcal{O}}^{1234(ab)}(y_i)\,, \tag{2.34}$$

where

$$C_{ab}^{1234}(\Delta,\rho) = I_{ac}^{1234}(\Delta,\rho)\, S(\mathcal{O}_3\mathcal{O}_4[\widetilde{\mathcal{O}}^\dagger])^c{}_b\,. \tag{2.35}$$

The conformal block decays for large real $\Delta > 0$, so the contour can be closed to the right and the integral is the sum of residues

$$-\operatorname*{Res}_{\Delta\to\Delta^*} C_{ab}^{1234}(\Delta,\rho^*) = \sum_I c^I_{12\mathcal{O}^*,a} c^I_{34\mathcal{O}^*,b}\,. \tag{2.36}$$

The sum over I in (2.36) is over degenerate operators with the quantum numbers (Δ^*,ρ^*). Degeneracies among multi-trace operators are natural in expansions around mean field theory.[1]

In section 2.2.2 we will use the partial wave expansion of the shadow transformed four-point function. To obtain it let us now apply the shadow transform in (2.10) to $\mathcal{O}_1$ and $\mathcal{O}_2$ on both sides of the partial wave expansion (2.29). Using (2.30) this gives

$$\begin{aligned}\langle \mathbf{S}[\mathcal{O}_1]\mathbf{S}[\mathcal{O}_2]\mathcal{O}_3\mathcal{O}_4\rangle = \sum_\rho \int_{\frac{d}{2}}^{\frac{d}{2}+i\infty} \frac{d\Delta}{2\pi i}\, I_{ab}^{1234}(\Delta,\rho) \\ \int dy\, \langle \mathbf{S}[\mathcal{O}_1]\mathbf{S}[\mathcal{O}_2]\mathcal{O}(y)\rangle^{(a)} \langle \mathcal{O}_3\mathcal{O}_4\widetilde{\mathcal{O}}^\dagger(y)\rangle^{(b)}\,.\end{aligned} \tag{2.37}$$

From (2.32), we thus obtain the partial wave expansion of the shadow transformed correlator

$$\langle \mathbf{S}[\mathcal{O}_1]\mathbf{S}[\mathcal{O}_2]\mathcal{O}_3\mathcal{O}_4\rangle = \sum_\rho \int_{\frac{d}{2}}^{\frac{d}{2}+i\infty} \frac{d\Delta}{2\pi i}\, I_{ab}^{\mathbf{S}[1]\mathbf{S}[2]34}(\Delta,\rho)\, \Psi_{\mathcal{O}}^{\widetilde{12}34(ab)}(y_i)\,, \tag{2.38}$$

where

$$\begin{aligned} I_{ab}^{\mathbf{S}[1]\mathbf{S}[2]34} &= I_{mb}^{1234}(\Delta,\rho)\, \frac{S(\mathcal{O}_1[\mathcal{O}_2]\mathcal{O})^m{}_n}{N_{\mathcal{O}_2}} \frac{S([\mathcal{O}_1]\widetilde{\mathcal{O}}_2\mathcal{O})^n{}_a}{N_{\mathcal{O}_1}}\,, \\ \Psi_{\mathcal{O}}^{\widetilde{12}34(ab)}(y_i) &= \int dy\, \langle \widetilde{\mathcal{O}}_1\widetilde{\mathcal{O}}_2\mathcal{O}(y)\rangle^{(a)} \langle \mathcal{O}_3\mathcal{O}_4\widetilde{\mathcal{O}}^\dagger(y)\rangle^{(b)}\,. \end{aligned} \tag{2.39}$$

There are examples of the S coefficients computed in [11] which tell us that they have the appropriate zeroes to kill the double-trace poles in I^{1234} and replace them with the poles for the double-traces of the shadows, as would be appropriate for $I^{\mathbf{S}[1]\mathbf{S}[2]34}$.

2.2.2 A derivation using harmonic analysis

We are ready to begin the derivation of the perturbative CFT optical theorem (2.5). $\mathbf{S}_5\mathbf{S}_6 A_{\text{tree}}^{1564}(y_i)$ in (2.5) is the coefficient of $1/N^2$ in the correlator $\langle \mathbf{S}[\mathcal{O}_6]^\dagger\mathbf{S}[\mathcal{O}_5]^\dagger\mathcal{O}_1\mathcal{O}_4\rangle$, and $A_{\text{tree}}^{3652}(y_i)$ is the coefficient of $1/N^2$ in $\langle \mathcal{O}_3\mathcal{O}_2\mathcal{O}_5\mathcal{O}_6\rangle$. Consider the following conformally invariant pairing

[1] A simple example built with spin 1 operators are the families $\mathcal{O}_5^\mu \Box^n \mathcal{O}_{6,\mu}$ and $\mathcal{O}_5^\mu \partial_\mu\partial_\nu \Box^{n-1}\mathcal{O}_6^\nu$, which we wrote schematically. Both these sets of operators have quantum numbers $\Delta = \Delta_5 + \Delta_6 + 2n$ and $\rho = \bullet$.

of two four-point functions

$$\int dy_5 dy_6 \, \langle \mathcal{O}_3 \mathcal{O}_2 \mathcal{O}_5 \mathcal{O}_6 \rangle \langle \mathbf{S}[\mathcal{O}_6]^\dagger \mathbf{S}[\mathcal{O}_5]^\dagger \mathcal{O}_1 \mathcal{O}_4 \rangle = \tag{2.40}$$
$$\sum_{\rho,\rho'} \int_{\frac{d}{2}}^{\frac{d}{2}+i\infty} \frac{d\Delta}{2\pi i} \frac{d\Delta'}{2\pi i} \, I_{ab}^{3256}(\Delta,\rho) \, I_{cd}^{\mathbf{S}[6]\mathbf{S}[5]14}(\Delta',\rho') \int dy_5 dy_6 \, \Psi_{\mathcal{O}}^{3256(ab)}(y_i) \, \Psi_{\mathcal{O}'}^{\widetilde{65}14(cd)}(y_i) \, .$$

To compute the y_5 and y_6 integrals, we use (2.30) and the following result for the pairing of the three-point structures by two legs, which is known as the bubble integral,

$$\int dy_1 dy_2 \langle \mathcal{O}_1 \mathcal{O}_2 \mathcal{O}(y) \rangle^{(a)} \langle \widetilde{\mathcal{O}}_1^\dagger \widetilde{\mathcal{O}}_2^\dagger \widetilde{\mathcal{O}}'^\dagger(y') \rangle^{(b)} = \frac{\left(\langle \mathcal{O}_1 \mathcal{O}_2 \mathcal{O} \rangle^{(a)}, \langle \widetilde{\mathcal{O}}_1^\dagger \widetilde{\mathcal{O}}_2^\dagger \widetilde{\mathcal{O}}^\dagger \rangle^{(b)} \right)}{\mu(\Delta,\rho)} \mathbf{1}_{yy'} \delta_{\mathcal{O}\mathcal{O}'} \, , \tag{2.41}$$

with $\delta_{\mathcal{O}\mathcal{O}'} \equiv 2\pi\delta(s-s')\delta_{\rho\rho'}$, where $\mathcal{O} = (s,\rho)$ and $\mathbf{1}_{yy'}$ is a delta function. Here $\mu(\Delta,\rho)$ is the Plancherel measure and the brackets denote a conformally invariant pairing of 3-point functions, given by

$$\left(\langle \mathcal{O}_1 \mathcal{O}_2 \mathcal{O}_3 \rangle, \langle \widetilde{\mathcal{O}}_1^\dagger \widetilde{\mathcal{O}}_2^\dagger \widetilde{\mathcal{O}}_3^\dagger \rangle \right) = \int \frac{dy_1 dy_2 dy_3}{\text{volSO}(d+1,1)} \, \langle \mathcal{O}_1 \mathcal{O}_2 \mathcal{O}_3 \rangle \langle \widetilde{\mathcal{O}}_1^\dagger \widetilde{\mathcal{O}}_2^\dagger \widetilde{\mathcal{O}}_3^\dagger \rangle \, . \tag{2.42}$$

Using (2.30) and the bubble integral in (2.41) we find

$$\int dy_5 dy_6 \Psi_{\mathcal{O}}^{3256(ab)}(y_i) \Psi_{\mathcal{O}'}^{\widetilde{65}14(cd)}(y_i) = \frac{\left(\langle \mathcal{O}_5 \mathcal{O}_6 \widetilde{\mathcal{O}}^\dagger \rangle^{(b)}, \langle \widetilde{\mathcal{O}}_6^\dagger \widetilde{\mathcal{O}}_5^\dagger \mathcal{O} \rangle^{(c)} \right)}{\mu(\Delta,\rho)} \, \delta_{\mathcal{O}\mathcal{O}'} \Psi_{\mathcal{O}}^{3214(ad)}(y_i) \, . \tag{2.43}$$

We can now plug (2.43) into (2.40) which gives

$$\int dy_5 dy_6 \langle \mathcal{O}_3 \mathcal{O}_2 \mathcal{O}_5 \mathcal{O}_6 \rangle \langle \mathbf{S}[\mathcal{O}_6]^\dagger \mathbf{S}[\mathcal{O}_5]^\dagger \mathcal{O}_1 \mathcal{O}_4 \rangle = \tag{2.44}$$
$$\sum_{\rho} \int_{\frac{d}{2}}^{\frac{d}{2}+i\infty} \frac{d\Delta}{2\pi i} \, I_{ab}^{3256}(\Delta,\rho) I_{cd}^{\mathbf{S}[6]\mathbf{S}[5]14}(\Delta,\rho) \frac{\left(\langle \mathcal{O}_5 \mathcal{O}_6 \widetilde{\mathcal{O}}^\dagger \rangle^{(b)}, \langle \widetilde{\mathcal{O}}_6^\dagger \widetilde{\mathcal{O}}_5^\dagger \mathcal{O} \rangle^{(c)} \right)}{\mu(\Delta,\rho)} \, \Psi_{\mathcal{O}}^{3214(ad)}(y_i) \, .$$

In the next steps we will show that the factor $\left(\langle \mathcal{O}_5 \mathcal{O}_6 \widetilde{\mathcal{O}}^\dagger \rangle, \langle \widetilde{\mathcal{O}}_6^\dagger \widetilde{\mathcal{O}}_5^\dagger \mathcal{O} \rangle \right)$ in (2.44) , along with the various shadow coefficients, will cancel the contribution of the OPE coefficients $c_{56[56]}^{\text{MFT}}$ in the spectral functions I^{3256} and $I^{\mathbf{S}[6]\mathbf{S}[5]14}$. In the simple case where at least one of the spectral functions in (2.44) belong to scalar MFT correlators (which requires pairwise equal operators) this is particularly easy to see, since [11]

$$I^{\text{MFT}}(\Delta,\rho) = \frac{\mu(\Delta,\rho)}{\left(\langle \mathcal{O}_1 \mathcal{O}_2 \widetilde{\mathcal{O}}^\dagger \rangle, \langle \widetilde{\mathcal{O}}_1^\dagger \widetilde{\mathcal{O}}_2^\dagger \mathcal{O} \rangle \right)} \, S([\widetilde{\mathcal{O}}_1]\widetilde{\mathcal{O}}_2\mathcal{O}) \, S(\mathcal{O}_1[\widetilde{\mathcal{O}}_2]\mathcal{O}) \, , \tag{2.45}$$

so that the pairing of three-point functions can be canceled directly with one of the spectral functions. The general case is less obvious because the cancellation happens on the level of

OPE coefficients, not spectral functions. Here we use (2.39) in (2.44), and extend the range of the principal series integral as in (2.34) by repeated use of (2.33). This gives

$$\int dy_5 dy_6 \langle \mathcal{O}_3\mathcal{O}_2\mathcal{O}_5\mathcal{O}_6\rangle \langle \mathbf{S}[\mathcal{O}_6]^\dagger \mathbf{S}[\mathcal{O}_5]^\dagger \mathcal{O}_1\mathcal{O}_4\rangle = \sum_\rho \int_{\frac{d}{2}-i\infty}^{\frac{d}{2}+i\infty} \frac{d\Delta}{2\pi i}\, I^{3256}_{ab} I^{6514}_{md} S(\mathcal{O}_1\mathcal{O}_4[\widetilde{\mathcal{O}}^\dagger])^d{}_l$$
$$\frac{S(\mathcal{O}_6[\mathcal{O}_5]\mathcal{O})^m{}_n}{N_{\mathcal{O}_5}} \frac{S([\mathcal{O}_6]\widetilde{\mathcal{O}}_5\mathcal{O})^n{}_c}{N_{\mathcal{O}_6}} \frac{\left(\langle \mathcal{O}_5\mathcal{O}_6\widetilde{\mathcal{O}}^\dagger\rangle^{(b)}, \langle \widetilde{\mathcal{O}}_6^\dagger \widetilde{\mathcal{O}}_5^\dagger \mathcal{O}\rangle^{(c)}\right)}{\mu(\Delta,\rho)} G^{3214(al)}_{\mathcal{O}}(y_i)\,. \tag{2.46}$$

Using (2.35) we can express (2.46) as

$$\int dy_5 dy_6 \langle \mathcal{O}_3\mathcal{O}_2\mathcal{O}_5\mathcal{O}_6\rangle \langle \mathbf{S}[\mathcal{O}_6]^\dagger \mathbf{S}[\mathcal{O}_5]^\dagger \mathcal{O}_1\mathcal{O}_4\rangle = \sum_\rho \int_{\frac{d}{2}-i\infty}^{\frac{d}{2}+i\infty} \frac{d\Delta}{2\pi i}\, C^{3256}_{ak} C^{6514}_{md}\, Q^{km}_{65\mathcal{O}}\, G^{3214(ad)}_{\mathcal{O}}\,, \tag{2.47}$$

where,

$$Q^{km}_{65\mathcal{O}} = \frac{S(\mathcal{O}_6[\mathcal{O}_5]\mathcal{O})^m{}_n}{N_{\mathcal{O}_5}} \frac{S([\mathcal{O}_6]\widetilde{\mathcal{O}}_5\mathcal{O})^n{}_c}{N_{\mathcal{O}_6}} \frac{\left(\langle \mathcal{O}_5\mathcal{O}_6\widetilde{\mathcal{O}}^\dagger\rangle^{(b)}, \langle \widetilde{\mathcal{O}}_6^\dagger \widetilde{\mathcal{O}}_5^\dagger \mathcal{O}\rangle^{(c)}\right)}{\mu(\Delta,\rho)} \frac{S(\mathcal{O}_5\mathcal{O}_6[\mathcal{O}^\dagger])^k{}_b}{N_{\mathcal{O}}}\,. \tag{2.48}$$

Next we analyze the pole structure of the spectral function in (2.47) and close the integration contour to obtain the block expansion. First let us consider the simple poles at the dimensions of the double-trace operators $\mathcal{O}_{[56]}$ in each of C^{3256} and C^{6514}. We will show that $Q_{65\mathcal{O}}(\Delta,\rho)$ has a zero at each of these dimensions, canceling one of the two poles from C^{3256} and C^{6514}. This ensures that in the MFT limit the spectral function in (2.47) has a simple pole for each double-trace dimension. This can be seen explicitly in specific examples for the S coefficients computed in [11], but in general let us note the following identity, which can be derived by applying Euclidean inversion on the expansion (2.29) for the MFT correlator [11]

$$\frac{I^{6565,\text{MFT}}_{ab}(\Delta,\rho)}{\mu(\Delta,\rho)} \left(\langle \mathcal{O}_6^\dagger \mathcal{O}_5^\dagger \widetilde{\mathcal{O}}^\dagger\rangle^{(b)}, \langle \widetilde{\mathcal{O}}_6\widetilde{\mathcal{O}}_5\mathcal{O}\rangle^{(c)}\right) = S([\widetilde{\mathcal{O}}_6]\widetilde{\mathcal{O}}_5\mathcal{O})^c{}_l\, S(\mathcal{O}_6[\widetilde{\mathcal{O}}_5]\mathcal{O})^l{}_a\,. \tag{2.49}$$

Since all operators are bosonic, (2.49) can be expressed as

$$(-1)^{2J} \frac{I^{6556,\text{MFT}}_{ab}(\Delta,\rho)}{\mu(\Delta,\rho)} \frac{S(\mathcal{O}_6[\mathcal{O}_5]\mathcal{O})^m{}_n}{N_{\mathcal{O}_5}} \frac{S([\mathcal{O}_6]\widetilde{\mathcal{O}}_5\mathcal{O})^n{}_c}{N_{\mathcal{O}_6}} \left(\langle \mathcal{O}_5\mathcal{O}_6\widetilde{\mathcal{O}}^\dagger\rangle^{(b)}, \langle \widetilde{\mathcal{O}}_6^\dagger \widetilde{\mathcal{O}}_5^\dagger \mathcal{O}\rangle^{(c)}\right) = \delta^m_a\,. \tag{2.50}$$

Using (2.34) and (2.48), we rephrase (2.50) as

$$C^{6556,\text{MFT}}_{ak}(\Delta,\rho)\; Q^{km}_{65\mathcal{O}}(\Delta,\rho) = \delta^m_a\,. \tag{2.51}$$

Let (Δ,ρ) be (Δ^*,ρ^*) for the double-trace operators $\mathcal{O}^I_{[56]^*}$, where I labels degenerate operators, as discussed previously. The coefficient $C^{6556,\text{MFT}}_{ak}$ has a simple pole at this location and

therefore (2.51) implies that $Q^{km}_{65\mathcal{O}}(\Delta,\rho)$ is its inverse matrix and has a corresponding zero at this value. Evaluated at $\Delta=\Delta^*$, (2.51) takes the form

$$\left(\sum_I c^{MFT,I}_{65[56]^*,a}c^{MFT,I}_{56[56]^*,k}\right) q^{km}=\delta^m_a\,, \tag{2.52}$$

where $c^{MFT,I}_{65[56]^*,a}c^{MFT,I}_{56[56]^*,k}$ is the contribution to the residue of $C^{6556,\text{MFT}}_{ak}$ corresponding to $\mathcal{O}^I_{[56]^*}$ and q^{km} is the coefficient of the first order zero of $Q^{km}_{65\mathcal{O}}$ at Δ^*.

Note that the matrix of OPE coefficients $c^{MFT,I}_{65[56]^*,a}c^{MFT,I}_{56[56]^*,k}$ for a specific double-trace operator is singular. In general, (2.51) and (2.52) imply that there are sufficiently many degenerate double-trace families so the matrix obtained by summing over all of them is not singular. In the case where there is a unique tensor structure, such as when $\mathcal{O}_5$ and $\mathcal{O}_6$ are scalars, the 1×1 matrix is of course non-degenerate, so degenerate double-trace operators need not exist. Contracting both sides of (2.52) with $c^{MFT,J}_{65[56]^*,m}$, we obtain

$$c^{MFT,I}_{56[56]^*,k}\,q^{km}\,c^{MFT,J}_{65[56]^*,m}=\delta^{IJ}\,. \tag{2.53}$$

Finally, using (2.36) and (2.53) we obtain the contribution of the (Δ^*,ρ^*) pole to the spectral integral in (2.47)

$$-\operatorname*{Res}_{\Delta\to\Delta^*} C^{3256}_{ak}C^{6514}_{md}\,Q^{km}_{65\mathcal{O}}\,G^{3214(ad)}_{\mathcal{O}}\big|_{\rho\to\rho^*}=\sum_I c^I_{32[56]^*,a}c^I_{14[56]^*,d}\,G^{3214(ad)}_{[56]^*}(y_i)\,. \tag{2.54}$$

Given that this is precisely the contribution of the double-trace operators $[\mathcal{O}_5\mathcal{O}_6]$ to the correlator $A^{3214}(y_i)$, this shows that the conformally invariant pairing we started with in (2.40) computes precisely this contribution, to leading order in $1/N^2$ because we used MFT expressions along the way. Thus

$$\Big(1+O\big(1/N^2\big)\Big)\,A(y_k)\big|_{[\mathcal{O}_5\mathcal{O}_6]}=\int dy_5dy_6\,A^{3652}(y_k)\,\mathbf{S}_5\mathbf{S}_6A^{1564}(y_k)\Big|_{[\mathcal{O}_5\mathcal{O}_6]}\,. \tag{2.55}$$

In the context of the the projector defined in the previous section in (2.17), this result can be phrased as

$$\sum_{n,\ell,I}\Big|[\mathcal{O}_5\mathcal{O}_6]^I_{n,\ell}\Big|=|\mathcal{O}_5\mathcal{O}_6|+O\big(1/N^2\big)\,. \tag{2.56}$$

The labels n,ℓ sum over the double-trace operators with different dimensions and spins, while I sums over degenerate operators. The projection $|_{[\mathcal{O}_5\mathcal{O}_6]}$ appears on the two sides of (2.55) for different reasons. On the left hand side it selects one family of double-trace operators among all the operators appearing in the OPE, while on the right hand side it serves to discard poles from shadow operators that we would pick up when we close the

contour in (2.47). For example, it is evident from the first equation in (2.39) that $Q(\Delta,\rho)$ has poles at the double-traces $\mathcal{O}^I_{[\widetilde{5}\widetilde{6}]}$ composed of $\widetilde{\mathcal{O}}_5$ and $\widetilde{\mathcal{O}}_6$ and we pick up these contributions too. Let us take for simplicity the case with $\mathcal{O}_5$ and $\mathcal{O}_6$ scalars and $\mathcal{O}$ with integer spin ℓ in 4 dimensions. The corresponding three-point function has only one tensor structure and the expressions for $S(\mathcal{O}_6[\mathcal{O}_5]\mathcal{O})$ and $S([\mathcal{O}_6]\widetilde{\mathcal{O}}_5\mathcal{O})$ are known [11]

$$S(\mathcal{O}_6[\mathcal{O}_5]\mathcal{O}) \sim \frac{\Gamma\left(\frac{\Delta_6+\widetilde{\Delta}_5-\Delta+\ell}{2}\right)}{\Gamma\left(\frac{\Delta_6+\Delta_5-\Delta+\ell}{2}\right)}, \qquad S([\mathcal{O}_6]\widetilde{\mathcal{O}}_5\mathcal{O}) \sim \frac{\Gamma\left(\frac{\widetilde{\Delta}_6+\widetilde{\Delta}_5-\Delta+\ell}{2}\right)}{\Gamma\left(\frac{\Delta_6+\widetilde{\Delta}_5-\Delta+\ell}{2}\right)}. \tag{2.57}$$

Therefore, the product has poles at the double-traces $[\widetilde{\mathcal{O}}_5\widetilde{\mathcal{O}}_6]$ (and zeroes at the double-traces $[\mathcal{O}_5\mathcal{O}_6]$). To determine such contributions in the same way as above, we should express I^{3256} in terms of $I^{32\mathbf{S}[5]\mathbf{S}[6]}$ by inverting (2.38) at (2.44) in the derivation above. We can follow the remaining steps and use an identity for the MFT spectral function similar to (2.49) (see [11]). This gives the contribution from the double-traces of shadows $\mathcal{O}^I_{[\widetilde{5}\widetilde{6}]}$ to be of the same form as in (2.54). Note that in the case of scalar MFT correlators, these poles in $Q(\Delta,\rho)$ are canceled by zeros in the MFT spectral function (2.45) and hence we do not have these contributions from the double-traces of shadows.

2.2.3 Discontinuities in the large N expansion

Equation (2.55) by itself is not very useful because of the $O(\frac{1}{N^2})$ error term. External double traces contribute already at $O(N^0)$ so that their contributions at $O(\frac{1}{N^2})$ are already not attainable by (2.55). This problem is solved by taking the double discontinuity of (2.55), which will ensure that both sides of the equation are valid to $O(\frac{1}{N^4})$ for all double traces $[\mathcal{O}_5\mathcal{O}_6]$, both external and internal.

The discontinuities are given by commutators in Lorentzian signature, hence we analytically continue the correlators to Lorentzian signature and take the difference of different operator orderings. Euclidean correlators can be continued to Wightman functions using the following prescription [5]

$$\langle\mathcal{O}_1(t_1,\vec{x}_1)\mathcal{O}_2(t_2,\vec{x}_2)\cdots\mathcal{O}_n(t_n,\vec{x}_n)\rangle = \lim_{\epsilon_i\to 0}\langle\mathcal{O}_1(t_1-i\epsilon_1,\vec{x}_1)\cdots\mathcal{O}_n(t_n-i\epsilon_n,\vec{x}_n)\rangle\,, \tag{2.58}$$

with $\tau_i = it_i$ where τ is Euclidean and t Lorentzian time. The limits are taken assuming $\epsilon_1 > \epsilon_2 > \cdots > \epsilon_n$.

Let us assume without loss of generality that $\mathcal{O}_4$ is in the future of $\mathcal{O}_1$, that $\mathcal{O}_2$ is in the future of $\mathcal{O}_3$ and that all other pairs of operators are spacelike from each other. Now we apply the epsilon prescription to $\langle\mathcal{O}_1\mathcal{O}_2\mathcal{O}_3\mathcal{O}_4\rangle$ with $\epsilon_4 > \epsilon_1$ and $\epsilon_2 > \epsilon_3$. The relative ordering

of epsilons is unimportant for the spacelike separated pairs. This gives the Lorentzian correlator $A^{\circlearrowleft} = \langle \mathcal{O}_2\mathcal{O}_3\mathcal{O}_4\mathcal{O}_1\rangle$, which is equal to the time ordered correlator for the assumed kinematics. Similarly, we obtain $A^{\circlearrowright} = \langle \mathcal{O}_3\mathcal{O}_2\mathcal{O}_1\mathcal{O}_4\rangle$ from the ordering $\epsilon_4 < \epsilon_1$, $\epsilon_2 < \epsilon_3$. The Euclidean configurations A_{Euc} correspond to the mixed orderings $\epsilon_4 > \epsilon_1$, $\epsilon_2 < \epsilon_3$ and $\epsilon_4 < \epsilon_1$, $\epsilon_2 > \epsilon_3$. We can then relate the dDisc_t to these four configurations by

$$\text{dDisc}_t A(y_i) = A_{\text{Euc}}(y_i) - \frac{1}{2}\left(A^{\circlearrowleft}(y_i) + A^{\circlearrowright}(y_i)\right) = -\frac{1}{2}\langle [\mathcal{O}_2, \mathcal{O}_3]\,[\mathcal{O}_4, \mathcal{O}_1]\rangle\,. \tag{2.59}$$

Using (2.24) this gives the conventional definition of the double discontinuity [6]

$$\begin{aligned}\text{dDisc}_t A(y_i) = T^{1234}(y_i)\Big[&\cos\left(\pi(a+b)\right)\mathcal{A}^{1234}(z,\bar{z}) - \\ &- \frac{1}{2}\left(e^{i\pi(a+b)}\mathcal{A}^{1234}(z,\bar{z}^{\circlearrowleft}) + e^{-i\pi(a+b)}\mathcal{A}^{1234}(z,\bar{z}^{\circlearrowright})\right)\Big],\end{aligned} \tag{2.60}$$

where $a = \Delta_{21}/2$ and $b = \Delta_{34}/2$. $\bar{z}^{\circlearrowleft}$ and $\bar{z}^{\circlearrowright}$ denote that $\bar{z}$ is analytically continued by a full circle counter-clockwise and clockwise around $\bar{z} = 1$, respectively.[2]

The gluing of correlators on the right hand side in (2.55), with the shadow integrals now written explicitly, is a sum of terms of the form

$$\frac{1}{N_{\mathcal{O}_5}N_{\mathcal{O}_6}}\int dy_5\, dy_6\, dy_7\, dy_8\, \langle \mathcal{O}_2\mathcal{O}_3\mathcal{O}_6\mathcal{O}_5\rangle\, \langle \widetilde{\mathcal{O}}_5\widetilde{\mathcal{O}}_7^{\dagger}\rangle\, \langle \widetilde{\mathcal{O}}_6\widetilde{\mathcal{O}}_8^{\dagger}\rangle\, \langle \mathcal{O}_7\mathcal{O}_8\mathcal{O}_1\mathcal{O}_4\rangle\,. \tag{2.61}$$

Note that $\mathcal{O}_5 = \mathcal{O}_7$ and $\mathcal{O}_6 = \mathcal{O}_8$ but we have used the different labels to denote the insertion points. We can apply the same ϵ-prescriptions on (2.61) while we hold y_5, y_6, y_7, y_8 to be Euclidean. Taking the same combinations as in (2.59) we arrive at

$$\frac{1}{N_{\mathcal{O}_5}N_{\mathcal{O}_6}}\int dy_5\, dy_6\, dy_7\, dy_8\, \langle [\mathcal{O}_2, \mathcal{O}_3]\,\mathcal{O}_6\mathcal{O}_5\rangle\, \langle \widetilde{\mathcal{O}}_5\widetilde{\mathcal{O}}_7^{\dagger}\rangle\, \langle \widetilde{\mathcal{O}}_6\widetilde{\mathcal{O}}_8^{\dagger}\rangle\, \langle \mathcal{O}_7\mathcal{O}_8\,[\mathcal{O}_4, \mathcal{O}_1]\rangle\,. \tag{2.62}$$

The commutators in (2.62) give discontinuities in the correlator as defined in (2.22).

We will now show that taking the dDisc of (2.40) ensures that the external double-traces $[\mathcal{O}_1\mathcal{O}_4]$ and $[\mathcal{O}_2\mathcal{O}_3]$ which usually appear at $O(N^0)$ are suppressed in $1/N$ so that they appear at the same order as other double trace operators. To this end, let us briefly discuss the $1/N$ expansion of correlators and associated CFT data. The leading contribution is A_{MFT}, which is simply the disconnected correlator if the external operators are pairwise equal and is absent otherwise. Because of this, the only operators that appear at $O(N^0)$ are the ones

[2]The relation between (2.59) and (2.60) can be obtained by assigning the phases $y_{ij}^2 \to y_{ij}^2 e^{\pm i\pi}$ to the timelike distances y_{14} and y_{23}.

appearing in the disconnected correlator,

$$\begin{aligned} c_{ij[\mathcal{O}_i\mathcal{O}_j]_{n,\ell}} &= c^{\text{MFT}}_{ij[\mathcal{O}_i\mathcal{O}_j]_{n,\ell}} + \frac{1}{N^2}\, c^{(1)}_{ij[\mathcal{O}_i\mathcal{O}_j]_{n,\ell}} + \cdots\,, \\ \Delta_{[\mathcal{O}_i\mathcal{O}_j]_{n,\ell}} &= \Delta_i + \Delta_j + 2n + \ell + \frac{1}{N^2}\,\gamma_{[\mathcal{O}_i\mathcal{O}_j]_{n,\ell}} + \cdots\,. \end{aligned} \tag{2.63}$$

Other double-trace operators can only appear at higher orders in the OPE, therefore

$$c_{ij[\mathcal{O}_k\mathcal{O}_l]_{n,\ell}} = \frac{1}{N^2}\, c^{(1)}_{ij[\mathcal{O}_k\mathcal{O}_l]_{n,\ell}} + \cdots\,, \qquad i,j \neq k,l\,. \tag{2.64}$$

The analytic continuation of a t-channel conformal block to the Regge sheet is given by the following simple expression

$$g^{3214}_{\mathcal{O}}\big(1-z,(1-\bar{z})e^{i\beta}\big) = e^{i\beta\frac{\tau_{\mathcal{O}}}{2}}\, g^{3214}_{\mathcal{O}}(1-z,1-\bar{z})\,. \tag{2.65}$$

As a result, the action of the single and double discontinuities on the t-channel block expansion in (2.27) is given by

$$\begin{aligned} \text{Disc}_{14}\, A^{1ij4}(y_k) &= \sum_{\mathcal{O}} 2i \sin\left(\tfrac{\pi}{2}(\tau_{\mathcal{O}} - \Delta_1 - \Delta_4)\right) c_{ij\mathcal{O}} c_{14\mathcal{O}}\, G^{ij14}_{\mathcal{O}}(y_k)\,, \\ \text{Disc}_{23}\, A^{3ji2}(y_k) &= \sum_{\mathcal{O}} 2i \sin\left(\tfrac{\pi}{2}(\tau_{\mathcal{O}} - \Delta_2 - \Delta_3)\right) c_{32\mathcal{O}} c_{ij\mathcal{O}}\, G^{32ij}_{\mathcal{O}}(y_k)\,, \\ \text{dDisc}_t A(y_k) &= \sum_{\mathcal{O}} 2 \sin\left(\tfrac{\pi}{2}(\tau_{\mathcal{O}} - \Delta_1 - \Delta_4)\right) \sin\left(\tfrac{\pi}{2}(\tau_{\mathcal{O}} - \Delta_2 - \Delta_3)\right) c_{32\mathcal{O}} c_{14\mathcal{O}}\, G^{3214}_{\mathcal{O}}(y_k)\,. \end{aligned} \tag{2.66}$$

The sines in the expansions are responsible for suppressing the contribution of external double-traces. Therefore, using (2.66), (2.63) and (2.64), the leading contribution to the discontinuity of a correlator is $O(1/N^2)$

$$\begin{aligned} &\text{Disc}_{14}\, A(y_i) = \frac{1}{N^2}\, \text{Disc}_{14}\, A_{\text{tree}}(y_i) + O(1/N^4) = \\ &\sum_{\mathcal{O}=[\mathcal{O}_1\mathcal{O}_4]} i\pi \frac{\gamma_{\mathcal{O}}}{N^2}\, c^{\text{MFT}}_{14\mathcal{O}} c_{32\mathcal{O}} G^{3214}_{\mathcal{O}} + \sum_{\mathcal{O}\neq[\mathcal{O}_1\mathcal{O}_4]} 2i \sin\left(\tfrac{\pi}{2}(\tau_{\mathcal{O}} - \Delta_1 - \Delta_4)\right) \frac{c^{(1)}_{14\mathcal{O}}}{N^2}\, c_{32\mathcal{O}} G^{3214}_{\mathcal{O}}\,, \end{aligned} \tag{2.67}$$

and similarly the leading contribution to the double discontinuity is $O(1/N^4)$

$$\text{dDisc}_t A(y_i) = \frac{1}{N^4}\, \text{dDisc}_t A_{\text{1-loop}}(y_i) + O(1/N^6)\,. \tag{2.68}$$

In particular, when acting with (2.21) on the left hand side of (2.40) we have

$$\begin{aligned}
\text{Disc}_{23}\, A^{3652} &= \sum_{\mathcal{O}=[\mathcal{O}_2\mathcal{O}_3]} i\pi \frac{\gamma_{\mathcal{O}}}{N^2}\, c^{\text{MFT}}_{32\mathcal{O}}\, c_{56\mathcal{O}}\, G^{3256}_{\mathcal{O}} \\
&\quad + \sum_{\mathcal{O}\neq[\mathcal{O}_2\mathcal{O}_3]} 2i \sin\left(\tfrac{\pi}{2}(\tau_{\mathcal{O}}-\Delta_2-\Delta_3)\right) \frac{c^{(1)}_{32\mathcal{O}}}{N^2}\, c_{56\mathcal{O}}\, G^{3256}_{\mathcal{O}}\,, \\
\text{Disc}_{14}\, A^{1\widetilde{5}\widetilde{6}4} &= \sum_{\mathcal{O}=[\mathcal{O}_1\mathcal{O}_4]} i\pi \frac{\gamma_{\mathcal{O}}}{N^2}\, c_{\widetilde{65}\mathcal{O}} c^{\text{MFT}}_{14\mathcal{O}}\, G^{\widetilde{6}\widetilde{5}14}_{\mathcal{O}} \\
&\quad + \sum_{\mathcal{O}\neq[\mathcal{O}_1\mathcal{O}_4]} 2i \sin\left(\tfrac{\pi}{2}(\tau_{\mathcal{O}}-\Delta_1-\Delta_4)\right) c_{\widetilde{65}\mathcal{O}} \frac{c^{(1)}_{14\mathcal{O}}}{N^2}\, G^{\widetilde{6}\widetilde{5}14}_{\mathcal{O}}\,.
\end{aligned} \tag{2.69}$$

Since every term is these expansions already has an explicit factor of $1/N^2$, the only operators that can contribute at this order are the ones with $c_{56\mathcal{O}} = O(N^0)$ or $c_{\widetilde{65}\mathcal{O}} = O(N^0)$, which are the double-traces $\mathcal{O} = [\mathcal{O}_5\mathcal{O}_6]$ and $\mathcal{O} = [\widetilde{\mathcal{O}}_5\widetilde{\mathcal{O}}_6]$. Applying the discontinuities to both sides of (2.55) leaves us with one of our main results, the perturbative optical theorem for the contributions of double-trace operators to the 1-loop dDisc of the correlator, as stated in the introduction

$$\text{dDisc}_t\, A_{1-\text{loop}}(y_i)\Big|_{\text{d.t.}} = -\frac{1}{2} \sum_{\substack{\mathcal{O}_5,\mathcal{O}_6 \\ \in \text{ s.t.}}} \int dy_5 dy_6\ \text{Disc}_{23}\, A^{3652}_{\text{tree}}(y_k)\, \mathbf{S}_5\mathbf{S}_6\, \text{Disc}_{14}\, A^{1564}_{\text{tree}}(y_k)\Big|_{[\mathcal{O}_5\mathcal{O}_6]}\,. \tag{2.70}$$

The integrals in this formula are over Euclidean space. It would be very interesting to derive a fully Lorentzian generalization of this formula. In [12] it was shown that there is a Lorentzian version of the shadow integral which computes the conformal block without the need to project out shadow operators. A Lorentzian version of (2.70) might have this feature as well. In section 2.4 we will propose a Lorentzian fomula that is valid in the Regge limit.

To obtain the full double discontinuity, this generally has to be supplemented by the contributions of single trace operators, which already had the appropriate form in terms of three-point functions of single trace operators from the start, as shown in (2.4). The two types of contributions are analogous to double and single line cuts of scattering amplitudes in the S-matrix optical theorem.

2.3 Review of flat space amplitudes

In this section we review the Regge limit in D-dimensional flat space. Then we review the optical theorem in impact parameter space and explain how the notion of a one-loop vertex function arises. Not only does this serve as a hopefully more familiar introduction before discussing the same concepts in AdS, but it also provides the results we need later when we take the flat space limit of our AdS results and match them to known flat space expressions.

To mimic the $1/N$ expansion in the CFT, it will be convenient to define an expansion in G_N for the flat space scattering amplitude

$$A(s,t) = \frac{2G_N}{\pi} A_{\text{tree}}(s,t) + \left(\frac{2G_N}{\pi}\right)^2 A_{\text{1-loop}}(s,t) + \dots , \tag{2.71}$$

and we use an identical expansion for the phase shifts $\delta(s,b)$ defined below.

2.3.1 Regge limit and Regge theory

We start by introducing the impact parameter representation, following [48]. Let us consider a tree-level scattering process with incoming momenta k_1 and k_3 that have large momenta along different lightcone directions. For simplicity we assume for now that all external particles are massless scalars. This process is dominated by t-channel exchange diagrams of the type

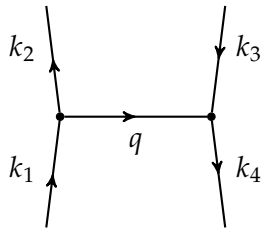

(2.72)

and the amplitude can be expressed in terms of the Mandelstam variables

$$s = -(k_1 + k_3)^2 , \qquad t = -(k_1 - k_2)^2 . \tag{2.73}$$

The amplitude now depends only on s and the momentum exchange q in the transverse directions, because we are considering the following configuration of null momenta, written in light-cone coordinates $p = (p^u, p^v, p_\perp)$

$$\begin{aligned} k_1^\mu &= \left(k^u, \frac{q^2}{4k^u}, \frac{q}{2}\right) , & k_3^\mu &= \left(\frac{q^2}{4k^v}, k^v, -\frac{q}{2}\right) , \\ k_2^\mu &= \left(k^u, \frac{q^2}{4k^u}, -\frac{q}{2}\right) , & k_4^\mu &= \left(\frac{q^2}{4k^v}, k^v, \frac{q}{2}\right) . \end{aligned} \tag{2.74}$$

Notice that we reserve the letter q for $(D-2)$-dimensional vectors in the transverse momentum space. In the Regge limit $k^u \sim k^v \to \infty$ the Mandelstams are given by

$$s \approx k^u k^v , \qquad t = -q^2 . \tag{2.75}$$

The tensor structures in such amplitudes are fixed in terms of the on-shell three-point amplitudes. For the case with two external scalars and an intermediate particle (labeled I) with

spin J there is only one possible tensor structure for the three-point amplitudes given by

$$\tilde{A}^{12I} = a_J(\epsilon_I \cdot k_1)^J\,, \qquad \tilde{A}^{34I} = a_J(\epsilon_I \cdot k_3)^J\,, \tag{2.76}$$

where we encode traceless and transverse polarization tensors in terms of vectors satisfying $\epsilon_i^2 = \epsilon_i \cdot k_i = 0$. We can then write the four-point amplitude as

$$A_{(m,J)}(s,t) = \frac{\sum_{\epsilon_I} \tilde{A}^{12I}\tilde{A}^{34I}}{t-m^2} \approx \frac{a_J^2\, s^J}{t-m^2}\,, \tag{2.77}$$

where we used that for large s the sum over polarizations is dominated by $\epsilon_{Iu}k_1^u \sim k^u$ and $\epsilon_{Iv}k_3^v \sim k^v$. The s^J behavior is naively problematic at high energies, especially if the spectrum contains particles of large spin, as is the case in string theory. However, boundedness of the amplitude in the Regge limit means there is a delicate balance between the infinitely many contributions in the sum over spin.[3] The precise framework to describe this phenomenon is Regge theory [49], which was reviewed for flat space in [4, 50].

In the Regge limit one has to consider the particle with the maximum spin $j(m^2)$ for each mass. The function $j(m^2)$ is called the leading Regge trajectory and the contributions from these particles get resummed into an effective particle with continuous spin $j(t)$. In this work we will focus on the leading trajectory with vacuum quantum numbers known as the Pomeron. At tree-level the amplitude for Pomeron exchange factorizes into three-point amplitudes involving a Pomeron and the universal Pomeron propagator $\beta(t)$. For example, in the case of 4-dilaton scattering in type IIB strings we have

$$A_{\text{tree}}(s,t) = \frac{8}{\alpha'}A^{12P}\beta(t)A^{34P}\left(\frac{\alpha' s}{4}\right)^{j(t)}\,, \tag{2.78}$$

with

$$\beta(t) = 2\pi^2\frac{\Gamma(-\frac{\alpha'}{4}t)}{\Gamma(1+\frac{\alpha'}{4}t)}\,e^{-\frac{i\pi\alpha'}{4}t}\,. \tag{2.79}$$

A^{ijP} are the three-point amplitudes between the external scalars and the Pomeron with the s-dependence factored out and normalized such that in the case of 4-dilaton scattering $A^{ijP} = 1$. This is convenient since later on, when we consider more general string states with spin,

[3] The couplings a_J are dimensionful, $[a_J] = 3 - D/2 - J$, and accommodate for higher derivatives in the couplings to higher spin fields. In string theory the dimensionful scale is α' and the dimensionless couplings are all proportional to the string coupling g_s.

the string three-point amplitudes defined this way will contain just tensor structures. Diagrammatically we can write (2.78) as

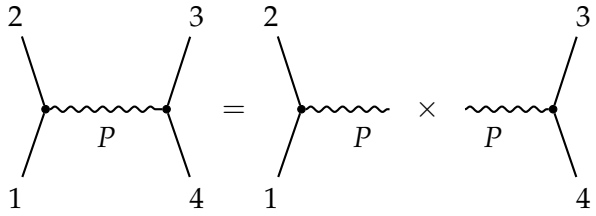

$$\times \frac{2G_N}{\pi}\frac{8}{\alpha'}\beta(t)\left(\frac{\alpha' s}{4}\right)^{j(t)} . \tag{2.80}$$

Amplitudes involving a Pomeron can be computed in string theory using the Pomeron vertex operator [39, 51, 52]. The factorization into three-point functions and a Pomeron propagator holds for general external string states [39, 53].

2.3.2 Optical theorem and impact parameter space

Next we consider the expression for the two-line cut of the one-loop amplitude in the impact parameter representation, which will be given in terms of the tree-level pieces we have discussed so far. The two-line cut receives a contribution from two-Pomeron exchange, which is the leading term in the Regge limit of the one-loop amplitude. Consider the following configuration of momenta

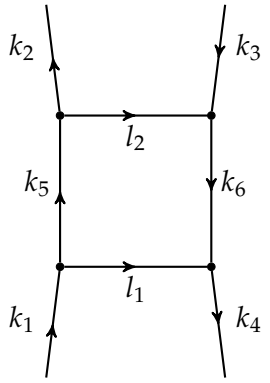

. (2.81)

The external momenta are again in the configuration (2.74) with Mandelstams (2.75). The optical theorem tells us to cut the internal lines of the diagram, putting the corresponding legs on-shell. This implies the following equation for the discontinuity of the amplitude

$$2\mathrm{Im}A_{\text{1-loop}}(s,q) = \sum_{\substack{m_5,\rho_5,\epsilon_5 \\ m_6,\rho_6,\epsilon_6}} \int \frac{dl_1}{(2\pi)^D} 2\pi i\delta(k_5^2+m_5^2)\, 2\pi i\delta(k_6^2+m_6^2) A^{3652}_{\text{tree}}(s,l_2)^* A^{1564}_{\text{tree}}(s,l_1) , \tag{2.82}$$

where one sums over all possible particles 5 and 6 with masses m, in Little group representations ρ and with polarization tensors ϵ. The sums over polarizations can be evaluated using completeness relations. In order to remove the delta functions we express k_5 and k_6 in terms of l_1 and the external momenta (2.74). Then we write the loop momentum as $l_1^\mu = (l^u, l^v, q_1)$

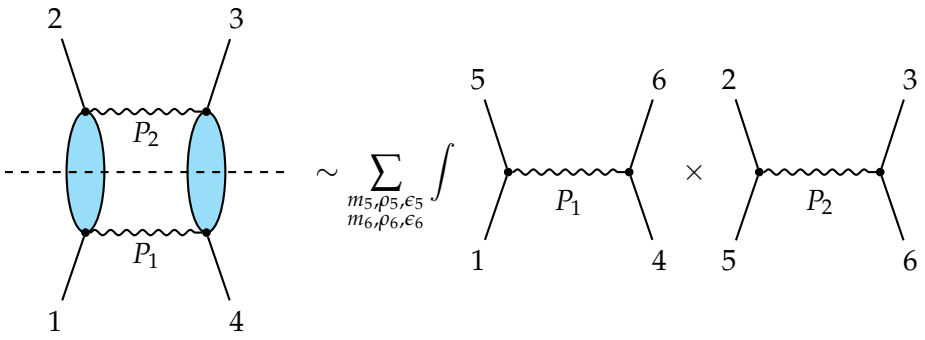

FIGURE 2.2: Optical theorem in the Regge limit in terms of Feynman diagrams. The tree-level correlators are dominated by s-channel Pomeron exchange. The ellipses on the l.h.s. indicate that all string excitations are taken into account.

and use the delta-functions to fix the forward components of the loop momentum l_u and l_v to

$$l^u = \frac{m_6^2 + q_1^2 + q \cdot q_1}{k^v}, \qquad l^v = -\frac{m_5^2 + q_1^2 - q \cdot q_1}{k^u}, \tag{2.83}$$

leaving only the transverse integration over q_1. We arrive at the equation

$$\mathrm{Im} A_{\text{1-loop}}(s,q) = \sum_{\substack{m_5,\rho_5,\epsilon_5 \\ m_6,\rho_6,\epsilon_6}} \int \frac{dq_1 dq_2}{(2\pi)^{D-2}} \frac{\delta(q - q_1 - q_2)}{4s} A^{3652}_{\text{tree}}(s,q_2)^* A^{1564}_{\text{tree}}(s,q_1), \tag{2.84}$$

where we introduced the transverse momentum $q_2 = q - q_1$ to write the expression in a more symmetrical way. Using that the tree-level amplitudes are given in the Regge limit by Pomeron exchange, we can write (2.84) diagrammatically as in figure 2.2. The optical theorem can be simplified even further by transforming it to impact parameter space. To this end the amplitude is expressed in terms of the impact parameter b, which is a vector in the transverse impact parameter space $\mathbb{R}^{D-2}$, using the following transformation

$$\delta(s,b) = \frac{1}{2s} \int \frac{dq}{(2\pi)^{D-2}} e^{iq\cdot b} A(s,t). \tag{2.85}$$

We can use this definition together with (2.84) to compute

$$\mathrm{Im}\delta_{\text{1-loop}}(s,b) = \frac{1}{2} \sum_{\substack{m_5,\rho_5,\epsilon_5 \\ m_6,\rho_6,\epsilon_6}} \delta^{3652}_{\text{tree}}(s,-b)^* \, \delta^{1564}_{\text{tree}}(s,b). \tag{2.86}$$

We conclude that the impact parameter representation absorbs the remaining phase space integrals in the optical theorem, resulting in a purely multiplicative formula. In fact, in the case where the particles on the left and right of the diagram do not change (i.e. 1,5,2 and 3,6,4 are identical particles), such a statement holds to all-loops, leading to exponentiation of the tree-level phase shift, which is the basis for the famous eikonal approximation.

2.3.3 Vertex function

Another notion we will use is that of the vertex function, which arises when combining the optical theorem (2.84) with the factorization of the tree-level amplitudes (2.78) into three-point amplitudes. By combining the two results one sees that the sums over particles and their polarizations factorize into separate sums for particles 5 and 6, which we call the vertex function V

$$V(q_1, q_2) \equiv \sum_{m_5, \rho_5, \epsilon_5} A^{15P_1}(q_1) A^{25P_2}(q_2)\,. \tag{2.87}$$

Moreover, such a sum over representations and polarizations for each mass is given by tree-level unitarity as the residue of the four-point amplitudes with two external Pomerons

$$\operatorname*{Res}_{k_5^2=-m_5^2} A^{12P_1P_2}(k_5, q_1, q_2) = \sum_{\rho_5, \epsilon_5} A^{15P_1}(q_1) A^{25P_2}(q_2)\,. \tag{2.88}$$

In terms of diagrams this reads

$V(q_1,q_2) \equiv \sum_{m_5,\rho_5,\epsilon_5}$ 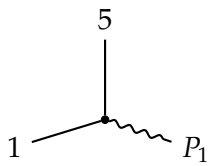 $\times$ 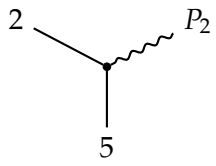 $= \sum_{m_5} \operatorname*{Res}_{k_5^2=-m_5^2}$ 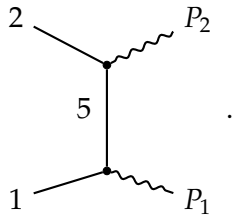 .

(2.89)

The vertex function combines all information about the exchanges of possibly spinning particles 5 and 6 into a single scalar function. In terms of the vertex function the optical theorem (2.84) in the Regge limit becomes

$$\begin{aligned}\mathrm{Im} A_{\text{1-loop}}(s,q) = -\frac{1}{4s}\int \frac{dq_1 dq_2}{(2\pi)^{D-2}}\,\delta(q-q_1-q_2) \\ \left(\frac{8}{\alpha'}\right)^2 \beta(t_1)^*\beta(t_2) V(q_1,q_2)^2 \left(\frac{\alpha' s}{4}\right)^{j(t_1)+j(t_2)}\,,\end{aligned} \tag{2.90}$$

where $t_i = -q_i^2$.

2.3.4 Spinning three-point amplitudes

Since it will be important later to compare tensor structures in AdS and flat space, we will provide here some more details on the tensor structures of the three-point amplitudes that appear in the unitarity cut of the four-point amplitude $A^{12P_1P_2}$ discussed above. The external momentum k_1 and the exchanged momentum l_1, with light-cone components given in the Regge limit by (2.83), fix the momentum $k_5 = k_1 - l_1$ as shown in the figure below. We may, however, change frame such that k_5 has no transverse momentum [53]. Such change of frame

does not alter the fact that the light-cone components of l_1 are subleading. The same applies to l_2. Thus in the Regge limit we can safely write

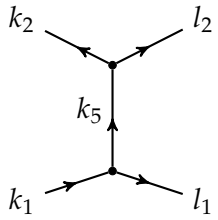

$$\begin{aligned} k_5 &\approx \left(k_5^u, \frac{m_5^2}{k_5^u}, 0\right), \\ l_2 &\approx (0,0,q_2), \qquad k_2 = k_5 - l_2, \\ l_1 &\approx (0,0,q_1), \qquad k_1 = k_5 + l_1. \end{aligned} \tag{2.91}$$

We focus on the three-point amplitude $A^{15P_1}(q_1)$, which is related to the four-point amplitude via the tree-level unitarity (2.88). In this relation we have a sum over a basis of possible polarizations ϵ_5, which can be evaluated using completeness relations, e.g. for massive bosons [54]

$$\sum_{\epsilon_5} \epsilon_5^{\mu_1\dots\mu_{|\rho|}} \epsilon_5^{\nu_1\dots\nu_{|\rho|}} = P_{5\gamma_1}^{\mu_1} \dots P_{5\gamma_\rho}^{\mu_\rho} \pi_\rho^{\gamma_1\dots\gamma_{|\rho|};\sigma_1\dots\sigma_{|\rho|}} P_{5\sigma_1}^{\nu_1} \dots P_{5\sigma_\rho}^{\nu_\rho}, \tag{2.92}$$

where π_ρ is the projector to the irreducible $SO(D-1)$ representation ρ and

$$P_{5\nu}^{\mu} = \delta_\nu^\mu - \frac{k_5^\mu k_{5\nu}}{k_5^2}, \tag{2.93}$$

is a projector to the space transverse to k_5. We will always absorb the projectors $P_{5\nu}^\mu$ into the three-point amplitudes, i.e. consider amplitudes in a transverse configuration. That means that the indices corresponding to particle 5 have to be constructed from the projected momenta of the other particles, which are identical

$$P_{5\nu}^\mu l_{1\mu} = P_{5\nu}^\mu k_{1\mu}. \tag{2.94}$$

Apart from that, massive particles can also have a longitudinal polarization v which satisfies

$$v \cdot k_5 = 0, \qquad v^2 = 1, \tag{2.95}$$

and is given in this frame explicitly by

$$v_\mu = \frac{1}{m_5}\left(k_5^u, -\frac{m_5^2}{k_5^u}, 0\right). \tag{2.96}$$

For the case that particle 1 is a scalar, we can then construct A^{15P} in terms of the following manifestly transverse tensor structures

$$A^{15P}_{m_5,\rho_5,\boldsymbol{\mu}} = \sum_{k=0}^{|\rho_5|} a^k_{m_5,\rho_5}(t_1)\, i^{|\rho_5|} \sqrt{\alpha'}^{|\rho_5|-k} v_{\mu_1} \dots v_{\mu_k} q_{1\mu_{k+1}} \dots q_{1\mu_{|\rho_5|}}, \tag{2.97}$$

where we introduced boldface indices $\boldsymbol{\mu}$ as multi-indices that stand for the $|\rho|$ indices for the irrep ρ. By abuse of language we defined the vector $q_1 \equiv (0,0,q_1)$, since q_1 is transverse. If particle 1 carries spin as well, as will be the case for the gravitons considered later on, we construct the polarization tensors out of the vector $\xi_1 = (\xi_1^u, \xi_1^v, \epsilon_1)$. In this case, again defining $\epsilon_1 \equiv (0,0,\epsilon_1)$, the amplitudes take the following form in the Regge limit

$$A^{15P}_{m_5,\rho_5,\boldsymbol{\mu}} = \sum_{n=0}^{\ell_1} \sum_{k=0}^{|\rho_5|-n} a^{k,n}_{m_5,\rho_5}(t_1)\, i^{|\rho_5|} \sqrt{\alpha'}^{|\rho_5|+\ell_1-2n-k} (\epsilon_1 \cdot q_1)^{\ell_1-n} \\ \epsilon_{1\mu_1} \dots \epsilon_{1\mu_n} v_{\mu_{n+1}} \dots v_{\mu_{n+k}} q_{1\mu_{n+k+1}} \dots q_{1\mu_{|\rho_5|}}\,, \tag{2.98}$$

as can be checked by comparing with the explicit amplitudes computed in [53]. These choices for the tensor structures are particularly convenient since $q_1 \cdot v = \epsilon_1 \cdot v = 0$. Contact with the momentum frame used in the previous subsections is made by identifying the Lorentz invariant $A^{12P_1P_2}$.

2.4 AdS impact parameter space

Our goal in this section is to compute the Regge limit of a scalar four-point function in a perturbative large N CFT at one-loop and finite Δ_{gap}. At finite Δ_{gap} we have to consider the t-channel exchange of all possible double-trace operators and also single-trace operators, which are respectively dual to tidal excitations of the external scattering states and to long-string creation in the string theory context. It was shown in [44] that the exchange of single-trace operators dual to the long-string creation effects is subleading in the Regge limit. Therefore we only need to consider the exchange of double-trace operators. This is where the new perturbative CFT optical theorem (2.5) takes a central role, as it allows us to compute the contributions of double-trace operators to the correlator starting from the corresponding tree-level correlators. The contribution of the leading Regge trajectory to the scalar tree-level correlators is known to leading order in the Regge limit [4, 40].

In this section we will therefore study (2.5) in the Regge limit, and this time we expand the tree-level correlators in the s-channel. In the Regge limit the four external points are in Lorentzian kinematics as depicted in figure 2.3. In this configuration all distances between points are spacelike except for $y_{14}^2, y_{23}^2 < 0$. The Regge limit is reached by sending the four-points to infinity along the light cones

$$y_1^+ \to -\infty, \quad y_2^+ \to +\infty, \quad y_3^- \to -\infty, \quad y_4^- \to +\infty\,. \tag{2.99}$$

The Regge limit can be directly applied to the left hand side of (2.5). The terms on the Regge sheets $A^{\circlearrowleft}(y_i)$ and $A^{\circlearrowright}(y_i)$ are dominant over the Euclidean terms in this limit. However,

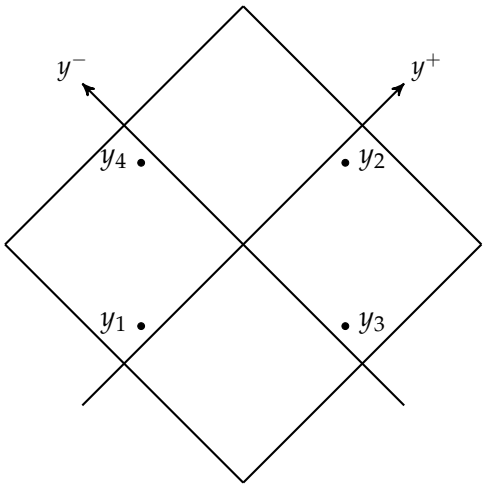

FIGURE 2.3: Kinematics in the central Poincaré patch with coordinates y_i. Time is on the vertical axis, transverse directions are suppressed.

we cannot apply the Regge limit directly to the right hand side of (2.5) as the shadow integrals range over Euclidean configurations. Hence we will apply Wick rotations on the points y_5, y_6, y_7, y_8 to obtain a gluing of the discontinuities of Lorentzian correlators. We will assume that in the Regge limit the dominant contribution to the gluing formula comes from the domain where the individual tree-level correlators are in the Regge limit themselves. We do not provide a proof of this assumption but we justify it in section 2.4.1.

When each four-point function in (2.61) is in the Regge limit, the points y_5, y_6, y_7, y_8 are placed in the same positions as y_1, y_4, y_2, y_3 in fig. 2.3, respectively. Thus y_7 is in the future of y_8 and this pair is spacelike from y_1, y_4, y_5, y_6. Similarly, y_6 is in the future of y_5 and is spacelike from y_2, y_3, y_7, y_8. For the chosen kinematics we put the pair y_5, y_6 in anti-time order using the epsilon prescription of (2.58) with $\epsilon_5 > \epsilon_6$, and the pair y_7, y_8 in time order using $\epsilon_7 > \epsilon_8$. Applying this on (2.70) gives the following formula for the Regge limit of the double discontinuity

$$\text{dDisc}_t A_{\text{1-loop}}(y_k)\Big|_{\text{d.t.}} = -\frac{1}{2}\sum_{\mathcal{O}_5,\mathcal{O}_6}\frac{1}{N_{\mathcal{O}_5}N_{\mathcal{O}_6}}\int dy_5 dy_6 dy_7 dy_8\, \langle[\mathcal{O}_2,\mathcal{O}_3]\mathcal{O}_5\mathcal{O}_6\rangle_{\text{tree}}\langle\widetilde{\mathcal{O}}_5\widetilde{\mathcal{O}}_7^\dagger\rangle \langle\widetilde{\mathcal{O}}_6\widetilde{\mathcal{O}}_8^\dagger\rangle\langle\mathcal{O}_7\mathcal{O}_8[\mathcal{O}_4,\mathcal{O}_1]\rangle_{\text{tree}}\Big|_{[\mathcal{O}_5\mathcal{O}_6]}. \quad (2.100)$$

The relative ordering between ϵ_5, ϵ_7 and ϵ_6, ϵ_8 is irrelevant as the pairs, appearing in the two-point functions on the right hand side of (2.100), are spacelike separated in the Regge configuration.

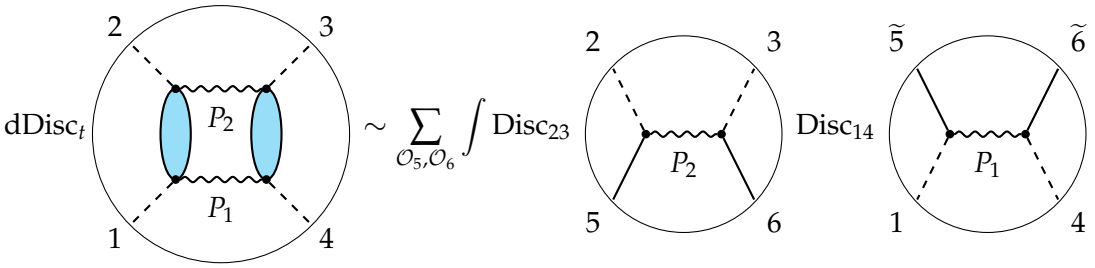

FIGURE 2.4: Optical theorem in the Regge limit in terms of Witten diagrams. The tree-level correlators are dominated by s-channel Pomeron exchange. The external operators are scalars, while $\mathcal{O}_5$ and $\mathcal{O}_6$ are summed over all states that couple to the external scalars and the Pomeron (tidal excitations). The ellipses on the l.h.s. indicate that all string excitations are taken into account.

In this section we define the discontinuities as the commutators inserted into the fully Lorentzian correlators

$$\begin{aligned} \text{Disc}_{14}\, A^{1874}(y_i) &:= \langle \mathcal{O}_7\mathcal{O}_8[\mathcal{O}_4,\mathcal{O}_1]\rangle = A^{1874^{\circlearrowleft}}(y_i) - A^{1874}_{\text{Euc}}(y_i)\,, \\ \text{Disc}_{23}\, A^{3652}(y_i) &:= \langle [\mathcal{O}_2,\mathcal{O}_3]\mathcal{O}_5\mathcal{O}_6\rangle = A^{3652}_{\text{Euc}}(y_i) - A^{3652^{\circlearrowleft}}(y_i)\,. \end{aligned} \tag{2.101}$$

This definition differs slightly from the one in (2.22). Stripping out the appropriate prefactors from (2.101), one can check that these single discontinuities can be equivalently defined as

$$\begin{aligned} \text{Disc}_{14}\, \mathcal{A}^{1234}(z,\bar{z}) &:= e^{i\pi(a+b)}\mathcal{A}^{1234}(z,\bar{z}^{\circlearrowleft}) - e^{-i\pi(a+b)}\mathcal{A}^{1234}(z,\bar{z})\,, \\ \text{Disc}_{23}\, \mathcal{A}^{1234}(z,\bar{z}) &:= \mathcal{A}^{1234}(z,\bar{z}) - \mathcal{A}^{1234}(z,\bar{z}^{\circlearrowleft})\,, \\ \text{Disc}_{23}\, \mathcal{A}^{3412}(z,\bar{z}) &= e^{-i\pi(a+b)}\mathcal{A}^{3412}(z,\bar{z}) - e^{i\pi(a+b)}\mathcal{A}^{3412}(z,\bar{z}^{\circlearrowleft})\,. \end{aligned} \tag{2.102}$$

Starting from the discontinuity defined in (2.22), these expressions result from continuing another half circle in $\bar{z}$, so that the different terms are either evaluated at the original position or continued a full circle around 1. The extra phase comes from the additional Wick rotations. The final result matches the definition of the discontinuity in [50]. Note that $\bar{z}$ is continued an extra half circle in opposite directions for the first two lines in (2.102), so that with these definitions the relation to the dDisc in (2.21) remains valid.[4] Therefore the optical theorem in the Regge limit can still be expressed as

$$\text{dDisc}_t A_{1-\text{loop}}(y_i)\Big|_{\text{d.t.}} = -\frac{1}{2}\sum_{\substack{\mathcal{O}_5,\mathcal{O}_6 \\ \in\, s.t.}}\int dy_5 dy_6\ \text{Disc}_{23}\, A^{3652}_{\text{tree}}(y_k)\, \mathbf{S}_5\mathbf{S}_6\, \text{Disc}_{14}\, A^{1564}_{\text{tree}}(y_k)\Big|_{[\mathcal{O}_5\mathcal{O}_6]}\,, \tag{2.103}$$

with the discontinuities as defined in the first and third lines of (2.102), and the gluing and shadow integrals now ranging over Minkowski space. This formula is also depicted in figure 2.4 in terms of Witten diagrams.

[4] For t-channel blocks, the new definitions for the discontinuities in (2.102) are related to the old definition in (2.22) by a phase, for example, for Disc$_{14}$ the relative phase is $e^{i\pi\tau_{\mathcal{O}}/2}$.

We should also note that for real $z, \bar{z}$, Disc_{23} in the third line of (2.102) is related to Disc_{14} in the first line by

$$\text{Disc}_{23}\,\mathcal{A}^{3412}(z,\bar{z}) = -\left(\text{Disc}_{14}\,\mathcal{A}^{1234}(z,\bar{z})\right)^*\Big|_{(a,b)\to(-b,-a)}\,, \quad 0<z,\bar{z}<1\,. \tag{2.104}$$

Applied to the correlators appearing in (2.103) this reads

$$\text{Disc}_{23}\,\mathcal{A}^{3652}(z,\bar{z}) = -\left(\text{Disc}_{14}\,\mathcal{A}^{1564}(z,\bar{z})\right)^*\Big|_{1564\to3652}\,. \tag{2.105}$$

To benefit from this useful relation, we will always strip out a pre-factor such that we obtain the correlator $\mathcal{A}^{3652}(z,\bar{z})$ on the right hand side of (2.103). Otherwise we would have to use the second line of (2.102) for Disc_{23}. Finally, in the Regge limit the analytically continued correlators are dominant over the Euclidean contributions so that we have

$$\begin{aligned}
\text{Disc}_{14}\,\mathcal{A}^{1234}(z,\bar{z}) &\approx e^{i\pi(a+b)}\mathcal{A}^{1234}(z,\bar{z}^{\circlearrowleft})\,,\\
\text{Disc}_{23}\,\mathcal{A}^{3412}(z,\bar{z}) &\approx -e^{i\pi(a+b)}\mathcal{A}^{3412}(z,\bar{z}^{\circlearrowleft})\,,\\
\text{dDisc}_{t}\,\mathcal{A}^{1234}(z,\bar{z}) &\approx -\frac{1}{2}\left(e^{i\pi(a+b)}\mathcal{A}^{1234}(z,\bar{z}^{\circlearrowleft}) + e^{-i\pi(a+b)}\mathcal{A}^{1234}(z,\bar{z}^{\circlearrowleft})\right)\,,
\end{aligned} \tag{2.106}$$

where the $\approx$ sign means we took the Regge limit. In order to account for the tidal excitations, the operators $\mathcal{O}_5$ and $\mathcal{O}_6$ can carry spin, in which case their indices are contracted with the ones of $\widetilde{\mathcal{O}}_5$ and $\widetilde{\mathcal{O}}_6$ and sums over tensor structures are implied. In subsections 2.4.1, 2.4.2 and 2.4.3 below we will mostly suppress the aspect of spinning correlators. We will come back to this issue in subsection 2.4.4.

2.4.1 Regge limit

To obtain the impact parameter representation, we first change the coordinate system placing each point on a different Poincaré patch as shown in figure 2.5. We use the following coordinate transformations

$$\begin{aligned}
x_i = \left(x_i^+, x_i^-, x_{i\perp}\right) &= -\frac{1}{y_i^+}\left(1, y_i^2, y_{i\perp}\right)\,, \quad i=1,2,5,7\,,\\
x_i = \left(x_i^+, x_i^-, x_{i\perp}\right) &= -\frac{1}{y_i^-}\left(1, y_i^2, y_{i\perp}\right)\,, \quad i=3,4,6,8\,.
\end{aligned} \tag{2.107}$$

In the new x_i coordinates, the Regge limit corresponds to placing the four external points at the origin of their respective Poincaré patches,

$$x_1, x_2, x_3, x_4 \to 0\,. \tag{2.108}$$

However, x_5 to x_8 are integrated over in the CFT optical theorem.

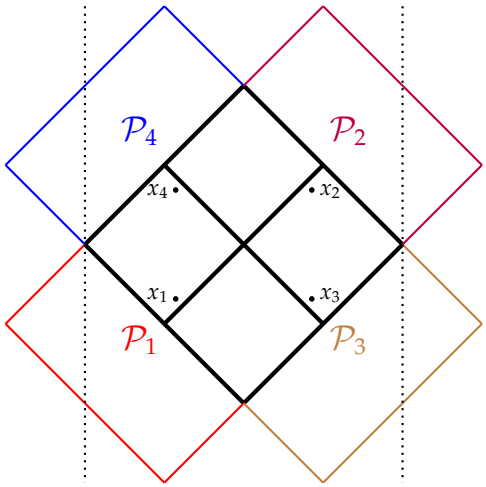

FIGURE 2.5: The external operators at coordinates x_i in their respective Poincaré patches $\mathcal{P}_i$. The black dotted lines are identified when the Poincaré patches are wrapped on the boundary of the global AdS cylinder.

Conformal correlators transform covariantly under the transformation (2.107). In the scalar case we have

$$A\left(y_i\right) = (-y_1^+)^{-\Delta_1}(y_2^+)^{-\Delta_2}(-y_3^-)^{-\Delta_3}(y_4^-)^{-\Delta_4}A\left(x_i\right) . \tag{2.109}$$

In the spinning case, one must additionally account for the Jacobian matrix $\partial y^a/\partial x^m$.[5]

Next we use conformal symmetry to express the correlator in terms of two vectors. This is similar to expressing the correlator in terms of two scalar cross-ratios, with the difference that here we fix two, instead of the customary three, positions using translations and special conformal transformations to express the correlator in terms of the remaining two position vectors. We can follow [43] and use a translation to send x_1 to 0 which, due to the different transformations in (2.107) (see also [55]), will act as a special conformal transformation on the Poincaré patches for x_3 and x_4,

$$x_1 \to 0\,, \quad x_2 \to x_2 - x_1\,, \quad x_{3,4} \to \frac{x_{3,4} - x_{3,4}^2 x_1}{1 - 2x_{3,4}\cdot x_1 + x_{3,4}^2 x_1^2}\,. \tag{2.110}$$

Next we implement a translation on the x_3 and x_4 patches (acting as special conformal transformation on $x_{1,2}$) to also map x_4 to 0 in its own patch and find that the correlator as a function of the Poincaré patch coordinates $A(x_i)$, as defined in (2.109), can always be expressed as

$$A(x_1, x_2, x_3, x_4) \approx A(0, -x, \bar{x}/\bar{x}^2, 0) \equiv A(x, \bar{x})\,, \tag{2.111}$$

[5]For external spinning operators, the conformal transformations have a non-trivial rotation matrix $\partial y^a/\partial x^m$. Conformal covariance of the correlators gives, in the representative example of two vectors and two scalars [43], $A^{ab}\left(y_i\right) = \left(-y_1^+ y_2^+\right)^{-1-\Delta_V}\left(-y_3^- y_4^-\right)^{-\Delta_S}\frac{\partial y_1^a}{\partial x_1^m}\frac{\partial y_2^b}{\partial x_2^n}A^{mn}\left(x_i\right)$. These matrices ensure that the inversion tensors are correctly mapped from y_i to x_i variables, preserving their form.

with

$$x \approx x_1 - x_2\,, \qquad \bar{x} \approx x_3 - x_4\,, \tag{2.112}$$

in the Regge limit (2.108).

It is further convenient to implement the coordinate change using embedding space coordinates $P^M \in \mathbb{R}^{2,d}$

$$P^M = \left(P^+, P^-, P^m\right), \qquad P \cdot P = -P^+P^- + \eta_{mn}P^mP^n\,. \tag{2.113}$$

These are related to the coordinates $y^m \in \mathbb{R}^{1,d-1}$ of physical Minkowski space by [43]

$$P^M = \left(y^+, y^-, 1, y^2, y_\perp\right) \quad \Rightarrow \quad P_{ij} \equiv -2P_i \cdot P_j = (y_i - y_j)^2\,, \tag{2.114}$$

and to the coordinates x_i by

$$\begin{aligned} P_1^M &= -y_1^+\left(-1, -x_1^2, x_1^m\right), \quad P_2^M = y_2^+\left(-1, -x_2^2, x_2^m\right), \\ P_3^M &= -y_3^-\left(-x_3^2, -1, x_3^m\right), \quad P_4^M = y_4^-\left(-x_4^2, -1, x_4^m\right). \end{aligned} \tag{2.115}$$

One can easily show that the cross-ratios (2.26) are given in terms of x and $\bar{x}$ as

$$z\bar{z} = x^2\bar{x}^2\,, \qquad (1-z)(1-\bar{z}) = 1 + x^2\bar{x}^2 + 2x\cdot\bar{x}\,, \tag{2.116}$$

and the kinematic prefactor (2.25) becomes

$$T^{1234} = \frac{(-y_1^+)^{-\Delta_1}(y_2^+)^{-\Delta_2}(-y_3^-)^{-\Delta_3}(y_4^-)^{-\Delta_4}}{x^{\Delta_1+\Delta_2}\bar{x}^{\Delta_3+\Delta_4}}\,. \tag{2.117}$$

When combining (2.24) and (2.109), the numerator of the last expression cancels the Jacobian prefactor in (2.109) to give,

$$A\left(x_i\right) = \frac{A^{1234}(z,\bar{z})}{x^{\Delta_1+\Delta_2}\bar{x}^{\Delta_3+\Delta_4}}\,. \tag{2.118}$$

If we now study the correlator $A^{3652}(x_i)$, a priori we have to take into account that only x_2 and x_3 are affected by the Regge limit. However, we will assume that the integration will be dominated by the region where the integration points are also boosted. Using the embedding space coordinates

$$P_5^M = -y_5^+\left(-1, -x_5^2, x_5^m\right), \qquad P_6^M = y_6^-\left(-x_6^2, -1, x_6^m\right), \tag{2.119}$$

we find

$$x' \approx x_5 - x_2\,, \qquad \bar{x}' \approx x_3 - x_6\,. \tag{2.120}$$

Where the primed variables are meant to emphasize that the points $1, 4$ are replaced by $5, 6$ in

this correlator as compared to (2.111). Performing these steps for all the correlators in (2.103) we find,

$$\begin{aligned} \text{dDisc}_t A_{\text{1-loop}}(x_{12}, x_{34}) = -\frac{1}{2} \sum_{\mathcal{O}_5, \mathcal{O}_6} \int dx_5 dx_6 \; \text{Disc}_{23} \, A^{3652}_{\text{tree}}(x_{36}, x_{52}) \\ \mathbf{S}_5 \mathbf{S}_6 \, \text{Disc}_{14} \, A^{1564}_{\text{tree}}(x_{15}, x_{64}) \Big|_{[\mathcal{O}_5 \mathcal{O}_6]} , \end{aligned} \tag{2.121}$$

where we stop explicitly mentioning that we are dealing with only the contribution of double-trace operators as single-trace contributions are subleading in the limit considered. Let us stress that in order to write the correlators on the right hand side in terms of two differences, we assumed that each of the individual tree-level correlators are in the Regge limit themselves. The easiest way to justify this is in Fourier space using the impact parameter transform defined below. Each tree-level position space correlator is dominated by a power $\sigma^{1-j(\nu)}$ in the Regge limit, which maps to a power of the AdS center of mass energy $S^{j(\nu)-1}$ in impact parameter space. Since the optical theorem is multiplicative in impact parameter space, subleading Regge trajectories or kinematical corrections from the conformal block at finite boost get mapped to smaller powers of S, and therefore do not contribute to the leading behavior. The eikonal approximation in AdS [37] gives additional intuition for this, since it means that even in AdS, the particles remain essentially undeflected, scattering forward each time they exchange a Pomeron. Furthermore, we will show in section 2.5 that this configuration reproduces the behavior at one-loop derived in [44].

2.4.2 Impact parameter space

Let us now consider the two-point functions $\langle \widetilde{\mathcal{O}}_5 \widetilde{\mathcal{O}}_7 \rangle$ and $\langle \widetilde{\mathcal{O}}_8 \widetilde{\mathcal{O}}_6 \rangle$ for the shadow transforms in (2.121). In the Regge configuration, x_5 is the patch of x_1, x_6 is the patch of x_4, x_7 is the patch of x_2 and x_8 is the patch of x_3. As explained in [12, 37], the two-point function between two coordinates on adjacent Poincaré patches has an additional phase factor $e^{i\pi\Delta}$ and this phase can be accounted for by switching from the $i\epsilon$ prescription of a Feynman propagator to that of a Wightman propagator (see [37]). The normalization of the shadow transform in (2.10) and (2.11) is obtained from the Fourier transform of a two-point function as the shadow transform acts multiplicatively in Fourier space (see section 3.2 of [11]). The normalization in (2.11) is obtained from the Fourier transform of a Euclidean two-point function, which matches the one of a Lorentzian two-point function with Feynman $i\epsilon$ prescription. The Wightman propagator in momentum space however has support only on the future lightcone and the coefficient of the Fourier transform is different (see Appendix B of [37] and section 2.1 of [56])

$$\int dx \frac{e^{-2iq\cdot x}}{\left[-(x^0 - i\epsilon)^2 + \vec{x}^2\right]^\Delta} = \mathcal{M}_\mathcal{O} \, \Theta(q^0) \, \Theta(-q^2) \left(-q^2\right)^{\Delta - \frac{d}{2}} , \tag{2.122}$$

with

$$\mathcal{M}_{\mathcal{O}} = \frac{2\pi^{\frac{d}{2}+1}}{\Gamma(\Delta)\Gamma\left(\Delta - \frac{d}{2}+1\right)}\,. \tag{2.123}$$

Consequently we change the normalization $N_{\mathcal{O}}$ of the shadow transform in (2.10) to (for scalar operators)

$$\mathcal{N}_{\mathcal{O}} = \mathcal{M}_{\mathcal{O}}\mathcal{M}_{\tilde{\mathcal{O}}}\,. \tag{2.124}$$

Next we define, following [40], the impact parameter representation as the Fourier transform of the discontinuity of the correlator in the two remaining vectors[6]

$$\text{Disc}_{14}\, A^{1jk4}(x_{1j}, x_{k4}) = \int dp\, d\bar{p}\, e^{-2ip\cdot x_{1j} - 2i\bar{p}\cdot x_{k4}} B^{1jk4}(p,\bar{p})\,, \tag{2.125}$$

where the function $B(p,\bar{p})$ has support only on the future Milne wedge of p and $\bar{p}$. Using (2.105) on (2.125) we get the Fourier transform of Disc_{23}.

$$\text{Disc}_{23}\, A^{3kj2}(x_{3k}, x_{j2}) = -\int dp\, d\bar{p}\, e^{-2ip\cdot x_{3k} - 2i\bar{p}\cdot x_{j2}} B^{3kj2}(-p,-\bar{p})^*\,. \tag{2.126}$$

The causal relations and thus the $i\epsilon$ prescription in (2.126) are opposite to those in (2.125) and the complex conjugation prescribed in (2.105) compensates for that. Inserting (2.125) into (2.121) and using that $A^{1\tilde{5}\tilde{6}4}_{\text{tree}}$ is a double shadow transform of A^{1784}_{tree} we obtain, upon using (2.105) for the Disc_{23},

$$\begin{aligned}\text{dDisc}_t A_{\text{1-loop}}(x_{12}, x_{34}) = \frac{1}{2}\sum_{\mathcal{O}_5,\mathcal{O}_6}\int dx_5\, dx_6\, dx_7\, dx_8 \int dp\, d\bar{p}\, dp'\, d\bar{p}' \\ \times e^{-2i(p'\cdot x_{36} + \bar{p}'\cdot x_{52} + p\cdot x_{17} + \bar{p}\cdot x_{84})} B^{3652}_{\text{tree}}(-p',-\bar{p}')^* B^{1564}_{\text{tree}}(p,\bar{p}) \\ \times \frac{T^{(\rho_5)}(x_{75})}{\mathcal{N}_{\mathcal{O}_5}\left[-(x^0_{75}-i\epsilon)^2 + \vec{x}^2_{75}\right]^{d-\Delta_5}} \frac{T^{(\rho_6)}(x_{68})}{\mathcal{N}_{\mathcal{O}_6}\left[-(x^0_{68}-i\epsilon)^2 + \vec{x}^2_{68}\right]^{d-\Delta_6}}\Bigg|_{[\mathcal{O}_5\mathcal{O}_6]}\,.\end{aligned} \tag{2.127}$$

$T^{(\rho)}(x_{ij})$ is the tensor structure for the two-point function of an operator with $SO(d)$ quantum number ρ. For example it is the familiar inversion tensor $\eta^{\mu\nu} - 2\frac{x^\mu x^\nu}{x^2}$ for spin 1 operators. Note that we have B^{1564}_{tree} instead of B^{1784}_{tree}, as the superscripts now only indicate the dimensions of the corresponding operators and $\Delta_5 = \Delta_7$, $\Delta_6 = \Delta_8$.

[6]The AdS impact parameter representation was previously defined in [31, 40, 41] as the Fourier transform of the correlator on the second sheet $A(z,\bar{z}^{\circlearrowleft})$. Since this contribution dominates in the Regge limit, it is indistinguishable from the discontinuity of the correlator in this limit. However, in the t-channel the two notions are clearly different and it was necessary to take the discontinuity to derive (2.5). In the next section we will see that the discontinuity is the better choice also in the s-channel.

We can now express the two-point functions from the shadow transforms in Fourier space by inverting (2.122)

$$\frac{T^{(\rho)}(x)}{[-(x^0-i\epsilon)^2+\vec{x}^2]^{d-\Delta}}=\frac{\mathcal{M}_{\tilde{\mathcal{O}}}}{\pi^d}\int\limits_M dq\, e^{-2iq\cdot x}\,\widehat{T}^{(\rho)}(q)\,(-q^2)^{\frac{d}{2}-\Delta}\,. \tag{2.128}$$

The Fourier space integral is over the future Milne wedge M as the Fourier transform has support only on this domain. $\widehat{T}^{(\rho)}(q)$ is the tensor structure of the two-point function in Fourier space, which has been discussed for example in [56]. It is a tensor composed of q^μ and $\eta^{\mu\nu}$ that can be factorized into a product of new tensors $t^{(\rho)}(q)$ as follows

$$\widehat{T}^{(\rho)}(q)^{\mu_1\dots\mu_{|\rho|}}_{\nu_1\dots\nu_{|\rho|}}=t^{(\rho)}(q)^{\mu_1\dots\mu_{|\rho|}}_{\sigma_1\dots\sigma_{|\rho|}}t^{(\rho)}(q)^{\sigma_1\dots\sigma_{|\rho|}}_{\nu_1\dots\nu_{|\rho|}}\,. \tag{2.129}$$

Using (2.128) in (2.127) we end up with four position integrals over x_5, x_6, x_7, x_8 and six integrals over $q, \bar{q}$ (from the four-point functions) and $p, \bar{p}, p', \bar{p}'$. The four position integrals give four Dirac delta functions with which we can eliminate the $q, \bar{q}, p', \bar{p}'$ integrals to obtain

$$\begin{aligned}\mathrm{dDisc}_t A_{\text{1-loop}}(x_{12},x_{34})=\frac{\pi^{2d}}{2}\sum_{\mathcal{O}_5,\mathcal{O}_6}\frac{1}{\mathcal{M}_{\mathcal{O}_5}\mathcal{M}_{\mathcal{O}_6}}\int dp\,d\bar{p}\,e^{-2i(p\cdot x_{12}+\bar{p}\cdot x_{34})}\\ \left.\frac{B^{3652}_{\text{tree}}(-\bar{p},-p)^*\;\widehat{T}^{(\rho_5)}(p)\,\widehat{T}^{(\rho_6)}(\bar{p})\;B^{1564}_{\text{tree}}(p,\bar{p})}{(-p^2)^{\Delta_5-\frac{d}{2}}(-\bar{p}^2)^{\Delta_6-\frac{d}{2}}}\right|_{[\mathcal{O}_5\mathcal{O}_6]},\end{aligned} \tag{2.130}$$

with an implicit index contraction between B^{1564}_{tree} and B^{3652}_{tree} and the tensor structures $\widehat{T}^{(\rho)}$. At this point we use (2.129) and absorb the $t^{(\rho)}(q)$ tensors into the definition of the phase shifts B_{tree}. This means that one needs to take it into account if one wants to relate tensor structures of CFT correlators and phase shifts, but we will not need to do such a basis change explicitly in this work. Using (2.106) we see that the double discontinuity corresponds to the quantity $-\mathrm{Re}B(p,\bar{p})$ in impact parameter space. Thus we find the following gluing formula for the impact parameter representation, which is purely multiplicative,

$$-\mathrm{Re}B_{\text{1-loop}}(p,\bar{p})=\frac{\pi^{2d}}{2}\sum_{\mathcal{O}_5,\mathcal{O}_6}\frac{1}{\mathcal{M}_{\mathcal{O}_5}\mathcal{M}_{\mathcal{O}_6}}\left.\frac{B^{3652}_{\text{tree}}(-\bar{p},-p)^*\,B^{1564}_{\text{tree}}(p,\bar{p})}{(-p^2)^{\Delta_5-\frac{d}{2}}(-\bar{p}^2)^{\Delta_6-\frac{d}{2}}}\right|_{[\mathcal{O}_5\mathcal{O}_6]}. \tag{2.131}$$

Let us consider the case when $\mathcal{O}_5=\mathcal{O}_1$ and $\mathcal{O}_6=\mathcal{O}_3$. In this case, it is useful to strip out a scale factor similar to that in (2.118) from the impact parameter representation

$$B^{jjkk}(p,\bar{p})=\frac{\mathcal{M}_{\mathcal{O}_j}\mathcal{M}_{\mathcal{O}_k}\,\mathcal{B}^{jjkk}(p,\bar{p})}{(-p^2)^{\frac{d}{2}-\Delta_j}\,(-\bar{p}^2)^{\frac{d}{2}-\Delta_k}}\,. \tag{2.132}$$

Using (2.122) one sees that with this choice of normalization the impact parameter representation of the MFT correlator is $\mathcal{B}^{jjkk}_{\text{MFT}}=1$, which is necessary for the eikonalization of the

phase shift in AdS gravity. Inspired by this fact we choose the normalization

$$B^{ijkl}(p,\bar{p}) = \frac{\sqrt{\mathcal{M}_{\mathcal{O}_i}\mathcal{M}_{\mathcal{O}_j}\mathcal{M}_{\mathcal{O}_k}\mathcal{M}_{\mathcal{O}_l}}\,\mathcal{B}^{ijkl}(p,\bar{p})}{(-p^2)^{\frac{d-\Delta_i-\Delta_j}{2}}(-\bar{p}^2)^{\frac{d-\Delta_k-\Delta_l}{2}}}\,, \tag{2.133}$$

for the general case. This gives the following compact form for the optical theorem in impact parameter space

$$-\text{Re}\mathcal{B}_{\text{1-loop}}(p,\bar{p}) = \frac{1}{2}\sum_{\mathcal{O}_5,\mathcal{O}_6}\mathcal{B}^{3652}_{\text{tree}}(-\bar{p},-p)^*\,\mathcal{B}^{1564}_{\text{tree}}(p,\bar{p})\Big|_{[\mathcal{O}_5\mathcal{O}_6]}\,. \tag{2.134}$$

We also introduce impact parameter variables later.

$$S = \sqrt{p^2\bar{p}^2}, \qquad \cosh L = -\frac{p\cdot\bar{p}}{\sqrt{p^2\bar{p}^2}}\,. \tag{2.135}$$

In [44], the Regge limit of a one-loop four-point function of scalars was studied in the large λ regime with $S \gg \lambda \gg 1$. The contribution of tidal excitations to the correlator is suppressed in this regime. It corresponds to just one term in the sum on the right hand side of (2.134) i.e. with $\mathcal{O}_5 = \mathcal{O}_1$ and $\mathcal{O}_6 = \mathcal{O}_3$. We show in section 2.5.1 that this term from our formula (2.134) reproduces the result from [44] in the large λ or equivalently the large Δ^2_{gap} limit. We do not need to discard any shadow double-trace contributions for this match. This motivates us to assume that the only non-zero contributions to the gluing of tree-level correlators in the Regge limit is from the physical double-traces $[\mathcal{O}_5\mathcal{O}_6]$, and we will drop the explicit projections henceforth. This is compatible with the intuition that there is no need to project out shadow operators in a Lorentzian CFT optical theorem.

2.4.3 *s*-channel discontinuities in the Regge limit

Next we have to analyze the discontinuities on the right hand side of the optical theorem (2.103). The discontinuity of the scalar s-channel block was recently computed in general without taking the Regge limit in [50] and we will review it here. The generalization to external spinning operators is done in section 2.4.4, after taking the Regge limit. Let us take the conformal partial wave expansion (2.29) in the s channel and use the symmetry of the integrand to extend the integration region at the cost of a factor $1/2$

$$A^{1234}(z,\bar{z}) = \frac{1}{2}\sum_J\int_{\frac{d}{2}-i\infty}^{\frac{d}{2}+i\infty}\frac{d\Delta}{2\pi i}\,I^{1234}(\Delta,J)\,\psi^{1234}_{\text{good},\mathcal{O}}(z,\bar{z})\,. \tag{2.136}$$

Let $\psi^{1234}(z,\bar{z})$ be the partial wave $\Psi^{1234}(y_i)$ with the prefactor T^{1234} stripped off. $\psi^{1234}_{\text{good},\mathcal{O}}(z,\bar{z})$ is the conformal partial wave with an additional term that vanishes for integer spin but

ensures favorable properties for non-integer spin [50]. The new partial wave is given by

$$\psi^{1234}_{\text{good},\mathcal{O}}(z,\bar{z}) = \psi^{1234}_{\mathcal{O}}(z,\bar{z}) + 2\pi\, S(\mathcal{O}_3\mathcal{O}_4[\widetilde{\mathcal{O}}^\dagger])\, K_{J+d-1,1-\Delta}\, \xi^{(a,b)}_{\Delta,J}\, g^{1234}_{J+d-1,1-\Delta}(z,\bar{z})\,, \tag{2.137}$$

where $g^{1234}_{\Delta,J}(z,\bar{z})$ is the usual conformal block, the constants a, b are defined below (2.60) and

$$\begin{aligned}
\xi^{(a,b)}_{\Delta,J} &= \left(s^{(a,b)}_{\Delta+J} - s^{(a,b)}_{\Delta+2-d-J}\right) \frac{\Gamma\left(-J-\frac{d-2}{2}\right)}{\Gamma(-J)}\,,\\
s^{(a,b)}_{\beta} &= \frac{\sin\left(\pi(a+\beta/2)\right)\,\sin\left(\pi(b+\beta/2)\right)}{\sin(\pi\beta)}\,,\\
K_{\Delta,J} &= \frac{\Gamma(\Delta-1)}{\Gamma\left(\Delta-\frac{d}{2}\right)}\,\kappa^{(a,b)}_{\Delta+J}\,,\\
\kappa^{(a,b)}_{\beta} &= \frac{\Gamma\left(\frac{\beta}{2}-a\right)\Gamma\left(\frac{\beta}{2}+a\right)\Gamma\left(\frac{\beta}{2}-b\right)\Gamma\left(\frac{\beta}{2}+b\right)}{2\pi^2\Gamma(\beta-1)\Gamma(\beta)}\,.
\end{aligned} \tag{2.138}$$

With this conformal partial wave it is possible to compute the discontinuity exactly [50]

$$\frac{\text{Disc}_{14}\ \psi^{1234}_{\text{good},\mathcal{O}}(z,\bar{z})}{S(\mathcal{O}_3\mathcal{O}_4[\widetilde{\mathcal{O}}^\dagger])} = \frac{R^{1234}_{\mathcal{O}}(z,\bar{z})}{\pi i \kappa^{(a,b)}_{\Delta,J}}\,. \tag{2.139}$$

Here R is the so-called Regge block

$$\begin{aligned}
R^{1234}_{\mathcal{O}}(z,\bar{z}) = g^{1234}_{1-J,1-\Delta} - \kappa'^{(a,b)}_{\Delta+J}\, g^{1234}_{\Delta,J} - \frac{\Gamma(d-\Delta-1)\Gamma\left(\Delta-\frac{d}{2}\right)}{\Gamma(\Delta-1)\Gamma\left(\frac{d}{2}-\Delta\right)}\,\kappa'^{(a,b)}_{d-\Delta+J}\, g^{1234}_{d-\Delta,J} +\\
+\frac{\Gamma(J+d-2)\Gamma\left(-J-\frac{d-2}{2}\right)}{\Gamma\left(J+\frac{d-2}{2}\right)\Gamma(-J)}\,\kappa'^{(a,b)}_{\Delta+J}\,\kappa'^{(a,b)}_{d-\Delta+J}\, g^{1234}_{J+d-1,1-\Delta}\,,
\end{aligned} \tag{2.140}$$

with $\kappa'^{(a,b)}_{\beta}$ defined as

$$\kappa'^{(a,b)}_{\beta} = \frac{r^{(a,b)}_{\beta}}{r^{(a,b)}_{2-\beta}}\,, \qquad r^{(a,b)}_{\beta} = \frac{\Gamma(\frac{\beta}{2}+a)\Gamma(\frac{\beta}{2}+b)}{\Gamma(\beta)}\,. \tag{2.141}$$

Disc_{23} in the 3412 OPE channel can be obtained by using (2.104) on (2.139)

$$\frac{\text{Disc}_{23}\ \psi^{3412}_{\text{good},\mathcal{O}}(z,\bar{z})}{S(\mathcal{O}_1\mathcal{O}_2[\widetilde{\mathcal{O}}^\dagger])} = \frac{R^{3412}_{\mathcal{O}}(z,\bar{z})}{\pi i \kappa^{(-b,-a)}_{\Delta,J}}\,, \tag{2.142}$$

which was the reason to consider this channel for the correlators on the right hand side of (2.103). The Regge block is dominated in the Regge limit by [6, 40, 50]

$$g^{1234}_{1-J,1-\Delta}(z,\bar{z}) = \frac{4\pi^{\frac{d}{2}}\Gamma\left(\Delta-\frac{d}{2}\right)}{\Gamma(\Delta-1)}\sigma^{1-J}\left(\Omega_{\Delta-\frac{d}{2}}(\rho)+O(\sigma)\right)\,. \tag{2.143}$$

The σ, ρ cross-ratios introduced here are defined as

$$\sigma = \sqrt{z\bar{z}} = \sqrt{x^2\bar{x}^2}\,, \quad \cosh(\rho) = \frac{z+\bar{z}}{2\sqrt{z\bar{z}}} = -\frac{x\cdot\bar{x}}{\sqrt{x^2\bar{x}^2}}\,. \tag{2.144}$$

$\Omega_{i\nu}(\rho)$ is the harmonic function on $d-1$ dimensional hyperbolic space H_{d-1} transverse to the scattering plane in AdS_{d+1} [30]

$$\begin{aligned}\Omega_{i\nu}(\rho) = &-\frac{i\nu\sin(\pi i\nu)\Gamma(h-1+i\nu)\Gamma(h-1-i\nu)}{2^{2h-1}\pi^{h+\frac{1}{2}}\Gamma\left(h-\frac{1}{2}\right)} \\ &{}_2F_1\left(h-1+i\nu, h-1-i\nu, h-\frac{1}{2}, \frac{1-\cosh(\rho)}{2}\right)\,.\end{aligned} \tag{2.145}$$

Inserting everything into (2.136), we find the following expression for the discontinuity of the correlator in the Regge limit

$$\mathrm{Disc}_{14}\, A^{1234}(z,\bar{z}) = 2\pi i \sum_J \int_{-\infty}^{\infty} d\nu\; \alpha(\nu, J)\, \sigma^{1-J}\Omega_{i\nu}(\rho)\,, \tag{2.146}$$

with

$$\alpha(\nu, J) = -\frac{\pi^{\frac{d}{2}-2}\, S\left(\mathcal{O}_3\mathcal{O}_4\left[\left(-i\nu-\frac{d}{2}\right)^{\dagger}\right]\right)\Gamma(i\nu)}{2\pi\kappa^{(a,b)}_{i\nu+\frac{d}{2},J}\,\Gamma\left(i\nu+\frac{d}{2}-1\right)}\, I^{1234}\left(i\nu+\frac{d}{2}, J\right)\,. \tag{2.147}$$

As in flat space the sum in (2.146) is dominated by the large J contributions in the Regge limit and only finite due to a conspiration of the coefficients to ensure Regge boundedness. The next step is therefore to perform a Sommerfeld-Watson resummation over J to evaluate (2.146). Also, note that the spectral function, as given by the Lorentzian inversion formula [6], is of the form

$$I^{1234}(\nu) = I^{1234,t}(\nu) + (-1)^J I^{1234,u}(\nu)\,. \tag{2.148}$$

Let us first consider the case of a correlator with pairwise equal external operators i.e. $a = b = 0$, $I^{1234,t} = I^{1234,u}$, where only even spins are exchanged. Now for the resummation we replace the sum by an integral,

$$2\sum_{J\,\text{even}} \to \int_C dJ \frac{e^{i\pi J}}{1-e^{i\pi J}}\,. \tag{2.149}$$

The contour C encloses all poles on the positive real axis (at even integers) in a clockwise direction. The leading Regge trajectory is given by the operators with the lowest dimension $\Delta(J)$ for every even spin J and $\alpha(\nu, J)$ has poles at $i\nu = \pm(\Delta(J) - d/2)$. Defining the inverse

function $j = j(\nu)$ of the spectral function $\Delta(J)$ by

$$\nu^2 + \left(\Delta(j(\nu)) - \tfrac{d}{2}\right)^2 = 0\,, \tag{2.150}$$

we see that the poles in ν translate into a single pole at $J = j(\nu)$. By deforming the J contour to the left one sees that the J integral is given by the residue at $J = j(\nu)$, i.e.

$$\text{Disc}_{14}\, A^{1234}(z,\bar{z}) = 2\pi i \int_{-\infty}^{\infty} d\nu\; \alpha(\nu)\, \sigma^{1-j(\nu)} \Omega_{i\nu}(\rho)\,, \tag{2.151}$$

where

$$\alpha(\nu) = -\operatorname*{Res}_{J=j(\nu)} i\, \frac{e^{i\pi J}}{1-e^{-i\pi J}}\, \frac{\pi^{\frac{d}{2}-2}\, S\big(\mathcal{O}_3\mathcal{O}_4\big[\big(-i\nu-\frac{d}{2}\big)^{\dagger}\big]\big)\,\Gamma(i\nu)}{\kappa^{(a,b)}_{i\nu+\frac{d}{2},J}\,\Gamma\big(i\nu+\frac{d}{2}-1\big)}\, I^{1234,t}\left(i\nu+\frac{d}{2},J\right). \tag{2.152}$$

When the operators are not pairwise equal, the even and odd spin operators organize into two analytic families as evident from the Lorentzian inversion formula [6]. To obtain the contribution of the leading Regge trajectory we still sum over the even spin exchanges. The result is of the same form as in (2.151) with $I^{1234,t}$ replaced by $\frac{1}{2}I^{1234}$ in $\alpha(\nu)$. For the other correlator we can use (2.104) to see that we get an analogous result with the complex conjugate spectral function

$$\text{Disc}_{23}\, A^{3412}(z,\bar{z}) = 2\pi i \int_{-\infty}^{\infty} d\nu\; \alpha(\nu)^*\, \sigma^{1-j(\nu)} \Omega_{i\nu}(\rho)\,. \tag{2.153}$$

One can show that the corresponding impact parameter representation is given in general by the same spectral function times a multiplicative factor which cancels poles for the external double-trace operators [31]

$$\mathcal{B}(p,\bar{p}) = 2\pi i \int_{-\infty}^{\infty} d\nu\; \beta(\nu)\, S^{j(\nu)-1} \Omega_{i\nu}(L)\,, \tag{2.154}$$

where

$$\beta(\nu) = \frac{4\pi^{2-d}(\sqrt{\mathcal{M}_{\mathcal{O}_1}\mathcal{M}_{\mathcal{O}_2}\mathcal{M}_{\mathcal{O}_3}\mathcal{M}_{\mathcal{O}_4}})^{-1}\,\alpha(\nu)}{\chi_{j(\nu)}(\nu)\,\chi_{j(\nu)}(-\nu)}\,, \tag{2.155}$$

with the definition

$$\chi_{j(\nu)}(\nu) = \Gamma\left(\frac{\Delta_1+\Delta_2+j(\nu)-d/2+i\nu}{2}\right)\Gamma\left(\frac{\Delta_3+\Delta_4+j(\nu)-d/2+i\nu}{2}\right). \tag{2.156}$$

The impact parameter space cross-ratios, analogous to (2.144), are

$$S = \sqrt{p^2 \bar{p}^2}, \qquad \cosh L = -\frac{p \cdot \bar{p}}{\sqrt{p^2 \bar{p}^2}} \,. \tag{2.157}$$

In the dual AdS scattering process these cross ratios are interpreted as the squared of the energy with respect to global time and as the impact parameter in the transverse space H_{d-1}.

2.4.4 Spinning particles and the vertex function

In this section we will introduce concrete expressions for the tree amplitudes with spinning external legs and show that the contributions of the contracted spinning legs can be expressed in terms of a scalar function of three spectral parameters which we call the vertex function, analogous to (2.87) in flat space. We construct tensor structures in terms of differential operators, which are a Regge limit version of weight-shifting operators that generate spinning conformal blocks from the scalar ones [57, 58]. It is convenient to work with tensor structures which are homogeneous in p and $\bar{p}$, i.e. independent of the cross-ratio S in (2.157), such that all tensor structures have the same large S behavior in the Regge limit. These differential operators can be constructed from the covariant derivative on the hyperboloid H_{d-1} and from $\hat{p} = p/|p|, \hat{\bar{p}} = \bar{p}/|\bar{p}|$ [7, 43]. The possible differential operators that generate spin for a single particle are

$$\mathcal{D}^{\rho,k}_{\mathbf{m}}(p) = \hat{p}_{m_1} \dots \hat{p}_{m_k} \nabla_{p\, m_{k+1}} \dots \nabla_{p\, m_{|\rho|}} \,, \qquad k = 0, \dots, |\rho| \,. \tag{2.158}$$

Tree diagrams for exchange of the Pomeron then have the form

$$\mathcal{B}^{(\Delta_5,\rho_5),(\Delta_6,\rho_6)}_{\mathbf{mn}}(p,\bar{p}) = 2\pi i \int_{-\infty}^{\infty} d\nu \, S^{j(\nu)-1} \mathfrak{D}^{(\Delta_5,\rho_5),(\Delta_6,\rho_6)}_{\mathbf{mn}}(\nu) \, \Omega_{i\nu}(L) \,. \tag{2.159}$$

Here $\mathcal{B}^{(\Delta_5,\rho_5),(\Delta_6,\rho_6)}_{\mathbf{mn}}(p,\bar{p})$ is defined just as in (2.125) and (2.133), but with tensor structures constructed from $\hat{p}$ and $\hat{\bar{p}}$. In (2.159) we introduced the following definition for the combination of spectral functions $\beta(\nu)$ and differential operators that generate different tensor structures

$$\mathfrak{D}^{(\Delta_5,\rho_5),(\Delta_6,\rho_6)}_{\mathbf{mn}}(\nu) = \sum_{k_5=0}^{|\rho_5|} \sum_{k_6=0}^{|\rho_6|} \beta^{k_5,k_6}_{(\Delta_5,\rho_5),(\Delta_6,\rho_6)}(\nu) \mathcal{D}^{\rho_5,k_5}_{\mathbf{m}}(p) \mathcal{D}^{\rho_6,k_6}_{\mathbf{n}}(\bar{p}) \,. \tag{2.160}$$

Notice that, in contrast to flat space, we do not impose a full factorization into three-point structures but rather allow for a separate spectral function for each combination of three-point structures.

The next step is to derive the general functional form of (2.134) after the contractions and sums have been done. We begin by inserting (2.159) into (2.134),

$$-\mathrm{Re}\mathcal{B}_{\text{1-loop}}(p,\bar{p}) = 2\pi^2 \sum_{\Delta_5,\Delta_6,\rho_5,\rho_6} \int_{-\infty}^{\infty} d\nu_1 d\nu_2\, S^{j(\nu_1)+j(\nu_2)-2} \tag{2.161}$$
$$\mathfrak{D}_{\mathbf{mn}}^{(\Delta_5,\rho_5),(\Delta_6,\rho_6)}(\nu_1)^*\, \Omega_{i\nu_1}(L)\, \pi_{\rho_5}^{\mathbf{m};\mathbf{p}} \pi_{\rho_6}^{\mathbf{n};\mathbf{q}}\, \mathfrak{D}_{\mathbf{pq}}^{(\Delta_5,\rho_5),(\Delta_6,\rho_6)}(\nu_2)\, \Omega_{i\nu_2}(L)\,.$$

Here π_ρ is the projector to the irreducible representation ρ of $SO(d)$, which is necessary because the operators (2.158) do not ensure the properties of irreducible representations such as tracelessness and Young symmetrization. Next we will show how one can replace the contractions and derivatives in the previous equation by spectral parameters. Note first that due to $p \cdot \nabla_p = 0$, all contractions involving $\hat{p}$ or $\hat{\bar{p}}$ give factors of their norm -1. The remaining contractions involve only covariant derivatives. These contracted derivatives can all be replaced by functions of the spectral parameters by using the Laplace equation for the harmonic function

$$\left(\nabla^2_{H_{d-1}} + \nu^2 + (d/2-1)^2\right) \Omega_{i\nu}(L) = 0\,. \tag{2.162}$$

Using this equation, factors of ∇_p^2 can directly be replaced. To evaluate contractions between derivatives acting on different harmonic functions we expand the product of two scalar harmonic functions as follows,

$$\Omega_{i\nu_1}(L)\Omega_{i\nu_2}(L) = \int_{-\infty}^{\infty} d\nu\, \Phi(\nu_1,\nu_2,\nu)\Omega_{i\nu}(L)\,, \tag{2.163}$$

where $\Phi(\nu_1,\nu_2,\nu)$ was computed (for the similar case of harmonic functions on AdS_{d+1}) in appendix D of [59].[7] By acting repeatedly with (2.162) on this equation, one can determine the function W_k that appears in

$$\nabla_{p_{m_1}} \dots \nabla_{p_{m_k}} \Omega_{i\nu_1}(L) \nabla_p^{m_1} \dots \nabla_p^{m_k} \Omega_{i\nu_2}(L) = \int_{-\infty}^{\infty} d\nu\, W_k\big(\nu_1^2,\nu_2^2,\nu^2\big)\, \Phi(\nu_1,\nu_2,\nu)\, \Omega_{i\nu}(L)\,. \tag{2.164}$$

W_k is a fixed kinematical polynomial of maximal degree k in its arguments. For example, the first non-trivial case is

$$\int_{-\infty}^{\infty} d\nu\, \Phi(\nu_1,\nu_2,\nu)\nu^2\, \Omega_{i\nu}(L) = \left(\nu_1^2+\nu_2^2+(\tfrac{d}{2}-1)^2\right) \Omega_{i\nu_1}(L)\, \Omega_{i\nu_2}(L) - 2\nabla_\mu \Omega_{i\nu_1}(L) \nabla^\mu \Omega_{i\nu_2}(L), \tag{2.165}$$

[7] Note that $\Phi_{\text{here}}\Omega_{i\nu}(0) = \Phi_{\text{there}}$.

from which one can read off W_0 and W_1 to be

$$W_0\big(\nu_1^2,\nu_2^2,\nu^2\big)=1\,,\qquad W_1\big(\nu_1^2,\nu_2^2,\nu^2\big)=\frac{1}{2}\Big(\nu_1^2+\nu_2^2-\nu^2+(d/2-1)^2\Big). \tag{2.166}$$

More generally, by acting with the Laplacian on both sides of (2.164) one can derive a recursion relation of the form

$$\begin{aligned}&\int d\nu\, W_{k+1}(\nu_i)\,\Phi(\nu_i)\,\Omega_{i\nu}(L)=\int d\nu\, W_k(\nu_i)\,W_1(\nu_i)\,\Phi(\nu_i)\,\Omega_{i\nu}(L)\\&+\frac{1}{2}\left([\nabla^2,\nabla_{m_1}\ldots\nabla_{m_k}]\Omega_{i\nu_1}(L)\nabla^{m_1}\ldots\nabla^{m_k}\Omega_{i\nu_2}(L)+(\nu_1\leftrightarrow\nu_2)\right)\,.\end{aligned} \tag{2.167}$$

The terms with commutators, which will vanish in the flat space limit, can be evaluated using the fact that the commutators of covariant derivatives can be replaced by Riemann tensors, which for the hyperboloid can be written in terms of the metric. This means that these terms have two derivatives less than the other terms, and will therefore produce less than maximal powers of ν_i. This shows that the maximal power of ν_i in W_k is just given by repeatedly multiplying W_1. Therefore we have

$$W_k\big(\nu_1^2,\nu_2^2,\nu^2\big)=\left(\frac{\nu_1^2+\nu_2^2-\nu^2}{2}\right)^k+O\Big(\nu_i^{2(k-1)}\Big)\,. \tag{2.168}$$

Having shown that all derivatives can be replaced by polynomials of the spectral parameters, we can define

$$\mathfrak{D}_{\mathbf{mn}}^{(\Delta_5,\rho_5),(\Delta_6,\rho_6)}(\nu_1)^*\,\Omega_{i\nu_1}(L)\,\pi_{\rho_5}^{\mathbf{m};\mathbf{p}}\pi_{\rho_6}^{\mathbf{n};\mathbf{q}}\,\mathfrak{D}_{\mathbf{pq}}^{(\Delta_5,\rho_5),(\Delta_6,\rho_6)}(\nu_2)\,\Omega_{i\nu_2}(L) \tag{2.169}$$

$$=\int_{-\infty}^{\infty}d\nu\,W_{(\Delta_5,\rho_5),(\Delta_6,\rho_6)}\big(\nu_1^2,\nu_2^2,\nu^2\big)\,\Phi(\nu_1,\nu_2,\nu)\,\Omega_{i\nu}(L)\,. \tag{2.170}$$

This gives the contribution of a given pair of intermediate states labeled by (Δ_5,ρ_5) and (Δ_6,ρ_6) to $-\mathrm{Re}\mathcal{B}_{\text{1-loop}}(p,\bar{p})$. Now we can define the vertex function $V(\nu_1,\nu_2,\nu)$, which is even in all its arguments, in analogy to (2.87) as the sum over all such contributions in (2.161)

$$\sum_{\Delta_5,\Delta_6,\rho_5,\rho_6,}W_{(\Delta_5,\rho_5),(\Delta_6,\rho_6)}\big(\nu_1^2,\nu_2^2,\nu^2\big)=\beta(\nu_1)^*\beta(\nu_2)V(\nu_1,\nu_2,\nu)^2\,, \tag{2.171}$$

and reach the following representation for the 1-loop amplitude

$$\begin{aligned}-\mathrm{Re}\mathcal{B}_{\text{1-loop}}(p,\bar{p})=2\pi^2\int_{-\infty}^{\infty}&d\nu d\nu_1 d\nu_2\,\beta(\nu_1)^*\beta(\nu_2)\,V(\nu_1,\nu_2,\nu)^2\\&S^{j(\nu_1)+j(\nu_2)-2}\Phi(\nu_1,\nu_2,\nu)\,\Omega_{i\nu}(L)\,.\end{aligned} \tag{2.172}$$

All the information about the spinning tree-level correlators and their contractions is encoded in the vertex function $V(\nu_1, \nu_2, \nu)$ which mirrors the role of its flat space analogue.

However, in order to compute the full impact parameter representation rather than just its real part, we have to go through a detour via the Lorentzian inversion formula, as described in [44]. We first Fourier transform back to $\text{dDisc}_t\, A_{1\text{-loop}}$ from which we obtain the s-channel OPE coefficients. Then we can compute $\text{Disc}_{14}\, A_{1\text{-loop}}$ which we can finally Fourier transform to obtain $\mathcal{B}_{1\text{-loop}}(p, \bar{p})$. Since in the Regge limit the difference between $\text{dDisc}_t\, A_{1\text{-loop}}$ and $\text{Disc}_{14}\, A_{1\text{-loop}}$ is just a phase factor (see [44]), the same happens for the impact parameter representation

$$\mathcal{B}_{1\text{-loop}}(p, \bar{p}) = -4\pi^2 \int_{-\infty}^{\infty} d\nu d\nu_1 d\nu_2 \, \frac{1 + e^{-i\pi(j(\nu_1)+j(\nu_2)-1)}}{1 - e^{-2\pi i(j(\nu_1)+j(\nu_2)-1)}} \, \beta(\nu_1)^* \beta(\nu_2) \, V(\nu_1, \nu_2, \nu)^2 \\ S^{j(\nu_1)+j(\nu_2)-2} \, \Phi(\nu_1, \nu_2, \nu) \, \Omega_{i\nu}(L) \, . \tag{2.173}$$

It is important to emphasize that this provides a finite Δ_{gap} description for the one-loop correlator in the Regge limit up to the knowledge of the vertex function $V(\nu_1, \nu_2, \nu)^2$. For CFTs that admit a flat space limit, we will see in sections 2.6 and 2.7 how one can fix part of this vertex function from the knowledge of its flat space analogue. In section 2.5 below, we make a comparison with the large Δ_{gap} limit studied in reference [44], and also describe the implications of (2.172) for t-channel CFT data.

2.5 Constraints on CFT data

2.5.1 Comparison with the large Δ_{gap} limit

In [44] the Regge limit of the four-point correlator of pairwise identical scalars was studied in an expansion in $1/N$ in the limit of large Δ_{gap}. The specific limit considered was $S \gg \Delta_{\text{gap}}^2 \gg 1$, so the result is sensitive to all the higher spin interactions in the leading Regge trajectory, but tidal excitations are ignored. Since we have kept Δ_{gap} finite, we should be able to obtain a match between the result for the one-loop correlator in [44] with our result (2.134) after dropping the tidal excitations $\mathcal{O}_5 \neq \mathcal{O}_1$ and $\mathcal{O}_6 \neq \mathcal{O}_3$.

We pick the term $\Delta_5 = \Delta_1$ and $\Delta_6 = \Delta_3$ that is the sole contribution to (2.134) in the large Δ_{gap} limit, and use (2.154) to obtain

$$-\text{Re}\mathcal{B}_{1\text{-loop}}(S, L) = 2\pi^2 \int d\nu_1 d\nu_2 d\nu \, \beta^*(\nu_1)\beta(\nu_2) \, \Phi(\nu_1, \nu_2, \nu) \, S^{j(\nu_1)+j(\nu_2)-2} \Omega_{i\nu}(L) \Big|_{[\mathcal{O}_5\mathcal{O}_6]} \, . \tag{2.174}$$

Now let us extract the corresponding result from [44]. Equation (3.15) of [44] gives the double discontinuity of the one-loop correlator $\mathcal{G}^{(2)}$ as follows (with $\Delta_\phi = \Delta_1$ and $\Delta_\psi = \Delta_3$)

$$\begin{aligned}\text{dDisc}_t[\mathcal{G}^{(2)}(z,\bar{z})] = \frac{\pi^4}{8}\int d\nu_1 d\nu_2 d\nu\, \chi_{j(\nu_1)+j(\nu_2)-1}(\nu)\,\chi_{j(\nu_1)+j(\nu_2)-1}(-\nu)\,\mathcal{N}\\ \widehat{\gamma}^{(1)}(\nu_1)\widehat{\gamma}^{(1)}(\nu_2)\,\Phi(\nu_1,\nu_2,\nu)(z\bar{z})^{\frac{2-j(\nu_1)-j(\nu_2)}{2}}\,\Omega_{i\nu}\left(\frac{1}{2}\log(z/\bar{z})\right),\end{aligned} \tag{2.175}$$

where $\chi_{j(\nu_1)+j(\nu_2)-1}(\nu)$ is defined in (2.156) but with $j(\nu)$ replaced by $j(\nu_1)+j(\nu_2)-1$, and with $\Delta_2 = \Delta_1$ and $\Delta_4 = \Delta_3$. It accounts for the double-trace exchanges $[\mathcal{O}_1\mathcal{O}_1]$ and $[\mathcal{O}_3\mathcal{O}_3]$ analytically continued to spin $j(\nu_1)+j(\nu_2)-1$. The operators contributing to the t-channel expansion in the large Δ_{gap} limit are the double-traces $[\mathcal{O}_1\mathcal{O}_3]_{n,\ell}$ with dimensions and OPE coefficients given by

$$\begin{aligned}\Delta_{h,\bar{h}} &= \Delta^{(0)}_{h,\bar{h}} + \frac{1}{N^2}\gamma^{(1)}_{h,\bar{h}} + \frac{1}{N^4}\gamma^{(2)}_{h,\bar{h}} + \cdots, \qquad \Delta^{(0)}_{h,\bar{h}} = \Delta_1+\Delta_3+2n+\ell,\\ P_{h,\bar{h}} &= P^{MFT}_{h,\bar{h}}\left(1+\frac{1}{N^2}\delta P^{(1)}_{h,\bar{h}} + \frac{1}{N^4}\delta P^{(2)}_{h,\bar{h}} + \cdots\right),\end{aligned} \tag{2.176}$$

where $h,\bar{h} = \Delta \mp \ell$. The tree-level anomalous dimensions $\gamma^{(1)}_{h,\bar{h}}$ and tree-level corrections to OPE coefficients $\delta P^{(1)}_{h,\bar{h}}$ can be extracted respectively from $\widehat{\gamma}^{(1)}(\nu)$ and $\widehat{\delta P}^{(1)}(\nu)$ by

$$\begin{aligned}\gamma^{(1)}_{h,\bar{h}} &\approx \int_{-\infty}^{\infty} d\nu\, \widehat{\gamma}^{(1)}(\nu)\,(h\bar{h})^{j(\nu)-1}\,\Omega_{i\nu}\big(\log(h/\bar{h})\big),\\ \delta P^{(1)}_{h,\bar{h}} &\approx \int_{-\infty}^{\infty} d\nu\, \widehat{\delta P}^{(1)}(\nu)\,(h\bar{h})^{j(\nu)-1}\,\Omega_{i\nu}\big(\log(h/\bar{h})\big).\end{aligned} \tag{2.177}$$

$\widehat{\gamma}^{(1)}(\nu)$ and $\widehat{\delta P}^{(1)}(\nu)$ can be obtained respectively from the real and imaginary parts of the phase shift, and are related to β by[8]

$$\begin{aligned}\widehat{\gamma}^{(1)}(\nu) &= 2\,\text{Re}\beta(\nu),\\ \widehat{\delta P}^{(1)}(\nu) &= -2\pi\,\text{Im}\beta(\nu).\end{aligned} \tag{2.178}$$

Taking the Fourier transform to impact parameter space on (2.175) and then using (2.178) gives[9]

$$-\text{Re}\mathcal{B}_{1\text{-loop}}(S,L) = 2\pi^2\int d\nu_1 d\nu_2 d\nu\,\text{Re}\beta(\nu_1)\,\text{Re}\beta(\nu_2)\,\Phi(\nu_1,\nu_2,\nu)S^{j(\nu_1)+j(\nu_2)-2}\,\Omega_{i\nu}(L). \tag{2.179}$$

We need to compare (2.174) with (2.179). The only difference are the real parts in (2.179),

[8] Note that due to difference in conventions, $\mathcal{N}\beta$ for us is equal to β, as defined in [44].

[9] In our conventions the Fourier transform takes $\text{dDisc}_t[\mathcal{G}^{(2)}(z,\bar{z})]$ to $-\mathcal{N}\text{Re}\mathcal{B}$ upto scaling factors.

however Imβ in (2.174) is related to tree-level corrections to the OPE coefficients and these are suppressed at large Δ_{gap} [44]. This can be seen for example from (2.178) and using in it the explicit expression for $\alpha(\nu)$ from [44]. The result is

$$\widehat{\delta P}^{(1)}(\nu) = \frac{-\pi \text{Im}\left(\frac{ie^{i\pi j(\nu)}}{1-e^{i\pi j(\nu)}}\right)}{\text{Re}\left(\frac{ie^{i\pi j(\nu)}}{1-e^{i\pi j(\nu)}}\right)} \widehat{\gamma}^{(1)}(\nu) = -\pi \tan\left(\frac{\pi}{2} j(\nu)\right) \widehat{\gamma}^{(1)}(\nu)\,. \tag{2.180}$$

The suppression is due to the tan factor, since for large N theories it is known that [4, 39, 40]

$$j(\nu) = 2 - 2\,\frac{\nu^2 + (d/2)^2}{\Delta_{\text{gap}}^2} + O\big(\Delta_{\text{gap}}^{-4}\big)\,. \tag{2.181}$$

The anomalous dimensions $\gamma^{(1)}_{h,\tilde{h}}$ are order 1, while the the corrections to the OPE coefficients $\delta P^{(1)}_{h,\tilde{h}}$ are at order Δ_{gap}^{-2}.

Thus we have matched our result for the Regge limit of the dDisc of a one-loop correlator at large Δ_{gap} to that of [44]. Note that we managed to reproduce the result without the need for any projections to the physical double-traces. Therefore it is reasonable to assume that the gluing of tree-level correlators in the Regge limit does not receive contributions from the double-traces of shadows and we can use the optical theorem (2.134) without the projections onto $[\mathcal{O}_5\mathcal{O}_6]$.

2.5.2 Extracting t-channel CFT data

Next we shall see how we can extract the CFT data for the double-trace operators exchanged in the t-channel to order $1/N^4$ from the vertex function $V(\nu_1^2, \nu_2^2, \nu^2)$. To this end we follow section 3.2 of [44] and extend the results therein by including tidal excitations, which make our statements valid at finite Δ_{gap}. As discussed in the previous section, the only operators contributing to the t-channel expansion in the large Δ_{gap} limit are the double-traces $[\mathcal{O}_1\mathcal{O}_3]$ [60]. The three-point function of these double-traces with their constituent operators $\mathcal{O}_1$ and $\mathcal{O}_3$ has the large N behavior

$$\langle \mathcal{O}_1\mathcal{O}_3[\mathcal{O}_1\mathcal{O}_3]\rangle \sim 1\,. \tag{2.182}$$

By including tidal excitations we have to include also double-traces $[\mathcal{O}_5\mathcal{O}_6]$ corresponding to additional double-traces coupling to $\mathcal{O}_1$ and $\mathcal{O}_3$. These satisfy

$$\langle \mathcal{O}_1\mathcal{O}_3[\mathcal{O}_5\mathcal{O}_6]\rangle \sim \frac{1}{N^2}\,, \qquad [\mathcal{O}_5\mathcal{O}_6] \neq [\mathcal{O}_1\mathcal{O}_3]\,, \tag{2.183}$$

so that only their classical dimension and leading OPE coefficient squared[10]

$$\Delta_{h',\bar{h}'} = \Delta_{\mathcal{O}_5} + \Delta_{\mathcal{O}_6} + 2n + \ell\,, \qquad P_{h',\bar{h}'} = \frac{1}{N^4} P^{\text{MFT}}_{h',\bar{h}'} \delta P^{(56)}_{h',\bar{h}'} + \dots\,, \tag{2.184}$$

appear in the one-loop correlator. This is compatible with the large N behavior for single-trace exchange in the direct channel,

$$\langle \mathcal{O}_1 \mathcal{O}_5 \mathcal{O}_{\Delta(J)} \rangle \sim \frac{1}{N}\,, \; \langle \mathcal{O}_{\Delta(J)} \mathcal{O}_6 \mathcal{O}_3 \rangle \sim \frac{1}{N}\,, \tag{2.185}$$

which justifies that the OPE coefficients $c_{\mathcal{O}_1\mathcal{O}_3[\mathcal{O}_5\mathcal{O}_6]}$ start at order $1/N^2$. As explained in [44], the cross channel expansion of the correlator is then dominated by the terms

$$\begin{aligned}\frac{\mathcal{A}^{\circlearrowleft}_{\text{1-loop}}(z,\bar{z})}{(z\bar{z})^{\Delta_\phi}} \approx & \sum_{h,\bar{h}} P^{MFT}_{h,\bar{h}} \left[i\pi\gamma^{(2)}_{h,\bar{h}} + \delta P^{(2)}_{h,\bar{h}} + i\pi\gamma^{(1)}_{h,\bar{h}}\, \delta P^{(1)}_{h,\bar{h}} - \frac{\pi^2}{2}\left(\gamma^{(1)}_{h,\bar{h}}\right)^2 \right] g_{h,\bar{h}}(1-z,1-\bar{z}) \\ & + \sum_{h',\bar{h}'} P^{MFT}_{h',\bar{h}'} \delta P^{(56)}_{h',\bar{h}'}\, g_{h',\bar{h}'}(1-z,1-\bar{z})\,. \end{aligned} \tag{2.186}$$

We shall now compare with our result for the one-loop correlator in the Regge limit and use it in the light of (2.186) to extract CFT data. We start with the dDisc of the correlator in the impact parameter representation as in (2.172). Doing an inverse Fourier transform on this and taking out the appropriate scale factors gives us the dDisc of the one-loop correlator in the Regge limit

$$\begin{aligned}\text{dDisc}_t \mathcal{A}_{\text{1-loop}}(z,\bar{z}) = \frac{\pi^4 \mathcal{N}}{4} \int_{-\infty}^{\infty} d\nu d\nu_1 d\nu_2 \left(\beta^*(\nu_1)\beta(\nu_2) + \beta(\nu_1)\beta^*(\nu_2)\right) V(\nu_1,\nu_2,\nu)^2 \\ \Phi(\nu_1,\nu_2,\nu)\, \chi_{j(\nu_1)+j(\nu_2)-1}(\nu)\, \chi_{j(\nu_1)+j(\nu_2)-1}(-\nu)\, \sigma^{2-j(\nu_1)-j(\nu_2)}\, \Omega_{i\nu}(\rho)\,, \end{aligned} \tag{2.187}$$

where we symmetrized the product of β's by using the symmetry of the expression under $\nu_1 \leftrightarrow \nu_2$. We can now use the Lorentzian inversion formula [6] on (2.187), as shown in [44], to obtain the one-loop correlator in the Regge limit, and then use (2.178) to express it as

$$\begin{aligned}\mathcal{A}^{\circlearrowleft}_{\text{1-loop}}(z,\bar{z}) \approx -\frac{\pi^4 \mathcal{N}}{4} \int_{-\infty}^{\infty} d\nu_1 d\nu_2 d\nu\, \frac{1+e^{-i\pi(j(\nu_1)+j(\nu_2)-1)}}{1-e^{-2\pi i(j(\nu_1)+j(\nu_2)-1)}}\, V(\nu_1,\nu_2,\nu)^2 \\ \Phi(\nu_1,\nu_2,\nu)\, \chi_{j(\nu_1)+j(\nu_2)-1}(\nu)\, \chi_{j(\nu_1)+j(\nu_2)-1}(-\nu)\, \sigma^{2-j(\nu_1)-j(\nu_2)}\, \Omega_{i\nu}(\rho) \\ \left[\widehat{\gamma}^{(1)}(\nu_1)\, \widehat{\gamma}^{(1)}(\nu_2) + \frac{1}{\pi^2} \widehat{\delta P}^{(1)}(\nu_1)\, \widehat{\delta P}^{(1)}(\nu_2) \right]. \end{aligned} \tag{2.188}$$

[10] We are free to insert P^{MFT} here, defining δP accordingly. This will be useful below in (2.191).

We now take the t-channel expansion (2.186), and use in it (2.177), (2.163), and the following ansatz,

$$\begin{aligned}\gamma^{(2)}_{h,\bar{h}} &\approx \int_{-\infty}^{\infty} d\nu_1 d\nu_2 d\nu\, \widehat{\gamma}^{(2)}(\nu_1,\nu_2,\nu)\,(h\bar{h})^{j(\nu_1)+j(\nu_2)-2}\,\Omega_{i\nu}\big(\log(h/\bar{h})\big)\,,\\ \delta P^{(2)/(56)}_{h,\bar{h}} &\approx \int_{-\infty}^{\infty} d\nu_1 d\nu_2 d\nu\, \widehat{\delta P}^{(2)/(56)}(\nu_1,\nu_2,\nu)\,(h\bar{h})^{j(\nu_1)+j(\nu_2)-2}\,\Omega_{i\nu}\big(\log(h/\bar{h})\big)\,,\end{aligned} \tag{2.189}$$

to obtain

$$\begin{aligned}(z\bar{z})^{-\Delta_\phi}\mathcal{A}^{\circlearrowleft}_{\text{1-loop}}(z,\bar{z}) \approx \int_{-\infty}^{\infty} d\nu_1 d\nu_2 d\nu \Bigg[&\sum_{h,\bar{h}} (h\bar{h})^{j(\nu_1)+j(\nu_2)-2}\,\Omega_{i\nu}(\log h/\bar{h})\,P^{MFT}_{h,\bar{h}} \\ &\Big[i\pi\widehat{\gamma}^{(2)}(\nu_1,\nu_2,\nu) + \frac{i\pi}{2}\Big(\widehat{\gamma}^{(1)}(\nu_1)\,\widehat{\delta P}^{(1)}(\nu_2) + \widehat{\gamma}^{(1)}(\nu_2)\,\widehat{\delta P}^{(1)}(\nu_1)\Big)\Phi(\nu_1,\nu_2,\nu) \\ &\quad - \frac{\pi^2}{2}\,\widehat{\gamma}^{(1)}(\nu_1)\,\widehat{\gamma}^{(1)}(\nu_2)\Phi(\nu_1,\nu_2,\nu) + \widehat{\delta P}^{(2)}(\nu_1,\nu_2,\nu)\Big]\, g_{h,\bar{h}}(1-z,1-\bar{z}) \\ &+ \sum_{h',\bar{h}'} P^{MFT}_{h',\bar{h}'}\,\widehat{\delta P}^{(56)}(\nu_1,\nu_2,\nu)(h'\bar{h}')^{j(\nu_1)+j(\nu_2)-2)}\,\Omega_{i\nu}(\log h'/\bar{h}')\,g_{h',\bar{h}'}(1-z,1-\bar{z})\Bigg]\,.\end{aligned} \tag{2.190}$$

We can approximate the $h,\bar{h}$ and $h',\bar{h}'$ sums with integrals, $\sum_{h,\bar{h}} \to \frac{1}{2}\int_0^\infty dh\, d\bar{h}$, and evaluate them using Bessel function integrals (see section 2.2 of [44]) to arrive at the result

$$\begin{aligned}\mathcal{A}^{\circlearrowleft}_{\text{1-loop}}(z,\bar{z}) \approx \frac{\pi^2\mathcal{N}}{4}\int_{-\infty}^{\infty} d\nu_1 d\nu_2 d\nu\, &\chi_{j(\nu_1)+j(\nu_2)-1}(\nu)\,\chi_{j(\nu_1)+j(\nu_2)-1}(-\nu)\,\sigma^{2-j(\nu_1)-j(\nu_2)}\,\Omega_{i\nu}(\rho) \\ &\Big[i\pi\widehat{\gamma}^{(2)}(\nu_1,\nu_2,\nu) - \frac{\pi^2}{2}\,\widehat{\gamma}^{(1)}(\nu_1)\,\widehat{\gamma}^{(1)}(\nu_2)\,\Phi(\nu_1,\nu_2,\nu) + \widehat{\delta P}^{(2)}(\nu_1,\nu_2,\nu) \\ &+\frac{i\pi}{2}\Big(\widehat{\gamma}^{(1)}(\nu_1)\,\widehat{\delta P}^{(1)}(\nu_2) + \widehat{\gamma}^{(1)}(\nu_2)\,\widehat{\delta P}^{(1)}(\nu_1)\Big)\Phi(\nu_1,\nu_2,\nu) + \widehat{\delta P}^{(56)}(\nu_1,\nu_2,\nu)\Big]\,.\end{aligned} \tag{2.191}$$

Comparing the real parts of the coefficient of $\chi(\nu)\chi(-\nu)\sigma^{2-j(\nu_1)-j(\nu_2)}\Omega_{i\nu}(\rho)$ in the integrands of (2.188) and (2.191), and using

$$\frac{1+e^{-i\pi(j(\nu_1)+j(\nu_2)-1)}}{1-e^{-2\pi i(j(\nu_1)+j(\nu_2)-1)}} = \frac{1}{2} + \frac{i}{2}\tan\Big(\frac{\pi}{2}\big(j(\nu_1)+j(\nu_2)\big)\Big)\,, \tag{2.192}$$

we conclude that

$$\begin{aligned}\widehat{\delta P}^{(2)}(\nu_1,\nu_2;\nu) + \widehat{\delta P}^{(56)}(\nu_1,\nu_2;\nu) = -\frac{1}{2}\Big[&\pi^2\Big(V(\nu_1,\nu_2,\nu)^2-1\Big)\widehat{\gamma}^{(1)}(\nu_1)\,\widehat{\gamma}^{(1)}(\nu_2) \\ &+ V(\nu_1,\nu_2,\nu)^2\,\widehat{\delta P}^{(1)}(\nu_1)\,\widehat{\delta P}^{(1)}(\nu_2)\Big]\Phi(\nu_1,\nu_2,\nu)\,.\end{aligned} \tag{2.193}$$

This is the general result for fixed Δ_{gap} that extracts OPE data from the AdS vertex function.

Let us now take the large Δ_{gap} limit to make contact with [44]. In this limit, $V(\nu_1,\nu_2,\nu)^2=1$ and $\widehat{\delta P}^{(1)}$, $\widehat{\delta P}^{(56)}$ are suppressed with respect to $\widehat{\gamma}^{(1)}$. Therefore $\delta P^{(2)}_{h,\bar{h}}=0$, as was obtained in [44].

Similarly, comparing the imaginary parts we have

$$\widehat{\gamma}^{(2)}(\nu_1,\nu_2;\nu)=-\frac{1}{2}\Bigg[\left(\widehat{\gamma}^{(1)}(\nu_1)\widehat{\delta P}^{(1)}(\nu_2)+\widehat{\delta P}^{(1)}(\nu_1)\widehat{\gamma}^{(1)}(\nu_2)\right)+\pi\tan\left(\frac{\pi}{2}(j(\nu_1)+j(\nu_2))\right)\\ V(\nu_1,\nu_2,\nu)^2\left(\widehat{\gamma}^{(1)}(\nu_1)\widehat{\gamma}^{(1)}(\nu_2)+\frac{1}{\pi^2}\widehat{\delta P}^{(1)}(\nu_1)\widehat{\delta P}^{(1)}(\nu_2)\right)\Bigg]\Phi(\nu_1,\nu_2,\nu)\,. \tag{2.194}$$

The term $\widehat{\delta P}^{(1)}(\nu_1)\,\widehat{\delta P}^{(1)}(\nu_2)$ is suppressed by Δ_{gap}^{-4} with respect to the other terms. At leading order in Δ_{gap}, we can discard this term and set $V(\nu_1,\nu_2,\nu)^2=1$. We can then use (2.180) to simplify the expression to,

$$\widehat{\gamma}^{(2)}(\nu_1,\nu_2;\nu)=-\frac{1}{2}\pi\tan\left(\frac{1}{2}\pi j(\nu_1)\right)\tan\left(\frac{1}{2}\pi j(\nu_2)\right)\tan\left(\frac{1}{2}\pi(j(\nu_1)+j(\nu_2))\right)\\ \times\,\widehat{\gamma}^{(1)}(\nu_1)\widehat{\gamma}^{(1)}(\nu_2)\Phi(\nu_1,\nu_2,\nu)\,. \tag{2.195}$$

This is the same result as obtained in [44] for $\widehat{\gamma}^{(2)}(\nu_1,\nu_2;\nu)$. More generally, knowledge of the vertex function $V(\nu_1,\nu_2,\nu)^2$ and of the $\langle\mathcal{O}_1\mathcal{O}_3[\mathcal{O}_5\mathcal{O}_6]\rangle$ OPE coefficients gives additional information about the one-loop CFT data of the $[\mathcal{O}_1\mathcal{O}_3]$ double-trace operators. It would be interesting to analyze these equations order by order in the $1/\Delta_{\text{gap}}^2$ expansion.

2.6 Flat space limit

Having fixed the general form of the impact parameter representation of the one-loop correlator from first principles in section 2.4, we now want to fix part of the dynamical data by taking the flat space limit, which relates it to the known flat space amplitudes. The prescription to achieve this was discovered in [40], where it was applied to scalar tree-level amplitudes. This limit is taken by sending the AdS radius R to infinity while scaling the relevant quantities in order to match them to flat space quantities in a sensible way. The dimensionless quantities S and L are sent to dimensionless combinations of R with the flat space center of mass energy s and impact parameter b as

$$S=\frac{R^2 s}{4}\,,\qquad L=\frac{b}{R}\,. \tag{2.196}$$

Note that L is the AdS impact parameter, as it describes the geodesic distance on H_{d-1} between the impact points in transverse space. If we impose the identification of Casimir eigenvalues

$$\Delta(\Delta - d) = R^2 m^2 \,, \tag{2.197}$$

for the states on the leading Regge trajectory and take this equation off-shell, it becomes

$$\nu^2 + \left(\frac{d}{2}\right)^2 = R^2 q^2 \,, \tag{2.198}$$

so for large R we further impose

$$\nu^2 = R^2 q^2 \,. \tag{2.199}$$

Our expressions in AdS are integrals in ν, while in flat space we have vector integrals in q, where we recall that q is a vector in the transverse space $\mathbb{R}^{D-2}$. In order to compare the expressions, it is instructive to do the flat space angular integrals and keep only the integral over the modulus $|q|$. In this way, the exponential is replaced by the harmonic function $\omega_q(b)$ according to

$$\int\limits_{\mathbb{R}^{D-2}} \frac{dq}{(2\pi)^{D-2}}\, e^{ib\cdot q} = 2\int\limits_0^\infty d|q|\, \omega_q(b) \,, \tag{2.200}$$

so that [61]

$$\omega_q(b) = q \int\limits_{\mathbb{R}^{D-2}} \frac{dp}{(2\pi)^{D-2}}\, e^{ib\cdot p}\, \delta(p^2 - q^2) = \frac{1}{2(2\pi)^{\frac{D-2}{2}}} \frac{|q|^{\frac{D-2}{2}}}{|b|^{\frac{D-4}{2}}} J_{\frac{D-4}{2}}(|q||b|) \,, \tag{2.201}$$

where J denotes the Bessel J-function and we recall that $\omega_q(b)$ only depends on the modulus of the vectors q and b. One can check that the flat space limit of the H_{d-1} harmonic function (2.145) yields the flat space harmonic function

$$R^{3-D}\Omega_{i\nu}(L) \to \omega_q(b) \,, \qquad \nu \geq 0 \,. \tag{2.202}$$

For even d this can be checked directly, while for general d it is convenient to use an integral representation for the hypergeometric function which under the limit is related to an integral representation for the Bessel function [62]. For even d the relation is also valid for $\nu < 0$.

In the context of string theory we further have the dimensionless coupling λ which is expressed in terms of α' and R as

$$\sqrt{\lambda} = \frac{R^2}{\alpha'} \,, \tag{2.203}$$

meaning we can also express S as

$$S = \frac{\sqrt{\lambda}\,\alpha' s}{4} \,. \tag{2.204}$$

To summarize, the flat space limit is taken by sending the AdS radius R to infinity while replacing

$$S = \frac{\sqrt{\lambda}\alpha' s}{4}, \quad L = \frac{b}{R}, \quad \nu^2 = R^2 q^2, \quad \nu_1^2 = R^2 q_1^2, \quad \nu_2^2 = R^2 q_2^2, \quad \sqrt{\lambda} = \frac{R^2}{\alpha'}, \tag{2.205}$$

and impact parameter representations can be compared by using (2.202). We can also use these relations to relate Δ_{gap} to λ taking as reference a string state of mass $m^2 = 4/\alpha'$, therefore

$$\Delta_{\text{gap}}^2 = \frac{4R^2}{\alpha'} = 4\sqrt{\lambda}\,. \tag{2.206}$$

2.6.1 Matching in impact parameter space

Let us now see what we can learn when we apply the flat space limit to the impact parameter representations studied in section 2.4. We begin with the tree-level correlator of four scalars for which the limit was originally imposed in [40]. The flat space limit of the AdS result $\mathcal{B}$ in (2.154) should match the flat space impact parameter representation $i\delta$ from (2.85) of the amplitude (2.78)[11]

$$\mathcal{B}_{\text{tree}}(p,\bar{p}) = 4\pi i \int_0^\infty d\nu\, \beta(\nu)\, S^{j(\nu)-1}\, \Omega_{i\nu}(L) \;\to\; i\delta_{\text{tree}}(s,b) = 2i \int_0^\infty d|q|\, \beta(t) \left(\frac{\alpha' s}{4}\right)^{j(t)-1} \omega_q(b)\,. \tag{2.207}$$

Here and below we do not always write the overall factors of R as in (2.202), but they do work out correctly when including the expansion parameters from (2.3) and (2.71) and using the relation

$$\frac{1}{N^2} = \frac{1}{R^{D-2}} \frac{2G_N}{\pi}\,. \tag{2.208}$$

From (2.202) and (2.204) we see that this does indeed match, provided the flat space limit of the AdS Regge trajectory and spectral function are sent to the flat space Regge trajectory and Pomeron propagator[12]

$$j(\nu) \;\to\; j(t)\,, \qquad \lambda^{\frac{j(\nu)-1}{2}} \beta(\nu) \;\to\; \frac{1}{2\pi}\,\beta(t)\,. \tag{2.209}$$

The power of λ in the relation of β's is necessary to cancel the powers of λ in the relation between S and $\alpha' s$. It is compatible with the expectation that each derivative in the couplings of the spin J operators forming the Pomeron comes at least with a power of $\lambda^{-\frac{1}{4}}$.

[11] The relative factor i in $\mathcal{B} \to i\delta$ can be determined by matching the exponents in the eikonal approximation for $\lambda \to \infty$.

[12] $j(\nu)$, $j(t)$ and $\beta(\nu)$, $\beta(t)$ are different functions and not the same function with different arguments.

Next we consider the optical theorem in AdS (2.134) and flat space (2.86)

$$-\text{Re}\mathcal{B}_{\text{1-loop}} = \frac{1}{2}\sum_{\substack{\Delta_5,\rho_5\\ \Delta_6,\rho_6}} \mathcal{B}^{3652\,*}_{\text{tree}}\mathcal{B}^{1564}_{\text{tree}} \;\to\; \text{Im}\delta_{\text{1-loop}}(b) = \frac{1}{2}\sum_{\substack{m_5,\rho_5,\epsilon_5\\ m_6,\rho_6,\epsilon_6}} \delta^{3652\,*}_{\text{tree}}\delta^{1564}_{\text{tree}}\,. \tag{2.210}$$

The similarity is striking, however we have to make sure the sums and summands are in fact related by the flat space limit. The additional sums over polarizations can be evaluated using completeness relations such as (2.92), which evaluate to contractions just as in the AdS equation. We also have to make sure that the labels ρ on both sides are irreducible representations of the same group $SO(d)$. This is indeed the case for massive particles if we consider the flat space limit $AdS_{d+1} \to \mathbb{R}^{1,d}$, which has the massive Little group $SO(d)$.

The next step is to match the tree-level correlators (2.159) and amplitudes (2.78) that involve spinning particles 5 and 6. In this case the flat space limit gives

$$\mathcal{B}^{(\Delta_5,\rho_5),(\Delta_6,\rho_6)}_{\mathbf{mn}}(p,\bar{p}) = 4\pi i\int_0^\infty d\nu\, S^{j(\nu)-1}\,\mathfrak{D}^{(\Delta_5,\rho_5),(\Delta_6,\rho_6)}_{\mathbf{mn}}(\nu)\,\Omega_{i\nu}(L) \;\to \tag{2.211}$$

$$\to i\delta^{(m_5,\rho_5),(m_6,\rho_6)}_{\mathbf{mn}}(s,b) = i\int_{\mathbb{R}^{D-2}}\frac{dq}{(2\pi)^{D-2}}\left(\frac{\alpha' s}{4}\right)^{j(t)-1} A^{12P}_{m_5,\rho_5,\mathbf{m}}(q,v)\,\beta(t)A^{34P}_{m_6,\rho_6,\mathbf{n}}(q,v)\,e^{iq\cdot b}$$

$$= 2i\int_0^\infty d|q|\left(\frac{\alpha' s}{4}\right)^{j(t)-1} A^{12P}_{m_5,\rho_5,\mathbf{m}}(-i\partial_b,v)\,\beta(t)A^{34P}_{m_6,\rho_6,\mathbf{n}}(-i\partial_b,v)\,\omega_q(b)\,,$$

where the derivative ∂_b is with respect to the components of the transverse vector b. The difference compared to (2.207) is that in AdS we have differential operators that generate tensor structures, while in flat space the tensor structures are the ones of the on-shell three-point amplitudes. As discussed in section 2.3.4, these three-point amplitudes are given in terms of the Pomeron momentum q and, for massive particles, the longitudinal polarization vector v, which is transverse to q. We will now study the relation of these two kinds of tensor structures to the flat space limit.

We begin with the covariant derivatives and will argue that they become derivatives in impact parameter in flat space, i.e.

$$\nabla^m_p\Omega_{i\nu}(L) \;\to\; R\partial^m_b e^{ib\cdot q} = Riq^m e^{ib\cdot q}\,. \tag{2.212}$$

In order to show this, we will act with two contracted covariant derivatives either on a single harmonic function or on two different ones, covering all situations that can occur. Acting on a single harmonic function we obtain, from (2.162) and (2.205),

$$\frac{1}{\sqrt{\lambda}}\,\nabla^2_p\,\Omega_{i\nu_{1,2}}(L) \;\to\; -\alpha' q^2_{1,2}\,\omega_{i\nu_{1,2}}(b)\,. \tag{2.213}$$

The action of contracted covariant derivatives on two different harmonic functions is captured by the functions W_k in (2.164), which is given in the flat space limit by the leading term (2.168)

$$\frac{W_k(\nu_1^2,\nu_2^2,\nu^2)}{(\sqrt{\lambda})^k} \;\to\; \left(\frac{\nu_1^2+\nu_2^2-\nu^2}{2\sqrt{\lambda}}\right)^k \;\to\; \left(\alpha'\,\frac{q_1^2+q_2^2-q^2}{2}\right)^k = (\alpha')^k(-q_1\cdot q_2)^k\,, \tag{2.214}$$

where we used that $q = q_1 + q_2$. This implies that the flat space limit of (2.164) is

$$\frac{1}{(\sqrt{\lambda})^k}\nabla_{p\,m_1}\ldots\nabla_{p\,m_k}\Omega_{i\nu_1}(L)\nabla_p^{m_1}\ldots\nabla_p^{m_k}\Omega_{i\nu_2}(L) \;\to \tag{2.215}$$

$$\to (-\alpha')^k q_{1\,m_1}\ldots q_{1\,m_k}e^{ib\cdot q_1}q_2^{m_1}\ldots q_2^{m_k}e^{ib\cdot q_2}\,. \tag{2.216}$$

We conclude that both (2.213) and (2.216) are compatible with (2.212). Apart from the covariant derivative, tensor structures depend also on the direction $\hat{p}$, which is normal to the transverse space H_{d-1} and satisfies $\hat{p}^2 = -1$. In flat space the only possible direction for polarizations that is normal to the transverse space is the unit vector v, hence we have to require that in the flat space limit

$$\hat{p}^m \;\to\; iv^m\,. \tag{2.217}$$

With the identifications (2.212) and (2.217), the matching in (2.211) works provided that the spectral functions $\beta^{k_5,k_6}_{(\Delta_5,\rho_5),(\Delta_6,\rho_6)}(\nu)$ in (2.160) are such that

$$\lambda^{\frac{j(\nu)-1}{2}}\mathfrak{D}^{(\Delta_5,\rho_5),(\Delta_6,\rho_6)}_{\mathbf{mn}}(\nu)\,\Omega_{i\nu}(L) \;\to\; \frac{1}{2\pi}A^{12P}_{m_5,\rho_5,\mathbf{m}}(-i\partial_b,v)\,\beta(t)\,A^{34P}_{m_6,\rho_6,\mathbf{n}}(-i\partial_b,v)\,\omega_q(b)\,. \tag{2.218}$$

Using the explicit tensor structures for three-point amplitudes in (2.97), the matching (2.218) can also be expressed for the spectral function for any given tensor structure

$$\lambda^{\frac{j(\nu)-1}{2}}\lambda^{\frac{|\rho_5|-k_5}{4}}\lambda^{\frac{|\rho_6|-k_6}{4}}\beta^{k_5,k_6}_{(\Delta_5,\rho_5),(\Delta_6,\rho_6)}(\nu) \;\to\; \frac{1}{2\pi}\,a^{k_5}_{m_5,\rho_5}(t)\,a^{k_6}_{m_6,\rho_6}(t)\,\beta(t)\,. \tag{2.219}$$

The powers of λ are again compatible with a factor of $\lambda^{-\frac{1}{4}}$ in $\beta^{k_5,k_6}_{(\Delta_5,\rho_5),(\Delta_6,\rho_6)}(\nu)$ for each derivative in the coupling. Such a scaling is expected from the general arguments of [7, 63]. We have now shown that all tree-level phase shifts appearing in the AdS and flat space optical theorems can be related by the flat space limit.

Let us also compare the vertex functions that appear in both AdS and flat space impact parameter representations of the one-loop amplitudes. The flat space limit of (2.172) is given by the impact parameter transform of (2.90), i.e.

$$-\mathrm{Re}\mathcal{B}_{\text{1-loop}}(p,\bar{p}) \;\to\; \mathrm{Im}\delta_{\text{1-loop}}(s,b)\,, \tag{2.220}$$

becomes

$$\begin{aligned} &2\pi^2 \int_{-\infty}^{\infty} d\nu d\nu_1 d\nu_2 \, \beta(\nu_1)^* \beta(\nu_2) \, V(\nu_1,\nu_2,\nu)^2 S^{j(\nu_1)+j(\nu_2)-2} \Phi(\nu_1,\nu_2,\nu) \, \Omega_{i\nu}(L) \;\to \\ \to \frac{1}{2} &\int_{\mathbb{R}^{D-2}} \frac{dq dq_1 dq_2}{(2\pi)^{2(D-2)}} \, \beta(t_1)^* \beta(t_2) \, V(q_1,q_2)^2 \left(\frac{\alpha' s}{4}\right)^{j(t_1)+j(t_2)-2} \delta(q-q_1-q_2) \, e^{iq\cdot b} \, . \end{aligned} \tag{2.221}$$

In this case we can use the delta function to write all the other scalar functions in terms of q_1^2, q_2^2 and q^2, however we need to do the angular integral over the delta function itself. To this end we can define

$$\int_{\mathbb{R}^{D-2}} \frac{dq_1 dq_2}{(2\pi)^{D-2}} \, \delta(q-q_1-q_2) = 4 \int_0^{\infty} d|q_1| d|q_2| \, \phi(q_1,q_2,q) \, . \tag{2.222}$$

Using this and (2.200), we can compute the angular integrals in

$$\int_{\mathbb{R}^{D-2}} \frac{dq_1 dq_2}{(2\pi)^{2(D-2)}} \, e^{ib\cdot(q_1+q_2)} = \int_{\mathbb{R}^{D-2}} \frac{dq_1 dq_2 dq}{(2\pi)^{2(D-2)}} \, \delta(q-q_1-q_2) \, e^{ib\cdot q} \, , \tag{2.223}$$

to find the flat space version of (2.163)

$$\omega_{q_1}(b) \, \omega_{q_2}(b) = 2 \int_0^{\infty} d|q| \, \phi(q_1,q_2,q) \, \omega_q(b) \, . \tag{2.224}$$

Using the explicit expressions for Φ and ϕ (which can be found for instance in appendix E of [59]), one can further check that under the flat space limit

$$R^{4-D} \Phi(\nu_1,\nu_2,\nu) \;\to\; \phi(q_1,q_2,q) \, . \tag{2.225}$$

With this relation is clear that the expressions in (2.221) are indeed related by the flat space limit provided that the vertex functions are related by

$$V(\nu_1,\nu_2,\nu) \;\to\; V(q_1,q_2) = V(t_1,t_2,t) \, . \tag{2.226}$$

2.6.2 Constraining AdS quantities

We saw above that all elements of the impact parameter optical theorems in AdS and flat space are related by the flat space limit provided that $j(\nu)$, $\beta(\nu)$, $\beta^{k_5,k_6}_{(\Delta_5,\rho_5),(\Delta_6,\rho_6)}(\nu)$ and $V\left(\nu_1^2,\nu_2^2,\nu^2\right)$ are given by their flat space counterparts in the limit. In this subsection, we briefly review

how the limit actually constrains these functions. All of these objects depend on two dimensionless quantities, the spectral parameters ν and the 't Hooft coupling λ. Let us discuss this for a generic function $f(\nu)$ that is required to satisfy the flat space limit

$$f(\nu,\lambda) \;\to\; f(t)\,. \tag{2.227}$$

Existence of the gravity limit requires the function to have an expansion in negative powers of $\sqrt{\lambda}$ of the form

$$f(\nu,\lambda) = \sum_{n=0}^{\infty} \frac{f_n(\nu)}{\lambda^{n/2}}\,. \tag{2.228}$$

In order for the flat space limit (2.205) of the function to be finite, the functions $f_n(\nu)$ must have an expansion in large ν with leading power not larger than $2n$,

$$f_n(\nu) = a_{n,n}\nu^{2n} + a_{n,n-1}\nu^{2(n-1)} + a_{n,n-2}\nu^{2(n-2)} + \dots\,, \tag{2.229}$$

which ensures finiteness of the limit order by order in the large λ expansion. The flat space limit of $f(\nu,\lambda)$ is then

$$f(\nu,\lambda) \;\to\; \sum_{n=0}^{\infty} a_{n,n}\left(\frac{\nu^2}{\sqrt{\lambda}}\right)^n \;\to\; \sum_{n=0}^{\infty} a_{n,n}(\alpha' q^2)^n\,. \tag{2.230}$$

At every order in $1/\sqrt{\lambda}$ the leading power of ν survives and is fixed by the flat space limit, while all the other powers are subleading, and cannot be determined from this condition. These considerations hold for $j(\nu)$, $\beta(\nu)$, $\beta^{k_5,k_6}_{(\Delta_5,\rho_5),(\Delta_6,\rho_6)}(\nu)$ and $V(\nu_1,\nu_2,\nu)$, fixing part of these functions. These facts have been explored in detail for the functions $j(\nu)$ and $\beta(\nu)$ in [4, 41].

2.7 Relating type IIB string theory in AdS and flat space

Let us now apply our general ideas to a concrete example, the scattering of four dilatons in type IIB superstring theory on $AdS_5 \times S^5$. In the flat space limit this is related to type IIB superstring theory on 10-dimensional flat space where the kinematics is restricted to the five dimensions arising from AdS. This happens since both the dilatons and the Pomerons are R-symmetry singlets, meaning the tidal excitations they couple to also have to be singlets. As a consequence, the Regge limit does not probe the 10 dimensional nature of the string scattering process, as we consider only states with the vacuum quantum numbers associated to the compact manifold S^5. For this case the discontinuity of the (finite α') one-loop amplitude in the Regge limit was computed in [35] and is precisely of the form (2.90) with $D = 5$. The regime of validity of this description was discussed in detail in [35]. All we need to specify are the four dynamic quantities that we already discussed in the previous section. For the

Regge trajectory and Pomeron propagator we have

$$j(t) = 2 + \frac{\alpha'}{2}\, t\,, \qquad \beta(t) = 2\pi^2 \frac{\Gamma\big(-\frac{\alpha'}{4}t\big)}{\Gamma\big(1+\frac{\alpha'}{4}t\big)}\, e^{-\frac{i\pi\alpha'}{4}t}\,. \tag{2.231}$$

As discussed in section 2.3.3 the vertex function can be obtained from the scattering amplitude of two dilatons and two Pomerons. This amplitude was computed in [35] and reads

$$A^{12P_1P_2}(k,q_1,q_2) = -\frac{\Gamma(1+\alpha' q_{12}/2)\,\Gamma\big(-\alpha'\frac{k^2}{4}-\alpha' q_{12}/2\big)\,\Gamma\big(\alpha'\frac{k^2}{4}\big)}{2\Gamma(-\alpha' q_{12}/2)\,\Gamma\big(1+\alpha' q_{12}/2+\alpha'\frac{k^2}{4}\big)\,\Gamma\big(1-\alpha'\frac{k^2}{4}\big)}\,, \tag{2.232}$$

where $q_{12} = q_1 \cdot q_2$. This amplitude has poles at the masses ($m^2 = 4n/\alpha'$) of the string states with residues

$$\operatorname*{Res}_{k^2=-4n/\alpha'} A^{12P_1P_2}(k,q_1,q_2) = \left(\frac{(-\alpha' q_{12}/2)_n}{n!}\right)^2\,, \qquad n = 0,1,2,\dots\,, \tag{2.233}$$

and the resulting vertex function is given by (2.89)

$$V(q_1,q_2) = \sum_{n=0}^{\infty}\left(\frac{(-\alpha' q_{12}/2)_n}{n!}\right)^2 = \frac{\Gamma\big(1+\alpha'\frac{t_1+t_2-t}{2}\big)}{\Gamma\big(1+\alpha'\frac{t_1+t_2-t}{4}\big)^2}\,. \tag{2.234}$$

Using the reasoning of section 2.6.2, this immediately fixes the leading terms in ν, ν_i of the AdS vertex function at every order in λ

$$V(\nu_1,\nu_2,\nu) = \frac{\Gamma\Big(1-\frac{\nu_1^2+\nu_2^2-\nu^2}{2\sqrt{\lambda}}\Big)}{\Gamma\Big(1-\frac{\nu_1^2+\nu_2^2-\nu^2}{4\sqrt{\lambda}}\Big)^2} + \text{vanishing in flat space limit}\,. \tag{2.235}$$

Thus, the first two corrections from expanding (2.235) at large λ are

$$\begin{aligned} V(\nu_1,\nu_2,\nu) = 1 &+ \Big(0\cdot\big(\nu_1^2+\nu_2^2-\nu^2\big)+c_{1,0}\Big)\frac{1}{\sqrt{\lambda}} \\ &+ \left(\frac{\pi^2}{96}\big(\nu_1^2+\nu_2^2-\nu^2\big)^2 + c_{2,1}\big(\nu_1^2+\nu_2^2\big) + c'_{2,1}\nu^2 + c_{2,0}\right)\frac{1}{\lambda} + \dots\,, \end{aligned} \tag{2.236}$$

where we also included the constants that are not fixed by the flat space limit. We note that the constants multiplying the leading power of ν at order $\big(\sqrt{\lambda}\big)^{-n}$ have a uniform transcendentality of weight n, which can be seen by explicitly expanding (2.235). It would be interesting to understand the relation of this property with features of maximal transcendentality in $\mathcal{N}=4$ SYM [64, 65].

Finally, all the spectral functions $\beta^{k_5,k_6}_{(\Delta_5,\rho_5),(\Delta_6,\rho_6)}(\nu)$ of tree-level correlators that contribute to the optical theorem are constrained by the flat space limit. Their flat space limit (2.219) is parameterized by on-shell three-point amplitudes in flat space. These amplitudes are in

principle encoded in the result (2.233), which separates the contributions of particles with different masses, but not the ones of particles in different representations ρ. The attempt to expand (2.233) into products of three-point amplitudes for different ρ and tensor structures k using (2.88) shows that this does not fully fix the $a^k_{m_5,\rho_5}(t)$ in (2.97) because the equations are quadratic. However the three-point amplitudes can of course be computed in string theory, which is what the next subsection is about. We will start with the 10D open superstring amplitudes of a massless vector, a Pomeron and an open string state up to mass level 2 which were computed in [53] by studying string-brane scattering. These amplitudes have to be squared to obtain closed string amplitudes. Then the irreducible representations of the 10D massive Little group $SO(9)$ have to be branched into irreducible representations of $SO(4)$ to match with the CFT irreps and account for the fact that we have five non-compact dimensions.

2.7.1 Massive tree amplitudes in flat space

Now we will discuss the flat space three-point amplitudes that take part in the process and that will fix part of the tree-level correlators with external spinning legs in AdS via the flat space limit. The goal is to derive the three-point amplitudes that appear in the unitarity cut (2.233) of the four-point amplitude of two dilatons and two Pomerons (2.232). It will be convenient to consider the more general case of two gravitons instead of dilatons, with polarizations $\epsilon_i^{\mu\nu} = \epsilon_i^\mu \epsilon_i^\nu$, and obtain the dilaton amplitudes in the very end by replacing $\epsilon_i^{\mu\nu}$ with $\eta^{\mu\nu}$. By using explicitly transverse three-point amplitudes and the completeness relation (2.92), we can write tree-level unitarity (2.88) in the form

$$\operatorname*{Res}_{k^2=-4n/\alpha'} A^{12P_1P_2}(k,q_{12}) = \left(\frac{(-\alpha' q_{12}/2)_n}{n!}\right)^2 (\epsilon_1\cdot\epsilon_2)^2 = \sum_{\rho,i} A^{15P_1}_{n,\rho,i,\mathbf{m}} \pi_\rho^{\mathbf{m},\mathbf{n}} A^{52P_2}_{n,\rho,i,\mathbf{n}}\,, \tag{2.237}$$

where for the massive levels, on which we will mostly focus, ρ is summed over irreducible representations of $SO(4)$ and i is summed over degenerate states in the same representation.

Our starting point will be the open string three-point amplitudes of a massless vector, a Pomeron and an arbitrary massive state up to mass level 2 (we give some simpler explicit examples in Appendix A.1). These amplitudes were computed in [53] by studying string-brane scattering. Since in flat space there is no interaction between the left- and right-moving string modes, the closed string amplitudes factorize into products of open string amplitudes. We can indeed check that the square root of the residues (2.237) matches the expansion in terms of the open string three-point amplitudes of [53]

$$\sqrt{\operatorname*{Res}_{k^2=-4n/\alpha'} A^{12P_1P_2}(k,q_{12})} = \frac{(-\alpha' q_{12}/2)_n}{n!}(\epsilon_1\cdot\epsilon_2) = \sum_{\rho_L} A^{15P_1}_{n,\rho_L,\boldsymbol{\alpha}} \pi_{\rho_L}^{\boldsymbol{\alpha},\boldsymbol{\gamma}} A^{52P_2}_{n,\rho_L,\boldsymbol{\gamma}}\,. \tag{2.238}$$

We did this consistency check for the first three mass levels, for which ρ_L is summed over the bosonic part (NS sector) of the chiral superstring spectrum in 10 dimensions, given by [66]

$$
\begin{aligned}
n = 0 : &\quad \square_8 \,, \\
n = 1 : &\quad \square\square_9 \oplus \begin{array}{|c|}\hline\ \\\hline\ \\\hline\end{array}_9 \,, \\
n = 2 : &\quad \square\square\square_9 \oplus \begin{array}{|c|c|}\hline\ & \\\hline\ \\\cline{1-1}\ \\\cline{1-1}\end{array}_9 \oplus \begin{array}{|c|c|}\hline\ & \\\hline\ \\\cline{1-1}\end{array}_9 \oplus \begin{array}{|c|}\hline\ \\\hline\ \\\hline\end{array}_9 \oplus \square_9 \,.
\end{aligned}
\tag{2.239}
$$

In order to obtain three-point amplitudes for closed strings in $10D$, we need to square (2.238) and expand again in irreducible representations. The first step is trivial

$$
\operatorname*{Res}_{k^2=-4n/\alpha'} A^{12P_1P_2}(k, q_{12}) = \sum_{\rho_L,\rho_R} A^{15P_1}_{n,\rho_L,\boldsymbol{\alpha}}\, A^{15P_1}_{n,\rho_R,\boldsymbol{\beta}}\, \pi^{\boldsymbol{\alpha},\gamma}_{\rho_L}\, \pi^{\boldsymbol{\beta},\delta}_{\rho_R}\, A^{52P_2}_{n,\rho_L,\gamma}\, A^{52P_2}_{n,\rho_R,\delta} \,, \tag{2.240}
$$

however expanding this into irreducible representations requires some more work. On an abstract level this is easily done in terms of the tensor product

$$
\rho_L \otimes \rho_R = \bigoplus_{\rho_C} \rho_C \,, \tag{2.241}
$$

which can be computed explicitly in terms of characters using e.g. the WeylCharacterRing implementation in SageMath [67]. For example, the closed string spectrum for the first two mass levels is

$$
n = 0 : \ \square_8 \otimes \square_8 = \square\square_8 \oplus \begin{array}{|c|}\hline\ \\\hline\ \\\hline\end{array}_8 \oplus \bullet \,, \tag{2.242}
$$

$$
\begin{aligned}
n = 1 : \ & \left(\square\square_9 \oplus \begin{array}{|c|}\hline\ \\\hline\ \\\hline\end{array}_9\right)^2 = \begin{array}{|c|c|}\hline\ & \\\hline\ & \\\hline\end{array}_9 \oplus \begin{array}{|c|c|}\hline\ & \\\hline\ & \\\cline{1-1}\ \\\cline{1-1}\end{array}_9 \oplus 2\begin{array}{|c|c|c|}\hline\ & & \\\hline\ \\\cline{1-1}\end{array}_9 \oplus 3\begin{array}{|c|c|}\hline\ & \\\hline\ \\\cline{1-1}\ \\\cline{1-1}\end{array}_9 \oplus \square\square\square\square_9 \\
& \oplus \begin{array}{|c|c|c|}\hline\ & & \\\hline\ \\\cline{1-1}\end{array}_9 \oplus 2\begin{array}{|c|c|}\hline\ & \\\hline\ & \\\hline\end{array}_9 \oplus \begin{array}{|c|c|}\hline\ & \\\hline\ \\\cline{1-1}\end{array}_9 \oplus \begin{array}{|c|}\hline\ \\\hline\ \\\hline\ \\\hline\end{array}_9 \oplus 2\begin{array}{|c|c|}\hline\ & \\\hline\ \\\cline{1-1}\end{array}_9 \oplus 3\begin{array}{|c|}\hline\ \\\hline\ \\\hline\end{array}_9 \oplus 2\square\square_9 \oplus 2\begin{array}{|c|}\hline\ \\\hline\ \\\hline\end{array}_9 \oplus 2\,\bullet \,.
\end{aligned}
$$

To use the tensor product in explicit calculations requires considerably more work and can be done by formulating (2.241) as an equation in terms of projectors to irreducible representations

$$
\pi^{\boldsymbol{\alpha};\gamma}_{\rho_L}\, \pi^{\boldsymbol{\beta};\delta}_{\rho_R} = \sum_{\rho_C \subset \rho_L \otimes \rho_R} p^{\boldsymbol{\alpha}\boldsymbol{\beta}}_{\rho_L\otimes\rho_R\to\rho_C,\boldsymbol{\mu}} \pi^{\boldsymbol{\mu};\boldsymbol{\nu}}_{\rho_C}\, p^{\gamma\delta}_{\rho_L\otimes\rho_R\to\rho_C,\boldsymbol{\nu}} \,. \tag{2.243}
$$

The tensors $p_{\rho_L\otimes\rho_R\to\rho_C}$ are constructed from Kronecker deltas and are uniquely determined by this equation. By inserting (2.243) into (2.240) we find the expansion of the residue

$$\operatorname*{Res}_{k^2=-4n/\alpha'} A^{12P_1P_2}(k,q_{12}) = \sum_{\rho_L,\rho_R,\rho_C} A^{15P_1}_{n,\rho_L\otimes\rho_R\to\rho_C,\boldsymbol{\mu}}\,\pi^{\boldsymbol{\mu},\boldsymbol{\nu}}_{\rho_C}\,A^{52P_2}_{n,\rho_L\otimes\rho_R\to\rho_C,\boldsymbol{\nu}}\,, \tag{2.244}$$

in terms of the closed string amplitudes

$$A^{15P_1}_{n,\rho_L\otimes\rho_R\to\rho_C,\boldsymbol{\mu}} = A^{15P_1}_{n,\rho_L,\boldsymbol{\alpha}}\;A^{15P_1}_{n,\rho_R,\boldsymbol{\beta}}\;p^{\boldsymbol{\alpha}\boldsymbol{\beta}}_{\rho_L\otimes\rho_R\to\rho_C,\boldsymbol{\mu}}\,. \tag{2.245}$$

The final step is to restrict the indices of the amplitudes to five dimensions and expand once again into irreducible representations, this times for the massive Little group $SO(4)$. In terms of representation theory, this is done by using branching rules to expand the $SO(9)$ representations in terms of irreps of the product $SO(4)\times SO(5)$,

$$\rho_C = \bigoplus_{(\rho,\sigma)\subset\rho_C} (\rho,\sigma)\,, \tag{2.246}$$

where, for massive levels, ρ is an irreducible representation of $SO(4)$ and σ of $SO(5)$. Since we consider Pomeron exchange, which caries the vacuum quantum numbers, we project onto the singlets of $SO(5)$

$$\rho_C|_{\bullet_5} = \bigoplus_{(\rho,\bullet)\subset\rho_C} (\rho,\bullet)\,. \tag{2.247}$$

This step is also abstractly implemented in SageMath. For example, we have

$$\square\square_9 = \left(\square\square_4,\bullet_5\right)\oplus\left(\square_4,\square_5\right)\oplus\left(\bullet_4,\square\square_5\right)\oplus\left(\bullet_4,\bullet_5\right). \tag{2.248}$$

and after projection to $SO(5)$ singlets

$$\square\square_9\Big|_{\bullet_5} = \square\square_4\oplus\bullet_4\,. \tag{2.249}$$

In this way we find the $SO(5)$ singlets for the closed string spectrum in terms of $SO(3)$ or $SO(4)$ irreps for the first two levels

$$\begin{aligned}
n=0:\quad & \square\square_3\oplus\square_3\oplus\,2\bullet\,,\\
n=1:\quad & \square\square\square\square_4\oplus\begin{array}{|c|c|c|}\hline\multicolumn{1}{|c}{}&\multicolumn{1}{c|}{}&\multicolumn{1}{c|}{}\\\hline\multicolumn{1}{|c}{}\\\cline{1-1}\end{array}_4\oplus 2\begin{array}{|c|c|}\hline\multicolumn{1}{|c}{}&\multicolumn{1}{c|}{}\\\hline\multicolumn{1}{|c}{}&\multicolumn{1}{c|}{}\\\cline{1-2}\end{array}_4\oplus 2\square\square\square_4\oplus 4\begin{array}{|c|c|}\hline\multicolumn{1}{|c}{}&\multicolumn{1}{c|}{}\\\hline\multicolumn{1}{|c}{}\\\cline{1-1}\end{array}_4\oplus 8\square\square_4\\
& \oplus 5\begin{array}{|c|}\hline\\\hline\\\hline\end{array}_4\oplus 10\square_4\oplus 9\,\bullet_4\,.
\end{aligned} \tag{2.250}$$

As for the tensor product, we can rephrase (2.247) as an equation in terms of projectors. In this case we get an equation for the $SO(9)$ projector with indices restricted to the $SO(4)$

directions $a = 1, \ldots, 4$

$$\pi_{\rho_C}^{\mathbf{a};\mathbf{b}} = \sum_{\rho \subset \rho_C|_{\bullet_5}} b^{\mathbf{a}}_{\rho_C \to \rho, \mathbf{m}} \, \pi_{\rho}^{\mathbf{m};\mathbf{n}} \, b^{\mathbf{b}}_{\rho_C \to \rho, \mathbf{n}} \,, \tag{2.251}$$

where the tensors $b_{\rho_C \to \rho}$ are uniquely determined by this equation and can be expressed in terms of Kronecker deltas and the $SO(4)$ Levi-Civita symbol. Since we are assuming the flat space limit kinematics to be restricted to five dimensions, we can simply insert this into (2.244) and obtain the residue in the anticipated form (2.237)

$$\operatorname*{Res}_{k^2 = -4n/\alpha'} A^{12P_1P_2}(k, q_{12}) = \sum_{\rho_L, \rho_R, \rho_C, \rho} A^{15P_1}_{n, \rho_L \otimes \rho_R \to \rho_C \to \rho, \mathbf{m}} \pi_{\rho}^{\mathbf{m},\mathbf{n}} A^{52P_2}_{n, \rho_L \otimes \rho_R \to \rho_C \to \rho, \mathbf{n}} \,, \tag{2.252}$$

with the $5D$ closed string amplitudes given by

$$A^{15P_1}_{n, \rho_L \otimes \rho_R \to \rho_C \to \rho, \mathbf{m}} = A^{15P_1}_{n, \rho_L \otimes \rho_R \to \rho_C, \mathbf{a}} b^{\mathbf{a}}_{\rho_C \to \rho, \mathbf{m}} \,. \tag{2.253}$$

2.7.1.1 Example

Let us now give a specific example of the procedure outlined above. We will consider the following chain of expansions at mass level 1, starting from the product of two open string massive spin 2 fields that give rise to a $5D$ scalar

$$\square\square_9 \otimes \square\square_9 \to \square\square_9 \to \bullet_4 \,. \tag{2.254}$$

In this example we discard the $5D$ massive spin 2 field that also appears in the projection (2.249). We alert the reader that whenever we write explicit amplitudes they are neither appropriately symmetrized nor traceless in order to write them more compactly. All explicit amplitudes should be understood as objects to be contracted with the projector for the associated representation.

We start with the open string amplitude for the state $(1, \square\square_9)$ from [53]

$$A^{15P_1}_{1, [2]_9, \alpha_1 \alpha_2} = -\sqrt{\frac{\alpha'}{2}} \left(\epsilon_{1\alpha_1} q_{1\alpha_2} + \frac{1}{2} (q_1 \cdot \epsilon_1) \, v_{\alpha_1} v_{\alpha_2} \right) . \tag{2.255}$$

Squaring this amplitude produces the following closed string states

$$\square\square_9 \otimes \square\square_9 = \square\square\square\square_9 \oplus \begin{array}{|c|c|c|}\hline & & \\ \hline \\ \cline{1-1} \end{array}_{\,9} \oplus \begin{array}{|c|c|}\hline & \\ \hline & \\ \hline \end{array}_{\,9} \oplus \begin{array}{|c|}\hline \\ \hline \\ \hline \end{array}_{\,9} \oplus \square\square_9 \oplus \bullet_9 \,. \tag{2.256}$$

To construct the relation (2.243) we need the projectors for all the representations in this list. They can be found in [68, 69], however here we just remind the reader of two of the most

familiar ones

$$\pi^{\mu_1\mu_2,\nu_1\nu_2}_{[2]_d} = \frac{1}{2}\left(\eta^{\mu_1\nu_1}\eta^{\mu_2\nu_2} + \eta^{\mu_1\nu_2}\eta^{\mu_2\nu_1}\right) - \frac{1}{d}\,\eta^{\mu_1\mu_2}\eta^{\nu_1\nu_2}\,, \qquad \pi_\bullet = 1\,, \tag{2.257}$$

and state that the closed string state $\square\!\square_9$ comes in (2.243) with the tensor

$$p^{\alpha_1\alpha_2\beta_1\beta_2}_{[2]_9\otimes[2]_9\to[2]_9,\mu_1\mu_2} = \sqrt{\frac{36}{91}}\,\pi^{\alpha_1\alpha_2;\gamma_1\gamma_2}_{[2]_9}\pi^{\beta_1\beta_2;\delta_1\delta_2}_{[2]_9}\eta_{\gamma_2\delta_1}\eta_{\gamma_1\mu_1}\eta_{\delta_1\mu_2}\,, \tag{2.258}$$

where we introduced additional projectors contracted with metrics in order to have the correct index properties. This determines the following closed string amplitude via (2.245)

$$\begin{aligned} A^{15P_1}_{1,[2]_9\otimes[2]_9\to[2]_9,\mu_1\mu_2} = \frac{\alpha'}{4\sqrt{91}}\Big[&\big(q_{1,\mu_1}(\epsilon_{1,\mu_2}q_1\cdot\epsilon_1 + 3q_{1,\mu_2}) \\ &+ \epsilon_{1,\mu_1}(q_{1,\mu_2}q_1\cdot\epsilon_1 - 3t_1\epsilon_{1,\mu_2}) + v_{\mu_1}v_{\mu_2}(q_1\cdot\epsilon_1)^2\big)\Big]\,. \end{aligned} \tag{2.259}$$

The branching rule for $\square\!\square_9$ was already considered in (2.249). Using the projectors (2.257) it is easy to see that we can write explicitly

$$\pi^{a_1a_2,b_1b_2}_{[2]_9} = \delta^{a_1}_{m_1}\delta^{a_2}_{m_2}\pi^{m_1m_2,n_1n_2}_{[2]_4}\delta^{b_1}_{n_1}\delta^{b_2}_{n_2} + \frac{5}{36}\,\delta^{a_1a_2}\pi_\bullet\delta^{b_1b_2}\,, \tag{2.260}$$

from which we read off

$$b^{a_1a_2}_{[2]_9\to[2]_4,m_1m_2} = \delta^{a_1}_{m_1}\delta^{a_2}_{m_2}\,, \qquad b^{a_1a_2}_{[2]_9\to\bullet_4} = \sqrt{\frac{5}{36}}\,\delta^{a_1a_2}\,. \tag{2.261}$$

Finally, inserting (2.259) and (2.261) into (2.253) we compute the $5D$ closed string amplitude

$$A^{15P_1}_{1,[2]_9\otimes[2]_9\to[2]_9\to\bullet_4} = \frac{1}{8}\sqrt{\frac{5}{91}}\alpha'\left((q_1\cdot\epsilon_1)^2 - 2t_1\right) \tag{2.262}$$

We derive the complete list of such level 1 three-point amplitudes in appendices A.2 and A.3.

2.7.2 Constraints on spinning AdS amplitudes

In this section we use the flat-space string amplitudes to constrain the high-energy, tree-level AdS_5 amplitudes with two dilatons and two spinning operators $\langle\phi\phi\mathcal{O}_5\mathcal{O}_6\rangle$. Since the operators in question are of stringy nature (i.e. the bulk fields have $m^2 \sim 4n/\alpha'$ for a very large AdS radius), their dimensions grow with the 't Hooft coupling ($\Delta \sim \lambda^{1/4}$) and transform in the $SO(4)$ representations discussed above in the flat space case. This means that generically $\mathcal{O}_5$ and $\mathcal{O}_6$ are in bosonic mixed-symmetry representations.

As discussed in section 2.6.1, the spectral functions that determine the spinning AdS correlators (2.159) via (2.160) are determined in the flat space limit by the three-point amplitudes

(2.97)

$$\lambda^{\frac{j(\nu)-1}{2}}\lambda^{\frac{|\rho_5|-k_5}{4}}\lambda^{\frac{|\rho_6|-k_6}{4}}\beta^{k_5,k_6}_{(\Delta_5,\rho_5),(\Delta_6,\rho_6)}(\nu)\ \to\ \frac{1}{2\pi}\,a^{k_5}_{m_5,\rho_5}(t)\,a^{k_6}_{m_6,\rho_6}(t)\beta(t)\,. \tag{2.263}$$

In other words, the leading term in ν at each order in λ is fixed by the flat space expression (see section 2.6.2)

$$\lambda^{\frac{j(\nu)-1}{2}}\lambda^{\frac{|\rho_5|-k_5}{4}}\lambda^{\frac{|\rho_6|-k_6}{4}}\beta^{k_5,k_6}_{(\Delta_5,\rho_5),(\Delta_6,\rho_6)}(\nu)=\frac{1}{2\pi}a^{k_5}_{m_5,\rho_5}(t)\,a^{k_6}_{m_6,\rho_6}(t)\beta(t)\Big|_{\alpha' t=-\frac{\nu^2}{\sqrt{\lambda}}}+\dots\,, \tag{2.264}$$

where $\dots$ are terms that vanish in the flat space limit. Let us now use this to study some specific examples. We begin with the example of section 2.7.1.1 where we computed an amplitude involving a graviton, a Pomeron and a particular scalar at mass level 1 in (2.262). In this result $\epsilon_{1,\mu}$ is such that $\epsilon_{\mu\nu}=\epsilon_{1,\mu}\epsilon_{1,\nu}$ parametrizes a general graviton polarization which must be replaced by the metric $\epsilon_{\mu\nu}\to\eta_{\mu\nu}$ to obtain the dilaton amplitude

$$A^{D5P_1}_{1,[2]_9\otimes[2]_9\to[2]_9\to\bullet_4}=a^0_{4/\alpha',[2]_9\otimes[2]_9\to[2]_9\to\bullet_4}(t)=-\frac{3}{8}\sqrt{\frac{5}{91}}\,\alpha' t\,, \tag{2.265}$$

where we used that $(q_1\cdot\epsilon_1)^2=-t_1$ for the dilaton case. Thus, for the AdS correlator of this particular scalar and three dilatons we have

$$\beta^{0,0}_{(2\lambda^{\frac{1}{4}}+\dots,\bullet),(4,\bullet)}(\nu)=\frac{3}{8}\sqrt{\frac{5}{91}}\frac{\nu^2}{\sqrt{\lambda}}\,\beta(\nu)+\text{vanishing in the flat space limit}\,. \tag{2.266}$$

Note that with respect to the case of four dilaton scattering we have an extra power of $1/\sqrt{\lambda}$, so the term of order λ^0 is absent, confirming that tidal excitations are suppressed at large λ, which in turn agrees with the considerations of [44] (we verified this fact for all amplitudes at level 1). In particular, this is consistent with the large λ suppression of $c_{\phi_1\phi_2 j(\nu)}$ for non-identical scalars, since our stringy mode is certainly different from the dilaton. Such a suppression is not a priori obvious from writing a bulk interaction between two different scalars and a spin J field (to be Sommerfeld-Watson transformed into a Pomeron), which makes this a non-trivial realization of the bounds derived in [7, 63]. This example is particularly simple, since there is a unique three-point structure in the case of the scalar.

More generally, we can consider amplitudes with several tensor structures constructed from v_a's and q_a's (equivalently, $\hat{p}$ and ∇_p in AdS). Let us take as a representative example, the case of the spin 4 operator at level 1. This operator is typically used to define Δ_{gap} and sits in the leading Regge trajectory. The corresponding graviton-Pomeron-spin 4 amplitude was worked out in Appendices A.2 and A.3, and reads

$$A^{a_1a_2a_3a_4}_{[2]_9\otimes[2]_9\to[4]_9\to[4]_4}(\epsilon_1)=\frac{1}{8}\alpha'\left(2\epsilon_{1,a_1}q_{1,a_2}+v_{a_1}v_{a_2}q_1\cdot\epsilon_1\right)\left(2\epsilon_{1,a_3}q_{1,a_4}+v_{a_3}v_{a_4}q_1\cdot\epsilon_1\right). \tag{2.267}$$

We again emphasize that it is understood that the amplitude should be contracted with $\pi^{\alpha;\beta}_{[4]_4}$. Furthermore, we are using the simplifying transverse kinematics discussed above. This means that upon doing the dilaton replacement, we have

$$A^{a_1a_2a_3a_4}_{[2]_9\otimes[2]_9\to[4]_9\to[4]_4} = \frac{\alpha'}{8}\big(-t_1 v_{a_1}v_{a_2}v_{a_3}v_{a_4} + 4v_{a_1}v_{a_2}q_{1,a_3}q_{1,a_4}\big)\,, \tag{2.268}$$

where we used the symmetry of the indices and note that transverse kinematics ensures that the term proportional to $\epsilon_{1,a_1}\epsilon_{1,a_2}$ gets mapped to a transverse metric which is annihilated by the projector to $[4]_4$. In this case we can directly use (2.218) to match both tensor structures at once

$$\begin{aligned}\mathfrak{D}^{(2\lambda^{\frac{1}{4}}+\ldots,[4]_4),(4,\bullet)}_{a_1a_2a_3a_4}(\nu) = \frac{\beta(\nu)}{8\sqrt{\lambda}}\big(\nu^2\hat{p}_{a_1}\hat{p}_{a_2}\hat{p}_{a_3}\hat{p}_{a_4} + 4\hat{p}_{a_1}\hat{p}_{a_2}\nabla_{p\,a_3}\nabla_{p\,a_4}\big)\\ + \text{vanishing in flat space limit}\,.\end{aligned} \tag{2.269}$$

We again note that these corrections are suppressed at large λ.

2.8 Conclusions

In this work, we derived a perturbative CFT optical theorem which computes the dDisc of a correlator in the $1/N$ expansion in terms of single discontinuities of lower order correlators. Notably, this allows the determination of double-trace contributions to a given one-loop holographic correlator, even when the intermediate fields have spin, which makes them much harder to handle using unitarity formulas in terms of the CFT data. This also clarifies the underlying CFT principles behind cutting formulas for AdS Witten diagrams, which so far used bulk quantities [27, 28].

Using the perturbative CFT optical theorem we fixed the form of the AdS one-loop four-point scattering amplitude in the high-energy limit, accounting for the physical effect of tidal excitations. This corresponds to box Witten diagrams with two-Pomeron exchange and general string fields as intermediate states. To do this, we transformed the optical theorem to CFT impact parameter space, in which the loop level phase shift is obtained as a contraction of tree-level phase shifts. Using the general structure of spinning correlators in the s-channel Regge limit, we rewrote all the tidal excitations in terms of a single scalar function, the AdS vertex function.

For the case of $\mathcal{N}=4$ SYM, dual to type IIB strings, we fixed part of the answer by relating our expression to the flat space results of [34–36] for high energy string scattering, requiring consistency with the flat space limit in impact parameter space. This procedure fixes part of the AdS vertex function and therefore also part of the CFT correlation function at one-loop in the Regge limit. Additionally, interpreting the previous result in terms of unitarity, we used

the flat-space behavior to constrain the spectral function for certain spinning CFT correlators at tree level in the Regge limit.

There are several open directions and applications of this work. First, we emphasize that the CFT optical theorem is quite general and does not rely on AdS ingredients. Moreover, it works directly at the level of correlators instead of having to extract the CFT data, which is very difficult to resum into correlators. It would be interesting to test and use this formula for more general holographic correlators and, since the expansion parameter does not necessarily need to be $1/N$, in weakly coupled CFTs such as ϕ^4 theory at the Wilson-Fisher fixed point in $4-\epsilon$ dimensions.

Another playground to apply our gluing formula is $\mathcal{N}=4$ SYM at weak 't Hooft coupling in the Regge limit. One could try to derive the order $1/N^4$ correlator explicitly at leading order in λ, using the techniques introduced in [41]. The corresponding double discontinuity should be the square of order $1/N^2$ correlators with impact factors that include the intermediate states.

In the Regge limit there are kinematical conditions in the CFT optical theorem that simplified the integrations over Lorentzian configurations. An interesting generalization would be to systematically study kinematic corrections to the Regge limit. In fact, in the recent work [50] the authors derived a Regge expansion for the correlator valid for any boost. It would be interesting to see how to incorporate this into our analysis, both in a general structural way, but also potentially to impose specific constraints from the flat space limit in a more general kinematic setup. More generally, it would be interesting to understand the Regge limit integrations in terms of light-ray operators [12], and to use the more general Lorentzian machinery of [11, 12] to write an intrinsically Lorentzian gluing formula in general kinematics.

A possible extension of this work is to consider a higher number of bulk loops. This was analyzed in the large Δ_{gap} limit in [44]. Let us give a few concrete ideas for the stringy generalization of that analysis. The leading contribution in the Regge limit at $k-1$ loops is expected to be k-Pomeron exchange, related to a k-fold product of tree-level phase shifts. By repeatedly using (2.163) one can define a generalization of the function Φ for such a product, so we expect that the contribution of intermediate states can again be expressed by a vertex function[13]

$$-\text{Re}\mathcal{B}_{k-1}(S,L)=\int_{-\infty}^{\infty}d\nu\left(\prod_{n=1}^{k}d\nu_n\,\beta^{(*)}(\nu_n)\right)V(\nu_1,\dots,\nu_k,\nu)^2\,S^{\sum_m j(\nu_m)-k}\,\Phi(\nu_1,\dots,\nu_k,\nu)\,\Omega_{i\nu}(L)\,, \tag{2.270}$$

[13]This corresponds to eikonalization in the operator sense of [35] where the phase shift is an operator in the string Hilbert space, with matrix elements between all possible string states.

where the product of $\beta(\nu_n)$ must be real, which means that the answer is slightly different depending on whether the number of loops is even or odd [44]. In order to find the flat space limit of this $(k-1)$-loop vertex function we would need to consider the flat space result for higher loops, which is known at least in integral form [34–36]

$$V_k(q_1,\ldots,q_k) = \int \prod_{i=1}^{k} \frac{d\sigma_i}{2\pi} \prod_{1\le j<l\le k} |e^{i\sigma_j} - e^{i\sigma_l}|^{\alpha' q_l\cdot q_j}\,. \tag{2.271}$$

Note that the symmetry of the integrand is such that only $k-1$ integrals are non-trivial. For example, the one-loop case just gives

$$V_2(q_1,q_2) = \int \frac{d\sigma_1 d\sigma_2}{(2\pi)^2}\,|e^{i\sigma_1} - e^{i\sigma_2}|^{\alpha' q_{12}} = \int \frac{d\sigma}{2\pi} |1-e^{i\sigma}\,|^{\alpha' q_{12}} = \frac{\Gamma\big(1+\alpha'\frac{t_1+t_2-t}{2}\big)}{\Gamma\big(1+\alpha'\frac{t_1+t_2-t}{4}\big)^2}, \tag{2.272}$$

recovering (2.234).

Appendix A

Appendices for Optical theorem

A.1 Additional examples of string amplitudes

In this appendix we provide some additional examples and comments on the chiral and closed string amplitudes.

A.1.1 Chiral Amplitudes

In the chiral case it is trivial to reproduce level 0. Here we have only the massless particles with residue

$$\sqrt{\underset{k^2=0}{\text{Res}} A^{12P_1P_2}(k,q_{12})} = \epsilon_1^\mu A^{15P_1}_{\mu\alpha} \pi^{\alpha;\beta}_{[1]_8} A^{52P_2}_{\beta\nu} \epsilon_2^\nu = \epsilon_1^\mu \eta_{\mu\alpha}\eta^{\alpha\beta}\eta_{\beta\nu}\epsilon_2^\nu = \epsilon_1\cdot\epsilon_2\,, \tag{A.1}$$

where we have used $A^{15P_1}_{\mu\alpha} = \eta_{\mu\alpha}$ and $\pi^{\alpha;\beta}_{[1]_8} = \eta^{\alpha\beta}$. At higher levels we will have non-trivial three-point functions. It will be convenient to absorb the external polarization into the amplitude

$$\epsilon_1^\mu A^{15P_1}_{n,\,\mu,\rho_5,\nu} \equiv A^{15P_1}_{n,\rho_5,\nu}\,, \tag{A.2}$$

to be more compact in writing the amplitudes (we are using the integer n to label the mass level of the state).

From the spectrum described above, we will have two amplitudes at level 1 which are $A^{15P_1}_{1,[1,1,1]_9,\boldsymbol{\alpha}}$ and $A^{15P_1}_{1,[2]_9,\boldsymbol{\alpha}}$.
Here we will keep in mind the Young diagrams explained above, along with the index symmetrization that comes with them, packaged in our boldface multi-index notation. The explicit level 1 three point amplitudes in the IIB superstring are

$$A^{15P_1}_{1,[1,1,1]_9,\boldsymbol{\alpha}} = \frac{\sqrt{6}}{m_1}\epsilon_{1\alpha_1}q_{1\alpha_2}v_{\alpha_3}\,,\; A^{15P_1}_{1,[2]_9,\boldsymbol{\alpha}} = -\sqrt{\frac{\alpha'}{2}}\left(\epsilon_{1\alpha_1}q_{1\alpha_2} + \frac{1}{2}(q_1\cdot\epsilon_1)v_{\alpha_1}v_{\alpha_2}\right)\,, \tag{A.3}$$

with $m_1 = 2/\sqrt{\alpha'}$ being the mass at level 1, and q_1 is the transverse momentum carried by the Pomeron P_1 (similarly for q_2 and the Pomeron P_2). All the relative factors between the different tensor structures and the overall normalization are fixed by computing the three-point amplitudes with the correctly normalized vertex operators for the excited NS states in IIB super string theory [53]. We can now contract the three-point amplitudes on each side using the projector for the appropriate representation and check the residue

$$\begin{aligned}\sqrt{\operatorname*{Res}_{k^2=-4/\alpha'} A^{12P_1P_2}(k,q_{12})} &= A^{15P_1}_{1,\boldsymbol{\alpha}}\pi^{\boldsymbol{\alpha};\boldsymbol{\beta}}_{[1,1,1]_9}A^{52P_1}_{1,\boldsymbol{\beta}} + A^{15P_2}_{1,\boldsymbol{\alpha}}\pi^{\boldsymbol{\alpha};\boldsymbol{\beta}}_{[2]_9}A^{52P_2}_{1,\boldsymbol{\beta}} \\ &= \frac{\alpha'}{2}(-q_1\cdot q_2)(\epsilon_1\cdot\epsilon_2),\end{aligned} \tag{A.4}$$

where we refrained from writing the representation labels in the amplitudes since they are contracted with a projector with the appropriate label. This matches what we extracted from $A^{\alpha_1\alpha_2}(q_{12})$, or equivalently from the vertex function. We can continue this procedure to the second level, where mixed symmetry tensors appear for the first time. For example, the $[2,1,1]_9$ tensor has the amplitude

$$A^{15P_1}_{2,[2,1,1]_9,\boldsymbol{\alpha}} = \sqrt{\frac{3}{8}}\sqrt{\frac{\alpha'}{2}}\left(\frac{4}{m_2}q_{1\alpha_2} + 2v_{\alpha_2}\right)\epsilon_{1\alpha_1}q_{1\alpha_3}v_{\alpha_4}, \tag{A.5}$$

where $m_2 = \sqrt{8/\alpha'}$ is the mass at level 2. It is important to emphasize that the level 2 amplitude contains a term with more powers of α' than any of the level 1 amplitudes. This would lead to further suppression in $1/\sqrt{\lambda}$ in the AdS theory.[1]

The remaining amplitudes can be found in section 5 of [53]. For our purposes it is just important to know that the amplitudes satisfy

$$\begin{aligned}\sqrt{\operatorname*{Res}_{k^2=-8/\alpha'} A^{12P_1P_2}(k,q_{12})} &= \sum_{\rho\in S} A^{15P_1}_{2,\rho,\boldsymbol{\alpha}}\pi^{\boldsymbol{\alpha};\boldsymbol{\beta}}_{\rho}A^{52P_2}_{2,\rho,\boldsymbol{\beta}} = \frac{(-\frac{\alpha'}{2}q_1\cdot q_2)_2}{2!}(\epsilon_1\cdot\epsilon_2)\,, \\ S &= \{[3]_9\,,\ [2,1,1]_9\,,\ [2,1]_9\,,\ [1,1]_9\,,\ [1]_9\}\,,\end{aligned} \tag{A.6}$$

which we explicitly checked. More generally, we can conclude that the square root of the residue at mass level n of $A^{12P_1P_2}(k,q_{12})$ can be recovered by unitarity if we account for all the covariant SO(9) representations corresponding to the massive NS states. This gives a microscopic interpretation for the vertex function at a given mass level. As already mentioned, summing over all these mass levels reconstructs the full vertex function.

[1] Clearly, states with higher spin, which can only appear at higher levels, can have higher powers of α' leading to a spin-dependent suppression of couplings, as is expected from the general arguments of [7, 63].

A.1.2 Closed string amplitudes

Here we consider the simple but instructive level 0 case for the closed string amplitudes, where the little group is SO(8). The square of the residue reads

$$A^{15P_1}_{L1,\alpha} A^{15P_1}_{R1,\beta} \left(\pi^{\alpha;\gamma}_{[1]_8} \pi^{\beta;\delta}_{[1]_8}\right) A^{52P_2}_{L1,\gamma} A^{52P_2}_{R1\delta} \tag{A.7}$$
$$= \sum_{\rho_C=[2]_8,[1,1]_8,\bullet_8} A^{15P_1}_{L1,\alpha} A^{15P_1}_{R1,\beta} (p^{\alpha\beta}_{[1]_8\otimes[1]_8\to\rho_C,\mu_1\mu_2} \pi^{\mu_1\mu_2;\nu_1\nu_2}_{\rho_C} p^{\gamma\delta}_{[1]_8\otimes[1]_8\to\rho_C,\nu_1\nu_2}) A^{52P_2}_{L1,\gamma} A^{52P_2}_{R1\delta} = (\epsilon_1\cdot\epsilon_2)^2 ,$$

where we used the group theoretical tensor product identity for projectors

$$\pi^{\alpha;\gamma}_{[1]_8} \pi^{\beta;\delta}_{[1]_8} = \sum_{\rho_C=[2]_8,[1,1]_8,\bullet_8} p^{\alpha\beta}_{[1]_8\otimes[1]_8\to\rho_C,\mu_1\mu_2} \pi^{\mu_1\mu_2;\nu_1\nu_2}_{\rho_C} p^{\gamma\delta}_{[1]_8\otimes[1]_8\to\rho_C,\nu_1\nu_2} . \tag{A.8}$$

We can solve this equation for the tensors p by contracting with polarization vectors for the left and right modes on both sides of the projector (z_L, z_R and $\bar{z}_L, \bar{z}_R$) and equating the polynomials in scalar products of z's. In practice we will always use this procedure, or a similar one where we contract with amplitudes to fix coefficients. In this case it is trivial to directly check that

$$\pi^{\alpha;\gamma}_{[1]_8} \pi^{\beta;\delta}_{[1]_8} = \eta^{\alpha\gamma}\eta^{\beta\delta} \equiv \pi^{\alpha\beta;\gamma\delta}_{[2]_8} + \pi^{\alpha\beta;\gamma\delta}_{[1,1]_8} + \frac{1}{8}\eta^{\alpha\beta}\eta^{\gamma\delta} \tag{A.9}$$
$$= \left(\frac{1}{2}(\eta^{\alpha\gamma}\eta^{\beta\delta} + \eta^{\alpha\delta}\eta^{\beta\gamma}) - \frac{1}{8}\eta^{\alpha\beta}\eta^{\gamma\delta}\right) + \frac{1}{2}(\eta^{\alpha\gamma}\eta^{\beta\delta} - \eta^{\alpha\delta}\eta^{\beta\gamma}) + \frac{1}{8}(\eta^{\alpha\beta}\eta^{\gamma\delta}) ,$$

where, obviously $p^{\alpha\beta}_{[1]_8\otimes[1]_8\to[2]_8,\mu_1\mu_2} = \delta^\alpha_{\mu_1}\delta^\beta_{\mu_2}$, $p^{\alpha\beta}_{[1]_8\otimes[1]_8\to[1,1]_8,\mu_1\mu_2} = \delta^\alpha_{\mu_1}\delta^\beta_{\mu_2}$ and $p^{\alpha\beta}_{[1]_8\otimes[1]_8\to\bullet_8} = \sqrt{\frac{1}{8}}\eta^{\alpha\beta}$ extracts traces, thereby projecting to a singlet state.

A.2 Tensor products for projectors

In this appendix we explain how to realize the tensor product of open string states into closed string states in terms of the corresponding projectors/tensors. We will consider mass level $n = 1$. The chiral spectrum at this level is

$$n = 1 : \quad \square\square_9 \oplus \begin{array}{|c|}\hline\ \\\hline\ \\\hline\end\,_9 . \tag{A.10}$$

We square the irreps using the tensor product as in the main text and analyze the decomposition term by term. For example, taking $\rho_L = \rho_R = [2]_9$ corresponds to the tensor product

$$\square\square_9 \otimes \square\square_9 = \square\square\square\square_9 \oplus \begin{array}{|c|c|c|}\hline\ &\ &\ \\\hline\ \\\cline{1-1}\end\,_9 \oplus \begin{array}{|c|c|}\hline\ &\ \\\hline\ &\ \\\hline\end\,_9 \oplus \square\square_9 \oplus \begin{array}{|c|}\hline\ \\\hline\ \\\cline{1-1}\end\,_9 \oplus \bullet_9 , \tag{A.11}$$

which we want to write in terms of SO(9) tensors as

$$\begin{aligned} \pi^{\boldsymbol{\alpha};\gamma}_{[2]_9}\pi^{\boldsymbol{\beta};\delta}_{[2]_9} &= \sum_{\rho_C\in S} p^{\boldsymbol{\alpha}\boldsymbol{\beta}}_{[2]_9\otimes[2]_9\to\rho_C,\boldsymbol{\mu}}\pi^{\boldsymbol{\mu};\nu}_{\rho_C}\, p^{\gamma\delta}_{[2]_9\otimes[2]_9\to\rho_C,\boldsymbol{\nu}}\,, \\ S &= \{[4]_9\,,[3,1]_9\,,[2,2]_9\,,[2]_9\,,[1,1]_9\,,\bullet_9\}\ . \end{aligned} \tag{A.12}$$

It will be useful to manifestly symmetrize the $\boldsymbol{\alpha}$ and $\boldsymbol{\beta}$ indices of the tensors p, in order to write down these tensors more compactly. Therefore, we will use

$$p^{\boldsymbol{\alpha}\boldsymbol{\beta}}_{\rho_L\otimes\rho_R\to\rho_C,\boldsymbol{\mu}} \equiv \pi^{\boldsymbol{\alpha}}_{\rho_L;\boldsymbol{\alpha}'}\pi^{\boldsymbol{\beta}}_{\rho_R;\boldsymbol{\beta}'}\tilde{p}^{\boldsymbol{\alpha}'\boldsymbol{\beta}'}_{\rho_L\otimes\rho_R\to\rho_C,\boldsymbol{\mu}}, \tag{A.13}$$

and we will present the simpler trial tensors $\tilde{p}$ for each case. In this case $\rho_L=\rho_R=[2]_9$ and we used the trial tensors[2]

$$\begin{aligned} \tilde{p}^{\alpha_1\alpha_2\beta_1\beta_2}_{[2]_9\otimes[2]_9\to[4]_9,\mu_1\mu_2\mu_3\mu_4} &= \delta^{\alpha_1}_{\mu_1}\delta^{\alpha_2}_{\mu_2}\delta^{\beta_1}_{\mu_3}\delta^{\beta_2}_{\mu_4} \equiv \delta^{\boldsymbol{\alpha}\boldsymbol{\beta}}_{\boldsymbol{\mu}}\,, & \tilde{p}^{\boldsymbol{\alpha}\boldsymbol{\beta}}_{[2]_9\otimes[2]_9\to[3,1]_9,\boldsymbol{\mu}} &= \delta^{\boldsymbol{\alpha}\boldsymbol{\beta}}_{\boldsymbol{\mu}}\,, \\ \tilde{p}^{\boldsymbol{\alpha}\boldsymbol{\beta}}_{[2]_9\otimes[2]_9\to[2,2]_9,\boldsymbol{\mu}} &= \sqrt{3}\delta^{\boldsymbol{\alpha}\boldsymbol{\beta}}_{\boldsymbol{\mu}}\,, & \tilde{p}^{\alpha_1\alpha_2\beta_1\beta_2}_{[2]_9\otimes[2]_9\to[2]_9,\mu_1\mu_2} &= \sqrt{\frac{36}{91}}\delta^{\alpha_1}_{\mu_1}\delta^{\beta_2}_{\mu_2}\eta^{\alpha_2\beta_1}\,, \\ \tilde{p}^{\alpha_1\alpha_2\beta_1\beta_2}_{[2]_9\otimes[2]_9\to[1,1]_9,\mu_1\mu_2} &= \sqrt{\frac{4}{11}}\delta^{\alpha_1}_{\mu_1}\delta^{\beta_2}_{\mu_2}\eta^{\alpha_2\beta_1}\,, & \tilde{p}^{\alpha_1\alpha_2\beta_1\beta_2}_{[2]_9\otimes[2]_9\to\bullet_9} &= \sqrt{\frac{1}{44}}\eta^{\alpha_1\beta_1}\eta^{\alpha_2\beta_2}\,. \end{aligned} \tag{A.14}$$

The remaining tensor products have some additional subtleties. Taking the cross term in the tensor product

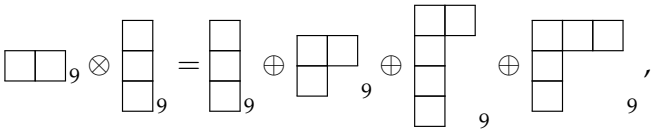

(A.15)

we note that there is a 4 row tensor appearing. When contracted with the amplitudes, this contribution will vanish, because we have only 3 independent vectors. However, from the point of view of the projector equation, we must still have

$$\begin{aligned} \pi^{\boldsymbol{\alpha};\gamma}_{[2]_9}\pi^{\boldsymbol{\beta};\delta}_{[1,1,1]_9} &= \sum_{\rho_C\in S'} p^{\boldsymbol{\alpha}\boldsymbol{\beta}}_{[2]_9\otimes[1,1,1]_9\to\rho_C,\boldsymbol{\mu}}\pi^{\boldsymbol{\mu};\nu}_{\rho_C}\, p^{\gamma\delta}_{[2]_9\otimes[1,1,1]_9\to\rho_C,\boldsymbol{\nu}}\,, \\ S' &= \{[3,1,1]_9\,,[1,1,1]_9\,,[2,1]_9\,,[2,1,1,1]_9\}\ . \end{aligned} \tag{A.16}$$

with a non-vanishing $p^{\boldsymbol{\alpha}\boldsymbol{\beta}}_{[2]_9\otimes[1,1,1]_9\to[2,1,1,1]_9,\boldsymbol{\mu}}$. However, by contracting directly with the amplitudes $A^{\boldsymbol{\alpha}}_{[2]_9}A^{\boldsymbol{\beta}}_{[1,1,1]_9}A^{\gamma}_{[2]_9}A^{\delta}_{[1,1,1]_9}$ we automatically eliminate the contribution of this tensor (this also avoids the computation of a complicated 4 row projector). With this in mind, we use

[2]For irreps with the same number of indices as the tensor product we will always take $\tilde{p}^{\boldsymbol{\alpha}\boldsymbol{\beta}}_{\boldsymbol{\mu}}\propto\delta^{\boldsymbol{\alpha}\boldsymbol{\beta}}_{\boldsymbol{\mu}}$.

again (A.13), with the trial projectors

$$\begin{aligned}
\tilde{p}^{\boldsymbol{\alpha\beta}}_{[2]_9\otimes[1,1,1]_9\to[3,1,1],\boldsymbol{\mu}} &= \sqrt{\frac{5}{4}}\delta^{\alpha_1}_{\mu_1}\delta^{\alpha_2}_{\mu_2}\delta^{\beta_1}_{\mu_3}\delta^{\beta_2}_{\mu_4}\delta^{\beta_3}_{\mu_5} \equiv \sqrt{\frac{5}{4}}\delta^{\boldsymbol{\alpha\beta}}_{\boldsymbol{\mu}}\,, \\
\tilde{p}^{\boldsymbol{\alpha\beta}}_{[2]_9\otimes[1,1,1]_9\to[1,1,1],\boldsymbol{\mu}} &= \sqrt{\frac{585}{352}}\eta^{\alpha_2\beta_1}\delta^{\alpha_1}_{\mu_1}\delta^{\beta_2}_{\mu_2}\delta^{\beta_3}_{\mu_3}\,,\ \tilde{p}^{\boldsymbol{\alpha\beta}}_{[2]_9\otimes[1,1,1]_9\to[2,1],\boldsymbol{\mu}} = \eta^{\alpha_2\beta_1}\delta^{\alpha_1}_{\mu_1}\delta^{\beta_2}_{\mu_2}\delta^{\beta_3}_{\mu_3}\,.
\end{aligned} \tag{A.17}$$

With these tensors and setting $p^{\boldsymbol{\alpha\beta}}_{[2]_9\otimes[1,1,1]_9=[2,1,1,1]_9,\boldsymbol{\mu}} \to 0$, which suffices for our purposes, we have that the identity (A.16) holds, but only when inserted between the amplitudes.

The remaining tensor product

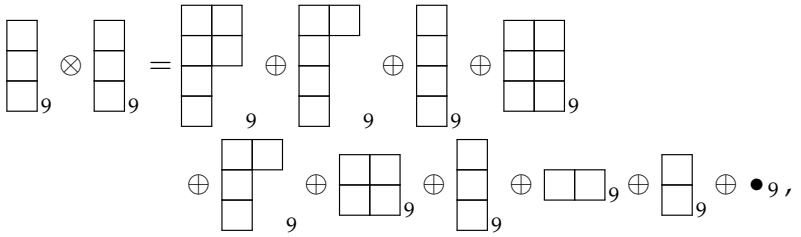

(A.18)

can be dealt with similarly, by contracting with only 3 independent polarizations instead of six, eliminating the contributions of the complicated 4 row tensors. The only non-vanishing contributions to projectors turn out to be

$$\begin{aligned}
\pi^{\boldsymbol{\alpha};\gamma}_{[1,1,1]_9}\pi^{\boldsymbol{\beta};\delta}_{[1,1,1]_9} &= \sum_{\rho_C\in S''} p^{\boldsymbol{\alpha\beta}}_{[1,1,1]_9\otimes[1,1,1]_9\to\rho_C,\boldsymbol{\mu}}\pi^{\boldsymbol{\mu};\nu}_{\rho_C}\, p^{\gamma\delta}_{[1,1,1]_9\otimes[1,1,1]_9\to\rho_C,\boldsymbol{\nu}}\,, \\
S'' &= \{[2,2,2]_9\,,[2,2]_9\,,[2]_9\,,\bullet_9\}\ .
\end{aligned} \tag{A.19}$$

where we used (A.13) and the trial projectors

$$\begin{aligned}
\tilde{p}^{\boldsymbol{\alpha\beta}}_{[1,1,1]_9\otimes[1,1,1]_9\to[2,2,2]_9,\boldsymbol{\mu}} &= \sqrt{8}\delta^{\alpha_1}_{\mu_1}\delta^{\alpha_2}_{\mu_2}\delta^{\alpha_3}_{\mu_3}\delta^{\beta_1}_{\mu_4}\delta^{\beta_2}_{\mu_5}\delta^{\beta_3}_{\mu_6} \equiv \sqrt{8}\delta^{\boldsymbol{\alpha\beta}}_{\boldsymbol{\mu}}\,, \\
\tilde{p}^{\boldsymbol{\alpha\beta}}_{[1,1,1]_9\otimes[1,1,1]_9\to[2,2]_9,\boldsymbol{\mu}} &= \sqrt{\frac{12}{5}}\eta^{\alpha_1\beta_1}\delta^{\alpha_2}_{\mu_1}\delta^{\beta_3}_{\mu_2}\delta^{\alpha_3}_{\mu_3}\delta^{\beta_2}_{\mu_4}\,, \\
\tilde{p}^{\boldsymbol{\alpha\beta}}_{[1,1,1]_9\otimes[1,1,1]_9\to[2]_9,\boldsymbol{\mu}} &= \sqrt{\frac{3}{7}}\eta^{\alpha_1\beta_1}\eta^{\alpha_2\beta_3}\delta^{\alpha_3}_{\mu_1}\delta^{\beta_2}_{\mu_2}\,, \\
\tilde{p}^{\boldsymbol{\alpha\beta}}_{[1,1,1]_9\otimes[1,1,1]_9\to\bullet_9} &= \sqrt{\frac{1}{84}}\eta^{\alpha_1\beta_1}\eta^{\alpha_2\beta_2}\eta^{\alpha_3\beta_3}\,,
\end{aligned} \tag{A.20}$$

where the unusual index ordering is to ensure that the resulting tensor doesn't vanish when we act with $\pi_{[1,1,1]_9}$ on the trial projectors $\tilde{p}$. This turns (A.19) into an identity which holds for two identical $[1,1,1]_9$ tensors, as will be the case for our amplitudes.

A.3 Branching relations for projectors

In this Appendix we provide a detailed account of all the branching relations for closed string state projectors utilized in section 2.7.1. Let us start by recalling the SO(9) closed string states at level 1

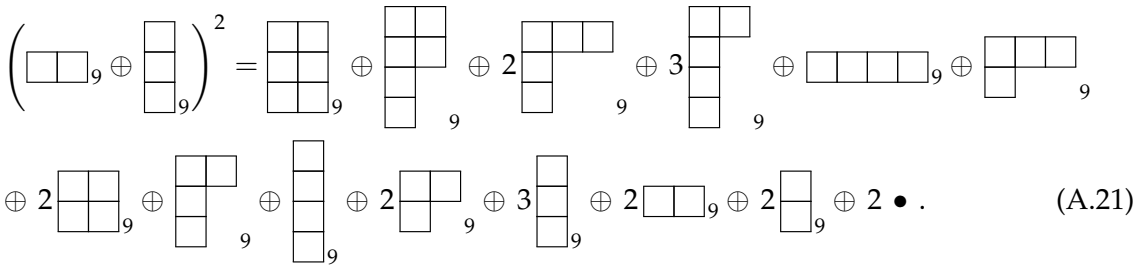

(A.21)

We recall that states with more than 3 columns will not contribute as we only have 3 different vectors to anti-symmetrize. We are going to perform the branching

$$\mathrm{SO}(9) \;\to\; \mathrm{SO}(4)\times\mathrm{SO}(5)|_{\bullet}\,, \tag{A.22}$$

where we denote the projection to singlets of SO(5) by $|_{\bullet}$. Note that certain representations can naturally be restricted to SO(4) by simply taking the 5d subset of 10d indices. It is obvious that

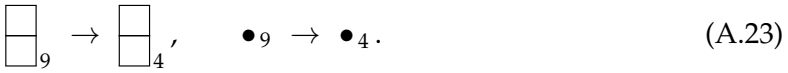

(A.23)

Additionally, the projector for these representations is identical for SO(9) and SO(4) (up to restriction of the indices $\alpha \to a$, $\beta \to b$, $\mu \to m$, ...)

$$\pi^{a_1a_2;b_1b_2}_{[1,1]_9} = \pi^{a_1a_2;b_1b_2}_{[1,1]_4} = \frac{1}{2}\left(\eta^{a_1b_1}\eta^{a_2b_2} - \eta^{a_1b_2}\eta^{a_2b_1}\right)\,. \tag{A.24}$$

Other representations admit a direct restriction, but can also give additional irreps, by the creation of SO(5) singlets, through the contraction of indices with legs on the compact manifold. For example the spin 2 states branch as

(A.25)

The spin 2 on the RHS is interpreted as the restriction of indices to the SO(4) and the singlet as a trace over the compact space indices. In terms of projectors the statement is simply

$$\pi^{a_1a_2;b_1b_2}_{[2]_9} = \pi^{a_1a_2;b_1b_2}_{[2]_4} + \frac{5}{36}\eta^{a_1a_2}\eta^{b_1b_2}\,. \tag{A.26}$$

Similarly, for the spin 4 case

$$\square\square\square\square_9 \;\to\; \square\square\square\square_4 \;\oplus\; \square\square_4 \;\oplus\; \bullet_4, \tag{A.27}$$

and the projector equation is

$$\pi^{\mathbf{a};\mathbf{b}}_{[4]_9} = \sum_{\rho=[4]_4,[2]_4,\bullet_4} b^{\mathbf{a}}_{[4]_9\to\rho,\mathbf{m}}\; \pi^{\mathbf{m};\mathbf{n}}_{\rho}\; b^{\mathbf{b}}_{[4]_9\to\rho,\mathbf{n}}\,. \tag{A.28}$$

It will be again convenient to manifestly symmetrize the tensors, in order to present them more compactly. We define

$$b^{\mathbf{a}}_{\rho_C\to\rho,\mathbf{m}} \equiv \pi^{\mathbf{a}}_{\rho_C,\mathbf{a}'}\tilde{b}^{\mathbf{a}'}_{\rho_C\to\rho,\mathbf{m}}\,, \tag{A.29}$$

and then present a list of the simpler $\tilde{b}$. In this case we have

$$\begin{aligned}\tilde{b}^{a_1a_2a_3a_4}_{[4]_9\to[4]_4,m_1m_2m_3m_4} &= \delta^{a_1}_{m_1}\delta^{a_2}_{m_2}\delta^{a_3}_{m_3}\delta^{a_4}_{m_4} \equiv \delta^{\mathbf{a}}_{\mathbf{m}}\\ \tilde{b}^{a_1a_2a_3a_4}_{[4]_9\to[2]_4,m_1m_2} &= \sqrt{\frac{39}{20}}\delta^{a_1}_{m_1}\delta^{a_2}_{m_2}\eta^{a_3a_4}\,,\; \tilde{b}^{a_1a_2a_3a_4}_{[4]_9\to\bullet_4} = \sqrt{\frac{143}{280}}\eta^{a_1a_2}\eta^{a_3a_4}\,.\end{aligned} \tag{A.30}$$

The fact that the direct restriction of the irrep $[4]_9 \to [4]_4$ comes with coefficient 1 is a non-trivial consistency check of the previous procedure.

There are other irreps that don't admit a direct restriction, because they have more than two columns (SO(4) Young tableaux have at most two columns, and traces can vanish by antisymmetry). For this we need to use the SO(4) Levi-Civita tensor. We will simply write it as $\varepsilon^{a_1a_2a_3a_4}$. The simplest case is the 3-form

$$\begin{array}{|}\hline\\\hline\\\hline\end{array}_9 \;\to\; \square_4\,, \tag{A.31}$$

and the corresponding projector equation is

$$\pi^{\mathbf{a};\mathbf{b}}_{[1,1,1]_9} = \frac{1}{6}\varepsilon^{a_1a_2a_3}{}_m\pi^{m;n}_{[1]_4}\,\varepsilon_n{}^{b_1b_2b_3} = 4\,\pi^{\mathbf{a}m;\mathbf{b}n}_{[1,1,1,1]_4}\,\pi_{[1]_4,m;n}\,, \tag{A.32}$$

From the first equation we can read off

$$b^{a_1a_2a_3}_{[1,1,1]_9\to[1]_4,m} = \sqrt{\frac{1}{6}}\varepsilon^{a_1a_2a_3}{}_m\,. \tag{A.33}$$

For the second equality in (A.32) we used the standard identity

$$\epsilon^{a_1a_2a_3a_4}\epsilon^{b_1b_2b_3b_4} = 4!\,\pi^{\mathbf{a};\mathbf{b}}_{[1,1,1,1]_4}\,. \tag{A.34}$$

This is convenient to square the three-point amplitudes when computing the residue of the

four-point function $A^{12P_1P_2}$. Using trace subtractions and products of epsilon tensors we can now derive branching identities for all the relevant irreps. Let us list the remaining identities, where we write the trace subtractions and the Levi-Civita tensors using the trial projectors $\tilde{b}$, but then appropriately symmetrize them through (A.29)

$$
\begin{aligned}
&\ydiagram{2,1,1}_{9} \to \ydiagram{2}_{4} \oplus \ydiagram{1,1}_{4}\,,\\
&\tilde{b}^{a_1a_2a_3a_4}_{[2,1,1]_9\to[2]_4,m_1m_2} = \sqrt{\frac{6}{4!}}\,\varepsilon^{a_1a_3a_4}{}_{m_1}\delta^{a_2}_{m_2}\,,\ \tilde{b}^{a_1a_2a_3a_4}_{[2,1,1]_9\to[1,1]_4,m_1m_2} = \sqrt{\frac{42}{4!5}}\,\varepsilon^{a_1a_3a_4}{}_{m_1}\delta^{a_2}_{m_2}\,,\\
&\ydiagram{2,1}_{9} \to \ydiagram{2,1}_{4} \oplus \ydiagram{1}_{4}\,,\\
&\tilde{b}^{\mathbf{a}}_{[2,1]_9\to[2,1]_4,\mathbf{m}} = \delta^{\mathbf{a}}_{\mathbf{m}}\,,\ \tilde{b}^{a_1a_2a_3}_{[2,1]_9\to[1]_4,m} = \sqrt{\frac{16}{5}}\,\delta^{a_1}_{m_1}\eta^{a_2a_3}\,,
\end{aligned}
\tag{A.35}
$$

$$
\begin{aligned}
&\ydiagram{3,1,1}_{9} \to \ydiagram{3}_{4} \oplus \ydiagram{2,1}_{4} \oplus \ydiagram{1}_{4}\,,\\
&\tilde{b}^{\mathbf{a}}_{[3,1,1]_9\to[3]_4,\mathbf{m}} = \sqrt{\frac{36}{4!5}}\,\varepsilon^{a_1a_4a_5}{}_{m_1}\delta^{a_2}_{m_2}\delta^{a_3}_{m_3}\,,\ \tilde{b}^{\mathbf{a}}_{[3,1,1]_9\to[2,1]_4,\mathbf{m}} = \sqrt{\frac{1152}{4!25}}\,\varepsilon^{a_1a_4a_5}{}_{m_1}\delta^{a_2}_{m_2}\delta^{a_3}_{m_3}\,,\\
&\tilde{b}^{a_1a_2a_3a_4a_5}_{[3,1,1]_9\to[1]_4,m} = \sqrt{\frac{22}{4!5}}\,\varepsilon^{a_1a_4a_5}{}_{m}\eta^{a_2a_3}\,,\\
&\ydiagram{3,1}_{9} \to \ydiagram{3,1}_{4} \oplus \ydiagram{1,1}_{4} \oplus \ydiagram{2}_{4}\,,\\
&\tilde{b}^{\mathbf{a}}_{[3,1]_9\to[3,1]_4,\mathbf{m}} = \delta^{\mathbf{a}}_{\mathbf{m}},\ \tilde{b}^{\mathbf{a}}_{[3,1]_9\to[1,1]_4,\mathbf{m}} = \sqrt{\frac{11}{10}}\,\delta^{a_1}_{m_1}\eta^{a_2a_3}\delta^{a_4}_{m_2},\ \tilde{b}^{\mathbf{a}}_{[3,1]_9\to[2]_4,\mathbf{m}} = \sqrt{\frac{27}{10}}\,\delta^{a_1}_{m_1}\eta^{a_2a_4}\delta^{a_3}_{m_2},\\
&\ydiagram{2,2}_{9} \to \ydiagram{2,2}_{4} \oplus \ydiagram{2}_{4} \oplus \bullet_{4}\,,\\
&\tilde{b}^{\mathbf{a}}_{[2,2]_9\to[2,2]_4,\mathbf{m}} = \delta^{\mathbf{a}}_{\mathbf{m}}\,,\ \tilde{b}^{\mathbf{a}}_{[2,2]_9\to[2]_4,\mathbf{m}} = \sqrt{\frac{42}{5}}\,\delta^{a_1}_{m_1}\eta^{a_2a_3}\delta^{a_4}_{m_2}\,,\ \tilde{b}^{\mathbf{a}}_{[2,2]_9\to\bullet_4} = \sqrt{\frac{7}{5}}\,\eta^{a_1a_4}\eta^{a_2a_3}\,,\\
&\ydiagram{2,2,2}_{9} \to \ydiagram{2}_{4} \oplus \bullet_{4}\,,\\
&\tilde{b}^{\mathbf{a}}_{[2,2,2]_9\to[2]_4,m_1m_2} = \frac{\sqrt{48}}{4!}\,\varepsilon^{a_1a_5a_3}{}_{m_1}\varepsilon^{a_4a_2a_6}{}_{m_2}\,,\ \tilde{b}^{\mathbf{a}}_{[2,2,2]_9\to\bullet_4} = \frac{\sqrt{28}}{4!}\,\varepsilon^{a_1a_5a_3}{}_{m}\varepsilon^{a_4a_2a_6m}\,.
\end{aligned}
\tag{A.36}
$$

Note that for the last diagram, which has more than 2 boxes in both columns, we are forced to use two pairs of epsilon tensors. Tensors with more than three rows aren't allowed by the 10d kinematics, but even if they were, their branchings do not contain singlets of SO(5) so we can simply discard them.

A.3.1 All 5d closed string amplitudes

Let us first write down in generality the 5d amplitudes using the relations derived in the main text. We have

$$A^{15P_1}_{n,\rho_L\otimes\rho_R\to\rho_C\to\rho,\mathbf{m}} = A^{15P_1}_{\rho_L,\boldsymbol{\alpha}}\, A^{15P_1}_{\rho_R,\boldsymbol{\beta}}\, p^{\boldsymbol{\alpha}\boldsymbol{\beta}}_{\rho_L\otimes\rho_R\to\rho_C,\mathbf{a}} b^{\mathbf{a}}_{\rho_C\to\rho,\mathbf{m}}\,. \tag{A.37}$$

With all the group theory identities established, we can enumerate all the amplitudes used in the main text to reproduce the residue at the cut with mass level 1. However, we again emphasize that we have not explicitly symmetrized the amplitudes by contracting with the respective projector, in order to maintain some compactness of the tables below. Namely, all amplitudes are to be contracted with the projector to the SO(4) irrep, and furthermore, amplitudes where $\text{rank}(\rho) = \text{rank}(\rho_L) + \text{rank}(\rho_R)$ are also not explicitly symmetrized with respect to ρ_L and ρ_R as in equation (A.13). Additionally, for amplitudes where the b tensors contain a Levi-Civita symbol, we write the square of the amplitude

$$\left(A^{\rho_L\otimes\rho_R\to\rho_C\to\rho}_{\mathbf{m}}\right)^2 \equiv A^{\rho_L\otimes\rho_R\to\rho_C\to\rho}_{\mathbf{m}}\, \pi^{\mathbf{m};\mathbf{n}}_{\rho}\, A^{\rho_L\otimes\rho_R\to\rho_C\to\rho}_{\mathbf{n}}\,, \tag{A.38}$$

since the amplitude itself cannot be written nicely in terms of $v_\alpha, q_\alpha, \epsilon_\alpha$. With these caveats in mind, we list the amplitudes starting by the ones with the most indices

$$
\begin{aligned}
&\square\square\square\square_4\\
A^{[2]_9\otimes[2]_9\to[4]_9\to[4]_4}_{m_1m_2m_3m_4} &= \frac{1}{8}\alpha'\left(2\epsilon_{1,m_1}q_{1,m_2}+v_{m_1}v_{m_2}q_1\cdot\epsilon_1\right)\\
&\times\left(2\epsilon_{1,m_3}q_{1,m_4}+v_{m_3}v_{m_4}q_1\cdot\epsilon_1\right),
\end{aligned}
$$

$$
\begin{aligned}
&2\begin{array}{|c|c|}\hline\ &\ \\\hline\ &\ \\\hline\end{array}_4\\
A^{[2]_9\otimes[2]_9\to[2,2]_9\to[2,2]_4}_{m_1m_2m_3m_4} &= \frac{1}{8}\alpha'\left(2\epsilon_{1,m_1}q_{1,m_2}+v_{m_1}v_{m_2}q_1\cdot\epsilon_1\right)\\
&\times\left(2\epsilon_{1,m_3}q_{1,m_4}+v_{m_3}v_{m_4}q_1\cdot\epsilon_1\right),
\end{aligned}
$$

$$
\begin{aligned}
A^{[1,1,1]_9\otimes[1,1,1]_9\to[2,2]_9\to[2,2]_4}_{m_1m_2m_3m_4} &= \frac{\alpha'}{4\sqrt{15}}[\left(v_{m_1}\epsilon_{1,m_3}-v_{m_3}\epsilon_{1,m_1}\right)\left(q_1\cdot\epsilon_1\left(v_{m_2}q_{1,m_4}-v_{m_4}q_{1,m_2}\right)\right.\\
&+t_1\left.\left(v_{m_2}\epsilon_{1,m_4}-v_{m_4}\epsilon_{1,m_2}\right)\right)\\
&+q_{1,m_1}\left(\epsilon_{1,m_3}\left(\epsilon_{1,m_2}q_{1,m_4}-\epsilon_{1,m_4}q_{1,m_2}\right)\right.\\
&+\left.v_{m_3}\left(v_{m_4}\left(\epsilon_{1,m_2}q_1\cdot\epsilon_1-q_{1,m_2}\right)+v_{m_2}\left(q_{1,m_4}-\epsilon_{1,m_4}q_1\cdot\epsilon_1\right)\right)\right)\\
&+q_{1,m_3}\left(\epsilon_{1,m_1}\left(\epsilon_{1,m_4}q_{1,m_2}-\epsilon_{1,m_2}q_{1,m_4}\right)\right.\\
&+\left.v_{m_1}\left(v_{m_4}\left(q_{1,m_2}-\epsilon_{1,m_2}q_1\cdot\epsilon_1\right)+v_{m_2}\left(\epsilon_{1,m_4}q_1\cdot\epsilon_1-q_{1,m_4}\right)\right)\right)],
\end{aligned}
$$

$$
\begin{aligned}
&\square\square\square_4\\
\left(A^{[2]_9\otimes[111]_9\to[311]_9\to[3]_4}_{\mathbf{m}}\right)^2 &= -\frac{\left(\alpha'\right)^2}{1152}\left(48\left(q_1\cdot\epsilon_2\right)^2\left(3\left(q_2\cdot\epsilon_1\right)^2+t_2\right)\right.\\
&+48t_1\left(\left(q_2\cdot\epsilon_1\right)^2+t_2\left(\epsilon_1\cdot\epsilon_2\right)^2\right)+48\left(q_1\cdot q_2\right)^2\left(1-3\left(\epsilon_1\cdot\epsilon_2\right)^2\right)\\
&+115(q_1\cdot q_2)(\epsilon_1\cdot\epsilon_2)(q_1\cdot\epsilon_1)(q_2\cdot\epsilon_2)\\
&\left.-115(q_1\cdot\epsilon_1)(q_1\cdot\epsilon_2)(q_2\cdot\epsilon_1)(q_2\cdot\epsilon_2)\right),
\end{aligned}
$$

$$
\begin{aligned}
&2\square_4\\
\left(A^{[2]_9\otimes[111]_9\to[311]_9\to[1]_4}_{\mathbf{m}}\right)^2 &= -\frac{625\left(\alpha'\right)^2}{12672}(q_1\cdot\epsilon_1)(q_2\cdot\epsilon_2)\\
&\times\left((q_1\cdot\epsilon_2)(q_2\cdot\epsilon_1)-(q_1\cdot q_2)(\epsilon_1\cdot\epsilon_2)\right),
\end{aligned}
$$

$$
\begin{aligned}
\left(A^{[2]_9\otimes[111]_9\to[111]_9\to[1]_4}_{\mathbf{m}}\right)^2 &= \frac{65\left(\alpha'\right)^2}{1408}(q_1\cdot\epsilon_1)(q_2\cdot\epsilon_2)\\
&\times\left((q_1\cdot q_2)(\epsilon_1\cdot\epsilon_2)-(q_1\cdot\epsilon_2)(q_2\cdot\epsilon_1)\right).
\end{aligned}
\tag{A.39}
$$

And

$$
\begin{aligned}
& 2\,\square\!\square\!\!\begin{array}{l}\square\\[-4pt]\square\end{array}_4 \\
A^{[2]_9\otimes[111]_9\to[21]_9\to[21]_4}_{m_1m_2m_3} &= \frac{\alpha'}{12\sqrt{6}}[(q_{1,m_1}\left(v_{m_3}\left(2\epsilon_{1,m_2}q_1\cdot\epsilon_1-3q_{1,m_2}\right)\right.\\
&+ v_{m_2}\left(3q_{1,m_3}-2\epsilon_{1,m_3}q_1\cdot\epsilon_1\right))\\
&+ 2q_1\cdot\epsilon_1\left(q_{1,m_3}\left(v_{m_2}\epsilon_{1,m_1}-v_{m_1}\epsilon_{1,m_2}\right)\right.\\
&+ q_{1,m_2}\left(v_{m_1}\epsilon_{1,m_3}-v_{m_3}\epsilon_{1,m_1}\right))\\
&+ 3t_1\epsilon_{1,m_1}\left(v_{m_2}\epsilon_{1,m_3}-v_{m_3}\epsilon_{1,\alpha_2}\right))],
\end{aligned}
\tag{A.40}
$$

$$
\begin{aligned}
\left(A^{[2]_9\otimes[111]_9\to[311]_9\to[21]_4}_{\mathbf{m}}\right)^2 &= \frac{5\left(\alpha'\right)^2}{1152}\left(6t_2\left(q_1\cdot\epsilon_2\right)^2+6t_1\left(\left(q_2\cdot\epsilon_1\right)^2+t_2\left(\epsilon_1\cdot\epsilon_2\right)^2\right)\right.\\
&+ (q_1\cdot q_2)(\epsilon_1\cdot\epsilon_2)(q_1\cdot\epsilon_1)(q_2\cdot\epsilon_2)\\
&- \left.(q_1\cdot\epsilon_1)(q_1\cdot\epsilon_2)(q_2\cdot\epsilon_1)(q_2\cdot\epsilon_2)+6\left(q_1\cdot q_2\right)^2\right),
\end{aligned}
$$

We also have the sixfold degenerate spin 2 states

$$
\begin{aligned}
& 6\,\square\!\square_4 \\
A^{[2]_9\otimes[2]_9\to[4]_9\to[2]_4}_{m_1m_2} &= \frac{\alpha'}{16}\sqrt{\frac{5}{39}}\left[q_{1,m_1}\left(5\epsilon_{1,m_2}(q_1\cdot\epsilon_1)+2q_{1,m_2}\right)\right.\\
&+ \epsilon_{1,m_1}\left(5q_{1,m_2}(q_1\cdot\epsilon_1)-2t_1\epsilon_{1,m_2}\right)\\
&+ \left.5v_{m_1}v_{m_2}\left(q_1\cdot\epsilon_1\right)^2\right],
\end{aligned}
$$

$$
\begin{aligned}
A^{[2]_9\otimes[2]_9\to[2,2]_9\to[2]_4}_{m_1m_2} &= \frac{\alpha'}{4}\sqrt{\frac{5}{42}}\left[-q_{1,m_1}\left(q_{1,m_2}-2\epsilon_{1,m_2}(q_1\cdot\epsilon_1)\right)\right.\\
&+ \epsilon_{1,m_1}\left(2q_{1,m_2}(q_1\cdot\epsilon_1)+t_1\epsilon_{1,m_2}\right)\\
&+ \left.2v_{m_1}v_{m_2}\left(q_1\cdot\epsilon_1\right)^2\right],
\end{aligned}
\tag{A.41}
$$

$$
\begin{aligned}
A^{[2]_9\otimes[2]_9\to[2]_9\to[2]_4}_{m_1m_2} &= \frac{\alpha'}{4\sqrt{91}}[(q_{1,m_1}\left(\epsilon_{1,m_2}(q_1\cdot\epsilon_1)+3q_{1,m_2}\right)\\
&+ \epsilon_{1,m_1}\left(q_{1,m_2}(q_1\cdot\epsilon_1)-3t_1\epsilon_{1,m_2}\right)\\
&+ \left.v_{m_1}v_{m_2}\left(q_1\cdot\epsilon_1\right)^2)\right],
\end{aligned}
$$

$$
\begin{aligned}
A^{[1,1,1]_9\otimes[1,1,1]_9\to[2,2]_9\to[2]_4}_{m_1m_2} &= \frac{\alpha'}{2\sqrt{14}}[(q_{1,m_1}\left(q_{1,m_2}-\epsilon_{1,m_2}(q_1\cdot\epsilon_1)\right)\\
&+\epsilon_{1,m_1}\left(-q_{1,m_2}\left(q_1\cdot\epsilon_1\right)-t_1\epsilon_{1,m_2}\right)\\
&+v_{m_1}v_{m_2}\left(-\left(q_1\cdot\epsilon_1\right)^2-t_1\right))]\,,\\
\\
A^{[1,1,1]_9\otimes[1,1,1]_9\to[2]_9\to[2]_4}_{m_1m_2} &= \frac{\alpha'}{4\sqrt{21}}[(q_{1,m_1}\left(\epsilon_{1,m_2}(q_1\cdot\epsilon_1)-q_{1,m_2}\right)\\
&+\epsilon_{1,m_1}\left(q_{1,m_2}(q_1\cdot\epsilon_1)+t_1\epsilon_{1,m_2}\right)\\
&+v_{m_1}v_{m_2}\left(\left(q_1\cdot\epsilon_1\right)^2+t_1\right))]\,,
\end{aligned}
\tag{A.42}
$$

$$
\begin{aligned}
\left(A^{[1,1,1]_9\otimes[1,1,1]_9\to[2,2,2]_9\to[2]_4}_{\mathbf{m}}\right)^2 &= \frac{(\alpha')^2}{1920}\left(37t_1\left(q_2\cdot\epsilon_1\right)^2-74t_1(\epsilon_1\cdot\epsilon_2)(q_2\cdot\epsilon_1)(q_2\cdot\epsilon_2)\right.\\
&+17\left(q_1\cdot\epsilon_1\right)^2\left(\left(q_2\cdot\epsilon_2\right)^2+t_2\right)+17t_1\left(\left(q_2\cdot\epsilon_2\right)^2+t_2\right)\\
&+\left(q_1\cdot\epsilon_2\right)^2\left(117\left(q_2\cdot\epsilon_1\right)^2+37t_2\right)\\
&-74(q_1\cdot\epsilon_1)(q_1\cdot\epsilon_2)\left((q_2\cdot\epsilon_1)(q_2\cdot\epsilon_2)+t_2(\epsilon_1\cdot\epsilon_2)\right)\\
&+\left(q_1\cdot q_2\right)^2\left(117\left(\epsilon_1\cdot\epsilon_2\right)^2-37\right)\\
&+q_1\cdot q_2\left(2q_1\cdot\epsilon_2\left(37q_2\cdot\epsilon_2-117\epsilon_1\cdot\epsilon_2q_2\cdot\epsilon_1\right)\right.\\
&\left.\left.+74q_1\cdot\epsilon_1\left(q_2\cdot\epsilon_1-\epsilon_1\cdot\epsilon_2q_2\cdot\epsilon_2\right)\right)-37t_1t_2\left(\epsilon_1\cdot\epsilon_2\right)^2\right)\,,
\end{aligned}
$$

and 8-fold degenerate spin 0 states

$$
\begin{aligned}
& 8\bullet_4\\
A_{[2]_9\otimes[2]_9\to[4]_9\to\bullet_4} &= \frac{1}{48}\sqrt{\frac{35}{286}}\alpha'\left(4t_1-15\left(q_1\cdot\epsilon_1\right)^2\right)\,,\\
\\
A_{[2]_9\otimes[2]_9\to[2,2]_9\to\bullet_4} &= \frac{1}{24}\sqrt{\frac{5}{7}}\alpha'\left(3\left(q_1\cdot\epsilon_1\right)^2+t_1\right)\,,\\
\\
A_{[2]_9\otimes[2]_9\to[2]_9\to\bullet_4} &= \frac{1}{8}\sqrt{\frac{5}{91}}\alpha'\left(\left(q_1\cdot\epsilon_1\right)^2-2t_1\right)\,,\\
\\
A_{[2]_9\otimes[2]_9\to\bullet_9\to\bullet_4} &= \frac{\alpha'}{8\sqrt{11}}\left(\left(q_1\cdot\epsilon_1\right)^2-t_1\right)\,,\\
\\
A_{[1,1,1]_9\otimes[1,1,1]_9\to[2,2]_9\to\bullet_4} &= \frac{1}{8}\sqrt{\frac{3}{7}}\alpha'\left(-\left(q_1\cdot\epsilon_1\right)^2-t_1\right)\,,
\end{aligned}
\tag{A.43}
$$

$$A_{[1,1,1]_9\otimes[1,1,1]_9\to[2]_9\to\bullet_4} = \frac{1}{8}\sqrt{\frac{5}{21}}\alpha'\left((q_1\cdot\epsilon_1)^2+t_1\right)\,,$$

$$A_{[1,1,1]_9\otimes[1,1,1]_9\to\bullet_9\to\bullet_4} = \frac{\alpha'}{8\sqrt{21}}\left((q_1\cdot\epsilon_1)^2+t_1\right)\,,$$

$$\begin{aligned}\left(A_{[1,1,1]_9\otimes[1,1,1]_9\to[2,2,2]_9\to\bullet_4}\right)^2 = \frac{(\alpha')^2}{4480}\,&\big(-49t_1\,(q_2\cdot\epsilon_1)^2+98t_1(\epsilon_1\cdot\epsilon_2)(q_2\cdot\epsilon_1)(q_2\cdot\epsilon_2)\\&-49\,(q_1\cdot\epsilon_2)^2\left((q_2\cdot\epsilon_1)^2+t_2\right)-29\,(q_1\cdot\epsilon_1)^2\left((q_2\cdot\epsilon_2)^2+t_2\right)\\&-29t_1\left((q_2\cdot\epsilon_2)^2+t_2\right)-49\,(q_1\cdot q_2)^2\left((\epsilon_1\cdot\epsilon_2)^2-1\right)\\&+98(q_1\cdot\epsilon_1)(q_1\cdot\epsilon_2)\left((q_2\cdot\epsilon_1)(q_2\cdot\epsilon_2)+t_2(\epsilon_1\cdot\epsilon_2)\right)\\&-98q_1\cdot q_2\,(q_1\cdot\epsilon_2\,(q_2\cdot\epsilon_2-(\epsilon_1\cdot\epsilon_2)(q_2\cdot\epsilon_1))\\&+q_1\cdot\epsilon_1\,(q_2\cdot\epsilon_1-(\epsilon_1\cdot\epsilon_2)(q_2\cdot\epsilon_2)))+49t_1t_2\,(\epsilon_1\cdot\epsilon_2)^2\big)\,.\end{aligned} \tag{A.44}$$

Upon contracting each of these amplitudes (with a Pomeron P_1) with the appropriate projector and another three-point amplitude (with a Pomeron P_2), we recover, upon summing over all 22 states, the level 1 residue of the four-point amplitude, as described in the main text.

Chapter 3

Conformal multi-Regge theory

In the previous chapter, we studied the consistency conditions on the correlation function of four scalar operators in a conformal field theory in the Regge limit. Consistency conditions also impose constraints on dynamical data at the level of more than four point correlation functions. These correlators give us access to much more data than their lower-point counterparts. Given that conformal blocks play a central role in conformal bootstrap, their higher-point analogues are studied in [70–76]. Although their structure is generically intricate, it simplifies drastically in the lightcone limit where bootstrap studies have been performed in [77, 78]. Higher-point correlation functions have also been considered in holographic theories [71, 79, 80].

An important tool in the analytical conformal bootstrap is the Regge limit [4, 31, 37]. The Regge limit of four-point correlation functions in CFTs is the conformal analogue of the limit of high centre of mass energy at fixed impact parameter of scattering amplitudes in quantum field theory. The main idea coming out of this study is that the CFT spectrum admits an elegant description in terms of a set of *Regge trajectories*. In particular, the spectrum admits an intriguing analyticity in spin quantum number, as established by the inversion formula [6]. This puts the analytical conformal bootstrap using the lightcone limit on a firm footing, by showing that the large spin expansion is not asymptotic, but convergent. Recently, these ideas have been tested on several physical models, with great success [9, 10]. This success calls for a deeper analysis of the Regge limit. In this chapter we start the discussion of the generalization of the Regge limit to higher-point functions, mostly focusing on the case of five-point functions.

The outline of the chapter is as follows. In Section 3.1, we review the literature on the multi-Regge limit for the S-matrix. In Section 3.2, we discuss the setup of five-point correlation functions in conformal field theories. We sketch the Euclidean OPE limit and the lightcone limit, and contrast it with our proposal for Regge limit. In Section 3.3, we discuss the analytic

properties of the correlator and its Mellin transfom. In subsection 3.3.4, we discuss the relation of the Reggeized correlator to the partial wave coefficients. Finally, we conclude with some open directions Section 3.4.

3.1 Scattering in flat-space and Regge theory

In this section, we review Regge theory for scattering amplitudes in flat space. We begin by reviewing the key ingredients in the case of $2 \to 2$ scattering process in four-dimensional Lorentzian spacetime. Then, we review the generalization to the case of higher-point scattering amplitudes. It will serve as the main inspiration for the conformal Regge theory that we will consider later.

Let us restrict to the more familiar case of $2 \to 2$ scattering, where we define the Mandelstam invariants as

$$s = -(k_1 + k_3)^2\,, \qquad t = -(k_1 + k_2)^2\,, \qquad u = -(k_1 + k_4)^2, \tag{3.1}$$

with k_i the external incoming momenta. The Regge limit corresponds to the high-energy limit of an amplitude, where $s \to \infty$ with fixed t. Regge theory, on the other hand, comes in play to address the experimental observation that s-channel processes exhibit a small t peak whenever there are exchanges of particles or resonances in the t-channel. One would like to understand this behaviour by considering a partial wave decomposition of the amplitude. Consider the scattering amplitude of four spinless particles with equal mass m in the t-channel decomposition

$$A(s,t) = \sum_{J=0}^{\infty} (2J+1) a_J(t) P_J(z)\,, \tag{3.2}$$

where $z = \cos\theta = 1 + 2s/(t-4m^2)$ and $P_J(z)$ is a Legendre polynomial of first kind of degree J. θ denotes the t-channel scattering angle and J is the angular momentum of the exchanged particles. This series converges in the t-channel physical region, namely the region $t > 4m^2$ and $s < 0$, and therefore is not reliable to study the large s limit. Note that the large s limit of a spin J partial wave behaves as s^J. The infinite sum over J gets more and more contributions from the higher J partial waves, in this limit. Regge theory provides a rewriting of (3.2) in a form that can be analytically continued to this large s region. This is done by complexifying angular momentum, extending Regge's idea [49], and allows to resum the contribution of a family of particles that correctly predict the observed large s behaviour.

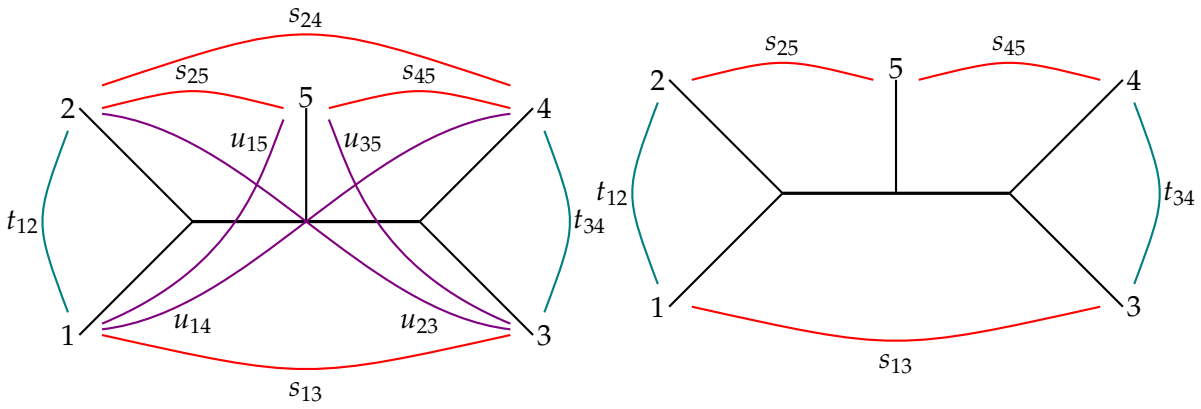

FIGURE 3.1: The ten two-body Mandelstam invariants of a five-point scattering amplitude (left) and our choice of five independent ones (right).

Naturally, one would like to extend Regge theory to multi-particle exchange amplitudes. The analytic structure of these amplitudes is less well understood than the four-point analogue. The increasing number of Mandelstam invariants turns this into a more technically-challenging goal, but there have been important contributions in the 70's that we now briefly review for the case of five-point amplitudes (see [81–91] for more details).

As represented in figure 3.1 (left), one can define ten two-body Mandelstam invariants for a five-point function, in an analogous way to the $2 \to 2$ scattering definition (3.1), i.e.

$$s_{ij} = -(k_i + k_j)^2 \,, \tag{3.3}$$

where k_i are again external incoming momenta. Similarly, we define t_{ij}- and u_{ij}-type invariants. Since not all the invariants are independent, we shall choose the following five as independent, $s_{13}, s_{25}, s_{45}, t_{12}, t_{34}$, as shown in figure 3.1 (right). We will be focusing on the double Regge limit where $s_{25}, s_{45} \to \infty$, and necessarily $s_{13} \to \infty$, while t_{12} and t_{34} are held fixed. It is also possible to define a single Regge limit by considering either $s_{25} \to \infty$ with s_{13}/s_{25} also fixed, or $s_{45} \to \infty$ with s_{13}/s_{45} fixed.[1] We note that the generalization of the double Regge limit to the case of n identical massive particles is given by [86],

$$s \text{ type :} \qquad s_{r+1,r+3} \,, \tag{3.4}$$

$$t \text{ type :} \qquad s_{1,r+2} \,, \tag{3.5}$$

$$\omega \text{ type (Toller angles) :} \qquad \frac{s_{p-2,p} s_{p-1,p+1}}{s_{p-2,p+1}} \,,$$

[1] Another interesting limit to consider is the helicity-pole limit where $s_{25} \to \infty$ with $s_{13}/s_{25} \to \infty$ while t_{12}, t_{34} and s_{45} are fixed (or the one where the roles of s_{25} and s_{45} are swapped). This limit is experimentally accessible in inclusive cross-sections [92]. It is also possible to consider the limit $s_{13} \to \infty$ with all the other Mandelstam invariants kept fixed.

where labels are in the following range $r = 1, \cdots, n-3$, $p = 4, \cdots, n-1$. We also use $s_{i,j} = -\left(k_{i+1} + \cdots + k_j\right)^2$.

Let us consider the partial-wave decomposition of an amplitude $A = A(s_{25}, s_{45}, \eta; t_{12}, t_{34})$ of five identical massive particles in the t_{12}, t_{34} channels,

$$A = \sum_{m=-\infty}^{\infty} \sum_{J_{1,2}=|m|}^{\infty} \prod_{i=1}^{2} (2J_i + 1) a_{J_1,J_2,m}(t_{12}, t_{34}) z^m d^{J_1}_{0m}(\cos\theta_1) d^{J_2}_{m0}(\cos\theta_2)\,, \tag{3.6}$$

where $\eta \equiv s_{13}/(s_{25}s_{45})$ and $z \equiv e^{i\theta_{\text{Toller}}}$, as defined below. Here m denotes the allowed helicities of exchanged particles. We also use Wigner-d functions which can be written in terms of Jacobi polynomials $\mathcal{P}^{\alpha,\beta}_J$ as

$$d^J_{m'm}(\cos\theta) = \left(\frac{(J+m)!\,(J-m)!}{(J+m')!\,(J-m')!}\right)^{\frac{1}{2}} \left(\sin\frac{\theta}{2}\right)^{m-m'} \left(\cos\frac{\theta}{2}\right)^{m+m'} \mathcal{P}^{m-m',m+m'}_{J-m}(\cos\theta)\,, \tag{3.7}$$

with

$$\mathcal{P}^{\alpha,\beta}_J(z) = \sum_{n=0}^{J} \frac{(-1)^n}{n!} \frac{J!}{(J-n)!} \frac{\Gamma(n+\alpha+1)\Gamma(J-n+\beta+1)}{\Gamma(J+\alpha+\beta+2)} z^{n+\alpha}\,(1-z)^{J-n+\beta}\,. \tag{3.8}$$

The scattering angles θ_1, θ_2 and θ_{Toller} have a clear physical meaning - see e.g. [86]. Consider the scattering process shown in the figure 3.1 with the exchanged momenta $q_1^2 = t_{12}$ and $q_2^2 = t_{34}$. Firstly, we lump together particles $3, 4$ and treat them as a single particle of momentum q_2. The angle θ_1 is defined as the scattering angle of the process $12 \to 5(34)$ which happens in a single plane in the center of mass frame. Secondly, we consider the rest frame of the exchanged momentum q_2. We denote the three momentum of particle-i by $\vec{p}_i$. As depicted in figure 3.2, we can choose a coordinate system where $\vec{p}_5$ is aligned with the z-axis and $\vec{p}_2$ lies somewhere in xz-plane. We define θ_2 as the zenith-angle of $\vec{p}_3$, whereas θ_{Toller} is the azimuth angle. Alternatively, the Toller angle can be thought of as the angle between the two scattering planes corresponding to the q_1 and q_2 rest frames, respectively.

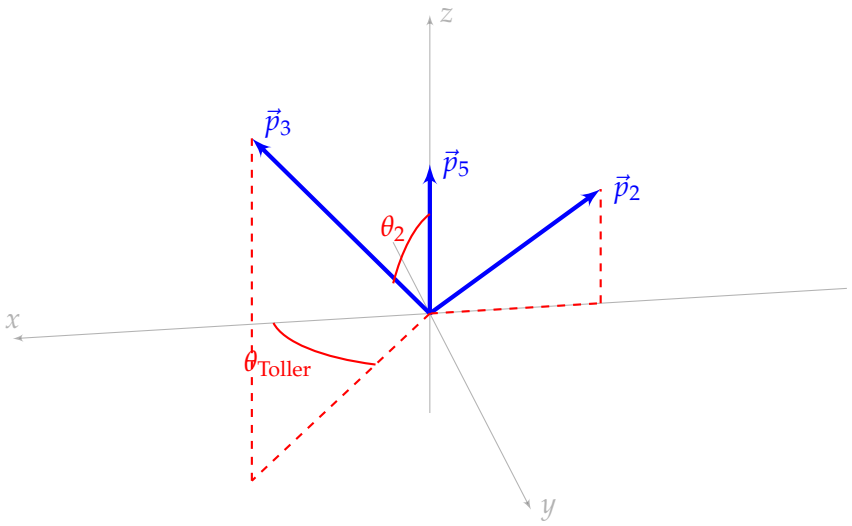

FIGURE 3.2: Scattering process shown in the resting frame of exchanged momentum q_2. This defines the angles θ_2 and θ_{Toller}. θ_1 is defined analogously in the rest frame of exchanged momentum q_1.

The scattering angles are related to the Mandelstam invariants in a nontrivial way - see e.g. [84, 87],

$$
\begin{aligned}
s_{25} &= 2m^2 + \frac{1}{2}\left(t_{34} - m^2 - t_{12}\right) + \frac{1}{2}\left(\frac{(t_{12}-4m^2)\lambda(t_{12},t_{34},m^2)}{t_{12}}\right)^{1/2}\cos\theta_1\,,\\
s_{45} &= 2m^2 + \frac{1}{2}\left(t_{12} - m^2 - t_{34}\right) + \frac{1}{2}\left(\frac{(t_{34}-4m^2)\lambda(t_{12},t_{34},m^2)}{t_{34}}\right)^{1/2}\cos\theta_2\,,\\
s_{13} &= 2m^2 + \frac{1}{4}\left(m^2 - t_{12} - t_{34}\right) + \frac{1}{4}\left(\frac{(t_{12}-4m^2)\lambda(t_{12},t_{34},m^2)}{t_{12}}\right)^{1/2}\cos\theta_1 \qquad (3.9)\\
&+\frac{1}{4}\left(\frac{(t_{34}-4m^2)\lambda(t_{12},t_{34},m^2)}{t_{34}}\right)^{1/2}\cos\theta_2 + \frac{1}{4}\left(\frac{(t_{12}-4m^2)(t_{34}-4m^2)}{t_{12}t_{34}}\right)^{1/2}\times\\
&\left(m^2 - t_{12} - t_{34}\right)\cos\theta_1\cos\theta_2 - \frac{1}{2}\left((t_{12}-4m^2)(t_{34}-4m^2)\right)^{1/2}\sin\theta_1\sin\theta_2\cos\theta_{\text{Toller}}\,,
\end{aligned}
$$

where we use $\lambda(a,b,c) = a^2 + b^2 + c^2 - 2ab - 2bc - 2ca$. Note that here m corresponds to the mass of the exchanged particles and should not be confused with helicity. We believe the context makes clear which one we refer to. We emphasize that only s_{13} depends on θ_{Toller}. Moreover, in the double Regge limit,

$$
\eta \sim \frac{2(t_{12}t_{34})^{1/2}\cos\theta_{\text{Toller}} + m^2 - t_{12} - t_{34}}{\lambda(t_{12},t_{34},m^2)}\,, \qquad (3.10)
$$

independently of θ_1 and θ_2. This map suffers from some kinematical singularities in terms of the variables t_{12}, t_{34}. These will be extracted from the possible types of singularities that we study below and we focus only on dynamical singularities.

To explore the double Regge region from the partial wave decomposition (3.6), we need a

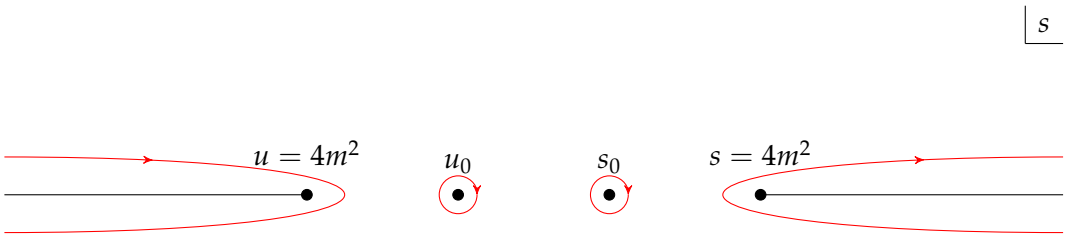

FIGURE 3.3: Singularities of $A(s,t)$ in the s complex-plane at fixed t.

well-defined analytic continuation of the amplitude. In contrast to the $2 \to 2$ scattering, for multiparticle scattering besides considering complex angular momentum, one also needs to account for helicity dependence. As stressed in [81–84], the analytic continuation of the amplitude to complex helicity values is also required. The proper procedure for analytic continuation and its uniqueness deserve some comments. Let us first review some concepts in the four-point case that will straightforwardly generalize to the five-point case we wish to analyse in more detail.

We assume that a $2 \to 2$ scattering amplitude has only singularities with dynamical origin. Namely, we only consider poles associated with bound states and branch-cuts starting at physical thresholds for particle production. In figure 3.3 we depict these singularities at fixed t in the complex s plane. We assume that the following dispersion relation at fixed t

$$A(s,t) = \frac{1}{2\pi i}\left(\int_0^{+\infty} ds' \, \frac{\text{Disc}_s(s',t,u')}{s'-s} + \int_0^{+\infty} du' \, \frac{\text{Disc}_u(s',t,u')}{u'-u}\right) = A_R(s,t) + A_L(u,t)\,. \tag{3.11}$$

Here, we have extended the notion of discontinuities Disc_s and Disc_u to include the contributions of bound-state poles.[2] We have also defined A_R and A_L with respect to each of the terms. As it is clear from the definition, each of the terms has only cut contributions along one of the directions in the s complex plane. This fact is crucial in performing the analytic continuation of the amplitude with good large J behaviour which happens to be unique as guaranteed by Carlson's theorem. It is also useful to define the *signatured amplitude* [3]

$$A^{\delta}(s,t) = \frac{1}{2}\big(A_R(s,t) + \delta\, A_L(s,t)\big), \tag{3.12}$$

[2] We assumed that no subtractions were needed in order to neglect contributions from arcs at infinity from the Cauchy integral that gives rise to the dispersion relation. If this is not the case, one should proceed considering instead a subtracted amplitude.

[3] The reader might be familiar with an equivalent decomposition of the full amplitude in terms of even and odd angular momentum contributions. These are composed of signatured amplitudes. Indeed we have $A^{\text{even}} = A^{+}(s,t) + A^{+}(-s,t)$ and $A^{\text{odd}} = A^{-}(s,t) - A^{-}(-s,t)$, where we use $u \sim -s$ in Regge limit.

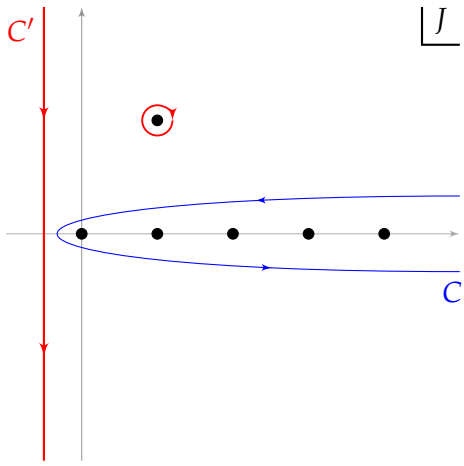

FIGURE 3.4: Contour integrals for the Sommerfeld-Watson transfom for the four partiacle scattering in the J-complex plane. As one deforms the contour from C to C' one has to consider the contribution from dynamical singularities which here we assume to be a Regge pole.

where $\delta = \pm 1$. Note that we replace u by s in A_L ensuring that there are only cuts in a single direction. The full amplitude can be easily reconstructed from the signatured amplitudes as

$$A(s,t) = \sum_{\delta=\pm 1} \Big(A^{\delta}(s,t) + \delta\, A^{\delta}(u,t) \Big) \,. \tag{3.13}$$

In what follows, we assume that the signatured amplitudes have the same analytic structure as the full amplitude. This assumption greatly simplifies the discussion of dynamical singularities of partial-wave amplitudes. We are entitled to consider the partial wave expansion of the signatured amplitude

$$A^{\delta}(s,t) = \sum_{J=0}^{\infty} (2J+1) a_J^{\delta}(t) P_J(z) \,. \tag{3.14}$$

Using the orthogonality of Legendre polynomials P_J and (3.12), we can write

$$a_J^{\delta}(t) = \frac{1}{4\pi i} \int_{z_0}^{+\infty} dz' \Big(\mathrm{Disc}_s A_R(s',t) + \delta\, \mathrm{Disc}_s A_L(s',t) \Big) Q_J(z') \,, \tag{3.15}$$

where z_0 is the branch point of the discontinuity and Q_J is the Legendre polynomial of the second kind given by

$$Q_J(z) = \int_{-1}^{1} d\zeta\, \frac{P_J(\zeta)}{z-\zeta} \,. \tag{3.16}$$

Using the symmetry $P_J(z) = (-1)^J P_J(-z)$, we perform a Sommerfeld-Watson transform of (3.14)

$$A^{\delta}(s,t) = \int_C \frac{dJ}{2\pi i} \frac{\pi}{\sin \pi J} (2J+1) a^{\delta}(J,t) P_J(-z)\,, \tag{3.17}$$

where C is the closed contour depicted in figure 3.4. Due to the good large J behaviour of the partial-wave P_J, one can continuously deform the contour from C to C', as shown in the same figure. We should account for all the possible singularities that may be encountered during this deformation. In this chapter, we always assume that these are pole type singularities [4]

$$a^{\delta}(J,t) \simeq \frac{\beta(t)}{J-\alpha(t)}\,, \tag{3.18}$$

where $\alpha(t)$ is a Regge trajectory and $\beta(t)$ is regular in t. Regularity follows from the assumption that $A^{\delta}(s,t)$ has the same analytic structure of the full amplitude $A(s,t)$. We also use the fact that Steinmann relations [93] impose the latter to have no double discontinuity in s and t. At large s, we keep the rightmost pole as it gives the leading contribution and write

$$A^{\delta}(s,t) \sim \frac{1}{2\pi i}(-s)^{\alpha(t)} \Gamma\big(-\alpha(t)\big)\beta(t)\,, \tag{3.19}$$

where we absorbed nonsingular factors into the definition of $\beta(t)$.

For the five-particle case we expect a similar analytic structure of the amplitude in the s_{25}, s_{45} and s_{13} complex planes as in the four-particle case. We would like to decompose the full amplitude in terms of signatured amplitudes with only right-hand or left-hand cuts for each s-type invariant. We immediately see that we have to consider $2^3 = 8$ possible signatures. Indeed, one writes

$$\begin{aligned} A(s_{ij},t_{ij}) = \sum_{\delta_{ij}=\pm 1} \Big\{ \Big(& A^{\delta_{25}\delta_{45}\delta_{13}}(s_{25},s_{45},\eta,t_{12},t_{34}) + \delta_{25} A^{\delta_{25}\delta_{45}\delta_{13}}(-s_{25},s_{45},\eta,t_{12},t_{34}) + \\ & \delta_{45} A^{\delta_{25}\delta_{45}\delta_{13}}(s_{25},-s_{45},\eta,t_{12},t_{34}) + \delta_{25}\delta_{45} A^{\delta_{25}\delta_{45}\delta_{13}}(-s_{25},-s_{45},\eta,t_{12},t_{34}) \Big) + \delta_{13}(\eta \to -\eta) \Big\}\,, \end{aligned} \tag{3.20}$$

where we make a slight abuse of notation by writing $u_{ij} \sim -s_{ij}$ as dictated by the double-Regge limit we are exploring. Indeed, note that each of the signatured amplitudes $A^{\delta_{25}\delta_{45}\delta_{13}}$ is a function with only right-hand cuts in each of the invariants s_{25}, s_{45} and s_{13}. While δ_{25}, δ_{45} are the already familiar signatures associated with angular momenta in the t_{12} and t_{34} channels, δ_{13} is a new signature related to the helicity at the central vertex.

[4] Other type of singularities like Regge cuts and nonsense-wrong-signature-fixed poles also exist. Moreover, singularities can also appear in a multiplicative manner but we neglect this scenario here for simplicity. The interested reader can find a discussion on those in [87] and references thereafter.

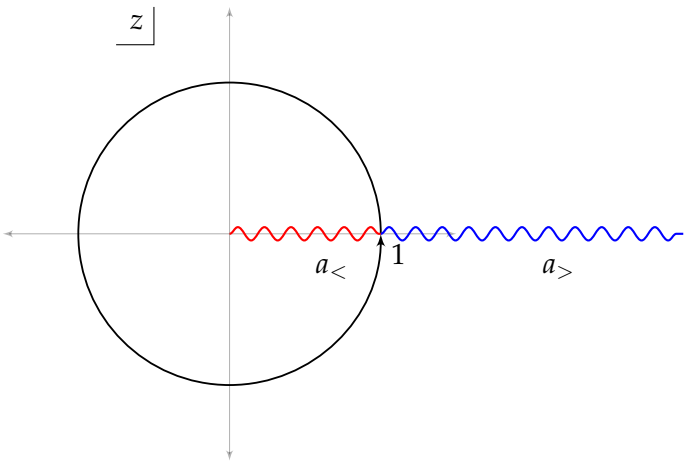

FIGURE 3.5: Contour deformation in $z = e^{i\theta_{\text{Toller}}}$ for doing the Froissart-Gribov continuation. The orthogonality relation holds on the black contours. We show the two different branch cuts corresponding to $a_{\gtrless}$ discussed in (3.24).

Following [81], we first analyse the analytic continuation of helicity m to complex values. Inspired by the form of the partial-wave decomposition (3.6), one expects the following dispersion relation to hold in the z-complex plane,

$$A(s_{ij},\eta,t_{ij}) = \frac{1}{2\pi i}\left(\int_{-\infty}^{-1-\epsilon} + \int_{-1+\epsilon}^{1-\epsilon} + \int_{1+\epsilon}^{+\infty}\right)\frac{\text{Disc}_z A(s_{ij},\eta',t_{ij})}{z'-z}\,dz'\,. \tag{3.21}$$

To have a well-defined analytic continuation, we need to consider amplitudes with cuts either only on the right or only on the left half plane in the respective Mandelstam variable. Thus, we consider signatured amplitudes as introduced in (3.20). We can write

$$A^{\delta_{13}}(z) = \sum_{m=-\infty}^{+\infty} a_m^{\delta_{13}} z^m\,, \tag{3.22}$$

where we suppress the dependence on labels or parameters that are irrelevant for this discussion. Using the fact that signatured amplitudes are functions with only right-hand cuts, [5] we have

$$a_m^{\delta_{13}} = \left(\frac{1}{2\pi i}\right)^2\left(\int_0^{1-\epsilon} + \int_{1+\epsilon}^{+\infty}\right)\int_{|z|=1}\frac{\text{Disc}_z A^{\delta_{13}}(z')}{z'-z}\,z^{-m-1}dz'dz\,. \tag{3.23}$$

For $z' > 1$ and $m < 0$ the z-integral gives 0, while for $m \geq 0$, it gives z'^{-m-1}. On the other hand, if $0 < z' < 1$ and $m \geq 0$, the residues at the two poles cancel and the integral yields 0,

[5] Note that taking $z \to -z$ is related with $\eta \to -\eta$ as one can see from (3.10).

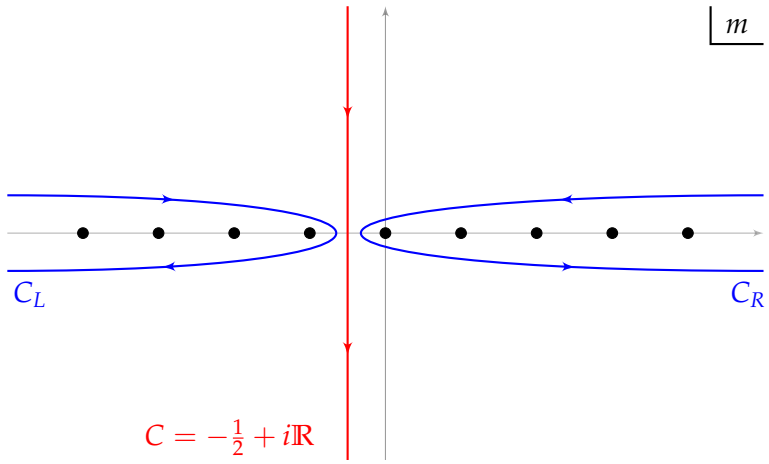

FIGURE 3.6: Contour integrals for the Sommerfeld-Watson transfom in the m-complex plane.

whereas for $m < 0$ we find $-z'^{-m-1}$. We can then define, as shown in figure 3.5,

$$a_{>}^{\delta_{13}}(m) = \frac{1}{2\pi i}\int_{1+\epsilon}^{\infty}(z')^{-m-1}\text{Disc}_z A^{\delta_{13}}(z')dz'\,, \tag{3.24}$$

$$a_{<}^{\delta_{13}}(m) = \frac{1}{2\pi i}\int_{0}^{1-\epsilon}(z')^{-m-1}\text{Disc}_z A^{\delta_{13}}(z')dz'\,, \tag{3.25}$$

where it is clear that $a_{>}^{\delta_{13}}$ has a good asymptotic behaviour in the right half-plane in the complex m variable, whereas $a_{>}^{\delta_{13}}$ does so on the left-half plane. We can thus perform a Sommerfeld-Watson transform in m and write

$$\begin{aligned} A^{\delta_{13}}(z) &= \sum_{m=0}^{\infty} a_{>}^{\delta_{13}}(m)z^m - \sum_{m=-\infty}^{-1} a_{<}^{\delta_{13}}(m)z^m \\ &= \frac{1}{2\pi i}\int_{C_R} dm \frac{\pi a_{>}^{\delta_{13}}(m)(-z)^m}{\sin\pi m} - \frac{1}{2\pi i}\int_{C_L} dm \frac{\pi a_{<}^{\delta_{13}}(m)(-z)^m}{\sin\pi m} \\ &= \frac{1}{2\pi i}\int_{C} dm \frac{\pi\left(a_{>}^{\delta_{13}}(m) + a_{<}^{\delta_{13}}(m)\right)}{\sin\pi m}(-z)^m\,, \end{aligned} \tag{3.26}$$

where the contours C_R, C_L and C are shown in figure 3.6. Recovering the previously suppressed dependences and parameters, we have

$$a_{\gtrless}^{\delta_{13}}(m) = \sum_{J_1,J_2=m}^{\infty}\left(\prod_{i=1}^{2}(2J_i+1)\right) a_{\gtrless,J_1,J_2,m}^{\delta_{25}\delta_{45}\delta_{13}}(t_{12},t_{34})d_{0m}^{J_1}(\cos\theta_1)d_{m0}^{J_2}(\cos\theta_2)\,, \tag{3.27}$$

which only makes sense if we also analytically continue in the two angular momenta,

$$a_{\gtrless}^{\delta_{13}}(m) = \left(\prod_{i=1}^{2}\int_{C_i}\frac{dJ_i}{2\pi i}\frac{\pi(2J_i+1)}{\sin\pi(J_i-m)}\right) a_{\gtrless}^{\delta_{25}\delta_{45}\delta_{13}}(J_1,J_2,m,t_{12},t_{34})d_{0m}^{J_1}(-z_1)d_{m0}^{J_2}(-z_2)\,, \tag{3.28}$$

with contours C_i as shown in figure 3.7 (left) and where $z_i = \cos\theta_i$. This is a reasonable but

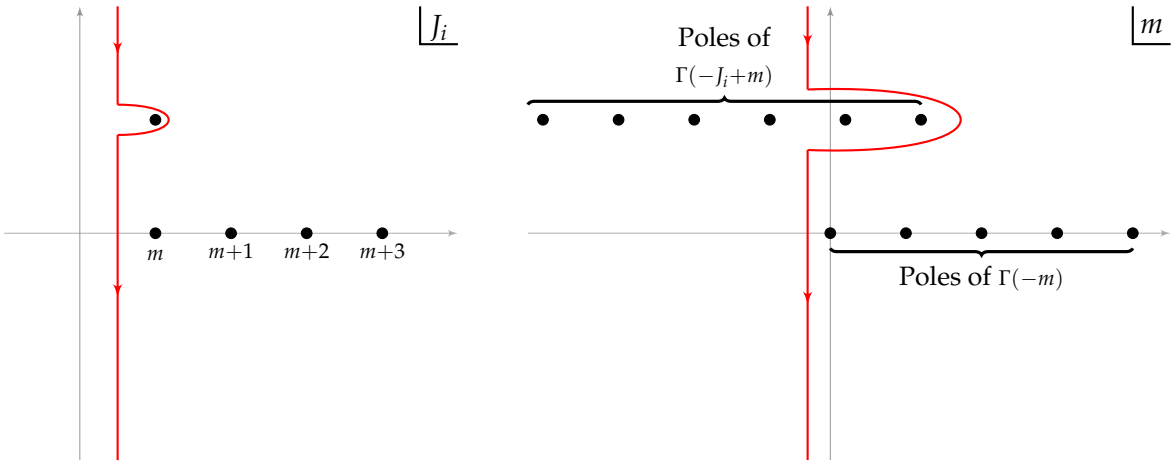

FIGURE 3.7: Contour of integration in J_i and m-complex planes when the respective variable is integrated first. Here, we only account for dynamical singularities given by Regge poles and ignore the existence of Regge cuts and fixed poles. Note that there are no dynamical singularities in the m-complex plane.

non-trivial claim. In fact, [82, 83] was only able to check a well-defined analytic continuation for a single angular momentum and helicity, but not the three simultaneously. To the best of our knowledge, there is no derivation of the latter. In the following, we assume that this defines a satisfactory analytic continuation of the signatured amplitude in terms of the scattering angles and of t_{12} and t_{34}. However, we would like to rewrite it in terms of the Mandelstam invariants alone. This can be done by using the map (3.9). To find the dependence on s_{25} and s_{45}, we mimic the analysis of the four-particle case. On the other hand, the η dependence requires one more comment. We assume that $A^{\delta_{13}}$ is an even function of the Toller angle and, in particular, a function of $\cos\theta_{\text{Toller}}$ (and thus invariant under $z \to 1/z$)[6]. This requirement follows from the realization that η is an even function of θ_{Toller} and therefore only even functions of θ_{Toller} can be rewritten in terms of η. This ends up imposing $a^{\delta_{13}}_{>}(m) = a^{\delta_{13}}_{<}(-m)$ and justifies dropping the subscripts when we write

$$A^{\delta_{13}}(\eta) = \frac{1}{2\pi i}\int_C dm\, \frac{\pi a^{\delta_{13}}(m)}{\sin \pi m}(-\eta)^m\,. \tag{3.29}$$

[6]See [87] for whenever this is not the case.

Note that, as we write z in terms of η, we redefine what we mean by $a^{\delta_{13}}$. [7] We can summarize the discussion on analytic continuations of five-particle amplitudes by writing

$$\begin{aligned} A^{\delta_{25}\delta_{45}\delta_{13}}(s_{25},s_{45},\eta,t_{12},t_{34}) &= \left(\frac{1}{2\pi i}\right)^3 \int_C dm \left(\prod_{i=1}^{2}\int_{C_i} dJ_i(2J_i+1)\right) \\ &\frac{\pi^3 d^{J_1}_{0m}(-\cos\theta_1) d^{J_2}_{m0}(-\cos\theta_2)(-\eta)^m}{\sin\pi m \sin\pi(J_1-m)\sin\pi(J_2-m)}\, a^{\delta_{25}\delta_{45}\delta_{13}}(J_1,J_2,m,t_{12},t_{34}) \\ &= \left(\frac{1}{2\pi i}\right)^3 \int_C dm\Gamma(-m) \left(\prod_{i=1}^{2}\int_{C_i} dJ_i(2J_i+1)\Gamma(-J_i+m)\right) \\ &(-s_{25})^{J_1-m}(-s_{45})^{J_2-m}(-s_{13})^m a^{\delta_{25}\delta_{45}\delta_{13}}(J_1,J_2,m,t_{12},t_{34})\,, \end{aligned} \tag{3.30}$$

where we used $\eta = s_{13}/(s_{25}s_{45})$ and in the second equality $a^{\delta_{25}\delta_{45}\delta_{13}}(J_1,J_2,m,t_{12},t_{34})$ was redefined.

Under the assumption that the analytic continuation of the signatured amplitude has a good asymptotic behaviour in J_1, J_2 and m such that we can ignore arcs at infinity, we focus on possible singularities that one might encounter as we move the contours to the left. In figure 3.7, we draw both m and J_i complex planes when the respective variable is integrated first. In particular, we show the possible singularities. As before, we restrict our analysis to Regge-pole-type of singularities and we refer interested readers to [86, 87] for more details on other type of singularities. One expects the singularities in m to the left of contour and that determine the asymptotic behaviour of the amplitude to be completely determined by the dynamical singularities in angular momenta. The reason for that is bi-folded. First, note that the amplitude has the asymptotic behaviour

$$(-s_{25})^{J_1-m}(-s_{45})^{J_2-m}(-s_{13})^m\,. \tag{3.31}$$

Generically, this expression has a nonzero double discontinuity in the partially-overlapping channel invariants, namely s_{25} and s_{45}. However, this is forbidden by Steinmann relations [93]. Therefore, it must be that either $J_1 - m$ or $J_2 - m$ is a non-negative integer after the capture of poles. It then follows that, in this limit, helicity singularities are fully determined by angular momentum ones as

$$m = \alpha - N\,, \tag{3.32}$$

where α is the location of a dynamical singularity in J_1 or J_2 and N is a non-negative integer. In the above argument, we naturally assume that the asymptotic behaviour is attained within a physical region for the amplitude. It is conceivable, however, that such asymptotics

[7] In particular, as commented before, there are kinematical singularities in the map that we shall ignore when we discuss dynamical singularities in $a^{\delta_{13}}(m)$.

do not correspond to a physical behaviour and thus the argument would require an extension of validity of Steinmann relations for those configurations. The second reason concerns the special nature of the helicity quantum number. The physical interpretation of dynamical singularities are associated with the existence of particles. As helicity is not a good Lorentz invariant and does not classify particles, as mass and spin do, we do not expect dynamical singularities in m [86, 88]. Besides, these assumptions seem to work well with specific models [86, 94] as we will see below.

We now focus on our particular case of interest, the contribution of two Regge poles $\alpha_1(t)$ and $\alpha_2(t)$ in the double Regge limit with

$$a^{\delta_{25}\delta_{45}\delta_{13}}(J_1, J_2, m, t_{12}, t_{34}) \approx \frac{\beta(m, t_{12}, t_{34})}{\big(J_1 - \alpha_1(t_{12})\big)\big(J_2 - \alpha_2(t_{34})\big)}\,. \tag{3.33}$$

In the Regge limit we move the C_1 and C_2 contours to the left in (3.30) and capture the poles in complex angular momentum. The leading contributions come from the rightmost poles. We find

$$\begin{aligned} A^{\delta_{25}\delta_{45}\delta_{13}}(s_{25}, s_{45}, \eta, t_{12}, t_{34}) &\sim \frac{1}{2\pi i}\int_C dm(2\alpha_1+1)(2\alpha_2+1)\Gamma(-m)\Gamma(-\alpha_1+m)\Gamma(-\alpha_2+m) \\ &\qquad \times (-s_{25})^{\alpha_1-m}(-s_{45})^{\alpha_2-m}(-s_{13})^{m}\beta(m, t_{12}, t_{34}) \\ &\sim (-s_{25})^{\alpha_1}(-s_{45})^{\alpha_2}\left((-\eta)^{\alpha_1}\sum_i \Gamma(-\alpha_1+i)\Gamma(\alpha_1-\alpha_2-i)\beta(\alpha_1-i, t_{12}, t_{34})\frac{\eta^{-i}}{i!}\right. \\ &\qquad \left. +(-\eta)^{\alpha_2}\sum_i \Gamma(-\alpha_2+i)\Gamma(\alpha_2-\alpha_1-i)\beta(\alpha_2-i, t_{12}, t_{34})\frac{\eta^{-i}}{i!}\right). \end{aligned} \tag{3.34}$$

From the first to second line we closed the C contour to the left, capturing all the α_i-dependent poles, and absorbed overall constants into β. In particular, if we consider the limit $\eta = s_{13}/(s_{25}s_{45}) \to \infty$, we can just keep the leading contribution

$$\begin{aligned} A^{\delta_{25}\delta_{45}\delta_{13}}(s_{25}, s_{45}, \eta, t_{12}, t_{34}) &\sim (-s_{13})^{\alpha_1}(-s_{45})^{\alpha_2-\alpha_1}\Gamma(-\alpha_1)\Gamma(\alpha_1-\alpha_2)\beta(\alpha_1, t_{12}, t_{34}) \\ &\quad + (-s_{13})^{\alpha_2}(-s_{25})^{\alpha_1-\alpha_2}\Gamma(-\alpha_2)\Gamma(\alpha_2-\alpha_1)\beta(\alpha_2, t_{12}, t_{34})\,, \end{aligned} \tag{3.35}$$

which clearly does not have double discontinuities in s_{25} and s_{45}, as follows from our construction. Note that the apparent singularities in $\alpha_1 = \alpha_2$ are just spurious, as they cancel each other.

There are many subtleties and unproven statements in deriving the Regge theory result (3.34), but the final form seems very reasonable in physical terms. We can analyze these claims in specific models. We consider a dual resonance model of a five-particle amplitude in the

so-called Bardakci-Ruegg representation [95]

$$B_5 = \int \frac{dx_1}{x_1}\frac{dx_2}{x_2}\, x_1^{-\alpha(t_{12})}\,(1-x_1)^{-1-\alpha(s_{25})}\, x_2^{-\alpha(t_{34})}\,(1-x_2)^{-1-\alpha(s_{45})} \times (1-x_1x_2)^{-\alpha(s_{13})+\alpha(s_{25})+\alpha(s_{45})}\,, \tag{3.36}$$

where the integral ranges from 0 to 1 in x_1 and x_2. We defined $\alpha(x) = \alpha_0 + x$ with α_0 the intercept of the Regge trajectory. As stated above, a single Regge limit happens when s_{25} (or s_{45}), $s_{13} \to \infty$ with their ratio fixed. In this limit, it can be shown [86] that the region $x_1 \approx 0$ dominates in the integral (3.36). For the values $0 < s_{25}/s_{13} < 1$, it can be shown that

$$B_5 = (-s_{13})^{\alpha(t_{12})} \sum_{n=0}^{\infty} p_n \left(-\frac{s_{25}}{s_{13}}\right)^n + (-s_{13})^{\alpha(t_{34})}\,(-s_{25})^{\alpha(t_{12})-\alpha(t_{34})} \sum_{n=0}^{\infty} q_n \left(-\frac{s_{25}}{s_{13}}\right)^n, \tag{3.37}$$

where

$$p_n(t_{12}, t_{34}, s_{45}) = \frac{\Gamma\big(n-\alpha(t_{12})\big)\,\Gamma(-n+t_{12}-t_{34})\,\Gamma\big(n-\alpha(s_{45})\big)}{\Gamma\big(t_{12}-t_{34}-\alpha(s_{45})\big)\,n!}\,, \tag{3.38}$$

$$q_n(t_{12}, t_{34}, s_{45}) = \frac{\Gamma\big(n-\alpha(t_{34})\big)\,\Gamma(-n+t_{34}-t_{12})\,\Gamma\big(n+t_{12}-t_{34}-\alpha(s_{45})\big)}{\Gamma\big(t_{12}-t_{34}-\alpha(s_{45})\big)\,n!}\,. \tag{3.39}$$

Note that there are no simultaneous singularities in the overlapping Mandelstam invariants. This follows from the explicit expressions of p_n and q_n. The first term has power-law behaviour in s_{13} and poles in s_{45}, while having no singularities in s_{25}. The second term, on the other hand, has power-law behaviour in both s_{25} and s_{13} times a function without any singularities in s_{45}. This is an instance of the Steinmann relations, which hold for the full amplitude. The double Regge limit corresponds to taking a further limit $s_{45} \to \infty$ with the ratio $\eta = s_{13}/\,(s_{25}s_{45})$ fixed. It leads to [86]

$$B_5 = (-s_{25})^{\alpha(t_{12})}\,(-s_{45})^{\alpha(t_{34})} \int_{-i\infty}^{i\infty} \frac{dm}{2\pi i}\,\Gamma\big(m-\alpha(t_{12})\big)\Gamma\big(m-\alpha(t_{34})\big)\Gamma(-m)\,(-\eta)^m\,, \tag{3.40}$$

which is of the same form as (3.34).

With the knowledge of the multi-Regge limit in S matrix theory, we are now in a position to study the multi-Regge limit in conformal field theories.

3.2 Kinematics of five-point conformal correlators

Correlation functions of local primary operators in any conformal field theory can be written in terms of a simple prefactor, that absorbs the weight of external operators, and a non-trivial function that depends on conformal invariant variables, usually called cross ratios, that contains all the dynamics of the correlator. In this chapter, we will be mostly focused in

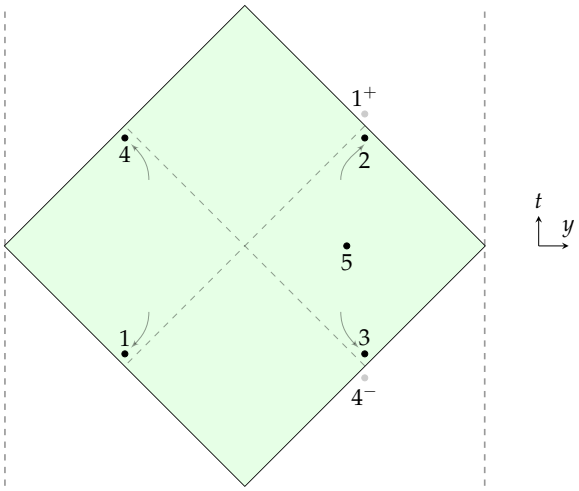

FIGURE 3.8: We show our proposal for the Regge limit of the five-point correlator.

correlators involving five operators. These depend on five different cross ratios through[8]

$$\langle \mathcal{O}(x_1)\mathcal{O}(x_2)\mathcal{O}(x_3)\mathcal{O}(x_4)\mathcal{O}(x_5)\rangle = \frac{\left(\frac{x_{23}^2}{x_{13}^2}\right)^{\frac{\Delta_{12}}{2}}\left(\frac{x_{14}^2}{x_{13}^2}\right)^{\frac{\Delta_{34}}{2}}}{(x_{12}^2)^{\frac{\Delta_1+\Delta_2}{2}}(x_{34}^2)^{\frac{\Delta_3+\Delta_4}{2}}}\left(\frac{x_{13}^2}{x_{15}^2x_{35}^2}\right)^{\frac{\Delta_5}{2}}\mathcal{G}(u_1\dots u_5)\,, \quad (3.41)$$

where $x_{ij}^2 = (x_i - x_j)^2$, we used the shorthand notation $\Delta_{ij} \equiv \Delta_i - \Delta_j$ and the cross ratios are defined as

$$u_1 = \frac{x_{12}^2 x_{35}^2}{x_{13}^2 x_{25}^2}\,, \qquad u_{i+1} = u_i|_{x_i \to x_{i+1}}\,. \quad (3.42)$$

It is worth emphasizing that this is just a particular choice of cross ratios which is obviously not unique. For instance, $\tilde{u}_3 \equiv u_3 u_2$ would be as valid a choice as u_3. The choice (3.42) has the nice feature that the cross ratios can be defined by transforming the x_i cyclically, *i.e.* $x_i \to x_{i+1}$. This is particularly interesting when studying observables that are cyclically symmetric [77, 78, 96].

In general, $\mathcal{G}(u_i)$ is an intricate function of the cross ratios with a complex analytic structure. One interesting question is, *what are the allowed singularities of a correlation function of five local operators and what is their physical meaning?* This is a hard question that we will not try to answer here in full generality (see [97] for progress in this direction). Instead, we shall focus on a particular singularity that is associated with the limit described in figure 3.8 and that is similar to the Regge limit of scattering amplitudes reviewed in the previous section. There are two other more common (and simpler) singularities, the Euclidean and lightcone OPE limits which will be relevant for the Regge limit analysis. Indeed, it is possible to extract

[8]This is the same number as independent Mandelstam invariants in flat space scattering amplitudes as reviewed in the previous section. The connection between correlation functions in conformal field theories and scattering amplitudes is more clear in Mellin space, as we shall see in the next section.

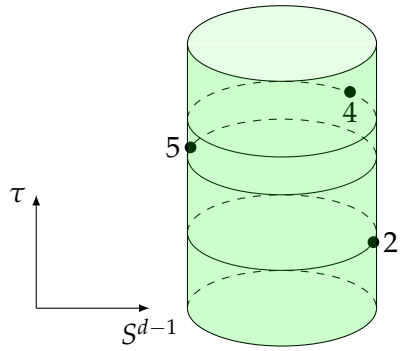

FIGURE 3.9: Position of points on the Euclidean cylinder. Two points 1 and 3, are at $\tau = -\infty$ and $\tau = \infty$.

some information about these singularities from the conformal block decomposition of five points

$$\mathcal{G}(u_i) = \sum_{k_1 k_2, \ell} P^{\ell}_{k_1 k_2} G^{\ell}_{k_1 k_2}(u_1, \dots u_5)\,, \tag{3.43}$$

where $G^{\ell}_{k_1 k_2}(u_1, \dots u_5)$ are conformal blocks in the channel (12) and (34), $P^{\ell}_{k_1 k_2}$ are products of three-point coefficients (to be described in more detail in the following subsection) and the sum is over all primary operators.

In the following subsections, we will review and explore the Euclidean and lightcone singularities and introduce the Regge limit for five-point correlation functions.

3.2.1 Euclidean limit

The simplest limit in a CFT is when two operators are brought close to each other. In this setup, the operator product expansion (OPE) is convergent and can be used safely. The OPE is perhaps one of the most important properties of a CFT. This feature tells that the product of two operators at distinct points can be replaced by a linear combination of operators

$$\mathcal{O}(x_1)\mathcal{O}(x_2) \approx \sum_k \frac{C_{12k}}{(x_{12}^2)^{\frac{\Delta_1+\Delta_2-(\Delta_k-J_k)}{2}}} F_k\big(x_{12}, D_z, \partial_{x_1}\big)\mathcal{O}_k(x_1, z)\,, \tag{3.44}$$

where the sum runs over all primary operators, C_{12k} are the OPE coefficients and F_k is a differential operator that takes into account the contribution of descendants. The auxiliary null variable z is used to encode the open indices of a symmetric and traceless spin J operator as

$$\mathcal{O}(x, z) \equiv z^{\mu_1} \dots z^{\mu_J} \mathcal{O}^{\mu_1 \cdots \mu_J}(x)\,, \tag{3.45}$$

while

$$D_{z^\mu} = \left(\frac{d}{2} - 1 + z\cdot\frac{\partial}{\partial z}\right)\frac{\partial}{\partial z^\mu} - \frac{1}{2}z^\mu\frac{\partial^2}{\partial z\cdot\partial z} \tag{3.46}$$

is used to recover the information about the indices. The exact form of F_k can be determined from consistency of two- and three-point correlation functions of local operators. It follows from a simple computation that, at the leading order and in the limit $x_2 \to x_1$, the function F_k is given by

$$F_k(x_{12}, D_z, \partial_{x_1}) = \frac{(x_{12}\cdot D_z)^{J_k}}{J_k!\left(\frac{d}{2}-1\right)_{J_k}} + \dots\,, \tag{3.47}$$

where $\dots$ represent subleading terms. One feature of this simple result is that it is evident that the limit is dominated by operators with lowest dimension Δ_k. In particular, this determines the dominant contribution of a five-point conformal block in the limits $x_2 \to x_1$ and $x_4 \to x_3$

$$\sum_\ell P^\ell_{k_1k_2} G^\ell_{k_1k_2}(u_1,\dots u_5) \approx \frac{C_{12k_1}C_{34k_2}(x_{12}\cdot D_z)^{J_1}(x_{34}\cdot D_{z'})^{J_2}}{(x_{12}^2)^{\frac{J_1-\Delta_{k_1}}{2}}(x_{34}^2)^{\frac{J_2-\Delta_{k_2}}{2}}}\langle\mathcal{O}_{k_1}(x_1,z)\mathcal{O}_{k_2}(x_3,z')\mathcal{O}(x_5)\rangle\,. \tag{3.48}$$

Note that the double limit in the pair of points (12) and (34) was taken to reduce the correlator to a three-point function which is fixed by symmetry as

$$\langle\mathcal{O}_{k_1}(x_1,z_1)\mathcal{O}_{k_2}(x_2,z_2)\mathcal{O}(x_3)\rangle = \sum_{\ell=0}^{\min(J_1,J_2)} \frac{C^\ell_{123}V_{123}^{J_1-\ell}V_{213}^{J_2-\ell}H^\ell_{12}}{(x_{12}^2)^{\frac{h_1+h_2-h_3}{2}}(x_{13}^2)^{\frac{h_1+h_3-h_2}{2}}(x_{23}^2)^{\frac{h_2+h_3-h_1}{2}}}\,, \tag{3.49}$$

where $h_i \equiv \Delta_i + J_i$ and

$$H_{12} = (z_1\cdot x_{12})(z_2\cdot x_{12}) - \frac{x_{12}^2(z_1\cdot z_2)}{2}\,, \quad V_{123} = \frac{(z_1\cdot x_{12})x_{13}^2 - (z_1\cdot x_{13})x_{12}^2}{x_{23}^2}\,. \tag{3.50}$$

It follows from (3.48) that the constants $P^\ell_{k_1k_2}$ are given by

$$P^\ell_{k_1k_2} = C_{12k_1}C_{34k_2}C^\ell_{k_1k_25}\,. \tag{3.51}$$

Conformal blocks are complicated functions which are not known in closed form for general dimensions. However, it is possible to compute them as an expansion around some limits. One method to obtain them takes advantage of the fact that they are eigenfunctions of the conformal Casimir differential equation

$$\left(\mathcal{D}_{12} - c_{\Delta_{k_1},J_1}\right)G^\ell_{k_1k_2} = 0\,, \tag{3.52}$$

with

$$c_{\Delta,J} = \Delta(\Delta - d) + J(d + J - 2)\,, \qquad \mathcal{D}_{12} = 2u_1^2\partial_{u_1}^2 + \dots\,, \tag{3.53}$$

where $\dots$ represent other subleading terms. We omitted an analogous equation in the (34) channel that can be obtained using symmetry.

The cross ratios (3.42) are not appropriate for all situations. For instance, in the limit considered above where $x_2 \to x_1$ and $x_4 \to x_3$, one has

$$u_1, u_3 \to 0\,, \qquad u_i \to 1 \quad (i = 2, 4, 5)\,, \tag{3.54}$$

which is insensitive to the angle at which the operators approach each other. For this limit, it is preferable to use instead another set of cross ratios[9][71]

$$\xi_1 = \frac{1 - u_5}{2\sqrt{u_1}}\,, \qquad \xi_2 = \frac{1 - u_4}{2\sqrt{u_3}}\,, \qquad \xi_3 = \frac{u_2 - 1}{2\sqrt{u_1}\sqrt{u_3}}\,, \tag{3.55}$$

which remain finite. These are related to the angles just mentioned above. The leading behavior, in the Euclidean OPE limit, of the five-point conformal block can be written in terms of these new cross ratios as

$$G^{\ell}_{k_1 k_2} = u_1^{\frac{\Delta_{k_1}}{2}} u_3^{\frac{\Delta_{k_2}}{2}} \mathcal{H}_\ell(\xi_i)\,, \tag{3.56}$$

with

$$\mathcal{H}_\ell(\xi_i) = \prod_{i=1}^{2} \frac{1}{J_i!\left(\frac{d}{2} - 1\right)_{J_i}} \frac{(x_{12}\cdot D_z)^{J_1}(x_{34}\cdot D_{z'})^{J_2}}{(x_{12}^2)^{\frac{J_{k_1}}{2}}(x_{34}^2)^{\frac{J_{k_2}}{2}}} \frac{V_{135}^{J_1-\ell} V_{315}^{J_2-\ell} H_{13}^{\ell}}{(x_{13}^2)^{\frac{J_1+J_3}{2}}(x_{15}^2)^{\frac{J_1-J_2}{2}}(x_{35}^2)^{\frac{J_2-J_1}{2}}}\,. \tag{3.57}$$

A brute force implementation of the action of the operators D_z and $D_{z'}$ on the previous expression for the function $\mathcal{H}_\ell$ will lead to a rather complicated sum [71] that we do not show since it will not be important in the discussion. A simple analysis reveals that the leading term of $\mathcal{H}_\ell$ in the limit $\xi_{1,2} \to \lambda\xi_{1,2}$, $\xi_3 \to \xi_3\lambda^2$ for large λ, which corresponds to considering lightcone limits[10] $x_{12}^2, x_{34}^2 \to 0$, is of the form

$$\mathcal{H}_\ell \approx \xi_1^{J_1-\ell}\xi_2^{J_2-\ell}\xi_3^{\ell} + \dots\,, \tag{3.58}$$

[9] We have decided to use slightly different angles as compared with [71] to make it appear more symmetric in the variables u_i.

[10] In this limit we can discard the second term in the differential operator D_z which in turn makes its action easier to implement. This just corresponds to throwing away the contribution of terms associated with traces.

where the ... represent subleading terms. Alternatively we can use the Casimir differential equation, in the Euclidean limit, to obtain subleading terms in (3.58)

$$\begin{aligned}&\left[(1-\xi_1^2)\partial_{\xi_1}^2+(1-\xi_3^2)\partial_{\xi_3}^2-(d-1)(\xi_1\partial_{\xi_1}+\xi_3\partial_{\xi_3})-2(\xi_1\xi_3+\xi_2)\partial_{\xi_1}\partial_{\xi_3}+C_{J_1}\right]\mathcal{H}_\ell=0\,,\\&\left[(1-\xi_2^2)\partial_{\xi_2}^2+(1-\xi_3^2)\partial_{\xi_3}^2-(d-1)(\xi_2\partial_{\xi_2}+\xi_3\partial_{\xi_3})-2(\xi_2\xi_3+\xi_1)\partial_{\xi_2}\partial_{\xi_3}+C_{J_2}\right]\mathcal{H}_\ell=0\,,\end{aligned}\tag{3.59}$$

with $C_J = J(J+2h-2)$. It is essential in extracting the dots in (3.58) from the Casimir equation to assume that $\mathcal{H}_\ell$ is polynomial in the variables ξ_i. However, this follows from the definition (3.57).

It turns out that, after changing the cross ratio ξ_3 to ζ defined by[11]

$$\xi_3 = -\xi_1\xi_2+\zeta\sqrt{(1-\xi_1^2)(1-\xi_2^2)}\,,\tag{3.60}$$

the Casimir differential equation becomes much simpler

$$\left[J_1\,(d+J_1-2)+\frac{(d-2)\zeta\partial_\zeta+(\zeta^2-1)\partial_\zeta^2}{\xi_1^2-1}+(1-d)\xi_1\partial_{\xi_1}+(1-\xi_1^2)\partial_{\xi_1}^2\right]\mathcal{H}\,,=0\tag{3.61}$$

with an analogous equation for J_2. This form of the differential equation allows to look for solutions with a factorized form

$$\tilde{\mathcal{H}} = f_1(\xi_1)f_2(\xi_2)g(\zeta)\,,\tag{3.62}$$

where we have used tilde to emphasize that the solution is factorized and possibly different from (3.57). The function $g(\zeta)$ satisfies a differential equation that can be read from (3.61)

$$\left[(\zeta^2-1)\partial_\zeta^2+(d-2)\zeta\partial_\zeta+\ell'(\ell'+d-3)\right]g_{\ell'}=0\,,\tag{3.63}$$

where the separation constant $\ell'(\ell'+d-3)$ was chosen for convenience. One solution to this differential equation that is polynomial in ζ is given by

$$g_{\ell'} = {}_2F_1\left(-\ell',\ell'+d-3,\frac{d-2}{2},\frac{1-\zeta}{2}\right) = \frac{\ell'!\Gamma(2h-3)}{\Gamma(2h+\ell'-3)}\,C_{\ell'}^{\frac{d-3}{2}}(\zeta)\,.\tag{3.64}$$

This is clearly a polynomial of degree ℓ'. It is also simple to check that

$$f_1(\xi_1) = (1-\xi_1^2)^{\frac{\ell'}{2}}C_{J_1-\ell'}^{\frac{d-2}{2}+\ell'}(\xi_1)\,,\tag{3.65}$$

is a solution to the differential equation arising from (3.61). The solution f_2 can be obtained

[11] These cross ratios were introduced in the context of conformal field theories in [73].

analogously. It can also be checked that this new solution $\tilde{\mathcal{H}}_{\ell'}$ is consistent with the non-factorized $\mathcal{H}_\ell$ in (3.57). Let us see how in more detail.

Both $\mathcal{H}_\ell$ and $\tilde{\mathcal{H}}_{\ell'}$ satisfy the same differential equation, however they are not the same function. Nevertheless it is possible to express $\mathcal{H}_\ell$ in terms of $\tilde{\mathcal{H}}$ and vice-versa, that is

$$\tilde{\mathcal{H}}_{\ell'} = \sum_{\ell=0}^{\ell'} C_{\ell\ell'} \mathcal{H}_\ell \,, \tag{3.66}$$

The coefficients $C_{\ell\ell'}$ can be thought as a change of basis of three-point functions. To determine them it is useful to take the limit $\xi_{1,2} \to \lambda\xi_{1,2}$ and $\xi_3 = \xi_3\lambda^2$, with λ large. In this limit the functions $\mathcal{H}_\ell$ and $\tilde{\mathcal{H}}_\ell$ behave as

$$\mathcal{H}_\ell \approx \xi_1^{J_1-\ell}\xi_2^{J_2-\ell}\xi_3^\ell + \dots \,, \qquad \tilde{\mathcal{H}}_{\ell'} \approx \xi_1^{J_1}\xi_2^{J_2} g_{\ell'}(\zeta) + \dots \,, \tag{3.67}$$

where $\zeta \to (\xi_1\xi_2 + \xi_3)/(\xi_1\xi_2)$ and the $\dots$ represent subleading terms. Using the previous equation and (3.66) we can find the coefficients. Let us start by $C_{\ell\ell'}$,

$$\xi_1^{J_1}\xi_2^{J_2} \sum_{\ell=0}^{\ell'} C_{\ell\ell'} \left(\frac{\xi_3}{\xi_1\xi_2}\right)^\ell = \xi_1^{J_1}\xi_2^{J_2} g_{\ell'}(\zeta) = \xi_1^{J_1}\xi_2^{J_2} \sum_{k=0}^{\ell'} \frac{(-\ell')_k\,(\ell'+d-3)_k}{k!\left(\frac{d-2}{2}\right)_k} \left(\frac{1-\zeta}{2}\right)^k \,, \tag{3.68}$$

where $\xi_3/(\xi_1\xi_2) = \zeta - 1$. The coefficients $C_{\ell\ell'}$ can be obtained straightaway leading to

$$C_{\ell\ell'} = \frac{(-\ell')_\ell\,(\ell'+d-3)_\ell}{\ell!\left(\frac{d-2}{2}\right)_\ell 2^\ell} \,. \tag{3.69}$$

To find the inverse relation we make use of the identity

$$\sum_{\ell'=0}^{\ell} \frac{(c)_\ell \binom{\ell}{\ell'} (b+2\ell')(-1)^{\ell'}}{(b+1+\ell')_\ell (b+\ell')} \,{}_2F_1\left(-\ell', b+\ell', c, \frac{x}{2}\right) = \left(\frac{x}{2}\right)^\ell \,, \tag{3.70}$$

for any variable x and constants b and c. Using this equation the inverse matrix $\tilde{C}_{\ell'\ell}$ follows immediately

$$\tilde{C}_{\ell'\ell} = \frac{(-1)^{\ell'}(d+2\ell'-3)\binom{\ell}{\ell'}\left(\frac{d-2}{2}\right)_\ell}{(d+\ell'-3)(d+\ell'-2)_\ell} \,. \tag{3.71}$$

This concludes the change of basis from (3.49) to the one that leads to (3.62), which we call factorized basis. In this basis, the three-point function can be written as [12]

$$\langle \mathcal{O}_{k_1}(x_1,z_1)\dots\mathcal{O}(x_3)\rangle = \frac{V_{123}^{J_1}V_{213}^{J_2}\sum_{\ell=0}^{\min(J_1,J_2)}\tilde{C}_\ell\ {}_2F_1\left(-\ell,\ell+d-3,\frac{d-2}{2},\frac{H_{12}}{2V_{123}V_{213}}\right)}{(x_{12}^2)^{\frac{h_1+h_2-h_3}{2}}(x_{13}^2)^{\frac{h_1+h_3-h_2}{2}}(x_{23}^2)^{\frac{h_2+h_3-h_1}{2}}}\,, \tag{3.72}$$

where $\tilde{C}_\ell$ are the OPE coefficients in the new basis. Let us remark that this is still polynomial in the structures V and H, as it should. The factorized basis for the leading behaviour of the block in the Euclidean OPE limit is a new result.

3.2.2 Lightcone limit

The distance between two operators, in Lorentzian kinematics, can be small when one of them approaches the lightcone of the other. This is in contrast with what has been analyzed in the previous subsection where the operators were actually close in the Euclidean sense. The OPE and more generally correlation functions are naturally organized, in this limit, in terms of distances between the almost null related operators. For example, the leading term in F_k of (3.44), in the limit $x_{12}^2\to 0$, is given by

$$F_k = (x_{12}\cdot\partial_{z_1})^{J_k}\int_0^1[dt]\,e^{tx_{12}\cdot\partial_{x_1}}\,, \tag{3.73}$$

where

$$[dt]\equiv\frac{\Gamma(\Delta_k+J_k)}{\Gamma^2(\frac{\Delta_k+J_k}{2})}\left(t(1-t)\right)^{\frac{\Delta_k+J_k}{2}-1}dt \tag{3.74}$$

for spin J_k operators. For exchanged scalar operators, it is also easy to write down the formula for F_k, including all subleading corrections,

$$F_k=\sum_{n=0}^{\infty}\frac{(-x_{12}^2)^n\left(\frac{\Delta-a}{2}\right)_n\left(\frac{\Delta+a}{2}\right)_n}{2^{2n}(\Delta)_{2n}\left(\frac{2\Delta-d}{2}\right)_n n!}\,{}_1F_1\left(\frac{2n+\Delta+a}{2},2n+\Delta,x_{21}\cdot\partial_{x_1}\right)(\partial_{x_1}^2)^n\,, \tag{3.75}$$

with $a=\Delta_{12}$ and ${}_1F_1(a,b,x)=\int_0^1 dt\,\frac{t^{a-1}(1-t)^{b-a-1}\Gamma(b)}{\Gamma(a)\Gamma(b-a)}\,e^{tx}$. In turn, these two formulae can be used to derive the five-point conformal blocks in the lightcone limit by just applying the OPE formula to a five-point correlator. For the leading term of spinning lightcone conformal

[12] Note that, for integer ℓ, the hypergeometric reduces to a polynomial,

$${}_2F_1\left(-\ell,\ell+d-3,\frac{d-2}{2},\frac{H_{12}}{2V_{123}V_{213}}\right)=\sum_{\ell'=0}^{\ell}\frac{(-\ell)_{\ell'}(\ell+d-3)_{\ell'}}{\ell'!\left(\frac{d-2}{2}\right)_{\ell'}2^{\ell'}}\left(\frac{H_{12}}{2V_{123}V_{213}}\right)^{\ell'}=\sum_{\ell'=0}^{\ell}C_{\ell'\ell}\left(\frac{H_{12}}{2V_{123}V_{213}}\right)^{\ell'}.$$

blocks we have

$$G^{\ell}_{k_1k_2,J_1,J_2} = u_1^{\frac{\Delta_{J_1}-J_1}{2}} u_3^{\frac{\Delta_{J_2}-J_2}{2}} (1-u_2)^{\ell} u_5^{\frac{\Delta_\phi}{2}} \int_0^1 [dt_1][dt_2]\, \mathcal{I} \tag{3.76}$$

with

$$\mathcal{I} = \frac{\left(1-t_1(1-u_2)u_4-u_2u_4\right)^{J_2-\ell}\left(1-t_2(1-u_2)u_5-u_2u_5\right)^{J_1-\ell}}{\left(1-(1-u_4)t_2\right)^{\frac{h_2-\tau_1-2\ell+\Delta_\phi}{2}}\left(1-(1-u_5)t_1\right)^{\frac{h_1-\tau_2-2\ell+\Delta_\phi}{2}}\left(1-(1-t_1)(1-t_2)(1-u_2)\right)^{\frac{h_1+h_2-\Delta_\phi}{2}}}\,. \tag{3.77}$$

For the scalar blocks in the lightcone we can write

$$G^{0}_{k_1k_200} = \sum_{n_1,n_2=0}^{\infty} u_1^{\frac{\Delta_{k_1}+2n_1}{2}} u_3^{\frac{\Delta_{k_2}+2n_2}{2}} u_2^{\frac{\Delta_{21}}{2}} u_4^{\frac{2n_1+\Delta_{34}-\Delta_5+\Delta_{k_1}}{2}} u_5^{\frac{2n_2+\Delta_{21}+\Delta_{k_2}}{2}} \int_0^1 dt_1 dt_2\, \tilde{\mathcal{I}}_{n_1,n_2}\,, \tag{3.78}$$

where the formula for $\tilde{\mathcal{I}}_{n_1,n_2}$ is shown in appendix B.1. The cross ratios u_i are appropriate to describe the lightcone limit $x_{12}^2, x_{34}^2 \to 0$, as only two of them go to zero while the others remain fixed.

One feature that is evident from the formulae above is that this limit is dominated by operators that have lowest twist, defined by $\Delta - J$. Hints of this property are already present in (3.44) and (3.47).

Another interesting attribute of the lightcone block is that it allows to probe Lorentzian regimes, this in sharp contrast with the Euclidean expansion (3.62) that is only valid when the point x_2 is in the vicinity of x_1. In particular, the integral formulation of both (3.73) and (3.75) is specially suitable to study monodromies of the block.

3.2.3 Regge limit

The limits described in the previous section shared a common feature as they could be taken in a kinematics where all points are still spacelike separated from each other. This is a significant restriction on the positions of operators and the physics that one is probing with a given correlation function. The goal of this subsection is to introduce and describe another limit, the Regge limit, as depicted in figure 3.8. The main novelty is that some points are timelike related, while others are still spacelike separated, more concretely the pairs of points $(1,4),(2,3),(3,5),(2,5)$ are timelike, while the other pairs remain spacelike. The configuration represented in figure 3.8 can be parametrized by the following variables

$$\begin{aligned} &x_1 = -r\,(\sinh\delta_1, \cosh\delta_1, \mathbf{0}_{d-2})\,, \quad x_2 = r\,(\sinh\delta_2, \cosh\delta_2, \mathbf{0}_{d-2})\,, \\ &x_3 = (-\sinh\delta_2, \cosh\delta_2, \mathbf{0}_{d-2})\,, \quad x_4 = (\sinh\delta_1, -\cosh\delta_1, \mathbf{0}_{d-2})\,, \qquad x_5 = (0, h_1, h_2, \mathbf{0}_{d-3})\,. \end{aligned} \tag{3.79}$$

where δ_i are being taken to infinity and r and h_i can assume generic values. Here we also use a d-dimensional vector of zeros denoted by $\mathbf{0}_d$. This configuration can also be written in terms of the cross ratios u_i as

$$\begin{aligned}
u_1 &= \frac{4r^2\left(x_5^2+1-2h_1\cosh\delta_2\right)}{\left(1+r^2+2r\cosh\delta\right)\left(x_5^2+r^2-2h_1r\cosh\delta_1\right)}, \qquad u_2 = \left(\frac{1+r^2-2r\cosh\delta}{1+r^2+2r\cosh\delta}\right)^2, \\
u_3 &= \frac{4\left(x_5^2+r^2-2h_1r\cosh\delta_1\right)}{\left(1+r^2+2r\cosh\delta\right)\left(x_5^2+1-2h_1\cosh\delta_2\right)}, \\
u_4 &= \frac{1}{\sqrt{u_2}}\frac{x_5^2+1+2h_1\cosh\delta_2}{x_5^2+1-2h_1\cosh\delta_2}, \qquad u_5 = \frac{1}{\sqrt{u_2}}\frac{x_5^2+r^2+2h_1r\cosh\delta_1}{x_5^2+r^2-2h_1r\cosh\delta_1},
\end{aligned} \tag{3.80}$$

where $\delta = \delta_1 + \delta_2$ and $x_5^2 = h_1^2 + h_2^2$. It is simple to see that both u_1 and u_3 approach zero as the δ_i are sent to infinity and that the remaining u_i go to 1 (note that u_2 approaches 1 faster then the other two cross ratios). This limit, in terms of cross ratios, is the same as the Euclidean OPE limit discussed in section 3.2.1. The main distinction between these two limits resides in the different causal ordering of the operators. The similarity to the Euclidean OPE limit should come as no surprise to the reader that is familiar with Regge limit for four points. In reality there is a simple reason for this to be the case as one can also interpret this configuration as an OPE limit between 1^+ and 2, as well as 3 and 4^-, where 1^+ and 4^- are defined respectively as the image of the points 1 and 4 on the next and previous Poincaré patch on the Lorentzian cylinder. This is shown in figure 3.8.

The fifth point is kind of a spectator in this limit. Nonetheless, it is important as it allows to introduce other parameters to differentiate the gaps δ_1 and δ_2. This is essentially the same as we already see in the Regge limit of five-point scattering amplitudes.

Note that in this section we made a choice of analytic continuation but there are other possible ways to attain Regge kinematics. Indeed, with some care, one can even move the fifth point in other directions and even boost it and find similar OPE behaviour after lightcones are crossed. The latter can be used as a guiding principle when we look for Regge kinematics. In Appendix B.4, we present some additional kinematics and path continuations that might be useful in understanding single-Reggeon exchanges or the Regge limit six-point functions in CFTs .

As mentioned before, the different causal relations between the points have important consequences. The analysis of the correlator in this setting is more elaborate and for this reason we devote the next section to it.

3.2.4 Conformal partial waves

The conformal block decomposition (3.43) is not the most appropriate option to analyze the Regge limit of corrrelation functions. A better alternative is to do the so-called conformal partial wave decomposition

$$\mathcal{G}(u_i) = \sum_{J_i=0}^{\infty} \sum_{\ell=0}^{\min(J_1,J_2)} \int_{-\infty}^{\infty} \frac{d\nu_1}{2\pi i} \frac{d\nu_2}{2\pi i}\, b^{\ell}_{J_1 J_2}(\nu_1,\nu_2)\, F_{\nu_1,\nu_2,J_1,J_2,\ell}(u_i)\,, \tag{3.81}$$

where the conformal partial wave coefficient $b^{\ell}_{J_1 J_2}(\nu_1,\nu_2)$ contains all the dynamical information of the correlation function, *i.e.* dimensions and OPE coefficients. The function $F_{\nu_1,\nu_2,J_1,J_2,\ell}(u_i)$ is the conformal partial wave defined by the integral

$$\begin{aligned} F_{\nu_1,\nu_2,J_1,J_2,\ell}(u_i) =& \frac{(x_{12}^2 x_{34}^2)^{\Delta_\phi} (x_{15}^2 x_{35}^2)^{\frac{\Delta_\phi}{2}}}{(x_{13}^2)^{\frac{\Delta_\phi}{2}}} \int d^d x_6\, d^d x_7\, \langle \mathcal{O}_{\frac{d}{2}-i\nu_1}(x_6, D_{z_1}) \mathcal{O}_{\frac{d}{2}-i\nu_2}(x_7, D_{z_2}) \mathcal{O}(x_5) \rangle^{(\ell)} \\ & \times \langle \mathcal{O}(x_1)\mathcal{O}(x_2)\mathcal{O}_{\frac{d}{2}+i\nu_1}(x_6,z_1)\rangle \langle \mathcal{O}(x_3)\mathcal{O}(x_4)\mathcal{O}_{\frac{d}{2}+i\nu_2}(x_7,z_2)\rangle\,, \end{aligned} \tag{3.82}$$

where the $\langle\rangle^{(\ell)}$ should be understood as the term proportional to C^{ℓ}_{123} in (3.49) (in other words, it is just the space dependence of the three-point function) and D_z is the differential operator defined in (3.46). It is simple to see that both integrals in x_6 and x_7 are conformal and that $F_{\nu_i,J_i,\ell}$ should satisfy the conformal Casimir equation in the channels (12) and (34) with eigenvalue $C_{\frac{d}{2}+i\nu_1,J}$ and $C_{\frac{d}{2}+i\nu_2,J_2}$, respectively. In particular, this implies that the conformal partial wave can be written as a linear combination of conformal blocks which solve the same equation

$$F_{\nu_1,\nu_2,J_i,\ell} = \sum_{\tilde{\ell}} \sum_{\alpha_1,\alpha_2=\pm} A^{\ell\tilde{\ell}}_{\alpha_1,\alpha_2} G^{\tilde{\ell}}_{\frac{d}{2}+i\alpha_1\nu_1,\frac{d}{2}+i\alpha_2\nu_2,J_i}(u_i)\,, \tag{3.83}$$

where we used the symmetry of the eigenvalue $C_{\frac{d}{2}+i\nu_i,J_i} = C_{\frac{d}{2}-i\nu_i,J_i}$. The sum over $\tilde{\ell}$ appears because the Casimir equation is not able to fix it, and so in principle we can have a sum over this number. The coefficients $A^{\ell\tilde{\ell}}$ were determined in [77] and are expressed in terms of several sums. It would be interesting to see if the coefficients in the new basis introduced in 3.2.1 are simpler and, more importantly for this work, analytic in spin. The conformal partial waves have the advantage that are Euclidean single valued[13]. Recall that the correlator also enjoys this property in contrast with a single conformal block.

[13]Conformal partial waves are single valued for integer J. It should be possible to add a term to them to make them single valued for positive real J as was done in [50] for four points. We hope to return to this point in the future.

3.3 Regge theory

3.3.1 Wick rotation or how to go Lorentzian

The Regge limit of a correlation function is an intrinsically Lorentzian limit that explores a specific causal configuration of the operators. On the other hand, CFTs have been better understood in Euclidean space. It is thus important to understand how to analytically continue from Euclidean to Lorentzian space and what can we say about convergence and other properties of the Lorentzian correlator from CFT axioms. These questions have only very recently been discussed in firmer grounds in [98, 99], extending the works of Lüscher and Mack [100, 101]. However, there the analysis focuses only on correlation functions of $n \leq 4$ points and no systematic study for higher-point functions exists to date. [14]

We want to consider Lorentzian invariant correlation functions of local operators that commute at spacelike separated points,

$$\mathcal{W}(x_1, x_2, \ldots, x_n) = \langle \mathcal{O}(x_1)\mathcal{O}(x_2)\ldots\mathcal{O}(x_n)\rangle \,. \tag{3.84}$$

These are called Wightman functions (or distributions). In particular, note that up to spacelike separated points, different orders of local operators give rise to different Wightman functions. We stress that these are not the standard time-ordered correlation functions one encounters in QFT textbooks. In fact, one can decompose time-ordered correlation functions in terms of Wightman functions[15]

$$\begin{aligned} &\langle\Omega|T\{\mathcal{O}(x_1)\mathcal{O}(x_2)\ldots\mathcal{O}(x_n)\}|\Omega\rangle = \\ &= \langle\Omega|\mathcal{O}(t_1,\mathbf{x_1})\mathcal{O}(t_2,\mathbf{x_2})\ldots\mathcal{O}(t_n,\mathbf{x_n})|\Omega\rangle\theta(t_1>t_2>\cdots>t_n) + \text{permutations} \\ &= \mathcal{W}(x_1,x_2,\ldots,x_n)\theta(t_1>t_2>\cdots>t_n) + \text{permutations}\,. \end{aligned} \tag{3.85}$$

One Wightman axiom states that Wightman functions are indeed tempered distributions even at coincident points. This means that when integrated against test functions belonging to Schwartz class $f(x_i) \in \mathcal{S}$, the following integral is finite

$$\int d^d x_1 \ldots d^d x_1 \mathcal{W}(x_1, \ldots, x_n) f(x_1)\ldots f(x_n) < \infty \,. \tag{3.86}$$

[14] This seems to be technically challenging (see discussion of Appendix B of [99]) but we hope that our results may also increase the motivation of community to tackle these questions on higher-point functions.

[15] We assume the existence of a Hilbert space with a unique vacuum Ω under the unitary action of the Poincaré group. We can however talk about Wightman distributions without making any such assumption since Wightman's reconstrution theorem guarantees that we would find a Hilbert space once we assumed spectral and positivity properties of the distributions - see [99, 102].

Our goal is to reach a Wightman correlation function with a given order starting from a translational- and rotational-invariant Euclidean one. The basic idea is that there should be some holomorphic function $G(x_1, \dots, x_n)$ that reduces to a Lorentzian correlator in a given limit and to a Euclidean one in another. Let us then consider a real-analytic (away from coincident points) Euclidean correlator, with operators at $x_i = (\tau_i, \mathbf{x}_i)$,

$$\langle \mathcal{O}(\tau_1, \mathbf{x}_1)\mathcal{O}(\tau_2, \mathbf{x}_2) \dots \mathcal{O}(\tau_n, \mathbf{x}_n)\rangle^E , \tag{3.87}$$

where Euclidean times τ_i are ordered $\tau_1 > \tau_2 > \cdots > \tau_n$. Recall that this ordering is necessary. If we assume the existence of a Hilbert space and a Hamiltonian that is bounded from below, we get that our Euclidean correlator can be rewritten as

$$\langle \Omega | \mathcal{O}(0, \mathbf{x}_1) e^{-H(\tau_1 - \tau_2)} \mathcal{O}(0, \mathbf{x}_2) e^{-H(\tau_2 - \tau_3)} \dots \mathcal{O}(\tau_n, \mathbf{x}_n) | \Omega \rangle^E , \tag{3.88}$$

where we use the Heisenberg representation of the field operators $\mathcal{O}$. To avoid high-energy states being exponentially enhanced, we immediately recognise that the Euclidean correlator needs to be "time-ordered".

To move towards a Lorentzian configuration, we want to consider an analytic continuation of the Euclidean correlator. This is achieved by taking $\tau_i \to \epsilon_i + i t_i$. Heuristically, adding the imaginary parts does not harm the convergence, as long as we keep $\epsilon_1 > \cdots > \epsilon_n$. This analytic continuation defines our function $G(x_1, \dots, x_n)$ that is holomorphic in $\tau_i = \epsilon_i + i t_i$ and real-analytic in $\mathbf{x}_i$. We can then find a Lorentzian correlator by sending $\epsilon_i \to 0$ while keeping the order of limits,

$$\langle \Omega | \mathcal{O}(t_1, \mathbf{x}_1) \dots \mathcal{O}(t_n, \mathbf{x}_n) | \Omega \rangle \equiv \lim_{\substack{\epsilon_i \to 0 \\ \epsilon_1 > \cdots > \epsilon_n}} \langle \Omega | \mathcal{O}(\epsilon_1 + i t_1, \mathbf{x}_1) \dots \mathcal{O}(\epsilon_n + i t_n, \mathbf{x}_n) | \Omega \rangle^E . \tag{3.89}$$

This formally defines our Wightman function $\mathcal{W}(x_1, \dots, x_n)$. Note that to achieve different orderings we should start from an Euclidean correlator in a different ordering. Holomorphicity may however be lost as we take $\epsilon_i \to 0$. We expect nonetheless the correlator to converge at least in a distributional sense. For CFT Wightman functions, the authors in [99] found powerlaw bounds and used Vladimirov's theorem to assure that indeed this limit converges at least in the distributional sense (even at coincident points) for $n \leq 4$-point functions in Minkowski space.[16]

We want to consider the Regge limit of CFT five-point functions of identical scalars. In this context, we are interested in correlation functions where the operator ordering is consistent

[16] All the remaining Wightman axioms were also proved from standard axioms of translational- and rotational-invariant Euclidean correlators.

with time ordering. Using the causal relations of figure 3.8, we take

$$\langle \phi(x_4)\phi(x_1)\phi(x_2)\phi(x_5)\phi(x_3)\rangle\,, \tag{3.90}$$

where permutations between spacelike separated operators are equivalent. As we approach the Regge kinematics, starting from a configuration where all operators are spacelike separated (essentially equivalent to a Euclidean configuration), we find branch-cut singularities whenever an operator crosses the lightcone of another. The way we deal with branch-cuts depends on the $i\epsilon$ prescription we adopted to reach this ordering of the Wightman function. In particular, as we move from fully spacelike separated points to the Regge kinematics we have $\{x_{14}^2, x_{23}^2, x_{25}^2, x_{35}^2\} \to \{|x_{14}^2|, |x_{23}^2|, |x_{25}^2|, |x_{35}^2|\} \times \exp(\pi i)$ which implies that the cross-ratios u_2, u_4 and u_5 go around 0 with the first going anticlockwise and the last two in clockwise direction. At the branch-cuts, OPEs $\phi_1 \times \phi_2$ and $\phi_3 \times \phi_4$, in which we block decompose our correlation function, are no longer convergent. We should then worry about boundedness in Regge limit. For a four-point function in the Regge limit and with operator ordering consistent with time ordering one can prove its boundedness. The general proof uses Rindler positivity [6, 103–105] and bounds the latter Wightman function with another correlator of different ordering where the OPE does converge. This proof does not work however with five-point functions. Nonetheless, we expect to be possible to find these type of bounds between different ordered Wightman functions or different channel decompositions but we will not make these considerations any more precise here. Conformal Regge theory, on the other hand, provides a method to resum divergent OPEs and exhibit the dominant Reggeon-exchange contributions. This resumation invokes an analytic continuation of OPE data in spin for which, in the case of four-point functions, the justification follows from the Lorentzian inversion formula [6, 106]. For higher-point functions, there are additional representation labels associated with the possible three-point structures between spinning operators.

In what follows we focus on double Reggeon-exchanges but similar analysis can be performed at the level of the single Reggeon exchanges, that we briefly discuss in Appendix B.4. The proper $i\epsilon$ prescription for these cases follows straightforwardly from the corresponding kinematics since we want to consider the operator orderings consistent with time ordering.

3.3.2 Mellin amplitudes

The similarities of Mellin and flat space scattering amplitudes make the former a suitable tool to build intuition. The goal of this section is to analyze the Regge limit for Mellin amplitudes [4]. We shall see that the Regge limit for five operators, as defined in the previous section, is dominated by the same kinematics of flat space scattering amplitudes reviewed in section 3.1.

In the following, we will review the definition of Mellin amplitudes, some of its properties and then analyze the Regge limit in this language. The definition of a Mellin amplitude, $\mathcal{M}(\delta_{ij})$, is given by

$$\langle \mathcal{O}(x_1)\dots\mathcal{O}(x_n)\rangle = \int [d\delta_{ij}]\, \mathcal{M}(\delta_{ij}) \prod_{1\le i<j\le n} \frac{\Gamma(\delta_{ij})}{(x_{ij}^2)^{\delta_{ij}}}\,, \tag{3.91}$$

where we decided to extract a standard prefactor containing Γ functions and the integration variables δ_{ij} run parallel to the imaginary axis. Since the Mellin variables are restricted by the condition $\sum_j \delta_{ij} = 0$, with $\delta_{ii} = -\Delta_i$, we shall use the following set of independent Mellin variables

$$\begin{aligned} &t_{12} = 2\Delta_\phi - 2\delta_{12}\,, && t_{34} = 2\Delta_\phi - 2\delta_{34}\,, && \\ &s_{13} = \Delta_\phi + 2\delta_{13}\,, && s_{25} = -2\delta_{25}\,, && s_{45} = -2\delta_{45}\,, \end{aligned} \tag{3.92}$$

which is the same number as conformal cross ratios - see figure 3.10. One advantage of Mellin amplitudes is that it is easy to analytically continue from the Euclidean configuration to Lorentzian, as the space-time dependence is simple [107]. For example, the configuration of figure 3.8 can be obtained just by adding a phase to the integrand [4]

$$\begin{aligned} G^{\circlearrowleft}(u_i) = \int [dt_{ij} ds_{ij}]\, u_4^{\frac{s_{45}}{2}}\, u_1^{\frac{t_{12}}{2}}\, u_3^{\frac{t_{34}}{2}}\, u_2^{\frac{s_{13}+s_{45}-t_{12}}{2}}\, u_5^{\frac{t_{34}-s_{25}-t_{12}}{2}}\, \mathcal{M}(s_{ij},t_{ij})\, e^{-i\pi\frac{2(s_{13}+s_{25}+s_{45})+\Delta_\phi}{2}} \\ \Gamma\Big(-\frac{s_{25}}{2}\Big)\Gamma\Big(-\frac{s_{45}}{2}\Big)\Gamma\Big(\frac{s_{13}+s_{25}+s_{45}}{2}\Big)\Gamma\Big(\frac{s_{13}-\Delta_\phi}{2}\Big) \\ \Gamma\Big(\frac{t_{12}-s_{13}-s_{45}}{2}\Big)\Gamma\Big(\frac{t_{34}-s_{13}-s_{25}}{2}\Big)\Gamma\Big(\frac{2\Delta_\phi-t_{12}}{2}\Big)\Gamma\Big(\frac{2\Delta_\phi-t_{34}}{2}\Big) \\ \Gamma\Big(\frac{\Delta_\phi+s_{25}+t_{12}-t_{34}}{2}\Big)\Gamma\Big(\frac{\Delta_\phi+s_{45}-t_{12}+t_{34}}{2}\Big) \end{aligned} \tag{3.93}$$

where $G^{\circlearrowleft}$ is the correlator analytically continued to the Regge kinematics. This particular phase seems to make the integrand divergent for large imaginary values of s_{ij}. However, the Γ functions in the definition of the Mellin amplitude cancel this apparent divergence. To see this in more detail we just have to use the identity

$$\Gamma\left(a+i\frac{x_i}{2}\right)\Gamma\left(b-i\frac{x_i}{2}\right) \approx 2\pi e^{i\frac{\pi}{2}(a-b)}\left(\frac{x_i}{2}\right)^{a+b-1} e^{-\frac{\pi}{2}x_i}\,, \tag{3.94}$$

in a regime where s_{13} goes faster to infinity than s_{45} and s_{25}. In the Regge limit, as defined in section 3.2.3, we have that the cross ratios $u_2 \to 1+\sigma_1\sigma_2\xi_3$, $u_4 \to 1-\sigma_2\xi_2$, $u_5 \to 1-\sigma_1\xi_1$, with $u_1 = \sigma_1^2, u_3 = \sigma_2^2$ going to zero while ξ_i are left fixed. This simplifies the dependence of

the Mellin amplitude on the cross ratios

$$u_4^{\frac{s_{45}}{2}}\, u_1^{\frac{t_{12}}{2}}\, u_3^{\frac{t_{34}}{2}}\, u_2^{\frac{s_{13}+s_{45}-t_{12}}{2}}\, u_5^{\frac{t_{34}-s_{25}-t_{12}}{2}} \to u_1^{\frac{t_{12}}{2}}\, u_3^{\frac{t_{34}}{2}}\, e^{\frac{i(y_{25}\sigma_1\xi_1+y_{45}\sigma_2\cosh\xi_2-y_{13}\sigma_1\sigma_2\xi_3)}{2}}\,, \tag{3.95}$$

where we made the change $s_{ij} = iy_{ij}$. Note that the exponent is not small provided σ_i and y_{ij} scale appropriately. By putting every piece together we obtain that in the Regge limit

$$\begin{aligned} G^{\circlearrowleft}(u_i) = \pi^4 \int [dt_{ij}]\, \Gamma\left(\frac{2\Delta_\phi - t_{12}}{2}\right) \Gamma\left(\frac{2\Delta_\phi - t_{34}}{2}\right) \frac{\sigma_1^{t_{12}}\sigma_2^{t_{34}}}{2^{\frac{t_{12}+t_{34}+\Delta_\phi-16}{2}}} e^{\frac{i\pi(\Delta_\phi+3t_{12}-t_{34})}{4}} \\ \int [dy_{ij}]\, y_{13}^{\frac{t_{12}+t_{34}-4-\Delta_\phi}{2}}\, y_{25}^{\frac{t_{12}+\Delta_\phi-t_{34}-2}{2}}\, y_{45}^{\frac{t_{34}+\Delta_\phi-t_{12}-2}{2}}\, e^{\frac{i(y_{25}\sigma_1\xi_1+y_{45}\sigma_2\cosh\xi_2-y_{13}\sigma_1\sigma_2\xi_3)}{2}}\, \mathcal{M}(t_{ij}, y_{ij})\,, \end{aligned} \tag{3.96}$$

where we have defined $u_1 = \sigma_1^2$, $u_3 = \sigma_2^2$ and we should take the leading behavior in $\mathcal{M}(t_{ij}, y_{ij})$ when $y_{ij} \to \infty$ with $y_{13}/y_{25}y_{25}$ fixed. Thus, in the remaining part of the section we shall analyze the Mellin amplitude in this limit. Let us just remark that the region of integration that dominates in the Regge limit is the same as for flat space scattering amplitudes.

One of the reasons to use Mellin amplitudes is their simple analytic structure. They are meromorphic functions of the Mellin variables δ_{ij} with just simple poles. This property follows, in a loose sense, from the structure of the OPE [108]. The exchange of primary operator with dimension Δ and spin J (and its conformal family) implies that the Mellin amplitude has a infinite set of poles whose residues are given by a dynamical part (related to OPE data) and a kinematical one, *i.e.* determined by symmetry

$$\mathcal{M}(\delta_{ij}) \approx \mathcal{M}_\Delta \equiv \frac{R_m(\delta_{ij})}{\delta_{LR} - (\Delta - J + 2m)}\,, \qquad m = 0, 1, \dots\,, \tag{3.97}$$

where

$$\delta_{LR} = \sum_{a=1}^{k} \sum_{i=k+1}^{n} \delta_{ai}\,, \tag{3.98}$$

m labels subleading twists and R_m is related with lower-point Mellin amplitudes whose precise form has been studied in [108]. This property is analogous to the factorization in flat space scattering amplitudes.

The residue itself, depending on the number of points, can have poles. To see this, take as an example the Mellin amplitude of a five-point correlator and look, without loss of generality, to poles in δ_{12} (this corresponds to setting $k = 2$ and $n = 5$ in (3.98)). The residue $R_m(\delta_{ij})$, as mentioned before, depends on a kinematical part and on the four-point Mellin amplitude $\mathcal{M}_{\mathcal{O}345}$, where $\mathcal{O}$ is the operator being exchanged. A four-point Mellin amplitude can also have poles for the very same argument.

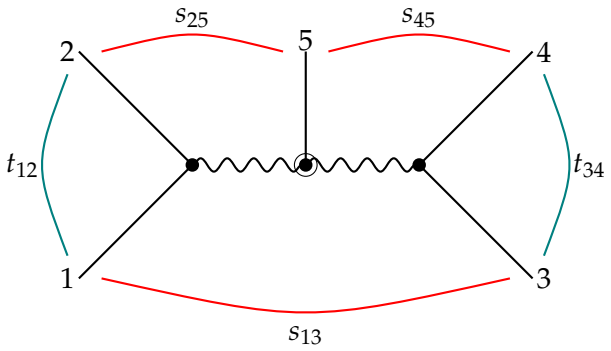

FIGURE 3.10: Regge kinematics for scattering amplitudes can be defined as $s_{13}, s_{25}^2, s_{45}^2 \to \frac{1}{x^2}, x \to 0$ while keeping t_{12} and t_{34} fixed. As can be seen in Mellin space the dominant contribution to the kinematics described in figure 3.8 is the same.

In this language, the exchange of operators of dimension Δ_1 and Δ_2 in the channels (12) and (34) is respectively encoded by the presence of poles in the Mellin amplitude $\mathcal{M}_5(s_{ij}, t_{ij})$ at $t_{12} = (\Delta_1 - J_1 + 2m_1)$ and $t_{34} = (\Delta_2 - J_2 + 2m_2)$,

$$\mathcal{M}_5(s_{ij}, t_{ij}) \approx \sum_{m_i} \frac{Q_{m_1,m_2}(s_{25}, s_{45}, s_{13})}{\big(t_{12} - (\tau_1 + 2m_1)\big)\big(t_{34} - (\tau_2 + 2m_2)\big)} + \dots , \tag{3.99}$$

where the $\dots$ represent regular terms (or poles at other locations). Notice that the poles with $m_1 = m_2 = 0$ are associated with the position space lightcone blocks 3.76 and $m_i > 0$ correspond to corrections around the lightcone. The residue for these sequential poles is related to three-point functions involving the operators that are exchanged.

Now it remains to analyze the large s_{ij} limit of the Mellin amplitude $\mathcal{M}(t_{ij}, s_{ij})$. As for the four-point case, the Casimir differential equations can be translated into Mellin space, where it transforms to a recurrence relation that we defer to (B.3) in appendix B.1. For the $m_i = 0$ sector, the difference equation simplifies considerably. Moreover, for each pair of spins (J_1, J_2), there are $1 + \min(J_1, J_2)$ polynomial solutions which can be labeled by an integer n and have the leading large s_{ij} behaviour

$$Q_{m_1,m_2}(s_{25}, s_{45}, s_{13}) = c_{\ell,m_1,m_2} s_{25}^{J_1-\ell} s_{45}^{J_2-\ell} s_{13}^{\ell} + \dots , \tag{3.100}$$

where $\dots$ represent lower degree terms in the Regge limit. Note that the ℓ denotes a different basis of tensor structure compared to the position space. We have Mellin transformed the lightcone blocks (3.76) and verified the behavior (3.100).

The recurrence relation (B.3) can be used to derive relations between c_{ℓ,m_1,m_2} with different values of m_i

$$\begin{aligned}&2m_1 c_{\ell,m_1,m_2}\big(d-2(J_1+m_1+\tau_1)\big)-c_{\ell,m_1-1,m_2}\left(\Delta_\phi+2J_2-2m_{12}-\tau_{12}-2\ell\right)\\&\times\left(2m_1+\tau_1-2\Delta_\phi\right)+c_{\ell,m_1-1,m_2-1}\left(2m_1+\tau_1-2\Delta_\phi\right)\left(2m_2+\tau_2-2\Delta_\phi\right)=0\,,\end{aligned}\tag{3.101}$$

for the (12) channel where $m_{ij}=m_i-m_j$. This particular limit is important in the Regge kinematics. It gives two recurrence relations for the coefficients c_{ℓ,m_1,m_2} that allow to fix them all in terms of the seed $c_{\ell,0,0}$. As mentioned before, the label m_i in the poles are related to corrections around the lightcone blocks. Fortunately, we have worked out all these corrections for scalar operators in position space in (B.1) and it is a simple exercise to translate the result into Mellin space, written in (B.2). In particular, this solution is consistent with (3.101).

It is possible to construct another solution to the scalar Casimir equation, written in Mellin space, by studying conformal partial waves (or alternatively, exchanged Witten diagrams using the split representation [61]). The idea behind this approach is simple, however the computation involves several steps and for this reason is given in the appendix B.2. The five-point scalar partial wave can be defined by

$$\begin{aligned}\mathcal{M}_{\nu_1,\nu_2,0,0,0}(\delta_{ij})=&\frac{\pi^{2h}\left[\prod_{i=1}^{2}\Gamma\left(\frac{\Delta_{2i-1}+\Delta_{2i}-t_{2i-1\,2i}}{2}\right)\left(\prod_{\sigma=\pm}\Gamma\left(\frac{h+\sigma(\Delta_{2i-1}-\Delta_{2i})+i\nu_i}{2}\right)\right)\right]^{-1}}{\Gamma(\Delta_5)\Gamma\left(\frac{\Delta_5-i\nu_1+i\nu_2}{2}\right)\Gamma\left(\frac{t_{12}-t_{34}+\Delta_5}{2}\right)\Gamma\left(\frac{2h-\Delta_5-i\nu_1-i\nu_2}{2}\right)\Gamma\left(\frac{h-t_{12}+\Delta_5-i\nu_2}{2}\right)}\\&\left[\left(\prod_{\sigma=\pm}\Gamma\left(\frac{h-t_{12}+\sigma\Delta_5-i\nu_2}{2}\right)\Gamma\left(\frac{\Delta_5+\sigma i\nu_1+i\nu_2}{2}\right)\right)\Gamma\left(\frac{h-t_{34}+i\nu_2}{2}\right)\Gamma\left(\frac{t_{12}-t_{34}+\Delta_5}{2}\right)\right.\\&{}_3F_2\left(\begin{matrix}\frac{t_{12}-t_{34}+\Delta_5}{2},\frac{\Delta_5-i\nu_1+i\nu_2}{2},\frac{\Delta_5+i\nu_1+i\nu_2}{2}\\ \Delta_5,\frac{2-h+t_{12}+\Delta_5+i\nu_2}{2}\end{matrix};1\right)+\Gamma(\Delta_5)\,\Gamma\left(\frac{t_{12}-h+\Delta_5+i\nu_2}{2}\right)\\&\left.\left(\prod_{\sigma=\pm}\prod_{i=1}^{2}\Gamma\left(\frac{h-t_{2i-1\,2i}+\sigma i\nu_i}{2}\right)\right)\,{}_3F_2\left(\begin{matrix}\frac{h-t_{12}-i\nu_1}{2},\frac{h-t_{12}+i\nu_1}{2},\frac{h-t_{34}-i\nu_2}{2}\\ \frac{2+h-t_{12}-\Delta_5-i\nu_2}{2},\frac{h-t_{12}+\Delta_5-i\nu_2}{2}\end{matrix};1\right)\right],\end{aligned}\tag{3.102}$$

where we use the notation $\delta_{ij}=(\Delta_i+\Delta_j-t_{ij})/2$. Obviously, the Mellin amplitude of the scalar conformal partial wave only depends on the variables t_{12} and t_{34} and it is symmetric under $\nu\to-\nu$. More importantly, it gives a solution valid at finite t_{ij} and reduces to the solution (B.2) when t_{ij} are at the poles. This leads us to study the casimir equation away from the poles. For this purpose let us write the Mellin amplitude as

$$\mathcal{M}_{J_1,J_2}(s_{ij},t_{ij})=s_{25}^{J_1-\ell}s_{45}^{J_2-\ell}s_{13}^{\ell}\,f(t_{12},t_{34})\,,\tag{3.103}$$

and plug it in the the recurrence relation (B.3). In turn, this leads difference equation for t_{12} and t_{34} that reads

$$f_{00}\left(t_{12}-\tau_1\right)\left(d-t_{12}-\tau_1-2J_1\right)+f_{-20}\left(2\Delta_\phi-t_{12}\right)\left(t_{34}-t_{12}+\Delta_\phi+2J_2-2\ell\right)$$
$$+f_{-2-2}\left(2\Delta_\phi-t_{12}\right)\left(2\Delta_\phi-t_{34}\right)=0\,, \tag{3.104}$$

where the subindices denote $f_{a_1a_2}\equiv f(t_{12}+a_1,t_{34}+a_2)$. This difference equation can be further simplified by redefining $f(t_{12},t_{34})$

$$\tilde{f}_{00}\left(\tau_1-t_{12}\right)\left(d-2J_1-\tau_1-t_{12}\right)+2\tilde{f}_{-20}\left(t_{12}-t_{34}-\Delta_\phi-2J_2+2\ell\right)-4\tilde{f}_{-2-2}=0 \tag{3.105}$$

where $\tilde{f}$ is given by

$$f(t_{12},t_{34})=\frac{\tilde{f}(t_{12},t_{34})}{\Gamma(\frac{2\Delta_\phi-t_{12}}{2})\Gamma(\frac{2\Delta_\phi-t_{34}}{2})}. \tag{3.106}$$

Note that this prefactor is precisely the same as the one that comes from the Gamma functions in the definition of Mellin amplitudes (3.91). It is now simple to see that the equation for $J_1=J_2$ and generic ℓ can be obtained from the scalar difference equation by doing the following shifts

$$\Delta_\phi\to\Delta_\phi+2(J_1-\ell),\quad d\to d-2J_1. \tag{3.107}$$

This suggests that the Mellin partial wave for equal spin $J_1=J_2$ and generic ℓ can be obtained from (3.102) by doing these replacements. One way to check this statement is to build solutions with the recursion relations in spin derived in [76] (we have rederived parts of these relations in the appendix B.1 using lightcone blocks) and verify that it agrees with the solution that we proposed above.

These solutions for Mellin amplitudes can then be inserted in (3.96) to obtain the conformal block in the Regge limit, that is

$$G^{\circlearrowleft}_{J_1,J_2,\ell,\nu_1,\nu_2}(\sigma_i,\rho_i)=\sigma_1^{1-J_1}\sigma_2^{1-J_2}\bar{\mathcal{H}}_{\nu_1\nu_2}(\xi_1,\xi_2,\xi_3)\,, \tag{3.108}$$

with

$$\bar{\mathcal{H}}_{\nu_1\nu_2}(\xi_1,\xi_2,\xi_3)=\int dt_{12}dt_{34}\,\Gamma\left(\frac{2\Delta_\phi-t_{12}}{2}\right)\Gamma\left(\frac{2\Delta_\phi-t_{34}}{2}\right)\Gamma\left(\frac{2\ell-\Delta_\phi+t_{12}+t_{34}-2}{2}\right)$$
$$\Gamma\left(\frac{2J_1-2\ell+\Delta_\phi+t_{12}-t_{34}}{2}\right)\Gamma\left(\frac{2J_2-2\ell+\Delta_\phi-t_{12}+t_{34}}{2}\right)\mathcal{M}_{\nu_1,\nu_2}(t_{12},t_{34})$$
$$\xi_1^{\frac{t_{34}-t_{12}-\Delta_\phi-2J_1+2\ell}{2}}\xi_2^{\frac{t_{12}-t_{34}-\Delta_\phi-2J_2+2\ell}{2}}\xi_3^{\frac{2-t_{12}-t_{34}+\Delta_\phi-2\ell}{2}}\,, \tag{3.109}$$

where $\mathcal{M}_{\nu_1,\nu_2}(t_{12},t_{34})$ is the conformal partial wave in Mellin space in the Regge limit. This expression highlights two properties of the Regge limit, firstly the limit is dominated by operators of high spin and, secondly, it depends on three fixed cross ratios that can be thought of as angles, which is similar to what happens in the Euclidean OPE limit as we mentioned before. In fact $\bar{\mathcal{H}}_{\nu_1\nu_2}$ solves the Casimir differential equation in the Euclidean region (3.59) but with a different eigenvalue C. Let us point out that the integral (3.109) can be done by picking up poles.

It follows from what was said above that $\bar{\mathcal{H}}_{\nu_1\nu_2}(\xi_1,\xi_2,\xi_3)$ must have the same form as (3.62), as it solves the same conformal Casimir equation.

3.3.3 Comment on position space

The analysis of the Regge limit in Mellin space of the previous section exposed the similarities to flat space scattering amplitudes but it does not emphasize enough the role of analytic continuation in the cross ratios in changing the behavior of the conformal block. This aspect is clearer in position space, in particular, in the lightcone expressions introduced in subsection 3.2.2. The kinematics of the Regge limit (where some pair of points are timelike while others are spacelike) can be reached from the Euclidean configuration after doing analytic continuations in u_2, u_4 and u_5 around 0 as explained in section 3.3.1.

The analysis is simpler for the discontinuities around $u_4, u_5 = 0$ in the lightcone blocks (3.76) and contains most of the physics we want to highlight in this subsection. These discontinuities come from the first two terms in the denominator of (3.76), provided that $u_2 > 0$. The origin of branch point at, say $u_5 = 0$, comes from the region $t_1 \approx 1/(1-u_5)$ where the denominator $(1-(1-u_5)t_1)$ changes sign. To deal with this it is convenient to divide the integration region in two parts,

$$\int_0^1 dt_1\,\mathcal{I} \;\to\; \int_0^{\frac{1}{1-u_5}} dt_1\,\mathcal{I} + (-1)^{(h_1-\tau_2-2\ell+\Delta_\phi)} \int_{\frac{1}{1-u_5}}^1 dt_1\,\mathcal{I}\,, \tag{3.110}$$

where the phase comes from the change of sign in the factor $(1-(1-u_5)t_1)$. The first term drops out when taking the discontinuity and so we obtain

$$\text{Disc}_{u_5=0} \int_0^1 dt_1\,\mathcal{I} = \left(1-(-1)^{(h_1-\tau_2-2\ell+\Delta_\phi)}\right) \frac{u_5}{u_5-1} \int_0^1 d\tau_1\,\mathcal{I}\,, \tag{3.111}$$

where we have changed variables to $t_1 = (u_5\tau_1 - 1)/(u_5-1)$ in order to have the integration running from 0 to 1 again. It is possible to repeat the same steps to take the discontinuity of u_4.

Recall that the cross ratios u_4, u_5 and u_2 approach 1 with $\frac{(1-u_2)}{(1-u_4)(1-u_5)} = \frac{1+\zeta}{2}$ fixed in the Regge limit. The discontinuity in u_4 and u_5 of the lightcone block after the Regge limit is given by

$$\lim_{\substack{u_4,u_5\to 1\\ \zeta \text{ fixed}}} \text{Disc}_{u_5,u_4=0}\mathcal{G} = \frac{u_1^{\frac{1-J_1}{2}} u_3^{\frac{1-J_2}{2}} (1+\zeta)^\ell}{\xi_2^{\Delta_2-1}\xi_1^{\Delta_1-1} 2^\ell} \sum_{m=0}^{\infty} \frac{\binom{\frac{\Delta_\phi-\tau_1-\tau_2-2J_1-2J_2}{2}}{m}\left(-\frac{1+\zeta}{2}\right)^m F_1 F_2}{\Gamma\left(\frac{2J_1+\Delta_\phi-2\ell+\tau_{12}}{2}\right)\Gamma\left(\frac{2J_2+\Delta_\phi-2\ell+\tau_{21}}{2}\right)}, \quad (3.112)$$

where we have used $\tau_{ij} = \tau_i - \tau_j$, the cross ratios (3.55) and

$$F_i = \frac{\pi\Gamma^2\left(\frac{\tau_i+2J_i}{2}\right)\Gamma(\tau_i+2J_i)\,\Gamma(\tau_i+2J_i+m-1)}{2^{J_i-\frac{1}{2}}\Gamma\left(\frac{\tau_1+\tau_2+2J_i+2m+2\ell-\Delta_\phi}{2}\right)} {}_2F_1\left(\begin{matrix}\ell-J_i, \tau_{i+1}+2J_{i+1}+m-1\\ \frac{2J_{i+1}+2m+2\ell+\tau_1+\tau_2-\Delta_\phi}{2}\end{matrix}; \frac{\zeta+1}{2}\right).$$

The discontinuities in u_4 and u_5 are enough to reveal that the discontinuities of conformal block behave with $\sigma_1^{1-J_1}\sigma_2^{1-J_2}$ in the Regge limit, which compares with $\sigma_1^{\Delta_1}\sigma_2^{\Delta_2}$ of the Euclidean block[17]. It can also be shown from the previous formula that three sequential discontinuities, $\text{Disc}_{u_2,u_4,u_5}$, evaluate to zero. Recall that four-point conformal blocks have vanishing double discontinuity. We believe that conformal blocks have this property away from the lightcone limit.

3.3.4 Conformal Regge theory for five points

Let us consider the representation of the five-point correlation function in terms of conformal partial waves, and its implications for the Regge limit. This basis is complete and orthogonal. Since we have more control over the analytic properties of the partial waves in Mellin space, we consider the expansion

$$\mathcal{M}(s_{ij},t_{ij}) = \sum_{J_1,J_2=0}^{\infty} \sum_{\ell=0}^{\min(J_1,J_2)} \int \frac{d\nu_1}{2\pi i}\frac{d\nu_2}{2\pi i}\, b_{J_1,J_2,\ell}(\nu_1,\nu_2)\mathcal{M}_{J_1,J_2,\ell}(s_{ij},t_{ij})\,. \quad (3.113)$$

We suppress the dependence of the Mellin partial wave $\mathcal{M}_{J_1,J_2,\ell}$ on the scaling dimensions, as the nontrivial analytic continuation occurs in other quantum numbers. We have introduced poles in the variables ν_1 and ν_2 with residues corresponding to the OPE coefficients, using

$$b_{J_1,J_2,\ell}(\nu_1,\nu_2) \approx \frac{P^\ell_{\nu_1,\nu_2,J_1,J_2}}{\left(\nu_1^2-(\Delta_1-h)^2\right)\left(\nu_2^2-(\Delta_2-h)^2\right)}, \quad (3.114)$$

[17] We also need to consider the monodromy of the lightcone block around the branch point at $u_2 = 0$. It is possible to do a Mellin transform of the lightcone block and apply the method of the previous subsection to derive all discontinuities. In the appendix, we provide several checks that the discontinuity of the block in u_2 has the same behavior.

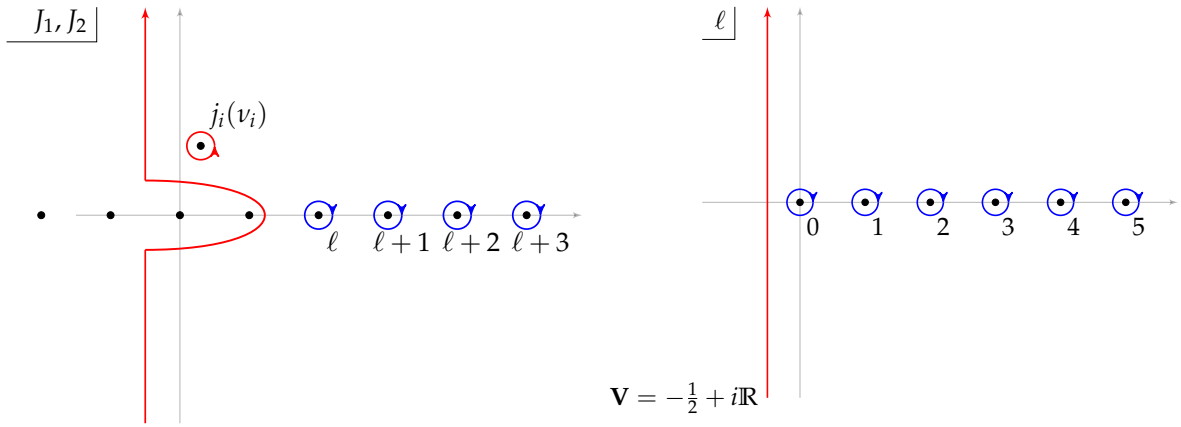

FIGURE 3.11: Integration contours for the spin quantum numbers J_1, J_2, as well as ℓ. The blue contour is the Euclidean contour, whereas the red contour is the Regge contour. We assume the leading Regge pole in the J_i-plane is located at $j_i(\nu)$ and that there are no dynamical poles in the ℓ plane. Red contour is understood to be deformed to the right of the other infinite series of poles depending on ℓ lying on the left in the J_i-plane.

where $\Delta_i = \Delta_i(J_i)$ is the dimension of the i-th exchanged operator of spin J_i. We remark that the product of the OPE coefficients $P^{\ell}_{\nu_1,\nu_2,J_1,J_2}$ in (3.114) is a linear combination of those in (3.51) that appear in the conformal block expansion.

We would like to provide a Sommerfeld-Watson representation of (3.113). First, we swap the range of summations as

$$\mathcal{M}(s_{ij},t_{ij}) = \sum_{\ell=0}^{\infty}\sum_{J_1,J_2=\ell}^{\infty}\int \frac{d\nu_1}{2\pi i}\frac{d\nu_2}{2\pi i}\, b_{J_1,J_2,\ell}(\nu_1,\nu_2)\mathcal{M}_{J_1,J_2,\ell}(s_{ij},t_{ij})\,. \tag{3.115}$$

Next, we analytically continue in the spin quantum numbers. However, the $b_{J_1,J_2,\ell}$ are not expected to have a unique analytic continuation in the quantum numbers. For that reason we need to consider their *signatured* counterparts.

Let us remind the reader the analogous construction [4] for the four-point correlator $\mathcal{A}(u,v)$ in terms of the cross ratios

$$u = \frac{x_{12}^2 x_{34}^2}{x_{14}^2 x_{23}^2}\,, \qquad v = \frac{x_{13}^2 x_{24}^2}{x_{14}^2 x_{23}^2}\,. \tag{3.116}$$

After expanding in Euclidean partial waves, we can write the correlation function as

$$\mathcal{A}(u,v) = \sum_{J=0}^{\infty}\int_{\frac{d}{2}+i\mathbb{R}}\frac{d\Delta}{2\pi i}\, c_{\Delta,J}\, F_{\Delta,J}(u,v)\,, \tag{3.117}$$

where $c_{\Delta,J}$ denotes the OPE function and $F_{\Delta,J}$ is the Euclidean partial wave. It can be transformed to Mellin space as

$$\mathcal{M}(s,t) = \sum_{J=0}^{\infty} \int_{\frac{d}{2}+i\mathbb{R}} \frac{d\Delta}{2\pi i}\, c_{\Delta,J}\, \mathcal{M}_{\Delta,J}(s,t)\,. \tag{3.118}$$

Again, the OPE function $c_{\Delta,J}$ is not uniquely defined in the complex J plane. Thus, we define the signatured OPE function $c^{\theta}_{\Delta,J}$ by

$$\mathcal{M}_{\theta}(s,t) = \sum_{J=0}^{\infty} \int_{\frac{d}{2}+i\mathbb{R}} \frac{d\Delta}{2\pi i}\, c^{\theta}_{\Delta,J}\, \mathcal{M}^{\theta}_{\Delta,J}(s,t)\,, \tag{3.119}$$

where the signatured Mellin partial waves are given by

$$\mathcal{M}^{\theta}_{\Delta,J}(s,t) = \frac{1}{2}\big[\mathcal{M}_{\Delta,J}(s,t) + \theta \mathcal{M}_{\Delta,J}(-s,t)\big]\,, \tag{3.120}$$

with $\theta = \pm$. The signatured Mellin amplitude allows for a unique analytic continuation of the signatured OPE function $c^{\theta}_{\Delta,J}$ [6]. The problem of the non-signatured OPE function can be traced back the factor of $(-1)^J$ that appears in the transformation $s \to -s$, which follows from the large s behaviour $\mathcal{M}_{\Delta,J}(s,t) \approx s^J$.

A similar construction can be done for five-point functions. We split the full correlator into eight parts depending on the *signature* denoted by $= (\theta_1, \theta_2, \theta_{12})$ where each component can be $\pm$. We define the *signatured* amplitudes as

$$\begin{aligned}\mathcal{M}_{\theta}(s_{25}, s_{45}, s_{13}) = \frac{1}{8}\big[&\mathcal{M}(s_{25}, s_{45}, s_{13}) + \theta_1 \mathcal{M}(-s_{25}, s_{45}, s_{13}) + \theta_2 \mathcal{M}(s_{25}, -s_{45}, s_{13}) \\ &+ \theta_1\theta_2 \mathcal{M}(-s_{25}, -s_{45}, s_{13}) + \theta_{12} \mathcal{M}(-s_{25}, -s_{45}, -s_{13}) + \theta_1\theta_{12} \mathcal{M}(s_{25}, -s_{45}, -s_{13}) \\ &+ \theta_{12}\theta_2 \mathcal{M}(-s_{25}, s_{45}, -s_{13}) + \theta_1\theta_{12}\theta_2 \mathcal{M}(s_{25}, s_{45}, -s_{13})\big]\,.\end{aligned} \tag{3.121}$$

This equation is suitable only for $s_{ij} \gg 1$. We also suppress the dependence on t_{ij} for brevity. We justify it by using the properties of the Mellin partial wave (3.103) which, in terms of $J'_i = J_i - \ell$, behaves in the Regge limit as

$$\mathcal{M}_{J'_1, J'_2, \ell}(s_{ij}, t_{ij}) = s_{25}^{J'_1} s_{45}^{J'_2}\, s_{13}^{\ell}\, f(t_{12}, t_{34})\,. \tag{3.122}$$

By analogy with the four-point case, we expect that OPE functions associated with the expansion of the signatured amplitudes in (3.121) have a unique analytic continuation in all quantum numbers J'_1, J'_2, ℓ. It would be interesting to put this on a firm footing by deriving dispersion relations along the lines of [6]. The full Mellin amplitude can then be written in

terms of the signatured Mellin amplitude as

$$\mathcal{M}(s_{25}, s_{45}, s_{13}) = \sum_{\theta \in \{-1,1\}^3} \mathcal{M}_\theta(s_{25}, s_{45}, s_{13})\,. \tag{3.123}$$

In terms of the signatured analogue of partial waves defined through (3.121), we write

$$\mathcal{M}_\theta(s_{ij}, t_{ij}) = \sum_{\ell=0}^{\infty} \sum_{J_1', J_2'=0}^{\infty} \int \frac{d\nu_1}{2\pi i} \frac{d\nu_2}{2\pi i}\, b^\theta_{J_1', J_2', \ell}(\nu_1, \nu_2) \mathcal{M}^\theta_{J_1', J_2', \ell}(s_{ij}, t_{ij})\,. \tag{3.124}$$

Next we perform a Sommerfeld-Watson transform on the ℓ contour. First, we replace the summation over ℓ by an integral over the blue contour shown in figure 3.11. Then we move the contour around the non-negative integers to a vertical contour $\mathbf{V}$ located at $-1/2 + i\mathbb{R}$, as shown in figure 3.11. We assume that we do not encounter any poles during this procedure. This assumption is inspired by an analogous procedure for the five particle S-matrix. Indeed the quantum number ℓ labels a choice of tensor basis for three-point functions and therefore should not have a dynamic content, just like the helicity quantum number for the S-matrix [88]. Thus after deforming the ℓ contour we have

$$\mathcal{M}_\theta(s_{ij}, t_{ij}) = \int_{\mathbf{V}} \frac{d\ell}{2\pi i} \frac{1}{\sin(\pi\ell)} \sum_{J_1', J_2'=0}^{\infty} \int \frac{d\nu_1}{2\pi i} \frac{d\nu_2}{2\pi i}\, b^\theta_{J_1', J_2', \ell}(\nu_1, \nu_2) \mathcal{M}^\theta_{J_1', J_2', \ell}(s_{ij}, t_{ij})\,. \tag{3.125}$$

Next we analytically continue in J_1' and J_2'. The analytic structure in these variables is analogous to the case of four-point correlation functions. Figure 3.11 shows the analytic structure of the integrand in (3.124). In particular there is a leading Regge pole in the J_i plane at $J_i = j_i(\nu_i)$ given by

$$\big[\Delta_i\big(j_i(\nu_i)\big) - h\big]^2 - \nu_i^2 = 0\,. \tag{3.126}$$

Picking the poles in the complex spin planes at $J_1' = j_1(\nu_1) - \ell$ and $J_2' = j_2(\nu_2) - \ell$, we obtain the following expression for the signatured correlators

$$\mathcal{M}_\theta = \int \frac{d\nu_1}{2\pi i} \frac{d\nu_2}{2\pi i}\, s_{25}^{j_1(\nu_1)} s_{45}^{j_2(\nu_2)} \int_{\mathbf{V}} \frac{d\ell}{2\pi i}\, \frac{b^\theta_{j_1(\nu_1), j_2(\nu_2), \ell}(\nu_1, \nu_2)\, f^\theta_{\nu_1, \nu_2, \ell}(t_{ij})\, \eta^\ell}{\sin(\pi\ell) \sin\big(\pi(j_1(\nu_1) - \ell)\big) \sin\big(\pi(j_2(\nu_2) - \ell)\big)}\,, \tag{3.127}$$

where $f^\theta_{\nu_1, \nu_2, \ell}$ is defined as the signatured analogue of f in (3.106). Thus, in the Regge limit the full correlator has the form

$$\mathcal{M} = \int \frac{d\nu_1}{2\pi i} \frac{d\nu_2}{2\pi i}\, s_{25}^{j_1(\nu_1)} s_{45}^{j_2(\nu_2)} \int_{\mathbf{V}} \frac{d\ell}{2\pi i}\, \eta^\ell g_{\nu_1, \nu_2, \ell}(t_{ij})\,, \tag{3.128}$$

where the function $g_{\nu_1, \nu_2, \ell}(t_{ij})$ is defined from replacing (3.127) in (3.123). This allows us to

represent the Reggeized Mellin amplitude in terms of the operator content of the leading Regge trajectories and their couplings to the external states.

3.4 Conclusions

We have discussed the generalization of the Regge limit to higher-point correlation functions in conformal field theories in general dimensions. For the case of five-point functions, we defined the five-variable generalization of the Mack polynomials, and discussed its properties. Using the leading order behavior of these polynomials, we studied the multi-Regge limit of the correlator which is dominated by the leading Regge trajectories.

By considering the implications of multi-Regge limit in Mellin space, we arrived at a proposal for the kinematics of the multi-Regge limit in position space. We studied the behavior of the conformal block in this limit, using the recent results on lightcone blocks for higher-point functions. To compute the monodromies of the conformal block, we also used some techniques from the study of hypergeometric functions.

Mellin space is a good place to study the multi-Regge limit of the correlators. We expect that the multi-Regge limit for conformal field theories in Mellin space is analogous to that of the flat space S matrix in Mandelstam space. The generalization of the partial wave expansion in the S matrix is done in [85], for four dimensional quantum field theories. Analogous generalization of the partial wave expansion is within reach for three dimensional CFTs for n-point functions. We would benefit from the fact that there are no representations of the rotation subgroup of the conformal group in three dimensions with more than one rows in the Young's tableaux. However, for higher dimensions, there will be proliferation of indices labelling the internal vertices.

In the process, we also discussed a novel basis of three-point functions of operators with spin $(J_1, J_2, 0)$, respectively. This basis is useful for study of Euclidean OPE limit as it leads to the analytic expression for the conformal block in this limit. These expressions appear to be a natural generalization of the Wigner d function used in the S matrix. This suggests that the basis used in the literature for three-point functions of operators with spin (J_1, J_2, J_3) might not be the most natural one for the study of Euclidean conformal blocks. Given the importance of conformal blocks in numerical bootstrap, it would be interesting to study the properties of this basis in more detail. The case of (J_1, J_2, J_3) three-point function is accessible in the Euclidean OPE limit of six-point function in the snowflake channel.

The new basis appears to be useful to arrive at a Euclidean inversion formula for the five-point functions, mainly due to simple orthogonality properties. While the study of analytic structure of the correlator of higher-point functions is still in its infancy, we expect that it

admits a drastic simplification in the multi-Regge limit. It would be interesting to derive an inversion formula and dispersion relation in the multi-Regge limit for CFTs, along the lines of [91]. An important ingredient is the multivariable generalization of the Cauchy formula, called the Bargman-Weil formula.

Finally, in the S matrix case, a crucial ingredient for the absence of singularities in ℓ was the use of Steinmann relations. It would be interesting to explore the analogue of Steinmann relations in CFTs.

Appendix B

Appendices for Multi-Regge theory

B.1 Lightcone blocks

The scalar five-point conformal blocks, mentioned in the main text, can be expressed in terms of an expansion around the lightcone (3.78) by acting with (3.75) on a three-point function. In (3.78) we have written it in terms of a function $\tilde{\mathcal{I}}_{n_1,n_2}$ given by

$$\tilde{\mathcal{I}}_{n_1,n_2} = \frac{\left(\frac{a-\Delta_5}{2}\right)_{n_1}\left(\frac{2n_1-\Delta_5+a}{2}\right)_{n_2}\left(\frac{a+4-\Delta_5-d}{2}\right)_{n_1}\left(\frac{2n_1-\Delta_5+a+4-d}{2}\right)_{n_2}}{\left(t_1^2u_1u_4-t_1(t_2(1-u_5)+t_2u_4(u_2u_5-1)+u_1u_4+u_5-1)+u_5\left(t_2^2u_3-t_2(u_3-u_2u_4+1)+1\right)\right)^{\frac{a+2n_1+2n_2-\Delta_5}{2}}} \tag{B.1}$$
$$\prod_{i=1}^{2}\frac{(-1)^{n_i}\Gamma(2n_i+\Delta_{k_i})\left(\frac{\Delta_{k_i}}{2}\right)_{n_i}^2(t_i(1-t_i))^{\frac{\Delta_{k_i}+2n_i}{2}-1}}{n_i!(\Delta_{k_i})_{2n_i}\left(\frac{2\Delta_{k_i}+4-d}{2}\right)_{n_i}\Gamma^2\left(\frac{2n_i+\Delta_{k_i}}{2}\right)}$$

where $a=\Delta_{k_1}+\Delta_{k_2}$. One nice feature of this result is that it allows to to analytic continuations in u_2,u_4,u_5 at all orders in u_1 and u_3, this is specially useful to verify that the analytic continuation of the conformal block has a distinct behavior in the Regge limit. With this expression in our hands we can also do a Mellin transform and obtain the Mellin amplitude associated with the scalar conformal block. For instance the function Q_{m_1,m_2} in (3.99) is given in this case by

$$Q_{m_1,m_2} = \sum_{n_i=0}\prod_{i=1}^{2}\frac{2(-1)^{m_i}\Gamma\left(\Delta_{k_i}\right)}{(m_i-n_i)!\Gamma^2\left(\frac{\Delta_{k_i}}{2}\right)\Gamma\left(\Delta_\phi-m_i-\frac{\Delta_{k_i}}{2}\right)\left(1-\frac{d}{2}+\Delta_{k_i}\right)_{m_i-n_i}}\frac{\left(\frac{\bar{\Delta}-\Delta_\phi}{2}\right)_{m_1-n_1}{}^{\left(n_1+n_2+\frac{\Delta_\phi}{2}-m_1-m_2-\frac{\bar{\Delta}}{2}\right)}_{n_1}}{\Gamma\left(\frac{\Delta_\phi+2m_1-2m_2+\Delta_{k_1}-\Delta_{k_2}}{2}\right)}$$
$$\times\frac{\left(\frac{\bar{\Delta}+2-d-\Delta_\phi}{2}\right)_{m_1-n_1}\left(\frac{2m_1+\bar{\Delta}-2n_1-\Delta_\phi}{2}\right)_{m_2-n_2}\left(\frac{2m_1+\bar{\Delta}+2-d-2n_1-\Delta_\phi}{2}\right)_{m_2-n_2}{}^{\left(\frac{2n_2+\Delta_\phi-2m_1-2m_2-\bar{\Delta}}{2}\right)}_{n_2}}{\Gamma\left(\frac{\Delta_\phi-2m_1+2m_2-\Delta_{k_1}+\Delta_{k_2}}{2}\right)\Gamma\left(\frac{2m_1+2m_2+\bar{\Delta}-\Delta_\phi}{2}\right)} \tag{B.2}$$

where $\bar{\Delta}=\Delta_{k_1}+\Delta_{k_2}$. Note that it does not depend on the variables s_{ij} as expected since the exchanged operators are scalars. The apparent asymetry in the channels (12) and (34) is

related with the choice of which differential operator F_k we decide to act first on a three-point function. Another advantage of having the Mellin amplitude for the scalar conformal block is that it can be used to generate some solutions for spinning blocks as we have shown in section 3.3.2.

We have checked that the solution (B.2) satisfies the Casimir recurrence equation, in the channel (12), given by

$$\begin{aligned}
&\big[\mathbf{d}_{00000}\big(2c_{\Delta_1 J_1} - a_1^2 + a_1(2a_4 + a_5 - a_3 - 2d + 3\Delta_\phi) - 2a_2(a_3 + a_4) + 2a_3^2 - 2a_3a_4 - 2a_3a_5 \\
&+ \Delta_\phi(5a_3 - 4a_4 - 2a_5 + 4d) + 2a_4^2 + a_4a_5 - 2\Delta_\phi^2\big) \\
&+ \mathbf{d}_{00-200}(a_1 - a_3 + a_4 - 2\Delta_\phi)(a_3 - 2a_2 - a_5 + 2\Delta_\phi) \\
&- \mathbf{d}_{000-20}(a_1 - 2a_2 + a_4 - \Delta_\phi)(a_1 - a_3 + a_4 - 2\Delta_\phi) - a_3\mathbf{d}_{002-20}(a_1 - 2a_2 + a_4 - \Delta_\phi) \\
&+ a_1\mathbf{d}_{-2000-2}(a_1 - 2a_2 - a_5 + \Delta_\phi) + a_1\mathbf{d}_{-2002-2}(a_1 - 2a_2 - a_5 + \Delta_\phi) + 2a_1a_2\mathbf{d}_{-2-2-200} \\
&+ 2a_1a_2\mathbf{d}_{-2-2000} + a_1a_5\mathbf{d}_{-20-220} + a_1a_5\mathbf{d}_{-20000} + a_4\mathbf{d}_{00-220}(2a_2 - a_3 + a_5 - 2\Delta_\phi) \\
&+ a_4\mathbf{d}_{00020}(a_3 - a_4 - a_5 + \Delta_\phi) + a_3\mathbf{d}_{00200}(a_4 + a_5 - a_3 - \Delta_\phi)\big] f(t_{ij}, s_{ij}) = 0
\end{aligned} \tag{B.3}$$

where $\mathbf{d}_{i_1i_2i_3i_4i_5}$ is defined by $\mathbf{d}_{i_1i_2i_3i_4i_5} f(t_{12}, t_{34}, s_{13}, s_{25}, s_{45}) = f(t_{12} + i_1, \ldots, s_{45} + i_5)$ and the coefficients a_i are given by

$$\begin{aligned}
&a_1 = 2\Delta_\phi - t_{12}, \quad a_2 = \frac{2\Delta_\phi - t_{34}}{2}, \quad a_3 = \Delta_\phi - s_{13}, \\
&a_4 = s_{25} + t_{12} - t_{34} + \Delta_\phi, \quad a_5 = s_{45} - t_{12} + t_{34} + \Delta_\phi\,.
\end{aligned} \tag{B.4}$$

This recurrence relation is also valid for spinning conformal blocks.

B.1.1 Spinning recursion relations

In [76] the authors have derived identities that blocks with different values of spin satisfy. It is possible to verify part of these relations using lightcone blocks for unequal external dimensions introduced in the previous subsection. Using (3.73) we can verify that the lightcone blocks satisfy

$$\begin{aligned}
&(2J_1 + 2\ell + \tau_1 + \tau_2 - 2 - \Delta_5) G^{\Delta_1,\Delta_5,\Delta_3}_{\tau_1,J_1,\tau_2,J_2,\ell} + 2(J_2 - \ell) G^{\Delta_1,\Delta_5,\Delta_3}_{\tau_1,J_1,\tau_2,J_2,\ell+1} \\
&+ \frac{4(2J_1 + \tau_1 - 2)(2J_1 + \tau_1 - 1)}{(2J_1 + \tau_1 - \Delta_{12} - 2)} \left[\frac{\sqrt{u_5} G^{\Delta_1+1,\Delta_5+1,\Delta_3}_{\tau_1+1,J_1-1,\tau_2,J_2,\ell}}{\sqrt{u_1}} - G^{\Delta_1,\Delta_5,\Delta_3}_{\tau_1,J_1-1,\tau_2,J_2,\ell}\right] = 0
\end{aligned} \tag{B.5}$$

where $G^{\Delta_1,\Delta_5,\Delta_3}_{\tau_1,J_1,\tau_2,J_2,\ell}$ represents the lightcone conformal block for the exchange of a twist τ_i and spin J_i in the channels (12) and (34) for external with dimension Δ_i,

$$G^{\Delta_1,\Delta_5,\Delta_3}_{\tau_1,J_1,\tau_2,J_2,\ell} = u_1^{\frac{\tau_1}{2}} u_3^{\frac{\tau_2}{2}} u_5^{\frac{\Delta_5}{2}} (1-u_2)^{\ell} \int [dt_1 dt_2] (1-u_2u_5+t_2(u_2-1)u_5)^{J_1-\ell} \tag{B.6}$$
$$\frac{(1-u_2u_4+t_1(u_2-1)u_4)^{J_2-\ell}}{(1+t_1(u_5-1))^{\frac{\Delta_5+2J_1+\tau_1-\tau_2-2\ell}{2}} (1+t_2(u_4-1))^{\frac{\Delta_5+2J_2-\tau_1+\tau_2-2\ell}{2}} (1+(1-t_1)(1-t_2)(u_2-1))^{\frac{2J_1+2J_2+\tau_1+\tau_2-\Delta_5}{2}}}$$

where $[dt_1dt_2] = \prod_{i=1}^{2} \frac{dt_i\,\Gamma(2J_i+\tau_i) t^{\frac{\tau_i+2J_i+a_i}{2}-1}(1-t_i)^{\frac{\tau_i+2J_i-a_i}{2}-1}}{\Gamma\left(\frac{\tau_i+2J_i+a_i}{2}\right)\Gamma\left(\frac{\tau_i+2J_i-a_i}{2}\right)}$ with $a_1 = \Delta_{12}, a_2 = \Delta_{34}$. As before, the index ℓ labels a particular structure in the three-point function (3.49)

By considering the Mellin transform of $G^{\Delta_1,\Delta_5,\Delta_3}_{\tau_1,J_1,\tau_2,J_2,\ell}$ we can phrase the recurrence relation in spin (B.5) in terms of a Mellin amplitudes

$$\frac{2(2J_1+\tau_1-2)(2J_1+\tau_1-1)((\Delta_5-2\delta_{25}+\tau_{12})\mathcal{M}^{\Delta_1+1,\Delta_5+1,\Delta_3}_{\tau_1+1,J_1-1,\tau_2,J_2,l} - \mathcal{M}^{\Delta_1,\Delta_5,\Delta_3}_{\tau_1,J_1-1,\tau_2,J_2,\ell})}{(2J_1+\tau_1-\Delta_{12}-2)}$$
$$+ (2J_1+2\ell+\tau_1+\tau_2-\Delta_5-2)\mathcal{M}^{\Delta_1,\Delta_5,\Delta_3}_{\tau_1,J_1,\tau_2,J_2,\ell} + 2(J_2-\ell)\mathcal{M}^{\Delta_1,\Delta_5,\Delta_3}_{\tau_1,J_1,\tau_2,J_2,\ell+1} = 0 \tag{B.7}$$

with

$$G^{\Delta_1,\Delta_5,\Delta_3}_{\tau_1,J_1,\tau_2,J_2,\ell} = u_1^{\frac{\tau_1}{2}} u_3^{\frac{\tau_2}{2}} \int [d\delta_{ij}] \mathcal{M}^{\Delta_1,\Delta_5,\Delta_3}_{\tau_1,J_1,\tau_2,J_2,\ell}(\delta_{ij}) u_4^{-\delta_{45}} u_5^{\delta_{25}+\frac{\tau_2-\tau_1}{2}} u_2^{\delta_{13}-\delta_{45}+\frac{\Delta_5-a_2-\tau_1}{2}} \prod_{i<j}\Gamma(\delta_{ij}) \tag{B.8}$$

where we have used the constraints to eliminate the some of the δ_{ij} and δ_{12} and δ_{34} are set to $\frac{\Delta_1+\Delta_2-\tau_1}{2}$ and $\frac{\Delta_3+\Delta_4-\tau_2}{2}$ respectively. We have suppressed the dependence on Mellin variables in (B.7) since there are no shifts in them.

There is an extra identity that is needed to turn (B.5) into a self-consistent recurrence relation

$$\frac{4(\tau_1+2\ell-1)(\tau_2+2\ell-1)(\tau_1+\tau_2+4\ell-\Delta_5-4)}{(\tau_1+2\ell-\Delta_{12}-2)(\Delta_{34}+\tau_2+2\ell-2)}\left[\frac{G^{\Delta_1+1,\Delta_5,\Delta_3-1}_{\tau_1+1,\ell-1,\tau_2+1,\ell-1,\ell-1}}{\sqrt{u_1}\sqrt{u_3}} - G^{\Delta_1,\Delta_5,\Delta_3}_{\tau_1,\ell-1,\tau_2,\ell-1,\ell-1}\right]$$
$$+ \frac{(\Delta_5-\tau_{12})(\tau_1+2\ell-1)}{(\tau_2+2\ell-2)(\tau_1+2\ell-\Delta_{12}-2)}\left[\frac{\sqrt{u_5}(\Delta_5+\tau_{12})G^{\Delta_1+1,\Delta_5+1,\Delta_3}_{\tau_1+1,\ell-1,\tau_2,\ell,\ell-1}}{\sqrt{u_1}} - 2G^{\Delta_1,\Delta_5,\Delta_3}_{\tau_1,\ell-1,\tau_2,\ell,\ell-1}\right]$$
$$- \frac{(\Delta_5+\tau_{12})(\tau_2+2\ell-1)(\tau_1+\tau_2+4\ell-\Delta_5-4)G^{\Delta_1,\Delta_5,\Delta_3}_{\tau_1,\ell,\tau_2,\ell-1,\ell-1}}{(\tau_1+2\ell-2)(\Delta_{34}+\tau_2+2\ell-2)}$$
$$+ (\tau_1+\tau_2+4\ell-\Delta_5-2)G^{\Delta_1,\Delta_5,\Delta_3}_{\tau_1,\ell,\tau_2,\ell,\ell} = 0. \tag{B.9}$$

B.2 Scalar Mellin partial-wave

In this appendix, we derive the Mellin partial-wave for scalar exchange within a five-point function. We start from partial-wave definition in position space

$$F_{\nu_1,\nu_2,0,0,0}(x_i) = \int dx_6 dx_7 \langle \phi_1\phi_2\phi(x_6)\rangle \langle \tilde{\phi}(x_6)\phi_5\tilde{\phi}(x_7)\rangle \langle \phi_3\phi_4\phi(x_7)\rangle \tag{B.10}$$

where the subscripts ans superscript 0 in $F_{\nu_1,\nu_2,0,0,0}$ denote the scalar exchanges and the superscripts refer to principal series representations of the exchanged operators. The notation $\langle \phi_i\phi_j\phi_k\rangle$ denotes kinematical structure of three-point functions

$$\langle \phi_1\phi_2\phi_3\rangle = \frac{1}{(-2P_1\cdot P_2)^{\frac{1}{2}(\Delta_1+\Delta_2-\Delta_3)}\,(-2P_1\cdot P_3)^{\frac{1}{2}(\Delta_1+\Delta_3-\Delta_2)}\,(-2P_2\cdot P_3)^{\frac{1}{2}(\Delta_2+\Delta_2-\Delta_1)}}\,, \tag{B.11}$$

where we use embedding space where $-2P_i\cdot P_j = x_{ij}^2$. Note that as we only consider scalar exchanges there is no sum over different possible tensor structures. In general, we consider unequal scalar fields labelled by their scaling dimensions Δ_i. For operators of fixed position we do the abuse of notation $\phi_i \equiv \phi(x_i)$ but we retain the dependence on integrated variables using $\phi(x_i)$. The latter notation corresponds to scalar operators of scaling dimension $h + i\nu_i$ with $h = d/2$. Moreover, shadow operators of scaling dimension $h - i\nu_i$ are denoted with an extra tilde.

In order to integrate over x_6 and x_7 we use the Schwinger parametrization

$$\frac{1}{(-2P_i\cdot P_j)^a} = \frac{1}{\Gamma(m+a)}\int_0^\infty \frac{dt_{ij}}{t_{ij}}\, t_{ij}^{m+a}(-\partial_{t_{ij}})^m e^{2t_{ij}P_i\cdot P_j}\,. \tag{B.12}$$

for any power a, $(-P_i\cdot P_j) > 0$ and some integer m such that $\mathrm{Re}(m+a) > 0$. For our purposes here, it is enough to take $m = 0$. It will also be useful to consider the following change of variables

$$\begin{aligned} &t_{12} = 2t_1t_2\,, \quad t_{16} = 2t_1t\,, \quad t_{26} = 2t_2t\,, \quad t_{34} = 2t_3t_4\,, \quad t_{37} = 2t_3s\,,\\ &t_{47} = 2t_4s\,, \quad t_{56} = 2t_5\bar{t}\,, \quad t_{57} = 2t_5\bar{s}\,, \quad t_{67} = 2\bar{t}\bar{s}\,, \end{aligned} \tag{B.13}$$

which is introduced to reproduce the form of integral one finds from considering a tree-level Witten diagram with two scalar exchanges using the notation of [59]. Here t_i's are related with bulk-to-boundary propagators of the external scalars whereas $t, \bar{t}, s, \bar{s}$ refer to split representations of the bulk-to-bulk propagators.

The integrals over x_6 and x_7 are easy to compute successively by noting [59]

$$\int_0^\infty \frac{dtd\bar{t}}{t\bar{t}} t^{\Delta_t}\bar{t}^{\Delta_{\bar{t}}}\int dP e^{2P\cdot(tX+\bar{t}Y)} = 2\pi^h\int_0^\infty \frac{dtd\bar{t}}{t\bar{t}} t^{\Delta_t}\bar{t}^{\Delta_{\bar{t}}} e^{(tX+\bar{t}Y)^2} \tag{B.14}$$

where $\Delta_t + \Delta_{\bar{t}} = 2h$ with X and Y two timelike vectors. We then find (dropping constants)

$$
\begin{aligned}
&F^0_{\nu_1,\nu_2,0,0}(x_i) \sim \int \frac{dt d\bar{t} ds d\bar{s}}{t\bar{t}s\bar{s}} t^{h+i\nu_1}\bar{t}^{h-i\nu_1}s^{h+i\nu_2}\bar{s}^{h-i\nu_2} \\
&\left(\prod_{i=1}^{5}\int\frac{dt_i}{t_i}t_i^{\Delta_i}\right)\exp\left[-t_1t_2x_{12}^2\left(t^2\left(\bar{s}^2\bar{t}^2+1\right)+1\right)\right. \\
&-t_1t_3x_{13}^2t\bar{t}s\bar{s}-t_1t_4x_{14}^2t\bar{t}s\bar{s}-t_1t_5x_{15}^2t\bar{t}\left(\bar{s}^2\left(\bar{t}^2+1\right)+1\right)-t_2t_3x_{23}^2t\bar{t}s\bar{s}-t_2t_4x_{24}^2t\bar{t}s\bar{s} \\
&\left.-t_2t_5x_{25}^2t\bar{t}\left(\bar{s}^2\left(\bar{t}^2+1\right)+1\right)-t_3t_4x_{34}^2\left(s^2+1\right)-t_3t_5x_{35}^2s\bar{s}\left(\bar{t}^2+1\right)-t_4t_5x_{45}^2s\bar{s}\left(\bar{t}^2+1\right)\right]
\end{aligned}
\tag{B.15}
$$

which is of the form of Symanzik's formula [109]

$$
2\int_0^\infty\prod_{i=1}^{n}\frac{dt_i}{t_i}t_i^{\Delta_i}e^{-\sum_{i<j}^{n}t_it_jQ_{ij}}=\frac{1}{(2\pi i)^{(n(n-3))/2}}\int d\delta_{ij}\prod_{i<j}^{n}\Gamma(\delta_{ij})Q_{ij}^{-\delta_{ij}}\,, \tag{B.16}
$$

with $Q_{ij} > 0$. The Mellin variables δ_{ij} are integrated along a contour parallel to the imaginary axis with $\mathrm{Re}(\delta_{ij}) > 0$ and obey the constraints

$$
\sum_{j\neq i}^{n}\delta_{ij}=\Delta_i\,. \tag{B.17}
$$

This allows us to find the inverse Mellin transform of the position-space partial-wave and the Mellin partial-wave

$$
F_{\nu_1,\nu_2,0,0,0}(x_i)=\frac{1}{(2\pi i)^5}\int d\delta_{ij}\mathcal{M}_{\nu_1,\nu_2,0,0,0}(\delta_{ij})\prod_{i<j}^{n}\Gamma(\delta_{ij})x_{ij}^{-2\delta_{ij}} \tag{B.18}
$$

The remaining integrations in $t, \bar{t}, s$ and $\bar{s}$ are straightforward to do. We then find

$$
\begin{aligned}
\mathcal{M}_{\nu_1,\nu_2,0,0,0}(\delta_{ij}) =&\frac{\pi^{2h}\left(\left(\prod_{i=1}^{2}\Gamma\left(\frac{\Delta_{2i-1}+\Delta_{2i}-t_{2i-1\,2i}}{2}\right)\left(\prod_{\sigma=\pm}\Gamma\left(\frac{h+\sigma\left(\Delta_{2i-1}-\Delta_{2i}\right)+i\nu_i}{2}\right)\right)\right)\right)^{-1}}{\Gamma(\Delta_5)\Gamma\left(\frac{\Delta_5-i\nu_1+i\nu_2}{2}\right)\Gamma\left(\frac{t_{12}-t_{34}+\Delta_5}{2}\right)\Gamma\left(\frac{2h-\Delta_5-i\nu_1-i\nu_2}{2}\right)\Gamma\left(\frac{h-t_{12}+\Delta_5-i\nu_2}{2}\right)} \\
&\left[\left(\prod_{\sigma=\pm}\Gamma\left(\frac{h-t_{12}+\sigma\Delta_5-i\nu_2}{2}\right)\Gamma\left(\frac{\Delta_5+\sigma i\nu_1+i\nu_2}{2}\right)\right)\Gamma\left(\frac{h-t_{34}+i\nu_2}{2}\right)\Gamma\left(\frac{t_{12}-t_{34}+\Delta_5}{2}\right)\right. \\
&{}_3F_2\left(\begin{matrix}\frac{t_{12}-t_{34}+\Delta_5}{2},\frac{\Delta_5-i\nu_1+i\nu_2}{2},\frac{\Delta_5+i\nu_1+i\nu_2}{2}\\ \Delta_5,\frac{2-h+t_{12}+\Delta_5+i\nu_2}{2}\end{matrix};1\right)+\Gamma\left(\Delta_5\right)\Gamma\left(\frac{t_{12}-h+\Delta_5+i\nu_2}{2}\right) \\
&\left.\left(\prod_{\sigma=\pm}\prod_{i=1}^{2}\Gamma\left(\frac{h-t_{2i-1\,2i}+\sigma i\nu_i}{2}\right)\right)\,{}_3F_2\left(\begin{matrix}\frac{h-t_{12}-i\nu_1}{2},\frac{h-t_{12}+i\nu_1}{2},\frac{h-t_{34}-i\nu_2}{2}\\ \frac{2+h-t_{12}-\Delta_5-i\nu_2}{2},\frac{h-t_{12}+\Delta_5-i\nu_2}{2}\end{matrix};1\right)\right]
\end{aligned}
\tag{B.19}
$$

where we use the notation $\delta_{ij} = \frac{\Delta_i+\Delta_j-t_{ij}}{2}$.

Let us finish this appendix by noting that a similar computation can be performed for spinning exchanges using Schwinger parametrization (B.12). To do so, at each moment, we multinomially expand the integrand decomposing it into sums over integrands of similar form to the ones encountered for scalar exchanges. In the end, one finds a spinning Mellin partial

wave written as several sums over scalar-type Mellin partial waves. In particular the sums are bounded by the values of spin of the exchanged operators. This is no-good for an analytic continuation in spin that we want to consider here. For that reason and due to its length we do not write that result here.

B.3 Explicit examples in position space

In this appendix, we single-out a conformal block contribution in position space and compute its Regge-limit behaviour.

We start with five-point conformal block lightcone limit in its integral representation

$$G_{k_1k_2\ell}(u_i) = u_1^{\frac{\tau_1}{2}} u_3^{\frac{\tau_2}{2}} (1-u_2)^{\ell} u_5^{\frac{\Delta_\phi}{2}} \int_0^1 [dt_1][dt_2] \tag{B.20}$$
$$\frac{\big(1-t_1(1-u_2)u_4-u_2u_4\big)^{J_2-\ell}\big(1-t_2(1-u_2)u_5-u_2u_5\big)^{J_1-\ell}}{\big(1-(1-u_4)t_2\big)^{\frac{h_2-\tau_1-2\ell+\Delta_\phi}{2}}\big(1-(1-u_5)t_1\big)^{\frac{h_1-\tau_2-2\ell+\Delta_\phi}{2}}\big(1-(1-t_1)(1-t_2)(1-u_2)\big)^{\frac{h_1+h_2-\Delta_\phi}{2}}},$$

where $\tau_i = \Delta_i - J_i$ is the twist and $h_i = \Delta_i + J_i$ the conformal spin of the i-th exchanged operator. The measure is given by $[dt] = \frac{\Gamma(\Delta_i+J_i)}{\Gamma^2(\frac{\Delta_i+J_i}{2})}(t(1-t))^{\frac{\Delta_i+J_i}{2}-1}$.

Generically, we do not know how to evaluate these integrals in terms of known analytic functions. However, when the exponents in the denominator of the integrand are integers, this is no longer the case.[1] As a matter of example we consider the simple case of $\Delta_i = \Delta_\phi = 2$ and $J_1 = J_2 = \ell = 0$. Note that this is just a choice and spinning cases would also have a similar discussion but with longer explicit expressions. In this case, equation (B.20) can be integrated and yields (apart from an overall constant)

$$\frac{u_1u_3u_5}{1-u_5+u_4\,(u_2u_5-1)}\,[\mathrm{Li}_2\,(u_2u_4)-\mathrm{Li}_2\,(u_4)+\mathrm{Li}_2\,(u_2u_5)-\mathrm{Li}_2\,(u_5)-\mathrm{Li}_2\,(u_2) \tag{B.21}$$
$$-\log\,(1-u_2)\log\,(u_2)-\log\,(1-u_4)\log\,(u_4)-\log\,(1-u_5)\log\,(u_5)$$
$$+\log\,(u_4)\log\,(u_5)+\log\,(u_2u_5)\log\,(1-u_2u_5)+\log\,(u_2u_4)\log\,(1-u_2u_4)+\zeta(2)]\ .$$

As we perform the analytic continuation from an Euclidean to double-Reggeon exchange kinematics that we presented in (3.79), we cross block branch-cuts and it mixes with other solutions of the Casimir equations. In particular, the discontinuities of the block contain the leading contributions in the Regge limit. Having an explicit expression to work with we can tell the full story.

As we perform the analytic continuation and as the lightcones are crossed, pairs of operators become timelike separated and cross-ratios u_2, u_4 and u_5 go around 0. Note then

[1] The package HyperInt [110] is particularly useful to evaluate these integrals.

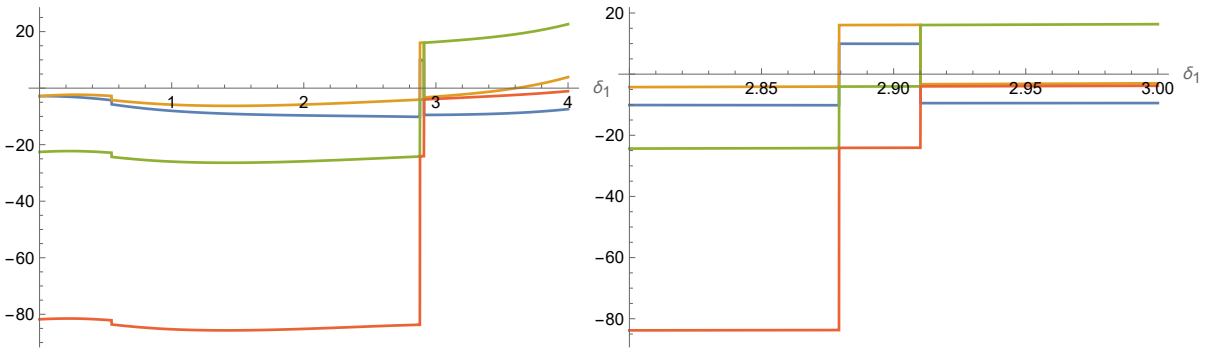

FIGURE B.1: Discontinuities of lightcone block under analytic continuation (3.79). In blue, the real part of the stripped-off lightcone block. In orange, the real part of the block with $\log(u_2) \to \log(u_2) + 2\pi i$. In green, the previous with $\log(u_4) \to \log(u_4) - 2\pi i$ and in red, the latter with $\log(u_5) \to \log(u_5) - 2\pi i$. On the right, a zoomed-in version of the same plot. The plots are obtained with $\delta_2 = 0.73\delta_1$.

that we are indeed crossing branch-cuts of the expression (B.21). In particular, we observe that only log terms in (B.21) can contribute to the discontinuity as u_i goes around 0 with $\log(x) \to \log(x) \pm 2\pi i$. The actual sign one picks is determined by how one moves around branch-cuts. As we reviewed in the main text, this depends on the ordering of operators of the Wightman function we consider. As before, here we take an ordering compatible with the time-ordering of Regge kinematics, i.e. $\langle \phi_4 \phi_1 \phi_2 \phi_5 \phi_3 \rangle$. Taking this ordering and the associated $i\epsilon$-prescription, we can perform the path continuation to Regge kinematics in our explicit-lightcone-block contribution and observe its discontinuities concretely. This is plotted in figure B.1.[2] As we move according to the chosen path for analytic continuation, we observe that the lightcone block (blue) has discontinuities. The first one can be removed if one replaces $\log(u_2) \to \log(u_2) + 2\pi i$ as shown by the orange line. Clearly, this shows that the discontinuity of the lightcone block is due to a logarithmic discontinuity in u_2. Similarly, when the orange line has a discontinuity, there is a continuation provided by the green line. The latter is defined from the former with the replacement $\log(u_4) \to \log(u_4) - 2\pi i$. We conclude that a discontinuity in u_4 has taken place. The same is true for the red line which provides the continuation of the green line once we take $\log(u_5) \to \log(u_5) - 2\pi i$ and once again a discontinuity, this time in u_5, has to be considered. This simple example shows in practice what we had already guessed: the lightcone block has discontinuities associated with u_2, u_4 and u_5 going around 0 and all of them are important. Let us then study the discontinuities of (B.21) on these variables.

[2] In this plot we only considered the terms within the brackets in (B.21). Note that only this part is relevant for the discontinuities we want to study.

It is possible to use the integral representation of the lightcone block to argue that there are no sequential discontinuities involving u_2, i.e.

$$\text{Disc}_{u_2}\text{Disc}_{u_4 \text{ or } u_5} G_{k_1,k_2,\ell} = \text{Disc}_{u_4 \text{ or } u_5}\text{Disc}_{u_2} G_{k_1,k_2,\ell} = 0\,. \tag{B.22}$$

In the expression (B.21) this is straightforward to see as there are no products of the type $\log(u_2)\log(u_4)$ or $\log(u_2)\log(u_5)$. As it was stated in the main text and as we will see below, it is actually the sum $\text{Disc}_{u_2} G_{k_1,k_2,\ell} + \text{Disc}_{u_5}\text{Disc}_{u_4} G_{k_1,k_2,\ell}$ that dominates the Regge behaviour of the correlation function.

The discontinuity of expression (B.21) as u_2 goes around 0 with fixed $u_4, u_5 > 0$ is given by

$$\pm 2\pi i \frac{u_1 u_3 u_5}{1 - u_5 + u_4(u_2 u_5 - 1)} \log\left(\frac{1-u_2}{(1-u_2 u_4)(1-u_2 u_5)}\right)\,, \tag{B.23}$$

which in the limit $u_4, u_5 \to 1$ with $\chi_2 = \frac{1-u_2}{(1-u_4)(1-u_5)}$ fixed simplifies to

$$\pm 2\pi i \frac{\sqrt{u_1}\sqrt{u_3}}{(\chi_2 - 1)\,\chi_4 \chi_5} \log(\chi_2)\,, \tag{B.24}$$

where we also use $\chi_4 = \frac{1-u_4}{\sqrt{u_3}}$ and $\chi_5 = \frac{1-u_5}{\sqrt{u_1}}$ which approach infinity due to the order of limits considered. This order of limits does not correspond to the actual Regge limit: indeed, we will call this ordered limit a boundary condition for Regge limit. The name simply follows from the fact that we use it below as a boundary condition for a set of recursion relations where we compute the Regge limit of a conformal block starting from the lightcone. Note, moreover, that the scaling in both u_1 and u_3 in the expression above agrees with the expected $u_i^{(1-J_i)/2}$ of Regge limit. As stated above we are indeed describing a double Reggeon exchange. This clearly contrasts with the Euclidean OPE scaling, $u_i^{\Delta_i/2}$, manifesting the difference between Regge and Euclidean kinematics. Perhaps a more striking example would follow from considering a spinning case from the beginning. The story is no different in those cases but the expressions grow considerably in size. We also note the existence of a log term in the case at hand. We point out that some other examples where the lightcone block can be integrated do not have these contributions in the above limit. Its existence in this case suggests however that a generic function for the discontinuity of the lightcone block as u_2 goes around 0 must contain log terms when the representation labels of the external and exchanged operators conspire in a certain way.

We now consider the discontinuity in u_4 with fixed and positive u_2, u_5. This gives

$$\pm 2\pi i \frac{u_1 u_3 u_5}{1 - u_5 + u_4(u_2 u_5 - 1)} \log\left(\frac{1-u_4}{(1-u_2 u_4)u_5}\right)\,, \tag{B.25}$$

which yields a boundary condition for Regge limit

$$\pm 2\pi i \frac{u_1\sqrt{u_3}}{\chi_4}\,. \tag{B.26}$$

From the symmetry of (B.21) between u_4 and u_5 we immediately see that a similar result follows for the discontinuity in u_5. Note that these terms are subdominant in the limit $u_1, u_3 \to 0$ when compared to (B.24). In particular, in expression (B.26) u_1 scales as $u_1^{\Delta_1/2}$ whereas u_3 scales as $u_3^{(1-J_2)/2}$. The converse happens in the discontinuity in u_5 complex plane. This behaviour should correspond to single Reggeon exchanges. Notably, the sequential discontinuity in u_4 and u_5 produces a dominant contribution for the double Reggeon kinematics. To see this, consider (B.25) and take the sequential discontinuity in u_5. This gives

$$\pm 4\pi^2 \frac{u_1 u_3 u_5}{1-u_5+u_4\,(u_2u_5-1)}\,, \tag{B.27}$$

which fixes the boundary condition for Regge limit

$$4\pi^2 \frac{\sqrt{u_1}\sqrt{u_3}}{(\chi_2-1)\,\chi_4\chi_5}\,, \tag{B.28}$$

that is as dominant as (B.24). We conclude in this simple example, the generic statement we have made in the main text that $\text{Disc}_{u_2} G_{k_1,k_2,\ell} + \text{Disc}_{u_5}\text{Disc}_{u_4} G_{k_1,k_2,\ell}$ provide the dominant contributions of the correlation function in Regge limit.

Even though the existence of log terms in the boundary condition for the Regge limit is not generic, we should however show how to deal with them when we compute the conformal blocks at Regge limit. If there are no log terms in your case of interest, simply set those terms to zero in the procedure below. We consider the Casimir equations in the limit of $u_1, u_3 \to 0$ with a block that scales as

$$\mathcal{G}_{k_1' k_2' \ell}(x_i) \propto u_1^{\frac{1-J_1}{2}} u_3^{\frac{1-J_2}{2}} \mathcal{H}(\chi_2,\chi_4,\chi_5)\,. \tag{B.29}$$

In this limit, the Casimir equations for $\mathcal{H}$ simplify and read

$$\begin{aligned}&\big[\chi_4^2\left(4(2\chi_2-1)(\partial_{\chi_2}-\chi_5\partial_{\chi_2}\partial_{\chi_5})-(d-1)\chi_5^3\partial_{\chi_5}-\left(\chi_5^2-4\right)\chi_5^2\partial_{\chi_5}^2\right)\\&+4\left((\chi_2-1)\chi_2\chi_4^2+1\right)\partial_{\chi_2}^2+(\Delta_1-1)(\Delta_1-d+1)\chi_4^2\chi_5^2\big]\,\mathcal{H}(\chi_2,\chi_4,\chi_5)=0\end{aligned} \tag{B.30}$$

with an entirely similar second equation obtained from the above by replacing Δ_1 by Δ_2 and permuting the roles of χ_4 and χ_5. In our particular case of study, in the limit of $u_1, u_3 \to 0$, large χ_4, χ_5 and fixed χ_2, the leading Regge contribution of the block behaves as

$$\frac{\sqrt{u_1}\sqrt{u_3}}{(\chi_2-1)\chi_4\chi_5}\,(a+b\log(\chi_2)) \tag{B.31}$$

where a and b are constants. We can thus further impose in (B.30)

$$\mathcal{H}(\chi_2,\chi_4,\chi_5)=\frac{\mathbb{H}(\chi_2,\chi_4,\chi_5)}{\chi_4\chi_5}\,. \tag{B.32}$$

According to (B.31) and considering a small-χ_2 limit, we can look for solutions of the Casimir equations of the form

$$\mathbb{H}(\chi_2,\chi_4,\chi_5)=\sum_{n_1,n_2,n_3} a_{n_1,n_2,n_3}\chi_2^{n_1}\chi_4^{-n_2}\chi_5^{-n_3}+b_{n_1,n_2,n_3}\log(\chi_2)\chi_2^{n_1}\chi_4^{-n_2}\chi_5^{-n_3} \tag{B.33}$$

where the coefficients a_{n_1,n_2,n_3} and b_{n_1,n_2,n_3} reduce to a and b, respectively, when all n_i are 0. The remaining expansion coefficients a_{n_1,n_2,n_3} and b_{n_1,n_2,n_3} are fixed by the Casimir equations. It is easy to see that this ansatz gives rise to terms in the Casimir equations of the form

$$\chi_2^{c_1+n_1}\chi_4^{c_2-n_2}\chi_5^{c_3-n_3}\times\begin{cases} a_{n_1,n_2,n_3}\\ b_{n_1,n_2,n_3}\\ b_{n_1,n_2,n_3}\log(\chi_2)\end{cases}\,. \tag{B.34}$$

Clearly, the terms that depend on log should cancel among each other in order to satisfy the Casimir equation. This leads to two constraints per Casimir equation, one for the log-dependent terms and one for the remaining. For the isolated log terms, we find recursion relations for the coefficients by removing the χ-dependence from the equations. To do so, we shift each term accordingly, i.e. $n_1\to n_1-c_1, n_2\to n_2+c_2$ and $n_3\to n_3+c_3$. This leads to the following recursion relations

$$\begin{aligned} b_{n_1,n_2,n_3}=\frac{1}{n_3(d-n_3-4)}\,&[4(n_1+1)\left((n_1+n_3)b_{n_1+1,n_2,n_3-2}-(n_1+2)b_{n_1+2,n_2-2,n_3-2}\right)\\ &-4(n_1+n_3-1)(n_1+n_3)b_{n_1,n_2,n_3-2}] \end{aligned} \tag{B.35}$$

with a similar one where we exchange the roles of n_3 and n_2. Clearly, the above recursion relation cannot be used whenever $n_3=0$. In such case, the other recursion relation can be used instead (and vice-versa). An entirely similar argument follows for the non-log-dependent terms. We find the recursion relations

$$\begin{aligned} a_{n_1,n_2,n_3}=\frac{4}{n_2(4-d+n_2)}\,&[(n_1+n_2-1)(n_1+n_2)a_{n_1,n_2-2,n_3}-(n_1+1)(n_1+n_2)a_{n_1+1,n_2-2,n_3}\\ &+(n_1+1)(n_1+2)a_{n_1+2,n_2-2,n_3-2}+(2n_1+2n_2-1)b_{n_1,n_2-2,n_3}-(2n_1+n_2+1)b_{n_1+1,n_2-2,n_3}\\ &+(2n_1+3)b_{n_1+2,n_2-2,n_3-2}] \end{aligned} \tag{B.36}$$

with another equivalent relation where the roles of n_2 and n_3 are swapped.

These recursion relations are only meaningful once one prescribes a boundary condition. We impose that

$$\begin{aligned} &a_{n_1,n_2,n_3} = b_{n_1,n_2,n_3} = 0 \qquad \text{if} \qquad n_1 < 0 \vee n_2 < 0 \vee n_3 < 0\,, \\ &a_{0,0,0} = a \qquad \text{and} \qquad b_{0,0,0} = b\,. \end{aligned} \tag{B.37}$$

It is easy to check that these recursion relations fix the behaviour of all the coefficients up to those of the form $a_{n_1,0,0}$ and $b_{n_1,0,0}$ but note that these can be read from (B.31) by expanding it on small χ_2 limit.

B.4 Other Regge kinematics

In this short appendix, we detail other possible Regge kinematics that we did not explore in detail in this paper but that might be worth studying in the future.

Single Reggeon exchange

Within a five-point function, one can consider a single Reggeon exchange. In terms of Mandelstam invariants s_{25} or s_{45} of figure 3.1 only one of the two becomes large. In the context of CFTs, this translates to having only two operators, one in the first and one in the second Poincare patches, approaching each other in such a way that there is only one cross-ratio going to 0 rather than two.

One possible analytic continuation that describes single Reggeon exchange is given by

$$\begin{aligned} &x_1 = -r\,(\sinh(\delta_1), \cosh(\delta_1), \mathbf{0}_{d-2}) \qquad x_3 = (0, 1, \mathbf{0}_{d-2}) \qquad x_5 = (0, h_1, h_2, \mathbf{0}_{d-3}) \\ &x_2 = r\,(\sinh(\delta_2), \cosh(\delta_2), \mathbf{0}_{d-2}) \qquad x_4 = (0, -1, \mathbf{0}_{d-2})\,. \end{aligned} \tag{B.38}$$

with positive rapidities δ_i and $\mathbf{0}_d$ denoting a d-dimensional vector of zeros. In the large-rapidities limit, one can check that $u_1 \to 0$ and $u_2, u_5 \to 1$ with unfixed u_3 and u_4. This agrees with the Euclidean OPE limit in the (12) channel. Again, we emphasize that this limit is attained after branch-cuts are crossed and thus in an intrinsically Lorentzian Regge sheet.

Six-point snowflake

The six-point conformal block of external scalars is known in the lightcone limit in the snowflake topology [77]. Even though we did not attempt in this paper to analyse the cut-structure of this block, we nonetheless write down an analytic continuation prescription to

achieve a Regge limit configuration that is consistent at the level of the cross-ratios with the OPE on channels (12), (34) and (56).

We use the set of 9 cyclic cross-ratios

$$\begin{aligned} u_1 &= \frac{x_{12}^2 x_{35}^2}{x_{13}^2 x_{25}^2} \quad u_{i+1} = u_i|_{x_i \to x_{i+1}} \mod 6 \\ U_1 &= \frac{x_{13}^2 x_{46}^2}{x_{14}^2 x_{36}^2} \quad U_{i+1} = U_i|_{x_i \to x_{i+1}} \mod 3\,. \end{aligned} \tag{B.39}$$

In the snowflake OPE limit $u_1, u_3, u_5 \to 0$ and the remaining all go to 1. In the Regge limit one should reobtain the same limiting values of the cross-ratios after some lightcones are crossed. We start with a totally spacelike configuration and perform the analytic continuation

$$\begin{aligned} x_1 &= -r_1\,(\sinh(\delta_1), \cosh(\delta_1), \mathbf{0}_{d-2}) & x_4 &= (\sinh(\delta_1), -\cosh(\delta_1), \mathbf{0}_{d-2}) \\ x_2 &= r_1\,(\sinh(\delta_2), \cosh(\delta_2), \mathbf{0}_{d-2}) & x_5 &= (r_2 \sinh(\delta_3), r_3, h, r_2 \cosh(\delta_3), \mathbf{0}_{d-4}) \\ x_3 &= (-\sinh(\delta_2), \cosh(\delta_2), \mathbf{0}_{d-2}) & x_6 &= (-r_2 \sinh(\delta_3), r_4, h, -r_2 \cosh(\delta_3), \mathbf{0}_{d-4})\,. \end{aligned} \tag{B.40}$$

where one can see that we use 9 degrees of freedom. Note as well that for six-point functions one can at most use the conformal symmetry to state that any generic correlation function is related to one that lives in some half-subspace in 4 dimensions [111]. Perhaps the most notorious difference in this case is the need to boost a pair of points along some different plane. It is easy to check however that this prescription indeed leads to the expected OPE behaviour for a snowflake six-point function.

Chapter 4

Conclusions

In this thesis, we have discussed two aspects of conformal Regge theory.

In the second chapter, we considered the generalization of the Optical theorem to AdS. This allowed us to write a formula that relates one loop CFT data in terms of tree level CFT data.

It would be interesting to use this formula to constrain CFT data at one loop in AdS in various supergravity approximations. More generally, there are various techniques in the scattering amplitude literature which deal with Feynman diagrams at higher loops which deal with only on-shell data. It would interesting if they have an analogous construction in AdS. Since unitarity plays an important role in those constraints, we expect our formula to be useful in that context.

It would be interesting if this formula can be generalized to higher loops. We commented about it in the conclusion of the second chapter. It is known that in the supergravity approximation, the loop diagrams can be resummed in the Regge limit. It would be interesting to generalize it beyond the supergravity approximation. Recently, there has been a lot of progress in the correlation functions on the boundary of AdS_3 in terms of Wess-Zumino-Witten models [112]. With or without supersymmetry, these models provide a good arena to test such a resummation procedure in AdS. It would provide a model of eikonal resummation at finite 't Hooft coupling which can be interpolated between weak and strong coupling.

In particular, cutting rules in flat space suggest that one can always decompose higher loop Feynman diagrams in terms of lower loop diagrams. Analogously, Witten diagrams might follow such a recursion.

In the third chapter, we considered the generalization of the Regge theory to higher point correlation functions. As the study of higher point correlation functions is in a nascent stage, there are several avenues of interest.

We have provided a novel basis for three point functions of spinning operators. This is necesary to establish the orthogonality of the conformal partial waves. It would be interesting

to explicitly write this orthogonality relation and the corresponding Euclidean inversion formula. Then, one can use the prescription for the Regge limit proposed in the third chapter along with boundedness assumption to arrive at an inversion formula. This would establish rigidity that is much stronger than the the one imposed by analyticity in spin.

More generally, the study of the causality constraints of the correlation functions has been done only in the four point case. It would be interesting to generalize this to higher point cases. Steinmann relations are known to be powerful in the weakly coupled maximally supersymmetric Yang-Mills theory in four dimension (SYM). It would be interesting to work out their implications in the strongly coupled limit.

Finally, the topic of Regge theory is chiefly inspired by the experimental data. It would be interesting if the lessons learnt from the higher supersymmetric examples teach us something about the Regge trajectories of the Quantum chromodynamics. After all, super Yang-Mills theory is a close cousin of the Quantum chromodynamics with a different matter content. Is there a way to deform the leading Regge trajectory to predict the correspoding leading Regge trajectory of Quantum chromodynamics? Hopefully, a more detailed understanding of the leading trajectory of conformal Regge theory and SYM will teach some lessons.

Bibliography

[1] David Poland, Slava Rychkov, and Alessandro Vichi. The Conformal Bootstrap: Theory, Numerical Techniques, and Applications. *Rev. Mod. Phys.*, 91:015002, 2019.

[2] V. N. Gribov. *The theory of complex angular momenta: Gribov lectures on theoretical physics*. Cambridge Monographs on Mathematical Physics. Cambridge University Press, 6 2007.

[3] Juan Martin Maldacena. The Large N limit of superconformal field theories and supergravity. *Int. J. Theor. Phys.*, 38:1113–1133, 1999.

[4] Miguel S. Costa, Vasco Goncalves, and Joao Penedones. Conformal Regge theory. *JHEP*, 12:091, 2012.

[5] Thomas Hartman, Sachin Jain, and Sandipan Kundu. Causality Constraints in Conformal Field Theory. *JHEP*, 05:099, 2016.

[6] Simon Caron-Huot. Analyticity in Spin in Conformal Theories. *JHEP*, 09:078, 2017.

[7] Miguel S. Costa, Tobias Hansen, and João Penedones. Bounds for OPE coefficients on the Regge trajectory. *JHEP*, 10:197, 2017.

[8] F. A. Dolan and H. Osborn. Conformal partial waves and the operator product expansion. *Nucl. Phys. B*, 678:491–507, 2004.

[9] David Simmons-Duffin. The Lightcone Bootstrap and the Spectrum of the 3d Ising CFT. *JHEP*, 03:086, 2017.

[10] Simon Caron-Huot, Murat Kologlu, Petr Kravchuk, David Meltzer, and David Simmons-Duffin. Detectors in weakly-coupled field theories. *JHEP*, 04:014, 2023.

[11] Denis Karateev, Petr Kravchuk, and David Simmons-Duffin. Harmonic Analysis and Mean Field Theory. *JHEP*, 10:217, 2019.

[12] Petr Kravchuk and David Simmons-Duffin. Light-ray operators in conformal field theory. *JHEP*, 11:102, 2018.

[13] Madalena Lemos, Pedro Liendo, Marco Meineri, and Sourav Sarkar. Universality at large transverse spin in defect CFT. *JHEP*, 09:091, 2018.

[14] Pedro Liendo, Yannick Linke, and Volker Schomerus. A Lorentzian inversion formula for defect CFT. *JHEP*, 08:163, 2020.

[15] Dean Carmi and Simon Caron-Huot. A Conformal Dispersion Relation: Correlations from Absorption. *JHEP*, 09:009, 2020.

[16] Simon Caron-Huot, Dalimil Mazac, Leonardo Rastelli, and David Simmons-Duffin. Dispersive CFT Sum Rules. 8 2020.

[17] Agnese Bissi, Parijat Dey, and Tobias Hansen. Dispersion Relation for CFT Four-Point Functions. *JHEP*, 04:092, 2020.

[18] Luis F. Alday. Large Spin Perturbation Theory for Conformal Field Theories. *Phys. Rev. Lett.*, 119(11):111601, 2017.

[19] Luis F. Alday. Solving CFTs with Weakly Broken Higher Spin Symmetry. *JHEP*, 10:161, 2017.

[20] Ofer Aharony, Luis F. Alday, Agnese Bissi, and Eric Perlmutter. Loops in AdS from Conformal Field Theory. *JHEP*, 07:036, 2017.

[21] Luis F. Alday and Simon Caron-Huot. Gravitational S-matrix from CFT dispersion relations. *JHEP*, 12:017, 2018.

[22] Luis F. Alday, Johan Henriksson, and Mark van Loon. Taming the ϵ-expansion with large spin perturbation theory. *JHEP*, 07:131, 2018.

[23] Edward Witten. Anti-de Sitter space and holography. *Adv. Theor. Math. Phys.*, 2:253–291, 1998.

[24] S.S. Gubser, Igor R. Klebanov, and Alexander M. Polyakov. Gauge theory correlators from noncritical string theory. *Phys. Lett. B*, 428:105–114, 1998.

[25] Junyu Liu, Eric Perlmutter, Vladimir Rosenhaus, and David Simmons-Duffin. d-dimensional SYK, AdS Loops, and $6j$ Symbols. *JHEP*, 03:052, 2019.

[26] Dmitry Ponomarev. From bulk loops to boundary large-N expansion. *JHEP*, 01:154, 2020.

[27] David Meltzer, Eric Perlmutter, and Allic Sivaramakrishnan. Unitarity Methods in AdS/CFT. *JHEP*, 03:061, 2020.

[28] David Meltzer and Allic Sivaramakrishnan. CFT unitarity and the AdS Cutkosky rules. *JHEP*, 11:073, 2020.

[29] A.Liam Fitzpatrick and Jared Kaplan. Unitarity and the Holographic S-Matrix. *JHEP*, 10:032, 2012.

[30] Lorenzo Cornalba, Miguel S. Costa, Joao Penedones, and Ricardo Schiappa. Eikonal Approximation in AdS/CFT: From Shock Waves to Four-Point Functions. *JHEP*, 08:019, 2007.

[31] Lorenzo Cornalba, Miguel S. Costa, Joao Penedones, and Ricardo Schiappa. Eikonal Approximation in AdS/CFT: Conformal Partial Waves and Finite N Four-Point Functions. *Nucl. Phys. B*, 767:327–351, 2007.

[32] David J. Gross and Paul F. Mende. The High-Energy Behavior of String Scattering Amplitudes. *Phys. Lett. B*, 197:129–134, 1987.

[33] David J. Gross and Paul F. Mende. String Theory Beyond the Planck Scale. *Nucl. Phys. B*, 303:407–454, 1988.

[34] D. Amati, M. Ciafaloni, and G. Veneziano. Superstring Collisions at Planckian Energies. *Phys. Lett. B*, 197:81, 1987.

[35] D. Amati, M. Ciafaloni, and G. Veneziano. Classical and Quantum Gravity Effects from Planckian Energy Superstring Collisions. *Int. J. Mod. Phys.*, A3:1615–1661, 1988.

[36] D. Amati, M. Ciafaloni, and G. Veneziano. Can Space-Time Be Probed Below the String Size? *Phys. Lett. B*, 216:41–47, 1989.

[37] Lorenzo Cornalba, Miguel S. Costa, and Joao Penedones. Eikonal approximation in AdS/CFT: Resumming the gravitational loop expansion. *JHEP*, 09:037, 2007.

[38] Richard C. Brower, Matthew J. Strassler, and Chung-I Tan. On the eikonal approximation in AdS space. *JHEP*, 03:050, 2009.

[39] Richard C. Brower, Joseph Polchinski, Matthew J. Strassler, and Chung-I Tan. The Pomeron and gauge/string duality. *JHEP*, 12:005, 2007.

[40] Lorenzo Cornalba. Eikonal methods in AdS/CFT: Regge theory and multi-reggeon exchange. 2007.

[41] Lorenzo Cornalba, Miguel S. Costa, and Joao Penedones. Eikonal Methods in AdS/CFT: BFKL Pomeron at Weak Coupling. *JHEP*, 06:048, 2008.

[42] Richard C. Brower, Matthew J. Strassler, and Chung-I Tan. On The Pomeron at Large 't Hooft Coupling. *JHEP*, 03:092, 2009.

[43] Lorenzo Cornalba, Miguel S. Costa, and Joao Penedones. Deep Inelastic Scattering in Conformal QCD. *JHEP*, 03:133, 2010.

[44] David Meltzer. AdS/CFT Unitarity at Higher Loops: High-Energy String Scattering. *JHEP*, 05:133, 2020.

[45] S. Ferrara, A.F. Grillo, G. Parisi, and R. Gatto. The shadow operator formalism for conformal algebra. Vacuum expectation values and operator products. *Lett. Nuovo Cim.*, 4S2:115–120, 1972.

[46] David Simmons-Duffin. Projectors, Shadows, and Conformal Blocks. *JHEP*, 04:146, 2014.

[47] V.K. Dobrev, G. Mack, V.B. Petkova, S.G. Petrova, and I.T. Todorov. *Harmonic Analysis on the n-Dimensional Lorentz Group and Its Application to Conformal Quantum Field Theory*, volume 63. 1977.

[48] Xian O. Camanho, Jose D. Edelstein, Juan Maldacena, and Alexander Zhiboedov. Causality Constraints on Corrections to the Graviton Three-Point Coupling. *JHEP*, 02:020, 2016.

[49] T. Regge. Introduction to complex orbital momenta. *Nuovo Cim.*, 14:951, 1959.

[50] Simon Caron-Huot and Joshua Sandor. Conformal Regge Theory at Finite Boost. 8 2020.

[51] M. Ademollo, A. Bellini, and M. Ciafaloni. Superstring Regge Amplitudes and Emission Vertices. *Phys. Lett. B*, 223:318–324, 1989.

[52] M. Ademollo, A. Bellini, and M. Ciafaloni. Superstring Regge Amplitudes and Graviton Radiation at Planckian Energies. *Nucl. Phys. B*, 338:114–142, 1990.

[53] Giuseppe D'Appollonio, Paolo Di Vecchia, Rodolfo Russo, and Gabriele Veneziano. Microscopic unitary description of tidal excitations in high-energy string-brane collisions. *JHEP*, 11:126, 2013.

[54] Rutger H. Boels and Tobias Hansen. String theory in target space. *JHEP*, 06:054, 2014.

[55] Manuela Kulaxizi, Gim Seng Ng, and Andrei Parnachev. Black Holes, Heavy States, Phase Shift and Anomalous Dimensions. *SciPost Phys.*, 6(6):065, 2019.

[56] Marc Gillioz. Momentum-space conformal blocks on the light cone. *JHEP*, 10:125, 2018.

[57] Miguel S. Costa, Joao Penedones, David Poland, and Slava Rychkov. Spinning Conformal Blocks. *JHEP*, 11:154, 2011.

[58] Denis Karateev, Petr Kravchuk, and David Simmons-Duffin. Weight Shifting Operators and Conformal Blocks. *JHEP*, 02:081, 2018.

[59] Joao Penedones. Writing CFT correlation functions as AdS scattering amplitudes. *JHEP*, 03:025, 2011.

[60] Daliang Li, David Meltzer, and David Poland. Conformal Bootstrap in the Regge Limit. *JHEP*, 12:013, 2017.

[61] Miguel S. Costa, Vasco Gonçalves, and João Penedones. Spinning AdS Propagators. *JHEP*, 09:064, 2014.

[62] Dean Carmi, Lorenzo Di Pietro, and Shota Komatsu. A Study of Quantum Field Theories in AdS at Finite Coupling. *JHEP*, 01:200, 2019.

[63] David Meltzer and Eric Perlmutter. Beyond $a = c$: gravitational couplings to matter and the stress tensor OPE. *JHEP*, 07:157, 2018.

[64] A.V. Kotikov and L.N. Lipatov. DGLAP and BFKL equations in the $N = 4$ supersymmetric gauge theory. *Nucl. Phys. B*, 661:19–61, 2003. [Erratum: Nucl.Phys.B 685, 405–407 (2004)].

[65] A.V. Kotikov, L.N. Lipatov, A. Rej, M. Staudacher, and V.N. Velizhanin. Dressing and wrapping. *J. Stat. Mech.*, 0710:P10003, 2007.

[66] Amihay Hanany, Davide Forcella, and Jan Troost. The Covariant perturbative string spectrum. *Nucl. Phys. B*, 846:212–225, 2011.

[67] The Sage Developers. *SageMath, the Sage Mathematics Software System (Version 9.1)*, 2020. `https://www.sagemath.org`.

[68] Miguel S. Costa, Tobias Hansen, Joao Penedones, and Emilio Trevisani. Projectors and seed conformal blocks for traceless mixed-symmetry tensors. *JHEP*, 07:018, 2016.

[69] Miguel S. Costa and Tobias Hansen. AdS Weight Shifting Operators. *JHEP*, 09:040, 2018.

[70] Vladimir Rosenhaus. Multipoint Conformal Blocks in the Comb Channel. *JHEP*, 02:142, 2019.

[71] Vasco Gonçalves, Raul Pereira, and Xinan Zhou. 20′ Five-Point Function from $AdS_5 \times S^5$ Supergravity. *JHEP*, 10:247, 2019.

[72] Ilija Buric, Sylvain Lacroix, Jeremy A. Mann, Lorenzo Quintavalle, and Volker Schomerus. From Gaudin Integrable Models to d-dimensional Multipoint Conformal Blocks. *Phys. Rev. Lett.*, 126(2):021602, 2021.

[73] Ilija Buric, Sylvain Lacroix, Jeremy A. Mann, Lorenzo Quintavalle, and Volker Schomerus. Gaudin models and multipoint conformal blocks III: comb channel coordinates and OPE factorisation. *JHEP*, 06:144, 2022.

[74] Ilija Buric, Sylvain Lacroix, Jeremy A. Mann, Lorenzo Quintavalle, and Volker Schomerus. Gaudin models and multipoint conformal blocks. Part II. Comb channel vertices in 3D and 4D. *JHEP*, 11:182, 2021.

[75] Ilija Buric, Sylvain Lacroix, Jeremy A. Mann, Lorenzo Quintavalle, and Volker Schomerus. Gaudin models and multipoint conformal blocks: general theory. *JHEP*, 10:139, 2021.

[76] David Poland and Valentina Prilepina. Recursion relations for 5-point conformal blocks. *JHEP*, 10:160, 2021.

[77] António Antunes, Miguel S. Costa, Vasco Goncalves, and Joao Vilas Boas. Lightcone bootstrap at higher points. *JHEP*, 03:139, 2022.

[78] Carlos Bercini, Vasco Gonçalves, and Pedro Vieira. Light-Cone Bootstrap of Higher Point Functions and Wilson Loop Duality. *Phys. Rev. Lett.*, 126(12):121603, 2021.

[79] Luis F. Alday, Vasco Gonçalves, and Xinan Zhou. Supersymmetric Five-Point Gluon Amplitudes in AdS Space. *Phys. Rev. Lett.*, 128(16):161601, 2022.

[80] Vasco Gonçalves, Carlo Meneghelli, Raul Pereira, Joao Vilas Boas, and Xinan Zhou. Kaluza-Klein Five-Point Functions from $AdS_5 \times S_5$ Supergravity. 2 2023.

[81] P. Goddard and A. R. White. Complex helicity and the sommerfeld-watson transformation of group-theoretic expansions. *Nuovo Cim. A*, 1:645–679, 1971.

[82] A. R. White. The signatured froissart-gribov continuation of multiparticle amplitudes to complex helicity and angular momentum. *Nucl. Phys. B*, 39:432–460, 1972.

[83] A. R. White. The analytic continuation of multiparticle unitarity in the complex angular momentum plane. *Nucl. Phys. B*, 39:461–478, 1972.

[84] A. R. White. Signature, factorization and unitarity in multi-regge theory - the five-point function. *Nucl. Phys. B*, 67:189–231, 1973.

[85] Alan R. White. The Analytic Foundations of Regge Theory. In *Institute on Structural Analysis of Multiparticle Collision Amplitudes in Relativistic Quantum Theory*, 2 1976.

[86] R. C. Brower, Carleton E. DeTar, and J. H. Weis. Regge Theory for Multiparticle Amplitudes. *Phys. Rept.*, 14:257, 1974.

[87] J. H. Weis. Singularities in complex angular momentum and helicity. *Phys. Rev. D*, 6:2823–2841, 1972.

[88] H. D. I. Abarbanel and A. Schwimmer. Analytic structure of multiparticle amplitudes in complex helicity. *Phys. Rev. D*, 6:3018–3031, 1972.

[89] Henry P. Stapp and Alan R. White. An Asymptotic Dispersion Relation for the Six Particle Amplitude. *Phys. Rev. D*, 26:2145, 1982.

[90] I. T. Drummond. Multi-reggeon behavior of production amplitudes. *Phys. Rev.*, 176:2003–2013, Dec 1968.

[91] Alan White. Analytic multi-regge theory and the pomeron in qcd - part 1. `https://www.osti.gov/servlets/purl/7002400`. [Online; accessed 15-November-2022].

[92] C. E. DeTar, C. E. Jones, F. E. Low, J. H. Weis, J. E. Young, and Chung-I Tan. Helicity poles, triple-regge behavior, and single-particle spectra in high-energy collisions. *Phys. Rev. Lett.*, 26:675–676, Mar 1971.

[93] Steinmann. Ueber den zusammenhang zwischen den wightmanfunktionen und den retardierten kommutatoren. `https://www.research-collection.ethz.ch/handle/20.500.11850/135473`. [Online; accessed 15-November-2022].

[94] John H. Schwarz. Dual resonance theory. *Phys. Rept.*, 8:269–335, 1973.

[95] K. Bardakci and H. Ruegg. Meson resonance couplings in a five-point veneziano model. *Phys. Lett. B*, 28:671–675, 1969.

[96] Carlos Bercini, Vasco Gonçalves, Alexandre Homrich, and Pedro Vieira. The Wilson Loop – Large Spin OPE Dictionary. 10 2021.

[97] Juan Maldacena, David Simmons-Duffin, and Alexander Zhiboedov. Looking for a bulk point. *JHEP*, 01:013, 2017.

[98] Petr Kravchuk, Jiaxin Qiao, and Slava Rychkov. Distributions in CFT. Part I. Cross-ratio space. *Jhep*, 05:137, 2020.

[99] Petr Kravchuk, Jiaxin Qiao, and Slava Rychkov. Distributions in CFT. Part II. Minkowski space. *Jhep*, 08:094, 2021.

[100] M. Luscher and G. Mack. Global Conformal Invariance in Quantum Field Theory. *Commun. Math. Phys.*, 41:203–234, 1975.

[101] G. Mack. Convergence of Operator Product Expansions on the Vacuum in Conformal Invariant Quantum Field Theory. *Commun. Math. Phys.*, 53:155, 1977.

[102] R. F. Streater and A. S. Wightman. *PCT, spin and statistics, and all that*. 1989.

[103] H. Casini. Wedge reflection positivity. *J. Phys. A*, 44:435202, 2011.

[104] Juan Maldacena, Stephen H. Shenker, and Douglas Stanford. A bound on chaos. *Jhep*, 08:106, 2016.

[105] Murat Kologlu, Petr Kravchuk, David Simmons-Duffin, and Alexander Zhiboedov. Shocks, Superconvergence, and a Stringy Equivalence Principle. *Jhep*, 11:096, 2020.

[106] David Simmons-Duffin, Douglas Stanford, and Edward Witten. A spacetime derivation of the Lorentzian OPE inversion formula. *JHEP*, 07:085, 2018.

[107] Gerhard Mack. D-independent representation of Conformal Field Theories in D dimensions via transformation to auxiliary Dual Resonance Models. Scalar amplitudes. 7 2009.

[108] Vasco Gonçalves, João Penedones, and Emilio Trevisani. Factorization of Mellin amplitudes. *JHEP*, 10:040, 2015.

[109] K. Symanzik. On Calculations in conformal invariant field theories. *Lett. Nuovo Cim.*, 3:734–738, 1972.

[110] Erik Panzer. Algorithms for the symbolic integration of hyperlogarithms with applications to Feynman integrals. *Comput. Phys. Commun.*, 188:148–166, 2015.

[111] Petr Kravchuk and David Simmons-Duffin. Counting Conformal Correlators. *Jhep*, 02:096, 2018.

[112] Lorenz Eberhardt. A perturbative CFT dual for pure NS–NS AdS_3 strings. *J. Phys. A*, 55(6):064001, 2022.